Optimising the operation of hydronic heating systems in existing buildings for connection to low temperature district heating networks

Michele Tunzi, MSc

Thesis submitted to the University of Nottingham
for the degree of Doctor of Philosophy

November 2016

"One difference between a quest and a "road trip" is the degree to which the traveller knows what he or she wants.....The appeal of the road trip is that the "point" is so deliberately minimal and the decisions involved so banal that the distinction between signal and noise becomes blurred."

Abstract

This thesis presents a new method developed to adapt existing hydronic systems in buildings to take advantage of low temperature district heating (LTDH). The work carried out was performed by extensive use of buildings' energy modelling, validated through recorded data. Two different case studies were investigated and the dynamic heat demand profiles, simulated for each building, were used to evaluate plate radiators connected to single and double string heating loops. The method considered an optimisation procedure, based on supply and return temperatures, to obtain the required logarithmic mean temperature difference (LMTD). The results of the analysis are presented as the average reduction of LMTD over the heating season compared to the base case design conditions.

The developed strategy was applied to a Danish single family house from the 1930s. Firstly it was hypothesised a heating system based on double string loop. Two scenarios were investigated based on the assumption of a likely cost reduction in the end users energy bills of 1% per each 1 °C reduction of return and average supply and return temperatures. The results showed possible discounts of 14% and 16% respectively, due to more efficient operation of the radiators. For the case of single loop system, the investigated scenario assumed a cost reduction in the end users energy bill of 1% per each 1 °C lower reduction of average supply and return temperature. Although low return temperatures could not be achieved, the implementation of the method illustrates how to efficiently operate these systems

and for the given scenario a possible discount of 5% was quantified.

The method was also applied to a UK small scale district heating (DH) network. The analysis began by assessing the buildings of the Estate having double string plate radiator systems. Assuming a likely cost reduction in the end users energy bills of 1% per each 1 °C reduction of return temperature, the optimisation led to obtain a possible discount in the end users energy bills of 14% with a possible yearly average return temperature of 41 °C, compared to the present 55 °C. Moreover, few improvements in the operation of the heat network were proposed. It was assumed to operate the buildings with underfloor heating systems (UFH) with average supply and return temperatures of 40/30 °C, whereas the ones with plate radiators with the optimised temperatures of 81/41 °C. The results shown that an overall average return temperature of 35.6 °C can be achieved operating the heat network as suggested. This corresponds to a decrease in the average return temperature of 18.6 °C compared to the present condition and to a reduction of 10% in the distribution heat losses. Finally, the lower average return temperature achievable would guarantee a better condensation of the flue gases, improving the overall efficiency of the biomass boiler. This was quantified as a possible reduction of fuel consumption of 9% compared to present conditions.

List of Publications

- Michele Tunzi, Dorte Skaarup Østergaard, Svend Svendsen, Rabah Boukhanouf and Edward Cooper. **Method to investigate and plan the application of low temperature district heating to existing hydraulic radiator systems in existing buildings**, *Published in Energy. July 2016*

- Michele Tunzi, Rabah Boukhanouf and Edward Cooper. **A Carbon Neutral Small Scale District Heating**, *14^th International Conference on Sustainable Energy Technologies. Nottingham (UK). September 2015*

Acknowledgments

I would like to deeply thank my supervisors, Dr. Rabah Bouhkanouf and Dr. Edward Cooper, for their support and guidance during my PhD but in particular for trusting the idea of this project since the beginning without any reserve.

A special thank to Mo for his enthusiasm and passion, which was a source of inspiration during these years. To Sasie Ltd and its team because it is Sasie Ltd who partially funded my project and gave me the opportunity to work on the interesting UK case study.

I cannot stop being grateful to Prof. Svend Svendsen. For his support, help and capacity of steering me in the right direction. My PhD would not have been the same! The period at DTU is unforgettable and I felt part of the crew and what a crew guys! It was pleasure to meet and work with Hongwei, Dorte, Maria, Xiaochen, Gunnlaug and with the two crazy guys Anton and Kevin who also shared crazy nights with me in the office.

A big thank to Tony and Helen, Steven and Sue, for being so sweet and helpful while connecting sensors, measuring temperature, essentially invading their own spaces. I really appreciate that.

Absolutely I cannot forget the guys of SRB and MGH who have shared the painful path until the end. We mastered our skills in everything, from Matlab and Simulink up to coffees, psychology, football and much more. What do we know at the end? Nothing, nothing at all. But that's the all point of research. To David and Vasilis the two big mates of this journey.

To Bexzabeide for sharing the long journey and for feeling the same difficulties especially in the last months. My return to Notts would have been much much more complicated without you. The taste of mezcal will be completely different that day.

To Gianluca who, despite the years, the persons and places is always there, no matter where I turn or where I sail to. We did not get rich with the model yet, but science will reward us for the effort one day!

To Ezio, Anna and Mario who represent my beloved Itaca. Itaca gave me the trip though, without asking anything back, and what a trip! To Melina, although she would not really get the sense of this, as she is the materialisation of my roots. There is no journey without knowing where you came from.

To Dori because NONE of this would even remotely happen without you on my side, giving me your unconditional support during the journey. You were my Muse!

Contents

List of Figures

List of Tables

List of Acronyms and nomenclature

- DH: District heating
- LTDH: Low-temperature district heating
- LMTD: Logarithmic mean temperature difference (°C)
- $LMTD_0$ Logarithmic mean temperature difference at design conditions (°C)
- ΔT: temperature difference between supply and return temperature
- TRV: Thermostatic radiator valve
- SH: Space heating
- DHW:Domestic hot water
- UFH: Underfloor heating
- ϕ: Heating power at operating temperatures (W)
- ϕ_0:Nominal heating power at design conditions (W)
- n: Radiator exponent
- $\dot{m}$: Mass flow rate (kg/h)
- $\dot{m}_0$: Max mass flow rate (kg/h)
- c_p: Specific heat capacity of water (J/kg °C)
- T_S: Supply temperature (°C)
- T_{S0}: Supply temperature at design conditions (°C)
- T_R: Return temperature (°C)
- T_{R0}: Return temperature at design conditions (°C)
- m_f: mass of fuel (tonne)
- CV: biomass calorific value (kWh/kg)
- eta_b: boiler efficiency (%)

Chapter 1

Introduction

1.1 Background

The background of this research project was related to the long-term objective to obtain a fossil fuel free society and guarantee energy security without compromising the environment and quality of life for the future generations.

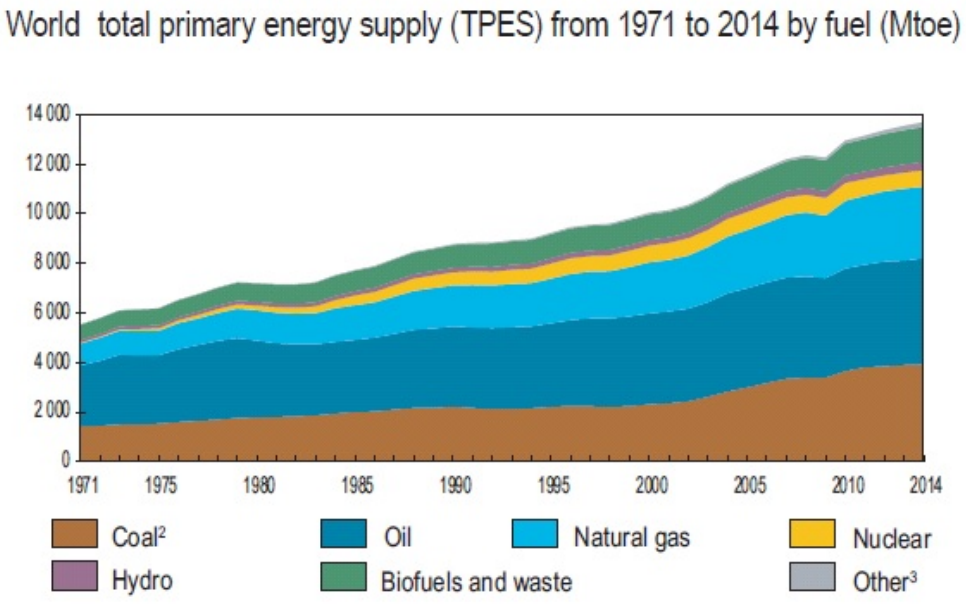

Figure 1.1: World total primary energy supply [1]. 1. World includes international aviation and international marine bunkers. 2. In these graphs, peat and oil shale are aggregated with coal. 3. Includes geothermal, solar, wind, heat etc.

The constant demographic growth and the increased demand for goods resulted in a consistent increase of the total energy supply over the last decades as presented in Figure 1.1. Although significant technical improvements have been achieved in the energy generation and distribution, improving the efficiency of traditional technologies as well as helping the penetration of renewable energy sources, at present conditions fossil fuels still account for 86% of the total primary energy supply as illustrated in Figure 1.2.

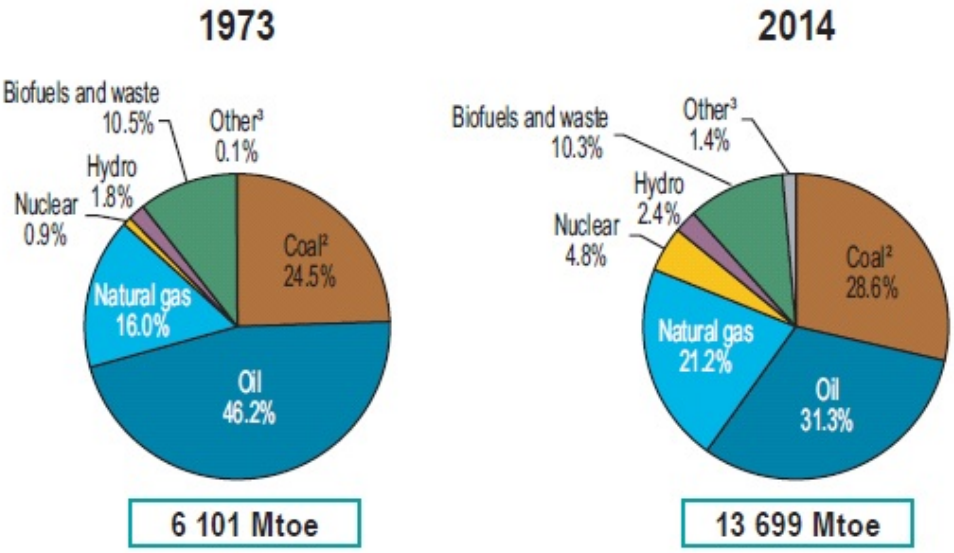

Figure 1.2: Fuel share of world total primary energy supply [1]. 1. World includes international aviation and international marine bunkers. 2. In these graphs, peat and oil shale are aggregated with coal. 3. Includes geothermal, solar, wind, heat etc.

Moreover, the energy consumption, as presented in Figure 1.3 for 2015, varies consistently in magnitude according to the specific geographical area considered, highlighting an unbalanced distribution.

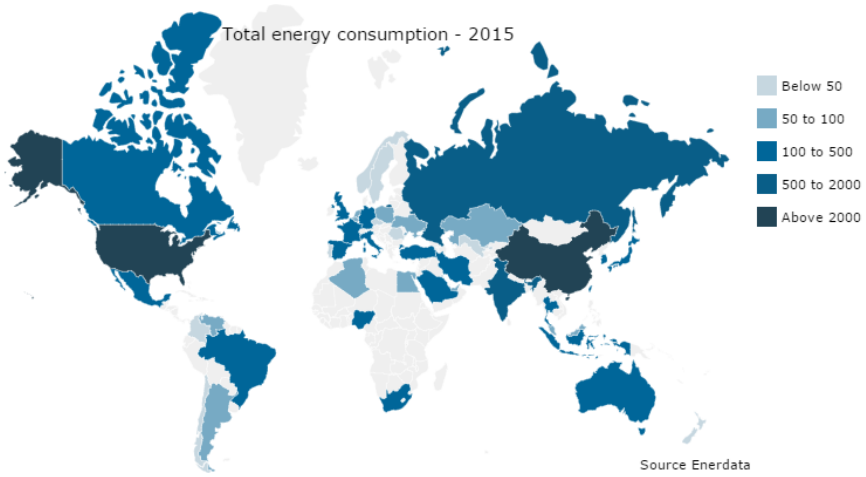

Figure 1.3: Energy consumption 2015 [2]

Similar trend has been experienced in the CO_2 emissions from fuel combustion as presented in Figure 1.4. It should be noted that, similarly to the total energy supply pattern — see Figure 1.1, the only drop experienced was related to the global economical crisis happened between 2008 and 2010.

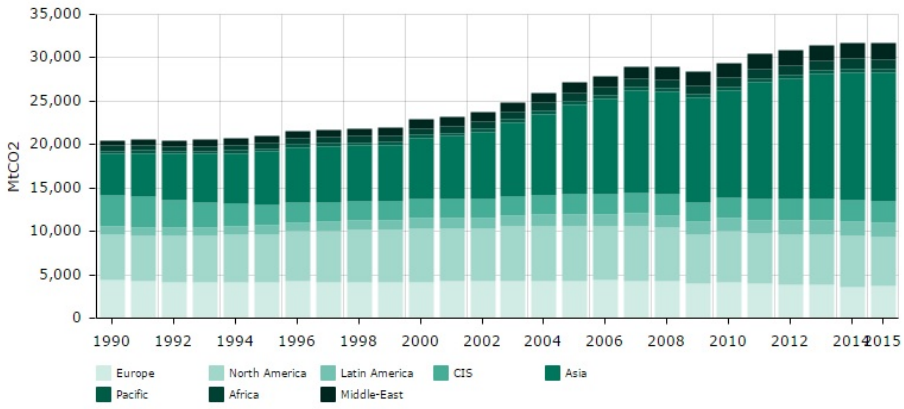

Figure 1.4: CO_2 emissions from fuel combustion [2]

As described in this IPCC publication [3] and reported in Figure 1.5 "Anthropogenic greenhouse gas emissions have increased since the pre-industrial era, driven largely by economic and population growth, and are now higher than ever. This has led to atmospheric concentrations of carbon dioxide, methane and nitrous

oxide that are unprecedented in at least the last 800,000 years. Their effects, together with those of other anthropogenic drivers, have been detected throughout the climate system and are extremely likely to have been the dominant cause of the observed warming since the mid-20th century".

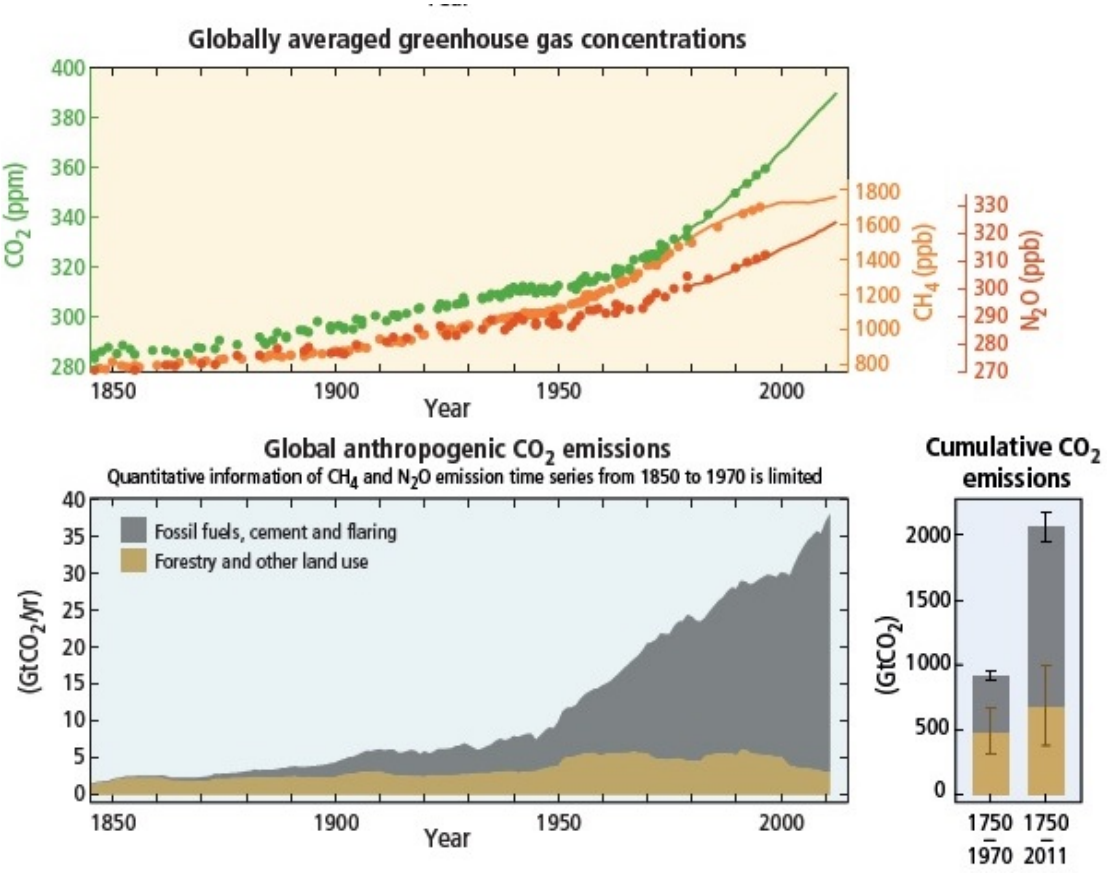

Figure 1.5: Top graphs describes atmospheric concentrations of the greenhouse gases carbon dioxide (CO_2, green), methane (CH_4, orange) and nitrous oxide (N_2O, red) determined from ice core data (dots) and from direct atmospheric measurements (lines). The global effects of the accumulation of CH_4 and N_2O emissions are summarised on the side. Bottom graph presents global anthropogenic CO_2 emissions from forestry and other land use as well as from burning of fossil fuel, cement production and flaring. Cumulative emissions of CO_2 from these sources and their uncertainties are shown as bars and whiskers, respectively, on the right hand side [3]

Future forecasts, as presented in Figure 1.6, highlight a likely change in the mean surface temperature in the range of 0.3 to 0.7 °C for the period between 2016–2035, while for the period up to 2100 this would depend from the assumed "Representative concentration pathways" (RCPs) scenarios. These in fact make

projections based on the level of GHG emissions and atmospheric concentrations, air pollutant emissions, land use and climate variability and in the worst scenarios (RCP 6.0 and 8.5) the change in the mean surface temperature could potentially exceed 2 °C.

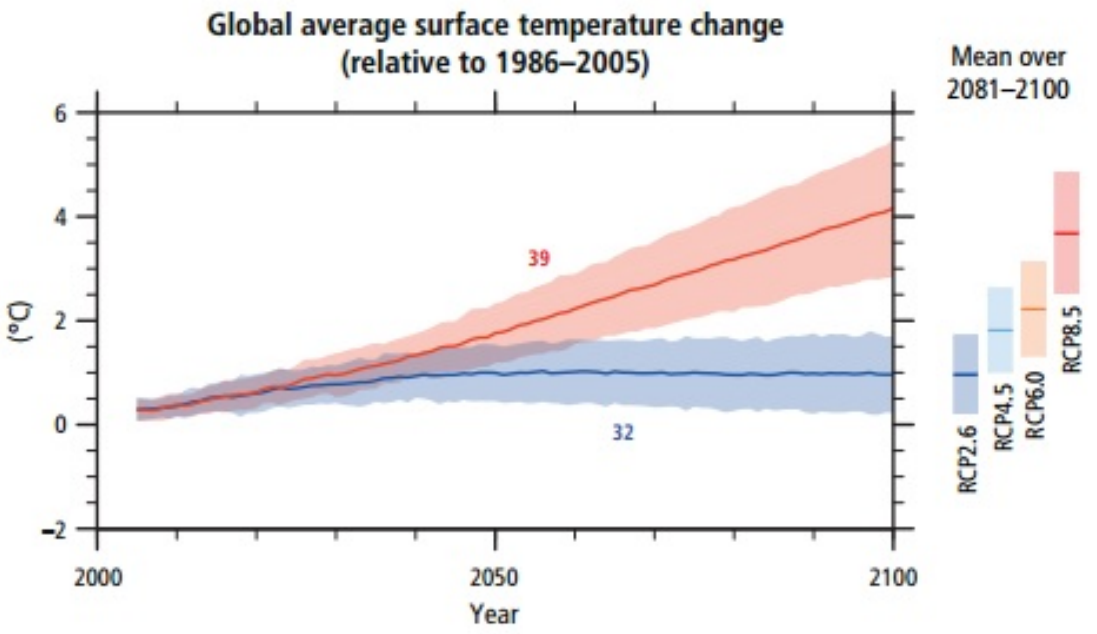

Figure 1.6: Global average surface temperature change from 2006 to 2100 as determined by multi-model simulations. All changes are relative to 1986–2005. Time series of projections and a measure of uncertainty (shading) are shown for scenarios RCP 2.6 (blue) and RCP8.5 (red). The mean and associated uncertainties averaged over 2081–2100 are given for all RCP scenarios as coloured vertical bars at the right hand side of the panel [3]

From this perspective, in the EU households, heating for space heating (SH) and domestic hot water (DHW) consumes 79% of the total final energy use (192.5 Mtoe), representing one of the largest carbon emitting sectors of the economy [4]. As a consequence, decarbonising the heat sector is being considered central to the EU energy policy agenda to foster a carbon neutral society and achieve the reduction in the greenhouse emission of 40% and 80% by 2030 and 2050 respectively to the level of 1990 [5–7]. Currently, heat supply in buildings in the EU is mainly provided by individual heat sources installed in buildings or alternatively

through district heating (DH) networks. The latter are widely used in Scandinavian, Eastern European countries and Russia. Driven by the need to use low carbon heat sources, the challenge is to meet SH and DHW demand with low temperatures. This would improve the overall efficiency of heat generation and support the integration of renewable sources.

1.2 Motivation and contribution to knowledge

There is an increased interest in energy sustainable and resilient communities using local heat and power generation sources. Low temperature district heating (LTDH) networks will form part of future solution to foster a sustainable society, augment local renewable energy penetration and support the decarbonisation of the heating sector in UK and EU. Several technical and economical questions need to be addressed to fully implement LTDH within the UK and EU energy market to both new and existing building stock. These questions can be summarised as follow:

- How can new and existing buildings be connected to LTDH?
- To what extent can temperatures be lowered?
- What is the economical impact of lower supply and return temperatures to both DH companies and end users?
- How do optimal operating temperatures of space heating systems vary according to the different DH networks?

The core of the investigation in the field in the last few years has been focused on the application of LTDH to community scheme mainly based on low energy

buildings. There is instead a research gap about the adoption of existing space heating (SH) and domestic hot water (DHW) systems to be operated with low temperatures. The work carried out in this thesis advances the knowledge in the field of LTDH in general developing an alternative method to investigate and plan the application of LTDH to existing buildings in particular. This is achieved by investigating an optimisation strategy that defines the best combination of supply and return temperatures to operate existing hydraulic radiators, the most common heat emitting element in EU buildings.

1.3 Aims and objectives

The main aim of the work developed in this thesis was to identify the optimum supply and return temperatures to operate DH networks and heating systems in buildings. An alternative methodology was developed to investigate and plan the implementation of low temperature district heating (LTDH) to existing buildings with plate radiators. This was obtained by expressing the heat demand as a function of logarithmic mean temperature difference (LMTD) between the water temperature in the hydraulic radiator and that of the heated building zone. The results of the investigation are expressed as an average reduction in LMTD over the heating season compared to the baseline design conditions. The needed LMTD, to satisfy the heat load, can be reached by numerous combinations of supply and return temperatures to the radiator. The optimum combination of supply and return temperatures supports maximum impact on both the end users' bills and heat network operator energy costs. This work achieved the following key research objectives:

i. Investigate and plan the application of LTDH to existing buildings

ii. Define the optimisation problem based on objective functions and constraints to identify the optimum operating temperature for existing plate radiators

iii. Customise the optimisation according to the economic impact that lower supply and return temperatures have in different DH networks

iv. Test the performances of the developed methodology to a Danish and UK case studies

1.4 Industrial and academic collaboration

This research project involved collaboration of academic and industrial partners. The industrial partner SASIE Ltd, a SME based in Nottingham specialised in renewable energy installations, partly supported the technical and financial investigation of the project. This support was related to investigate the potential of the introduction of LTDH within the UK energy market, using a small scale DH network case study located in Nottinghamshire. The initial work was focused on developing a computer model using MATLAB software to optimise the operation of the DH network. However, the project objectives were realigned with the industrial partner's business focus on demonstrating the applicability of LTDH in Nottingham. Hence, the focus of this project changed and moved to the definition of an alternative methodology to investigate and plan the connection of existing buildings with plate radiators to LTDH. The work also benefited from the academic collaboration with the department of Civil Engineering of DTU (Technical University of Denmark), recognised worldwide for over 30 years of research in the

field of DH technology. This collaboration culminated in joint research work and publications.

1.5 Thesis outline

This thesis is structured into seven chapters and represented schematically in Figure 1.7. After the introduction given in Chapter 1, the first part comprises Chapter 2 and 3 which extensively review DH and LTDH technology. In addition, Chapter 4 illustrates in details the methodology developed in this research project, while Chapter 5 and 6 describe the two case studies and present the results obtained. Finally, Chapter 7 summarises the discussions, conclusions and future work.

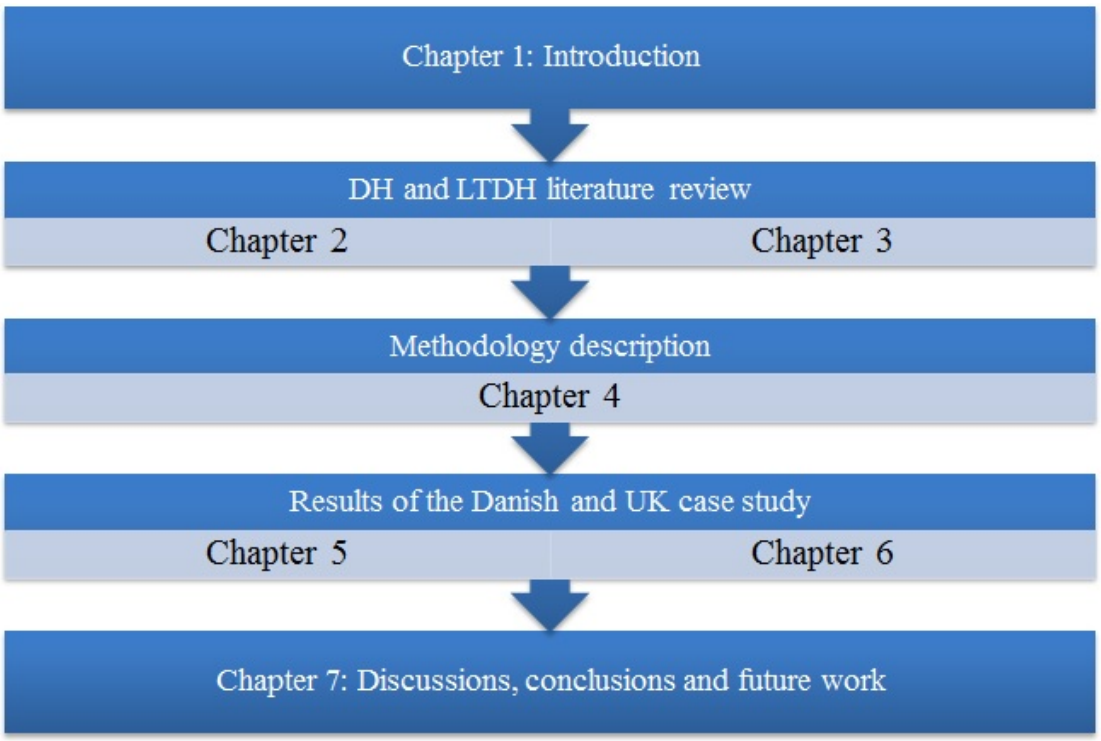

Figure 1.7: Structure of the thesis

Chapter 2 and 3 review the DH and LTDH technology, illustrating their potential role in the transition towards a low carbon society. Firstly, an overview

of the actual DH market is provided focusing on the European context, followed by a detailed description of the actual and future perspectives for DH in the UK heating market. Next, the new generation of DH is introduced, highlighting its potentials to fully exploit the renewable and low carbon heat sources due to the operation with low temperatures. In addition, the challenges of operating heat networks and existing heating systems with load dependent temperature with a target of 50/20 °C are deepened, emphasizing this as the actual focus of the research in the field.

Chapter 4 introduces the method developed to calculate the optimum temperatures to operate existing heating systems based on plate radiators. The methodology assesses the capability of the radiators to be operated with lower temperatures introducing an optimisation problem which takes into account the economic impact that lower supply and return temperatures have to both DH networks and end users.

Chapter 5 presents the results for a typical Danish single-family house from 1930s used as case study. The methodology was applied to different scenarios, including double and single string plate radiator systems. The capability of these systems to be operated with lower temperatures was assessed as well as the influence of different DH systems and the economic impacts of lower supply and return temperatures in the definition of the optimal operating temperatures.

Chapter 6 describes the results related to the analysis of the UK small scale

DH network. The analysis began with the calculation of the optimal operating temperatures of the buildings with double string plate radiators connected to the network. The second part of the investigation presents the results obtained from the simulations of the heat network and compares the outputs achieved operating the system at present and optimised conditions. The results were quantified in the possible improvements achievable in the heat generation and distribution according to new operating temperatures calculated.

Chapter 7 concludes this thesis by analysing the results derived from the application of the developed method to the investigated case studies. It also critically discusses the results obtained and recognises new area of research as future expansion of the work developed.

Chapter 2

District heating technology

2.1 Introduction

This chapter begins with a general introduction to the district heating (DH) technology and its potential role in the transition towards a low carbon society. This is presented by highlighting the high flexibility of this technology to connect and take advantages of a number of different heat sources, including heat recovery processes and renewables.

A review is provided about the present DH market, illustrating the development of the technology in some of the European countries, with particular emphasis to the experience of Denmark as leader in the sector. Next, the future goals of the European commission are described in terms of emissions limits and strategies for the heating market, including a selection of studies presenting possible scenarios with different level of penetration of renewables and DH.

UK has been recognized in the last few years as an emerging market for DH technology. A review of UK future perspective for DH as presented in DECC strategies is also undertaken as part of this investigation. A number of barriers affecting the development of DH, including technical, economical and policy limitations are discussed.

2.2 District heating background

The district heating technology is a particular way of producing managing and delivering heat energy to end users. The core idea is to manage different technologies and develop synergies between production and supply of heat. Differently from individual heat solutions, DH systems allow to distribute energy on community base, which can include neighbourhoods, villages or large cities. Heat is produced by taking advantage of low-cost heat generation or heat recovery and it is moved by distribution pipes using steam or pressurized water as carrier. Historically, the first generation DH network was built in US in the 1880s, using steam as energy carrier. Typical supply temperatures in steam based DH application are consistently above 100 °C. Although steam does not require to be pumped and has a higher energy density, the technology eveolved into the second generation of DH in the late 1930s where pressurized water was introduced as heat medium. Supply temperatures in the second generation DH were still above 100 °C. According to Harvey [8], the main advantages of using pumped hot water directly for heat distribution include:

- Improvement in power generation efficiency where steam turbines are used

- lower distribution heat losses
- lower maintenance costs
- longer distances pipe network
- no pipe corrosion
- easier to meter and store hot water
- simplified equipment to delivery heat to end-users
- possibility of using low cost plastic pipe
- require electricity to pump and circulate hot water

The third generation of DH, known as "The Scandinavian DH technology", started in the late 1970s as a response to the oil crisis to secure energy and remove the dependence from fossil fuels at national level. The supply temperatures of the hot water is often below 100 °C [9]. This type of DH is still present in many countries, although the DH technology is now evolving towards the future low-temperature district heating (LTDH), known as the forth generation (4GDH). This is the focus of the present research in the field, aiming to operate the future networks with target supply and return temperatures of 50/20 °C. A detailed overview of the concept of 4GDH is given in Chapter 3. Generally, DH technology can be divided into four major areas: heat supply, distribution network, end user substation and heating systems [10]. Figures 2.1 shows a schematic view of a typical distribution heat network with heat generated at the heat supply centre and distributed through insulated pipes. Heat is then delivered to end users

through hydraulic interface unit connecting each building to the main network as presented in Figure 2.2.

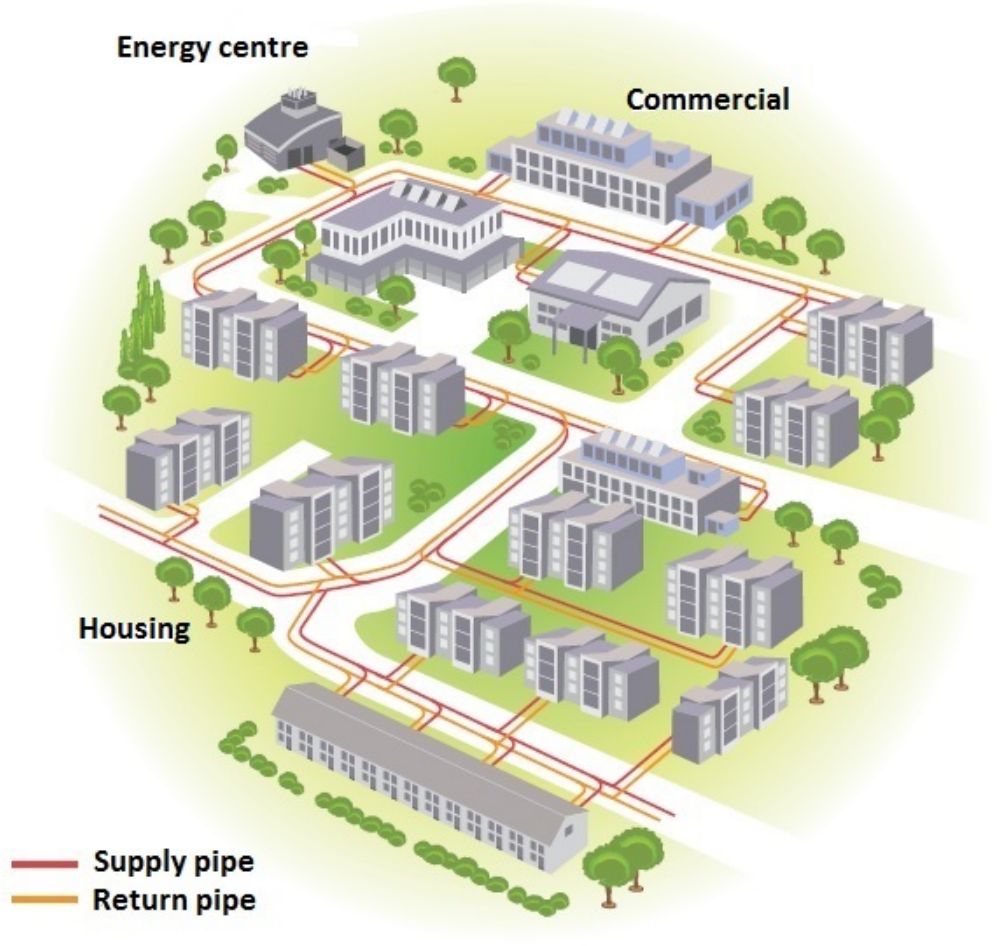

Figure 2.1: Schematic view of a DH system: generation, distribution and end users [11]

Various heat sources and fuels can be used to generate heat for DH including CHP plants burning fossil fuels, waste, biomass, heat recovery, geothermal and renewable sources using large solar field [8, 12]. The high flexibility of the system and the capacity of combining several heat sources is not only convenient for energy management, due to the fast response to different loads, but also because it improves significantly the energy efficiency of heat generation, making it competitive compare to individual/local solutions.

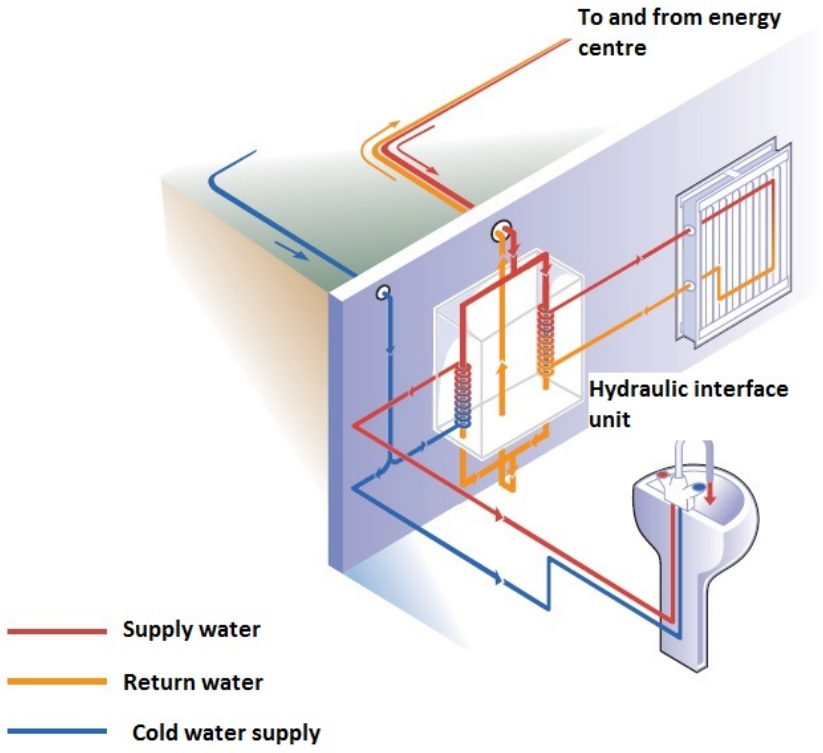

Figure 2.2: Schematic view of customer substation: interface between distribution network and end users heating systems [13]

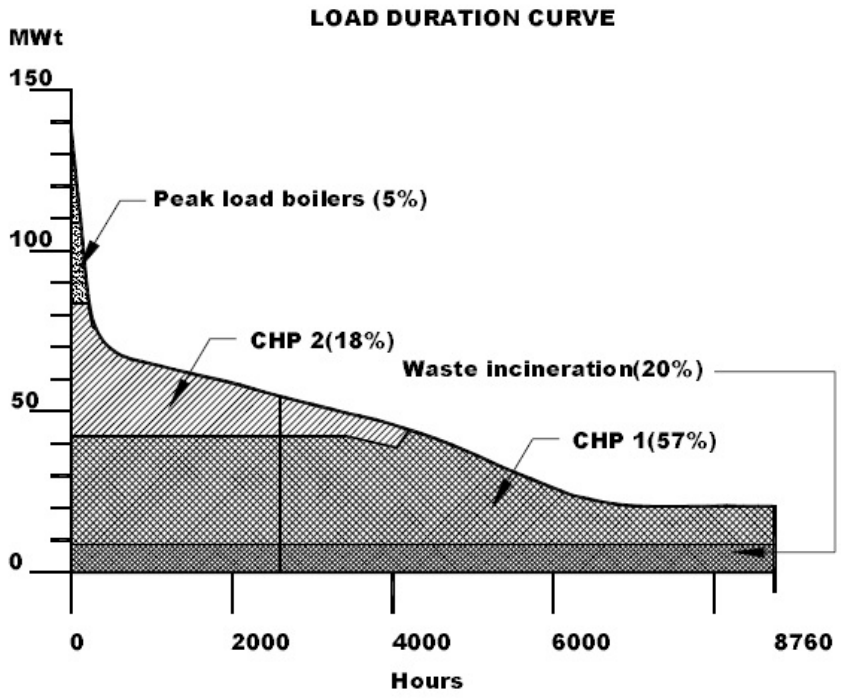

Figure 2.3: Example of load duration curve indicating the proportion of different heat sources [14]

An example of the integration of different heat generation sources in a load duration curve is presented in Figure 2.3. This shows that the efficient and cheap energy is produced by CHP plants and waste incinerators covering the base heat load of the system; whereas, only when peak load demand occurred, the more expensive boilers are switched on.

A recent study [15], comparing at city level "business as usual" and "modern district energy system" shows, as presented in Figure 2.4, that community schemes are more competitive technically, economically and environmentally. In fact, the same energy demand could be covered by the district energy system with a reduction of 51% in total primary energy consumption compared to the reference scenario. This would be possible due to a better exploitation of CHP technology and the integration of renewable energy sources. The overall benefits can be summarised as follow :

- increased energy security and reduced dependence on fossil fuel
- reduced energy import and fuel consumption
- ability to better use of renewable energy sources
- reduced greenhouse gas emissions

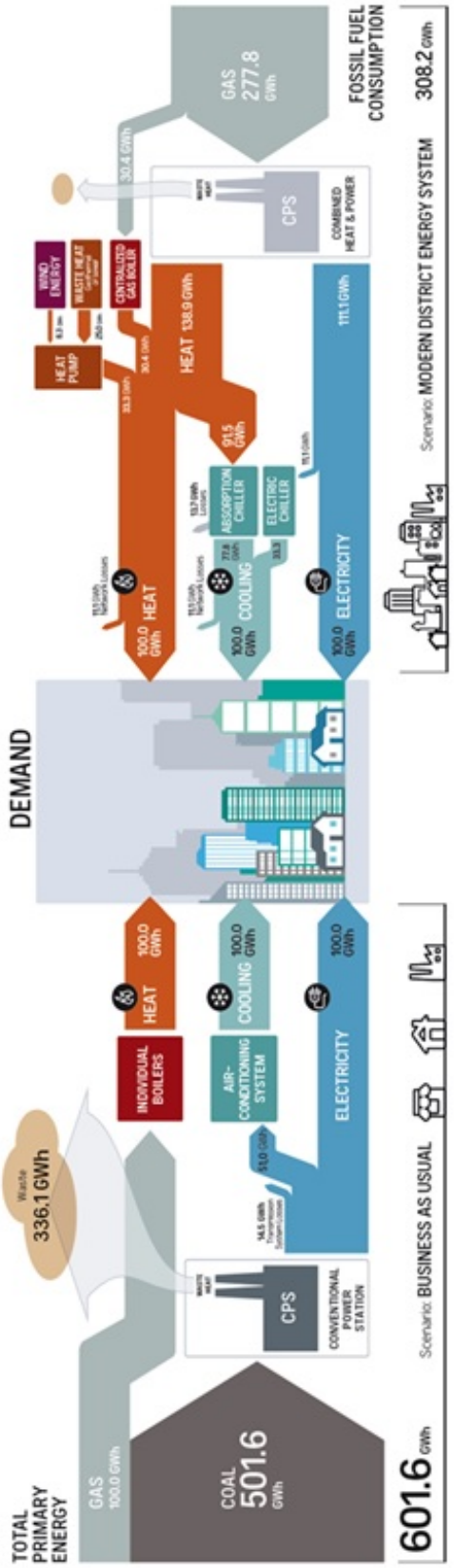

Figure 2.4: Sankey diagram of business-as-usual heat/electricity/cooling system against modern district energy system [15]

The DH technology is a capital intense technology and some of key costs are associated to the distribution network and the connections to end users. The distribution network is composed of pre-insulated buried pipes for supply and return line. Heat is transferred from the DH supply line (primary side) through the substation to the heat carrier of the end user heating system (secondary side) [10, 11]. The potential saving achievable by more effiecient heat generation can be offset by the aforemention costs, hence keeping these as low as possible is vital for the competitiveness of DH technology [16]. The associated costs of the infrastructure are a function of the linear heat density as depicted in Figure 2.5. The *linear heat density* is the ratio of the annual heat delivered to the consumers and the trench length of the DH network serving the area [13]; hence, the higher the linear heat density, the lower the levelised cost of the network and connections to end users [15] as presented in Figure 2.5. This highlights that dense areas and multi-storeys buildings all characterised by higher density and heat demand are more attractive from the DH point of view.

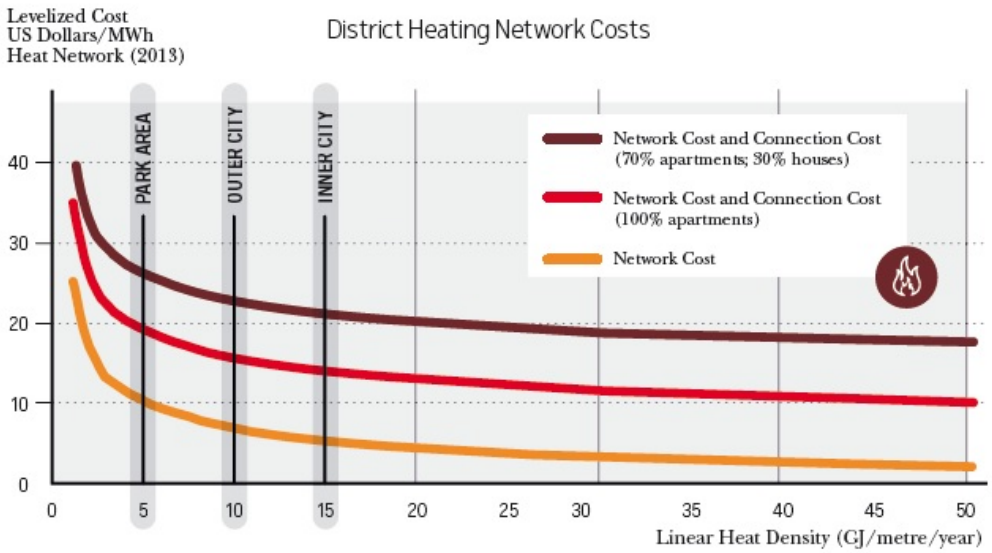

Figure 2.5: Network costs for district energy [15]

2.3 Present European district heating market and future outlook

The challenging objectives of decarbonising the EU economy and achieving the long term goal of an energy system completely based on renewable sources was the key aspect in the definition of the EU commission policy and strategy for the next three decades. In the short term vision, the EU commission agreed on the "20-20-20" package solutions, to cut the green house gases (GHG) emissions by 20% compared to 1990 levels, to increase by 20% the energy efficiency and to produce 20% of total energy consumed by renewable energy sources [6]. Further agreements were formalised by the EU member States with the envisaged strategy in the long run to cut the GHG emissions by 85-90% compared to the 1990 levels [7].

Heating and cooling in buildings and industries accounts for almost 50% of the total energy consumption in EU countries and it is one of the largest carbon emitting sectors [17]. The final energy consumption for heating and cooling is presented in Figure 2.6 for all EU member States, showing higher DH shares in Scandinavian and Eastern European countries. A recent report published by the EU commission highlights heating and cooling sector as crucial to tackle the decarbonisation of the EU economy and DH as a key technology in the transition towards a low carbon society [18].

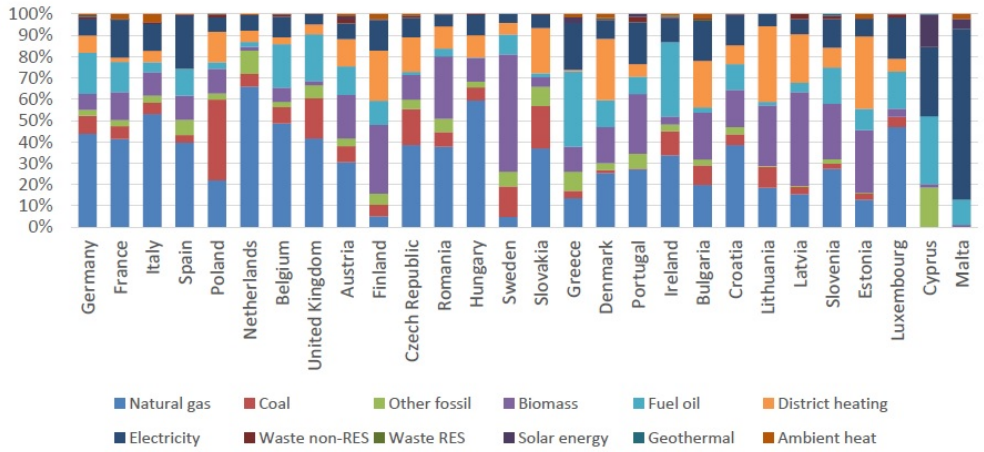

Figure 2.6: Final energy consumption for heating and cooling, 2012 [18]

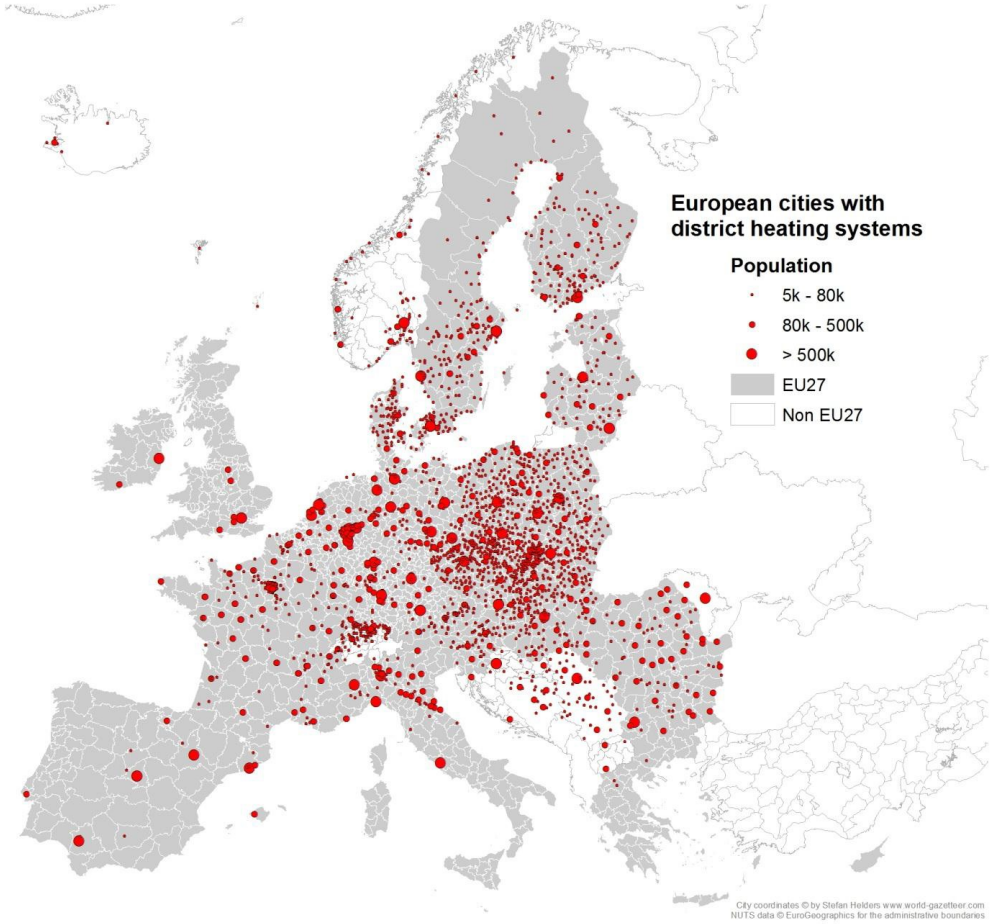

Figure 2.7: District heating systems in Europe by city size and for cities having more than 5000 inhabitants. The map shows 2428 cities with 2779 systems [19]

DH systems actually meet 12% of the total European heat demand for residential buildings and service sector as well as 9% of the industrial one with total turnover of approximately 30€ billion per year and an overall network length of 200.000 km [19]. An overview of the geographical DH networks distribution is presented in Figure 2.7 where it can be noted the non-uniformity across Europe.

Scandinavian and Eastern European countries have by far the largest DH penetration and in particular Denmark (63%) and Latvia (65%) are among the nations with the highest share, as depicted in Figure 2.8. Historically DH development took advantage by the exploitation of CHP technology and in fact Denmark, worlwide leader in the sector, has at present situation approximately 70% of the supplied heat in DH produced by CHP plants. [10, 15, 20].

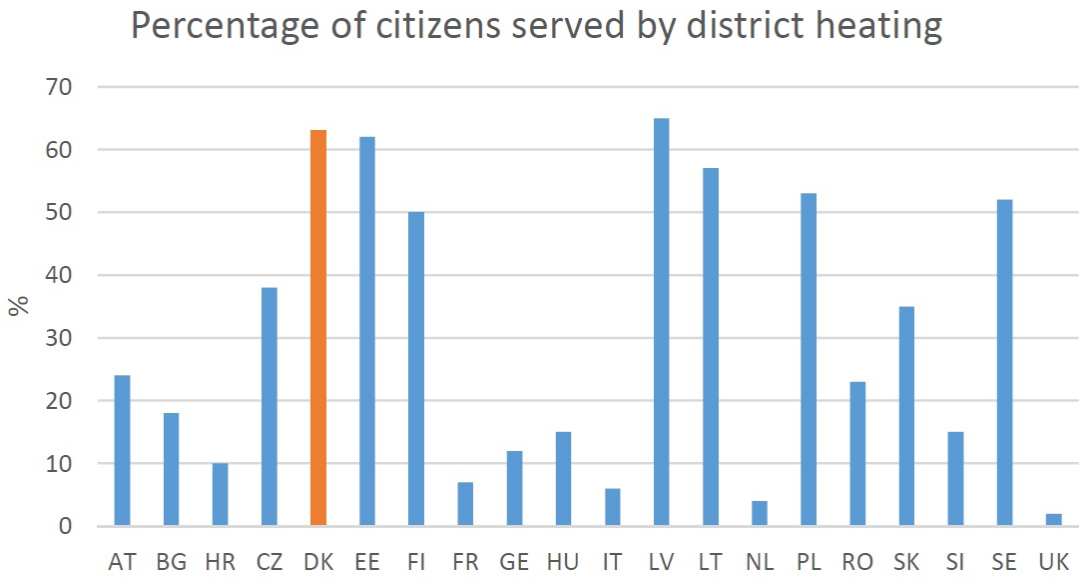

Figure 2.8: Percentage of citizens supplied by DH, 2013 [20]

Denmark is expecting to achieve 50% of the electricity consumption by 2020 covered by wind energy and to have by 2050 the national energy demand entirely

covered by renewable energy sources. In order to meet the challenge, as reported by the Danish Energy Agency (DEA) [20], due to his flexibility the DH technology will have a key role to face the challenge. The support in the integration of the expected high share of wind energy production can be summarised in three main areas:

- **Heating storage**. At time when electricity demand can be covered by wind energy, DH plants can reduce their CHP production and heat can be supplied from heating storages
- **Electric boilers and heat pumps**. DH plants can use excess of wind electricity to run electric boilers and heat pumps
- **Bypass of power turbines**. In case of excess of electricity in the system, CHP plants can produce heating only

Lund and Mathiesen [21] described the design of the future Danish energy sytem based on 100% renewable energy sources and its efficient operation. The results are presented for the overall energy market in Figure 2.9 and the main focus for the heating sector was envisaged in the concurrent strategies to expand the penetration of DH – increasing the exploitation of CHP, renewable energy and the capability to recover waste heat – and reduce the overall heat demand at the end users level.

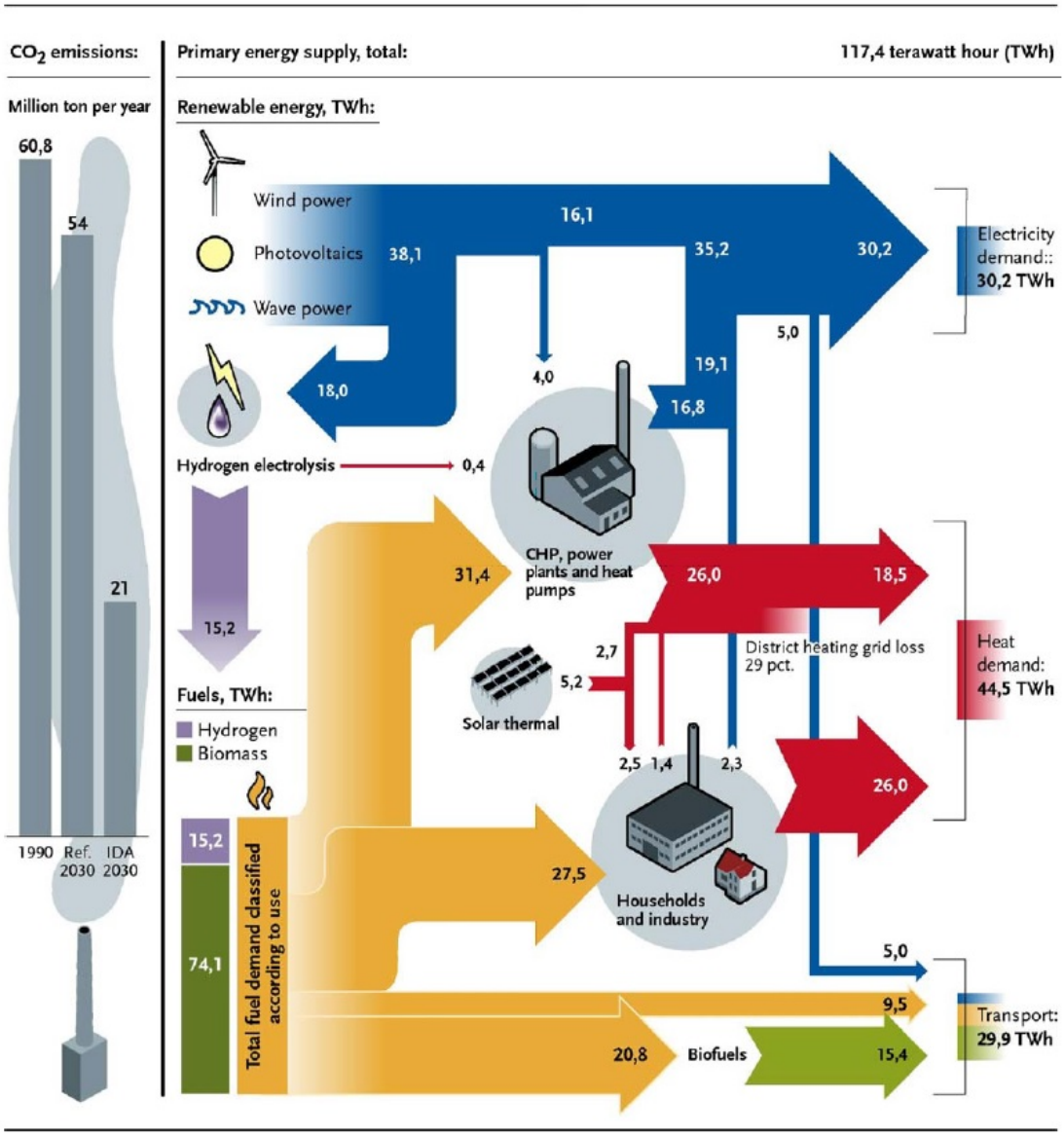

Figure 2.9: Flow Diagram of the 100% renewable energy system [21]

Likewise, the European heating sector has been studied by assessing several scenarios with different level of DH and renewable energy penetration. It was evaluated the relative effect on the overall primary energy consumption and CO_2 emissions. The performed analyses compared present situation with medium and long term perspective – 2030 and 2050 – by considering as reference scenario the "Current Policy Initiative" (CPI) and DH penetration at 10% [19]. As clearly illustrated in Figure 2.10, the effect of higher DH shares in the EU heating market

could potentially generate a consistent reduction in primary energy consumption and CO_2 emissions compare to the reference scenario for the heating building sector.

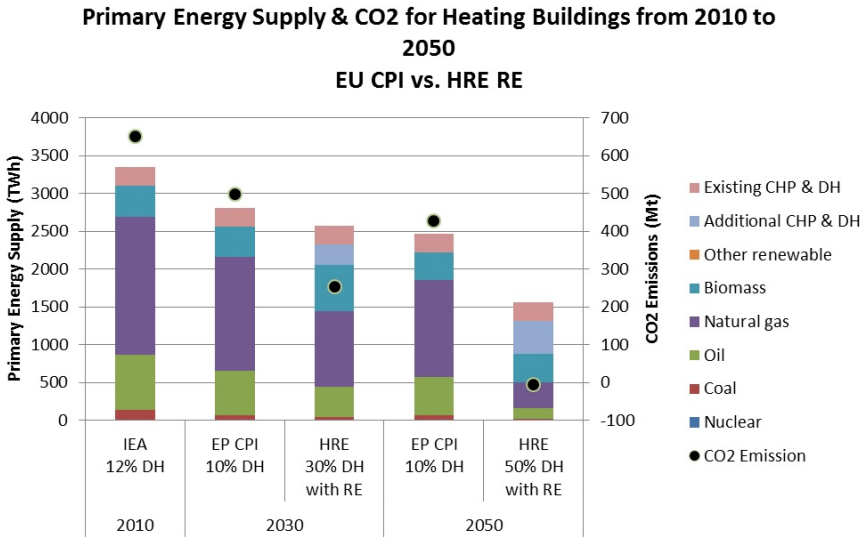

Figure 2.10: Primary energy supply and carbon dioxide emissions from hot water and the heating of buildings in the 2010, 2030, and 2050 EU27 energy system under a business-as-usual scenario and if district heating and CHP is expanded to 30% in 2030 and to 50% in 2050, in combination with the expansion of industrial waste heat, waste incineration, geothermal, and solar thermal heat for district heating [19]

2.4 District heating in the UK market

In line to the EU targets for CO_2 emissions, UK has outlined its own domestic emissions' targets through the "Climate Change Act", where a reduction of 50% and 80% to the 1990 carbon emissions level were set respectively for 2027 and 2050 [22]. Decarbonising the heat market, which consumes the largest portion of the total UK primary energy of around 44% [23], will be crucial to achieve the aforementioned targets and it became central in the UK political agenda. A detailed study commissioned by the Department of Energy & Climate Change (DECC) identified three main areas to tackle the challenge [24]:

- demand side management
- decarbonising heating and cooling supply in buildings
- decarbonising heat in industrial processes

In this direction, due to its flexibility and capacity of offering a faster and cheaper integration of renewable sources, DH was recognized as one of the key technologies in the transition towards a low carbon society for the UK heating market. The actual market share is about 2% and accounts for 1765 heat networks (75% are small networks) serving about 210,000 dwellings and 2000 commercial and pubblic buildings [25–28]. A detailed map of main existing schemes is presented in Figure 2.11. Historically, the presence of DH started in the 1950s, but only few schemes managed to be competitive in the UK heating market. A selection of the most relevant ones is provided:

- **Plinco DH Utility**. Established in early 1950s in London was serving a new housing development in Westminister. Heat is actually mainly produced by a gas-fired CHP plant [9]
- **Nottingham DH**. It is one of the most successful schemes in the UK. Heat is produced by waste incinerator CHP plant, serving 5000 households and 100 business. It forms part of an EU research project (Remourban), expanding the network into the Sneinton area [29, 30]
- **Birmingham DH**. The Birmingham DH includes two schemes built by using national fundings available through "Community Energy Programmes". Heat in both schemes is mainly produced by gas engine CHP units: 1.6 MW_e

(Broad Street scheme), 1.6 and 3 MW_e (East Side scheme). Additional gas-fires top up boilers and adsorption chillers are available on site [31]

- **Aberdeen DH**. The Aberdeen heat and power is a Scottish scheme which has been expanding since 1999 and now serving 2000 flats and 13 public building by taking advantage from CHP units [32]

- **Citigen DH**. The Citigen scheme was established in London and provide heating and cooling to major buildings of city of London (including barbican and Arts centre) using dual-fuel reciprocating engines [9]

- **Sheffield DH**. The Sheffield DH scheme delivers heat to 140 buildings around the city and makes use of a waste incinerator [33]

- **Southampton DH**. The Southampton district energy scheme (SDES)is a pioneering project, serving 45 energy users in the public and private sector, utilising as heat sources CHP, supplemented by geothermal energy and conventional boilers [34]

- **Coventry DH**. The DH of Coventry, operated by the Coventry District Energy Company (CDEC), buys heat from an energy-to-waste plant and delivers heat through a 6.6 km of network to end-users in the city centre [35]

- **Leicester DH**. The Leicester District Energy Scheme comprises a 7 km city network, with a further three smaller networks covering an additional 7 km in outlying areas. It provides energy-efficient heat from CHP plants to 2,800 homes, along with council offices, schools, De Montfort Hall and the University of Leicester [36]

- **Queen Elizabeth Olympic park DH**. Built in London it is the largest decentralised scheme in UK. It has a heat capacity of 45.6 MW from CHP plants serving venues, commercial buildings and residential properties [37]

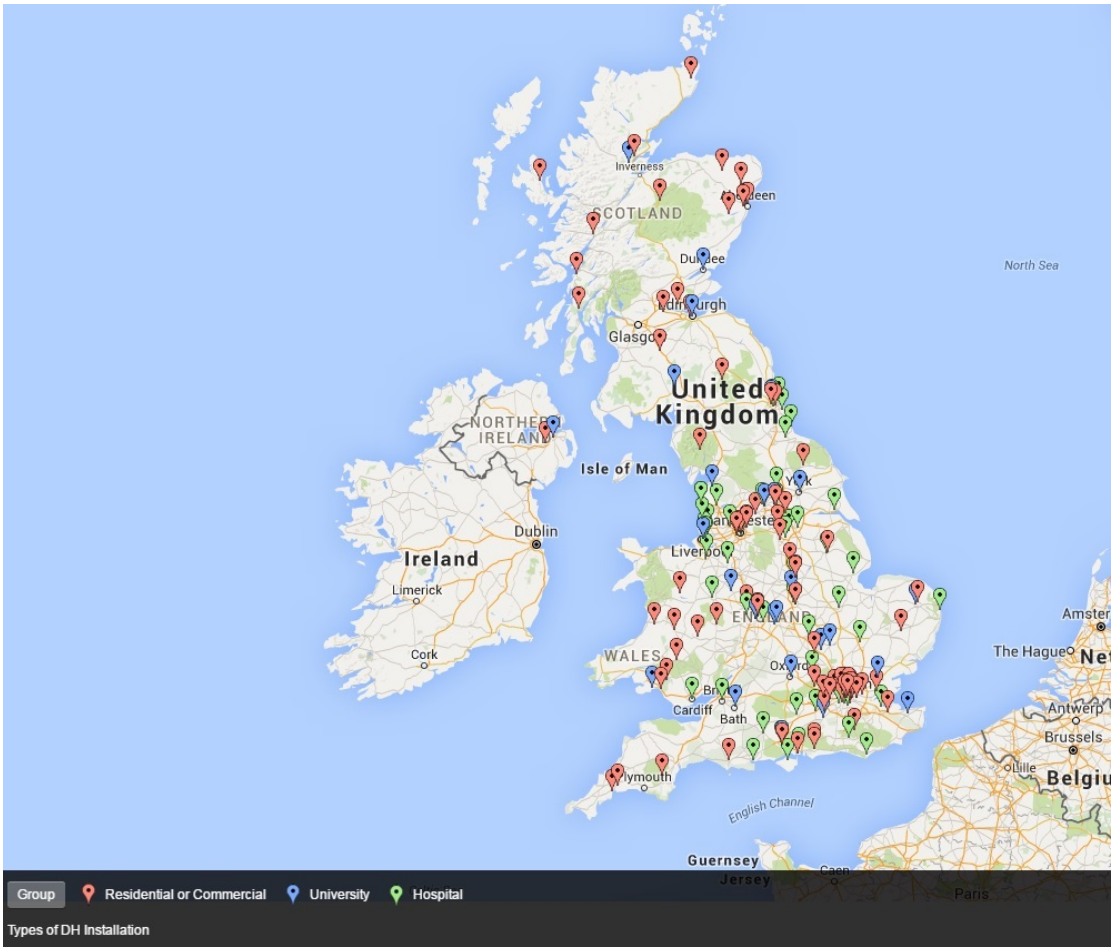

Figure 2.11: Existing UK district heating schemes [38]

Future forecasts instead, supported by the concurrent interest on increasing the CHP penetration, highlight how the DH technology could achieve respectively 14% and 43% of the UK heating demand in buildings in a cost effect way by 2030 and 2050 [23]. Hence, in order to enhance the development of DH in UK, it was recognised the necessity of improving the synergies between all the stakeholders involved. This is clearly described in Figure 2.12, where, due to the nature of DH technology, it is emphasised the importance of the engagement of local authorities

and central government with academia, industries and developers [26]. In particular, an interesting study for the UK [39], based on a qualitative analysis using the "Technological Innovation System", identified how local authorities will play a decisive role in the next years for the penetration of DH technology. They are in fact the subjects who will coordinate the different local organisations, allocating the areas and resources to develop the infrastructures and guaranteeing the connections to the DH networks of public buildings, large commercial areas and social housings. This is crucial because it would provide the base heat load for the DH systems, reducing costs and risks associated to this technology.

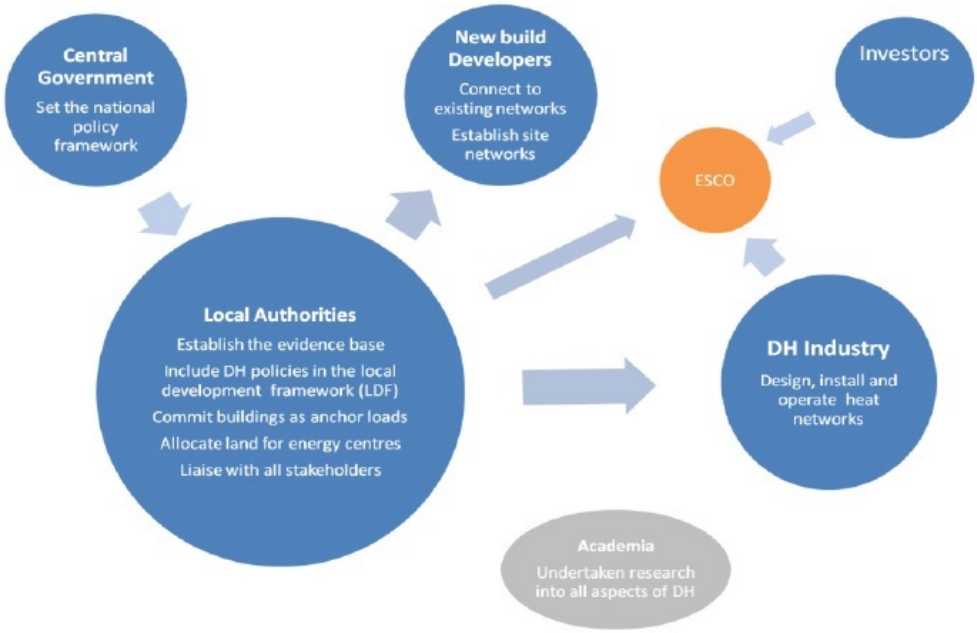

Figure 2.12: Development of district heating networks: flow chart showing principal stakeholders and the essential lines of communication between them [26]

As heat networks are going to play an important part within the future low carbon energy market in UK, there was the necessity to outline a common reference code of practise. To this extent, the release in July 2015 of the joint publication by

CIBSE and the "Association for Decentralised Energy" (ADE) *"Heat Networks: Code of practice for the UK"* was an important step forward to unify the requirements related to heat networks and define the minimum standards and best practise to ensure the quality and reliability of the future installations [40].

2.5 Barriers in the UK district heating development

The actual DH share in the UK heating market accounts for less than 2% and it did not reach large scale applications which could have guaranteed the possibility of taking advantage from low-cost heat sources and being competitive with other technologies. This was also the result of the UK energy strategy back in the 1970s. In fact, the large natural gas reserves in the North Sea and consequent cheap price led to individual gas boilers becoming the main heat source covering at present condition up to 85% of the total domestic heating demand [9]. Also, recent studies for UK identified the main barriers for the widespread deployment of the technology in order to outline the solutions to overcome the actual market limitations [9, 25, 26, 41–43]. These can be summarised as follow:

Financial risk and high capital costs

DH is a capital intensive technology due to high infrastructure costs. This is even more relevant for UK, where data show that DH infrastructure costs were 20% higher compared to more mature DH market – i.e. Northern European countries. This was mainly related to a lack of experience, ex-

pertise and standardisation of the processes. As a consequence, high discount rate of 10% was usually associated to this technology, reducing its competitiveness with other heat sources.

Technical limitations and lack of expertise

In the past, the combination of low thermal performance of houses with DH systems poorly installed seriously affected the reliability of the heating networks, which in some cases were also abandoned and replaced by individual gas boilers. This was also reflected into an evident gap in the technological development and in the policy framework compare to countries with more mature DH markets. However, the publication of the CIBSE and ADE code of practise for heat networks and the new interest of the heating sector in the political agenda is helping industry to cover the gap.

Lack of data and customer dissatisfaction

DECC reports that almost 75% of the existing residential networks are unmetered schemes. Also, there is a lack of data available in terms of energy consumption, price per kWh of heat and efficiency. The combination of all these factor ends with low transparency and uncertainties in the bill prices, which provokes dissatisfaction in the customers' experience with DH.

Local authorities and central government role

Local authorities and central government are the most important players into the mechanism of deploying DH in UK. Their role is on one hand to secure the necessary financial support to instigate the scheme and overcome the lack of knowledge. On the other hand, they have to protect customers

with a clear policy framework to ensure their rights, as well as guaranteeing a fair taxation, business rate and health safety by regulating allocation of areas and emissions limits.

2.6 Summary

An introduction to DH systems was highlighted in this chapter, providing main concepts and a detailed description of the evolution of this technology. The analysis covered the flexibility of DH to make use of low-cost heat sources, heat recovery and renewable sources, illustrating the potentials in the transition towards a low carbon economy.

A detailed overview was provided about the actual heating and cooling sector in the EU context and the relative policy framework. It was assessed the DH penetration in the EU energy market, presenting how DH already represents a robust technology in Scandinavian and Eastern European countries. To this extent, the case of Denmark among the others, was analysed more in details. In fact, Denmark is the leading country in the DH industry and part of the research work performed in this investigation and presented in Chapter 5 was related to a Danish case study.

Further analysis was presented for the heating and cooling market, focusing on both Danish and European future scenarios, illustrating the role of DH systems in the transition towards a low carbon economy and 100% renewable energy system.

The UK is recognised within the EU context as an emerging country for DH

development and it became central in the national political agenda as one of the key technologies to decarbonise the UK heating sector. A detailed description was provided about the current DH share and the future previsions according to latest DECC guidelines. Finally, it was presented an outline of the barriers for the UK energy sector that limited in the past the deployment, competitiveness and the reliability of DH technology.

This review identifies the background necessary to introduce the concept of LTDH, which is the core of the present research in the field — as reported in details in Chapter 3 — and links DH technology to the UK actual and future context as this was one of the main driver of the research work of this investigation.

Chapter 3

Low-temperature district heating

3.1 Introduction

This chapter starts with a description of the concept of LTDH, highlighting how the new generation of DH is aiming to exploit the full potentiality of renewable and low-temperature heat sources and face the challenge of supplying heat in the future energy market.

A review of current literature is provided in order to define the present works in the field, focusing on the implementation of LTDH for low-energy buildings to cover the heat demand for space heating (SH) and domestic hot water (DHW). Further details are included about the advantages of reducing working temperatures in the network both at generation and delivery point.

The analysis follows by introducing the challenge of integrating the LTDH to the existing stock of buildings, which was the main focus of this investigation as

presented in more details for the selected cases study in Chapter 5 and Chapter 6. In particular, existing heat elements for SH demand were analysed and it was illustrated the modelling performances of different types and their relative capability to be operated with low temperatures.

3.2 Description of the low-temperature district heating concept

District heating offers high flexibility for the integration of renewable heat sources, though still faces the technical challenge of matching different heat sources' supply temperature and demand. Driven by the need to use low carbon heat sources, the current focus is to develop LTDH systems (referred to as forth generation district heating 4GDH). One key design parameters in the development of LTDH is the reduction of supply and return temperatures. In mature Scandinavian DH markets, the standard average supply and return temperatures are 80/40 °C with heat distribution losses amount to about 20% [44]. The aim of LTDH is to achieve load dependent temperatures with a target of 50/20 °C. The overall concept and the comparison with previous DH generations is illustrated in the work of Lund et al. [45] and summarised in the infographics of Figure 3.1 . It is shown in fact that due to the technological improvements in the passage between each DH generation a corresponding reduction in the operating temperatures and an improvement in the overall efficiency were experienced.

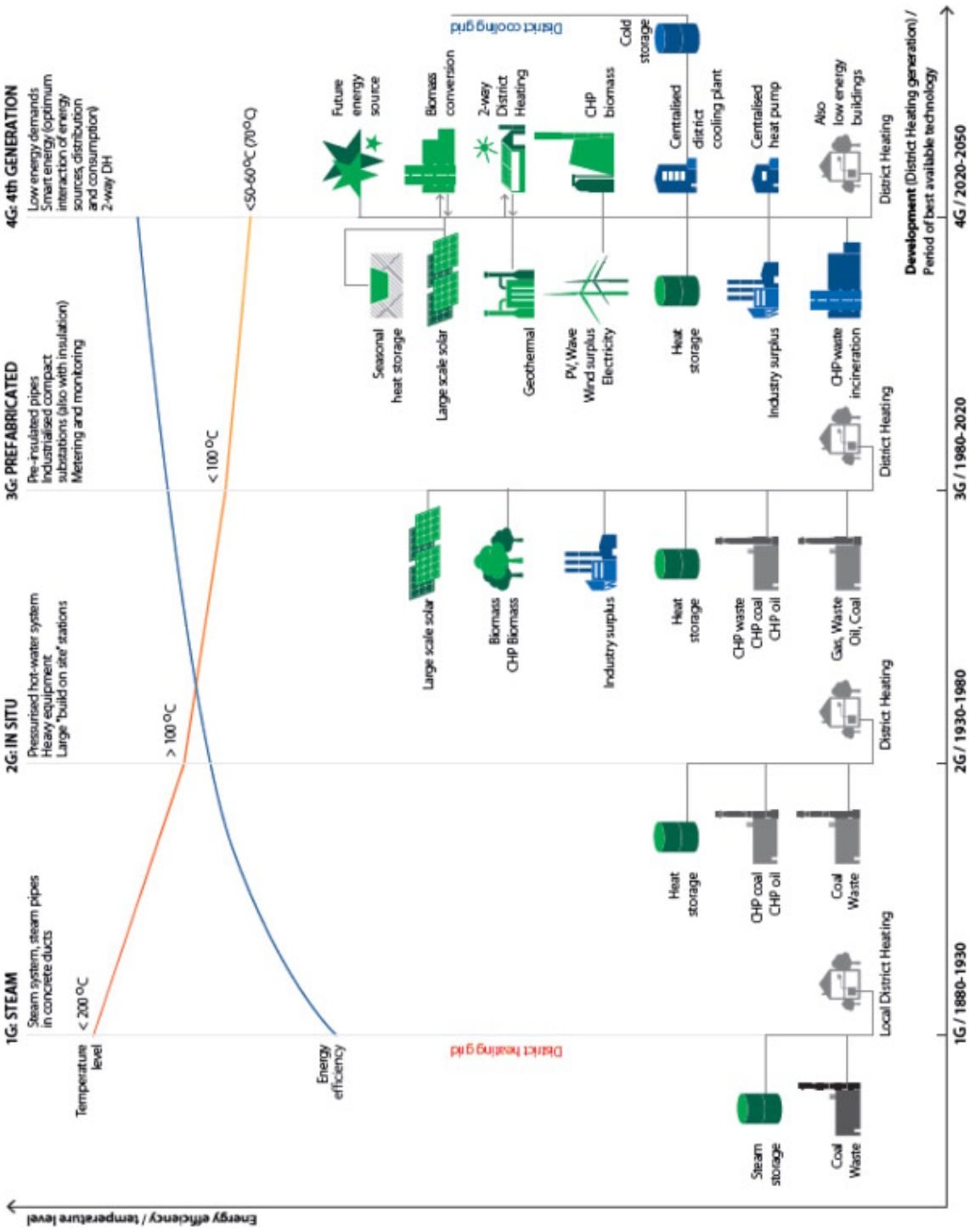

Figure 3.1: Illustration of the concept of 4th Generation District Heating in comparison to the previous three generations [45]

The implementation of LTDH will result in a number of advantages in the future energy market in relation to heat generation, distribution and consumption [46–48]. These can be summarised as follow:

- **Heat recovery from power stations**. In large CHP plants heat is often recovered from back pressure or extraction steam turbines. The efficiency and power output of these power generation systems strongly depend on heat sink temperature. The ratio between useful thermal energy and power output is defined as *Z-Ratio*. The power output decreases as the coolant temperature in the condenser increases. As a consequence, the lower the heat network return temperature, the higher the useful thermal energy will be for each unit of lost power generation as shown in Figure 3.2

- **Increased efficiency of fossil fuel heat generation plant**. Low return temperatures augment the condensation of flue gas, which increases the efficiency of the heat generation. This is relevant especially with fuels as biomass or waste due to their higher content of moisture

- **Integration of renewable energy and low temperature sources**. Supply temperatures below 60 °C allow the integration of both geothermal plants and large heat pump applications. Lower temperatures are also beneficial for solar thermal installations as well as for the re-utilisation of excess/waste heat from industrial processes or by heat recovery from cooling processes

- **Reduced distribution losses**. Low supply and return temperatures and low thermal conductivity of pipes contribute to decreasing the overall network heat losses

- **Increased efficiency of energy supply**. Reduced energy demand in new and renovated building and the use of low temperature heating elements allow to comfortably supply energy to end users with lower temperatures

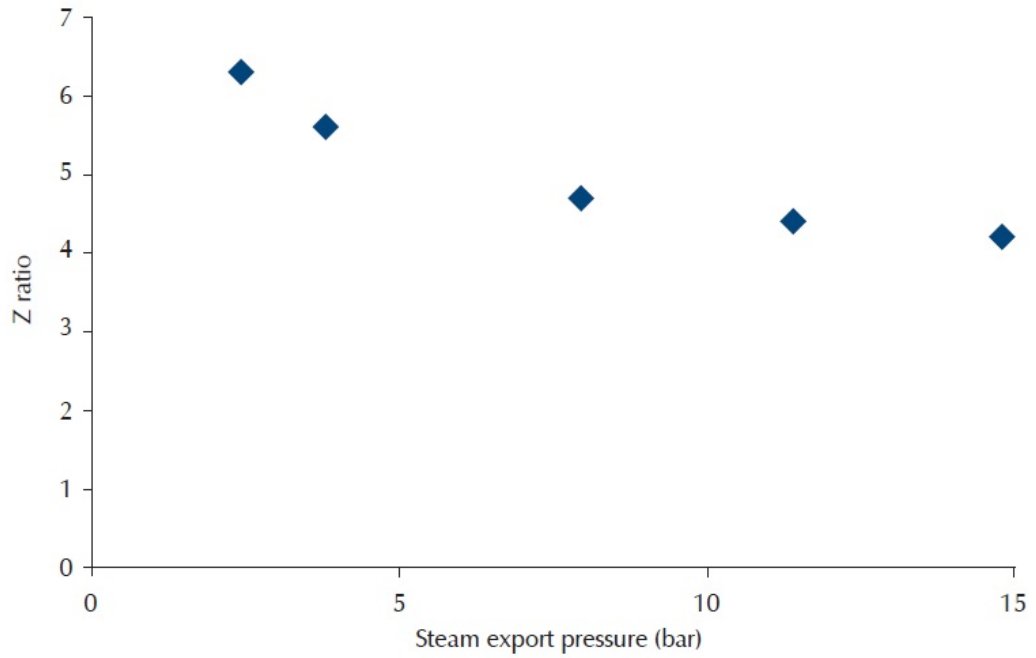

Figure 3.2: Variation of *Z-Ratio* with steam export pressure for a thermal power station [47]

3.2.1 Space heating and domestic hot water preparation with low-temperature district heating

As DH in the majority of cases covers the heat demand for SH and DHW, the lower limit for the supply temperature of 50 °C is imposed to avoid health problems due to Legionnaires' disease in sanitary water [45, 49, 50]. Legionella bacteria growth occurs at water temperatures in the range of $20 - 45$ °C, with optimum multiplication temperature within the range of $32 - 42$ °C. The growth of the bacteria is largely inhibited and slows down at temperatures of $50 - 55$ °C, gradually sterilized between $55 - 60$ °C and killed almost instantaneously at 70 °C [51]. An extensive document pubblished by the "European Committee for Standardization" provides detailed reccomandations for good practice to prevent the Legionella growth in drinking water installations, but the existing national regulations still remain the

reference policy [49]. For the UK, the national standards define, for the case of water storage, a minimum control temperature of 60 °C. For distribution pipes supplying to any thermostatic mixing valve (TMV), it has to be secured that the hot water reaches the outlet point in one minute with a temperature not lower than 50 °C (55 °C for healthcare premises) [52–54].

Similarly, recent studies show that buildings can be maintained at comfortable space temperature levels with low supply temperatures for the majority of the heating season using LTDH. However, this requires a flexible system to be able to adjusting the supply temperatures according to heat demand during extreme low outdoor temperatures. This would improve the overall efficiency of the heat generation and reduce the heat losses in the network [46, 55, 56]. Therefore, one of the challenges in the implementation of LTDH is the calculation of the optimal combination of supply and return temperature to operate the heating systems according to heat demand. In fact, reducing supply temperature to 50 °C poses few technical problems in regard to the capability of existing heating systems to guarantee the same thermal comfort. Commensurate with low-energy buildings, which use efficient heat emitters such as low-temperature radiators or underfloor heating, water supply temperatures of 50 °C or even lower would be technically adequate to meet SH demand for all of the year [57–59]. Hence, the core of this study was to investigate how to adapt the existing large building stock and the already installed hydronic heating systems to the applicability of LTDH, without any major design and construction intervention, yet adjusting water temperatures to meet heat demand.

3.3 Modelling performance of different types of heating elements for low-temperature operation

Lower return temperatures are beneficial for DH technology, by reducing the network distribution losses and mass flow rates, as well as improving the efficiency of energy generation [14,60–62]. This is even more important for the LTDH concept, where return temperatures have to be cooled to almost indoor temperature. In mature DH markets such as in Denmark, Sweden and Finland, LTDH has been successfully applied and tested in real projects. Good results proved the concept in case of low-energy buildings [46, 63, 64] and further investigations have been carried out for existing buildings at different levels of refurbishment [65,66]. However, none of these published papers includes an optimization process, based on the economic value of lower supply and return temperatures both for DH companies and end users. Existing buildings with radiator based heating systems are by far the most used and installed heating elements in Europe and to address correctly the challenge of operating existing hydronic radiators with low water supply temperatures, necessary considerations must be given both to the design of the heat emitting radiators (hardware) and the modelling analysis to optimize the performance.

3.3.1 Hardware part — type of heating systems

Hardware considerations include the different types of heating elements, the way they are operated and controlled in order to perform efficiently. Commonly, flat

panel radiators are manufactured by combining up to three flat plates and incorporating fins to augment the heat transfer area [67,68]; they can have a high or low profile. By far the most used hydraulic configuration for radiators is the double string system, consisting of one supply and one return water pipes as highlighted in Figure 3.3.

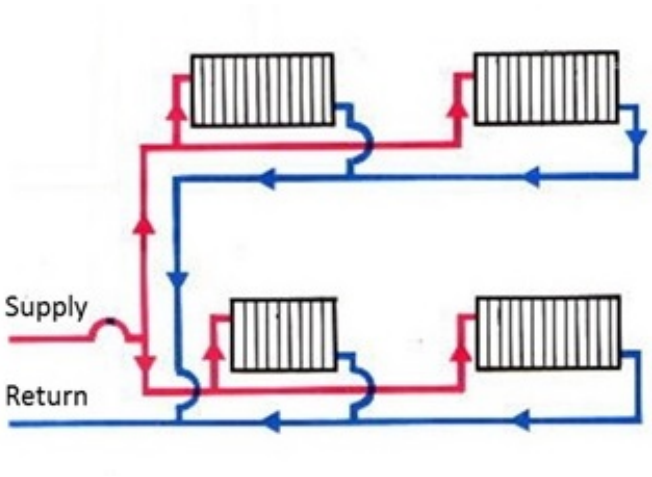

Figure 3.3: Schematic view of double string radiator system

In this type of radiators, hot water is supplied at the top of the radiator with water flowing vertically and cooling gradually before leaving from the opposite bottom [69]. Although low panel radiators are used in some cases, especially if there are space issues, they can lead to slightly higher return temperatures compared to taller ones, due to the reduced height; hence particular attention is necessary during the selection of the element if low return temperatures have to be attained.

Another possible hydraulic configuration for radiators is the one string system, characterized by only one pipe for both supply and return; the radiators are connected in a way that a fraction of the water flow in the main string runs through the radiator and back to the main string as presented in Figure 3.4. The

temperature though is gradually reduced as this enters to each successive radiator.

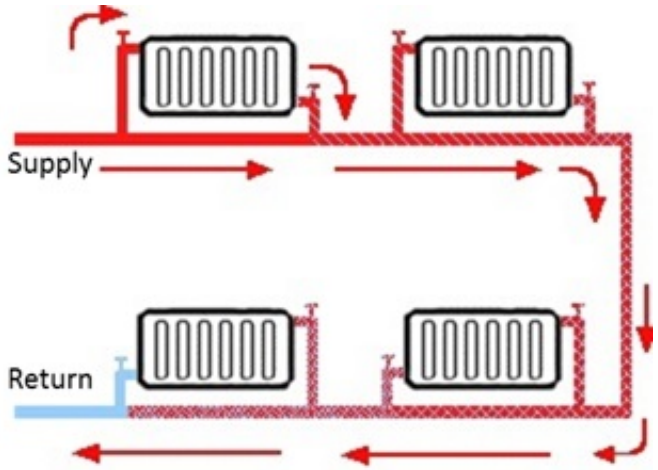

Figure 3.4: Schematic view of single string radiator system

This solution fosters the system to work with higher mass flow rate and lower ΔT. If carefully designed by increasing the size of each successive radiator [70], as presented in this Swedish report [71], return temperatures can be as low as in double string systems in typical DH network. Nonetheless, as difficult to properly control, it is common to experience higher return temperatures and smaller ΔT in the substation, hence this reduced their attractiveness in comparison to double string systems, in particular when connected to district heating [10]. Similarly to the radiators with single string hydraulic configuration, convectors lead to higher return temperatures due to high flow rate and low ΔT. They are characterized by heat transfer to the surrounding mainly by convection and the most common lay-out consists of a finned long tube, which generally follows the perimeter of exposed walls and/or windows [67–69, 72, 73]. These heating elements — likewise radiators with single string layout — are not very common and not recommended for DH in general and in particular not for LTDH application, where return temperatures close to room temperatures have to be achieved.

Central in the hardware discussion is also the way how radiator elements are controlled, typically by thermostatic radiator valves (TRVs). These regulate the flow of water circulating according to the temperature set-point defined by a thermostat in the room; this guarantees the required indoor comfort in an efficient way as well as the expected cooling of return temperatures. It also allows the heat output to modulate and compensate for emitters that can be over-dimensioned during some periods of the heating season [74–76]. However, it is quite common in real applications for TRVs to operate badly and negatively affect the overall system efficiency.

A study conducted in the UK by Ziao et al. [77] depicted how in hydronic radiator systems, although TRVs were installed in almost all the systems surveyed, in 65% of the cases they were performing poorly, mostly due to occupants misuse, and generating thermal discomfort and wasted energy. Therefore it is important to limit the side effect of human behavior on the effectiveness of TRVs [78], as these have a decisive role in overall system efficiency and in the cooling of return temperatures. In fact, the investigations of V. Monetti et al. [79], Xu et al. [80] and McNamara [81] illustrate that when properly installed and controlled, the TRVs can ensure an energy saving up to 10% in the first study and 12.4% and 15% in the second and third, with relatively low-cost retrofitting investment and short payback periods.

3.3.2 Modelling part — calculation of heat demand of rooms and heat power of radiators

Regardless of the operating temperature, the thermal performance of existing hydronic radiator systems operating at lower temperature must comply with current EU design practices and standards [82, 83]. The use of computer modelling tools allows accurate prediction of water temperature profiles in the radiator and determine accordingly the heating capacity [84,85]. It is important that the emitters are correctly sized and operated to deliver the heat needed; thus the challenge is to outline the optimal temperature of supply and return to meet the heat demand.

Hydronic systems are typically sized based on the worst case scenario of steady-state heat output that meets winter design conditions and do not consider sources of casual heat gains. This leads often to over-sizing systems and guarantees a larger radiator heat emitting surface area and a positive effect when lowering temperatures [14, 60, 66, 86]. Lauenburg [87] showed that heating systems sized for design temperatures only required full load during a short period when outdoor temperatures are very low, demonstrating that for most of the heating season consistently lower water supply temperatures can be appropriate to meet the heat demand.

The reliability of software outputs is crucial because it provides a powerful tool for professionals at the time of investigating and foreseeing the use of low temperatures to existing radiators. It is important to choose an adequate radiator element and correctly define the physical characteristics of the heating element,

including TRV controls. For instance, the open-source EnergyPlus, one of the most used and powerful software for energy simulations, only gives the user the option of a *"hot water baseboard heater with radiation and convection"* [88, 89]. This element has both radiative and convective components as with a radiator, but in reality is a convector. Therefore, the user can still perform accurate dynamic energy simulations for the building in analysis, but the accuracy could be affected if the focus of the investigation is specifically related to the cooling of the return temperatures in existing hydronic radiator elements at time of lowering the operating temperatures of the system. As a consequence, the choice made for this investigation was to simulate the buildings and the radiator elements using the commercial software IDA-ICE as presented in Chapter 4, 5 and 6. This allowed to perform accurate analysis of the operation of plate radiators.

From this perspective, the focus of this investigation is to develop an alternative method to investigate and plan the application of LTDH to existing buildings. In particular, as flat plate radiators are the most used heating elements in Europe, the goal of this research seeks to outline an optimization strategy to define the best combination of supply and return temperatures to operate existing hydraulic radiators in relation to LTDH implementation.

3.3.3 National codes and design temperatures for hydronic systems based on radiator units

Although the market penetration of underfloor heating in domestic buildings is increasing and ventilation systems are in some cases used in office/commercial

spaces, hydraulic radiators are still the most used heating elements across all Europe. As illustrated in Section 3.3.1, radiators are normally designed to guarantee the indoor comfort during the most extreme outside temperatures and typically buildings heat losses tend to be overestimated. Also, it is the case for existing buildings to experience over the years a certain level of renovation, which has a positive effect on their thermal performances. The combination of these aspects lead to generally oversizing the hydraulic radiator elements and as a consequence, for the majority of the heating season, operating temperatures lower than design ones are enough to ensure the required indoor comfort [87].

Hence, the radiator units for the majority of the heating season can be operated by either reducing supply temperatures or by reducing flow rates — if correct use of TRVs is in place — in order to avoid overheating of rooms [90]. By implementing the low-flow strategy, lower return temperatures can be achieved which have an important effect on the overall DH efficiency and costs. As reported in a study from Zinko et at. [91], 60% of malfunctioning equipment, which is the causes of higher return temperatures in DH systems, are associated to heating systems.

To define the degree of oversizing of the heating elemets and to which extent temperatures can be reduced, it is important to assess the design temperatures used. These vary according to national practise and policy. In mature DH market as Denmark and Finland radiator design temperatures for supply and return are 70/40 °C; for UK instead it was normal practice to use 82/70 °C. However, the new CIBSE publication related heat networks [40] highlights how radiators should

be designed according to 70/40 °C, which represents a step forward to align UK to more advance countries for DH technology. A selection of EU countries and relative radiator design temperatures are presented in Table 6.6 [14]. The case of Sweden highlights a pretty unique scenario as temperature above 60 °C are not allowed in new heating systems since 1982. This was directly related to the will of increasing the penetration of renewable sourceas and low-temperature heating systems [87].

Table 3.1: Radiator design temperatures in different EU countries

Country	**Supply Temp (°C)**	**Return Temp (°C)**
Denmark	70	40
Finland	70	40
Sweden*	60	40
United Kingdom	82	70
Germany	80	60
Russia	95	75

* Alternative design temperatures for Sweden 60/45 °C and 55/45 °C used today

3.4 Summary

A description of the LTDH concept was introduced in this chapter as well as the advantages and its role within the future energy market. The analysis highlighted the aim of the next DH generation to achieve a load dependent temperatures with a target for supply and return of 50/20 °C .

The evaluation also illustrated the challenges that the target temperatures will pose in the future DH network. This was deepened in particular for the SH and DHW demand at building level, emphasising on one hand, the reason to limit supply temperatures at 50 °C due to the risk of Legionnaires' disease; on the other hand, by addressing the capability and differences of heating systems in both low-energy and existing buildings to guarantee the expected indoor comfort with lower operating temperatures.

Furthermore, the target of the review focused in details on the application of the new generation DH to the existing stock of building. This was presented by highlighting the core of this investigation, related to assess the possibility of connecting existing heating systems, based on hydraulic radiators, to LTDH.

To this extent, a detailed analysis addressed the capability of plate radiators to achieve low-return temperatures according to design and operative conditions. Several aspects were emphasised and they can be summarised as follow:

- design conditions and typical over-sizing of heating element

- importance of TRVs to control flow-rates and heat emitted from the hydraulic radiators
- importance of energy software to model hydraulic radiator performances at lower operating temperatures
- capability to operate the heating systems at lower temperatures for the majority of the heating season

Chapter 4

Methodology

4.1 Introduction

The objective of this chapter is to present the methodology implemented to perform the research work of this investigation. The description begins with an outline of the main hypotheses of the work carried out, based on the concepts presented in Chapter 1, 2 and 3.

This is followed by a detailed overview of the strategy used to perform the analysis. This was centred on the characterisation of the different heating elements — mainly focusing on flat plate radiators — and on the implementation of an optimisation procedure to calculate the specific operating temperatures of the hydronic radiators as function of the heat emitted.

4.2 Research hypotheses

The research hypotheses are the synthesis of some of the main ideas illustrated in Chapter 1, 2 and 3, which were the leitmotif to develop the work of this investigation. These can be summarised as follow:

- community energy schemes will increase their share in the future European energy market and district heating and cooling will be more competitive compared to individual energy generation
- DH technology due to its high flexibility and capacity to integrate renewable energy sources will play an important role in the future energy market to decarbonise the UK heating sector and help achieving the carbon emission limits
- the possibility and the strategy to connect existing stock of buildings to LTDH is one of the main challenges in the progression of DH technology. This poses the problem of finding solutions to adapt and operate existing heating systems with lower temperatures

4.3 Methodology

The methodology developed in this research project is divided in two parts: textcolorredthe hardware part, which evaluates the different type of heating systems and the modelling part, which describes the strategy to optimise the operating temperatures of the selected heating elements. The focus is to investigate and plan the application of LTDH to existing hydronic radiator systems through two case studies:

1. optimisation of operation of plate radiators based on a Danish single-family house in the plan of connecting to LTDH as given in Chapter 5

2. optimisation of operation of an existing small scale DH network based in UK aiming to introduce lower temperatures as detailed in Chapter 6

4.3.1 Hardware part — type of heating system

The investigation related to the application of LTDH to existing buildings started with a characterization of heating systems with respect to the type of heating loop and heating elements. The characterization mainly addressed the differentiation between the possibilities of operating the specific systems with low return temperatures, as it was described in section 3.3.1. An example of a system with low return temperature is a double string system with panel radiator, whereas the examples of systems with high return temperature are:

- single string with all type of heating elements
- double string or single string with convectors

4.3.2 Modelling part — calculation of heating demand of rooms and heating power of radiators

The modelling method used in this work is carried out in a sequence of steps to investigate the applicability of LTDH to existing buildings with hydronic radiators. The stepwise procedure to calculate and optimise the operating temperatures of the plate radiators is presented as follows:

Step a: calculation of part load duration curve

Step a defines the part load duration curves for each room of the building considered. The starting point was the characterization of the design conditions of the heating system: this was made for the case study by performing steady-state simulations to outline the design heat load for each room according to Danish and UK standards [92, 93], assuming no heat gains and the specific design winter temperatures for both countries. Once the design conditions were defined, detailed dynamic simulations were performed to outline the realistic heat load distribution for an entire year using a weather file for Copenhagen based on a 10 year historical database and the CIBSE set of data for Nottingham [94, 95]; this allowed the specific part load duration curves to be obtained for each room on an hourly basis.

Step b: calculation of the relationship between part load and logarithmic mean temperature difference of the hydronic radiator elements

The objective of *step b* is to assess for each room the operation plate radiators to meet the heat demand outlined in *step a*. This was established by associating to each part load the specific logarithmic mean temperature difference (LMTD) for the specific radiator size of the room.

Hydronic radiator formulation

The empirical formula used to evaluate radiator performance and the capacity of cooling the return water temperatures is based on analysis of the heat emitted as a function of the mean temperature difference (MTD) between radiator

and ambient temperature. The arithmetic mean temperature difference (AMTD), between supply and return temperatures (T_S and T_R) of the radiators and surronding (T_i), is used in the formulation included in the EU standards EN 442-1 and EN 442-2 [84, 85]:

$$AMTD = \left(\frac{T_S + T_R}{2}\right) - T_i \tag{4.1}$$

Nonetheless, when the difference between supply and return temperatures are large, the AMTD does not provide an accurate evaluation as the temperature distribution on the radiator is not linear [96]. Hence, more detailed results can be obtained by using the LMTD. The empirical formula to define the heat emitted by radiators as function of LTMD is expressed as follows:

$$\Phi = \left(\frac{LMTD}{LMTD_0}\right)^n \cdot \Phi_0 \tag{4.2}$$

where Φ is the heating power at the operating temperatures (W); Φ_0 is the nominal heating power at design conditions (W); LMTD is the logarithmic mean temperature difference between radiator and surroundings at the operating temperatures (°C); $LMTD_0$ is the logarithmic mean temperature difference between radiator and surroundings at design conditions (°C); n is the radiator exponent typically equals to 1.3 for standard hydraulic radiators [59]. It defines the exponential relationship between the mean temperature difference and the heat emitted from the given radiator.

The general logarithmic mean temperature for the heat transfer between the

radiators surface and its surronding is expressed as follows [97]:

$$LMTD = \frac{T_S - T_R}{ln\left(\frac{T_S - T_i}{T_R - T_i}\right)} \tag{4.3}$$

where T_S is the supply temperature (°C), T_R is the return temperature (°C) and T_i is the indoor temperature (°C).

Step c: calculation of LMTD duration curve

The LMTD duration curve in this step is established for the hourly heat load duration curve calculated in *step a* and the relation of part load and LMTD obtained in *step b*. The method is then applied to each room of the building to calculate its respective LMTD duration curve as a prior analysis to connecting to LTDH.

Within all the curves, the worst cases represented by the highest LMTD duration curves have to be carefully assessed and possibly excluded from the analysis. These may represent typical errors in radiator design, undersized systems or unheated rooms. Therefore, a separate investigation need to be carried out and possibly improved by reducing heating demand or increasing heating capacity of radiators in order to operate more efficiently and guarantee the expected cooling of return temperatures.

This requires full access to the building heated area to measure the radiators operating parameters (temperatures, flow rates, etc) and check proper functioning of TRVs. If access to the buildings is not possible (as it was the case for the case studies of this investigation) the analysis has to be based on the design conditions

according to national building regulations.

Step d: calculation of the optimal supply and return temperature to provide the necessary logarithmic mean temperature difference

Step d is the calculation of the optimal combination of supply and return temperatures to provide the necessary LMTD obtained from *step c*. The needed LMTD can be reached by numerous combinations of supply and return temperatures to the radiators. The optimal combinations presented for all relevant LMTD was obtained by minimising the operating temperatures through an optimisation problem based on the *objective function* and *constraints*. This assesses the different economic benefits that lower supply and return temperatures have in the DH operation for both DH utility companies and end-users, as described in the results proposed in Chapter 5 and 6.

4.4 Data collection

The methodology implemented in this investigation project was used to analyse two case studies. The first case involved close research collaboration with the Civil Engineering Department of DTU, Denmark. The second one is related to an isolated Estate in the Nottinghamshire countryside, where a small scale DH network was installed.

For both cases experimental data were collected to define: buildings' thermal characteristics and indoor comfort; operating temperatures of different heating elements; operating temperatures of substations and boilers. Some limitations

in relation to the data gathering were linked to: technical problems, budget for equipment and in some cases privacy issues.

4.5 Modelling analyses

Several calculations and modelling of different scenarios have been performed by extensive use of computer-base simulations. Three main families of software have been used to analyse indoor comfort and energy consumption of buildings, as well as operation and performances of heating networks. A description of their capabilities is presented as follow:

- **IDA-ICE**. It is an innovative and trusted whole-year detailed and dynamic multi-zone simulation application for study of thermal indoor climate as well as the energy consumption of the entire building [98]. IDA-ICE can be used for complete energy and design studies, involving the envelop, glazing, HVAC systems, controls, light, indoor quality, comfort and energy consumption of buildings [66]. Every underlying equation can be browsed, and every variable can be logged and customised, giving great flexibility to the critical user. In addition, as documented in the investigations of M. Maivel and J. Kurnitsky [99, 100] and D. S. Østergaard and S. Svendesen [96], IDA-ICE has been largely used to perform detailed analyses in relation to low temperature heating systems and to the capability of existing plate radiators to be operated with low temperatures.

- **TERMIS**. It is a hydraulic modeling tool, which simulates flow, pressure and thermal behavior in the distribution network. It is the most advanced

software for real-time planning and optimisation of district heating and cooling network operations. This enables operators to make better and smarter decisions and to optimise production and enhance economic performance. It also allows to optimise the supply temperature leading to a reduction in the distribution losses and simulate the expansion of the network in new areas as illustrated in the published work of Della Rosa et al. [56]. Termis is in daily operation in more than 500 cities worldwide and provides reliable energy to more than 100 million homes [101]

- **MATLAB**. The MATLAB platform is optimised for solving complex engineering and scientific problems and its matrix-based language is largely used in both academia and industry. It has been used in this investigation to perform the calculations of the optimal operating temperatures for the plate radiators on one hand; to define an algorithm for simulating the operating conditions of DH networks on the other hand. However, due to the realignment of the objectives of this project — as described in Section 1.4 — the developed algorithm was not expanded further and it has been included in this thesis only as an appendix — see Appendix G.

4.6 Summary

The chapter begins by summarising the main hypotheses which were the main drivers to develop this investigation. These are related to the role that district energy scheme will have in the future energy scenarios across EU and in UK in order to help decarbonising the heating sector in the prevision of a low-carbon society. From this perspective, it was emphasised the relevance of investigating the implementation and connection of existing buildings with hydronic radiators to the future LTDH.

It is also deepened and illustrated in a number of steps the methodology used in this investigation to plan the connection of existing building with plate radiators to LTDH. The core idea is to define the optimal combination of supply and return temperature to operate the selected heat elements for each LMTD by formulating on optimisation problem which takes into account the economic benefits that could be potentially generated to both DH utility companies and end-users by lowering supply and return temperatures .

The last part highlights the methods related to experimental data collection — which will be presented in Chapter 5 and 6 — as well as the description of the software families used to perform calculations and computer-based simulations.

Chapter 5

Heat emitting radiators optimisation: case of a Danish single-family dwelling

5.1 Introduction

This chapter presents the results of the joint research work carried out in collaboration with the department of Civil Engineering of the Technical University of Denmark and published as an article to the Elsevier journal *Energy*.

The analysis begins with a detailed description of case study based on a Danish single-family house from 1930. The physical model built with the energy software IDA-ICE, in accordance to Danish building regulations, and dynamic simulation outputs are presented. A comparison between real measurements and simulation outputs is outlined in order to identify the capability of the software to correctly

model the cooling of return temperatures with hydronic radiators.

This is followed by the application of the method proposed to investigate and plan the connection of existing building with plate radiators to LTDH. This is illustrated by presenting the results of the optimisation of the operating temperatures of the chosen heating systems, assessing the economic benefits that lower supply and return temperatures have to both DH utility companies and end-users. Two different scenarios were assumed for the heating system in the single-family house: one with double-string and one with single-string plate radiators.

5.2 Description of the Danish single-family house

The method was tested by the use of a specific case based on a typical detached Danish single-family house from the 1930s, sited in Copenhagen. A model was created in the dynamic simulation software IDA-ICE [102] — see Figure 5.1— as a result of the collaboration with the DH reserach group of the department of Civil Engineering of DTU. The software has been validated in accordance with standard DS/EN 15265, which describes dynamic simulation of energy performance of buildings [103, 104].

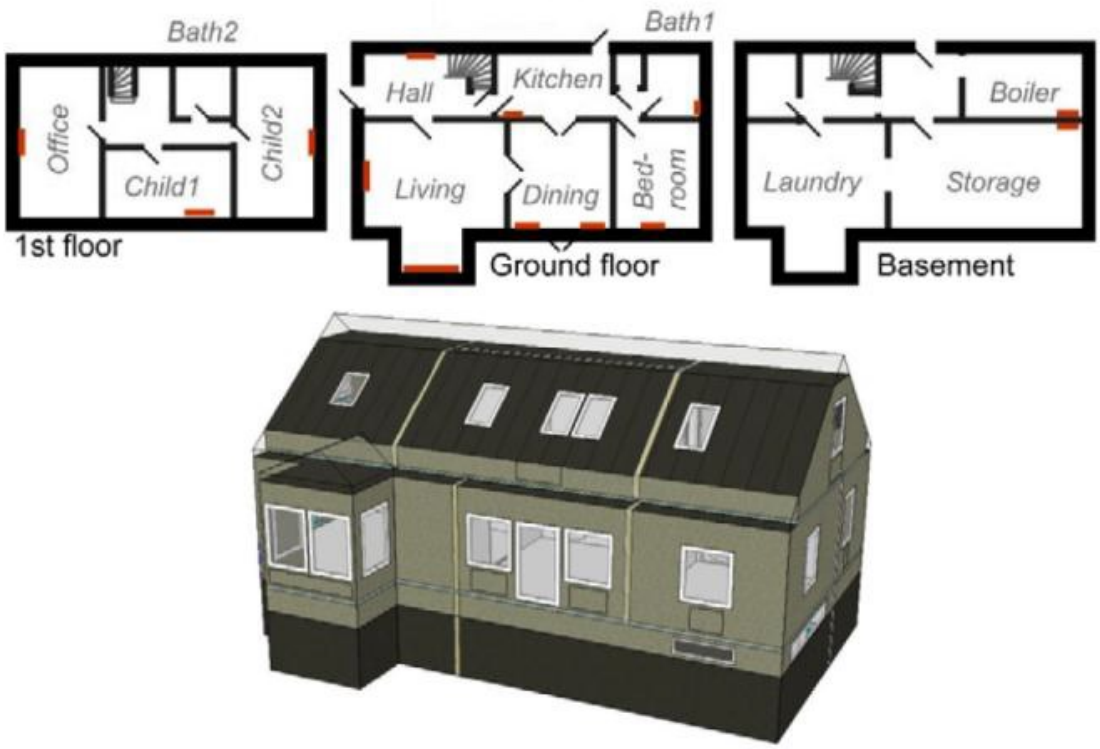

Figure 5.1: Floor plans, radiators (in red) and IDA-ICE model of the Danish single-family house [102]

The building has a basement and is made of brick cavity walls and red tile roof. As common for Danish buildings from 1930s, old windows and radiators have been replaced over the years, as well as improvements to roof insulation. This in fact represents an example of a typical building from 1930s that a Danish DH utility company can encounter when planning the expansion of the network to new urban areas. Table 5.1 summarises the main properties of the house used to build the physical model in IDA-ICE.

Table 5.1: Key data and construction elements

General parameters	
Number of occupants	2
Total floor area/basement area (m^2)	320/118
Heated part of basement (m^2)	47
Room Height (m)	2.7
Annual heating consumption (MWh)	20
Design winter temperature (°C)	−12
Building construction elements	**U-value (W/m^2K)**
External wall — insulated cavity brick wall	0.78
Roof-tiles, wood beams and insulation	0.15
Windows — 2 pane energy efficient glazing	1.55

The occupancy profiles, taking into account the two tenants and the different zones of the house, were modelled considering hourly variation, differentiating the patterns according to working days and weekends. The use of the equipment was modelled in similar way, assuming the specific profiles, use and characteristic. Typically, the average values for internal heat gains in domestic buildings according to Danish regulation are 1.5 W/m^2 for occupants and 3.5 W/m^2 for equipment [104]. The choice for the specific internal heat gains in the schedules added up to 0.81 and 1.55 W/m^2 on average for occupants and equipment respectively. The modelled heat gain was in the conservative end, but corresponds with the findings from earlier studies, that identified typical values for internal heat

gains to range between 2-5 W/m^2 [105]. The natural ventilation was assumed to be fixed at 0.3 l/s $\cdot m^2$ of floor area, which corresponds to the standard ventilation required in the Danish Building Code [104], and includes infiltration from opening of windows and doors in the winter time. Finally, in the definition of the model, it was not considered the windows and doors dynamic operation.

5.2.1 Software capability to predict cooling of return temperatures for hydronic radiators

The importance of having reliable software to assess the capability of hydronic radiators to be operated with low temperatures has been discussed in Section 3.3.2. Hence, a comparison was made between real measurements and the simulations' outputs to evaluate the capacity of IDA-ICE to correctly model the cooling of return temperatures. The analysis was performed considering the real radiators installed in the single-family house considered.

The radiator formula presented in Section 4.3.2 — Equation 4.2 and 4.3 — are used as model for the heating element performance in the simulation program IDA-ICE. The house was examined and the size and type of radiators in all rooms was measured and checked; the number and the exact location of each of them in each room are shown in the plans of Figure 5.1 in red. Also, indoor temperatures, heating system temperatures and heating consumption over the course of one month, between 10^{th} March and 13^{th} April 2015, were monitored and collected on an hourly basis.

During the monitored period, the energy demand for SH and DHW was provided by a condensing natural gas boiler, placed together with a hot water tank of 110 litres in the basement. The building was switched to district heating during the following June, after the measurements in the house had been taken. The real heating system consists of double string plate radiators, but electric floor heating is installed in both bathrooms. The existing radiators in the house were placed in the simulation model using their correct dimensions, design temperatures and heat power, exact location, and a TRV was set for each of them.

In order to accurately model the operating conditions of the hydronic system and achieve reliable results, the simulations were run using the real hourly weather data for the period in analysis; the recordings were obtained from measurements taken by the Danish Meteorological Institute, whereas the diffuse and direct sunlight were collected at the weather station of the Technical University of Denmark, which is close to the case study and therefore the values can be assumed to be appropriate [106].

Also, the performance of the heating elements available in the software were evaluated by running the simulations using the supply temperature obtained from the measurements, and the simulated results for the return temperatures out of the radiators in selected rooms were compared to the measured ones on an hourly basis. The average supply temperatures in the period recorded for the SH demand was 45 °C and it was enough to guarantee the expected indoor comfort; the mean outdoor temperature was 5.3 °C and the lowest value registered was −2.5 °C.

The comparison between the IDA-ICE outputs and the real return temperatures collected from the radiators over 24 hours, using dedicated temperature sensors, is presented in Figure 5.2 and 5.3 for two selected rooms. The importance of comparing the results over an interval of 24h was driven by the necessity of testing the accuracy of the software to reflect the influence that all the dynamic variables involved have on the performances of the radiators throughout a typical day.

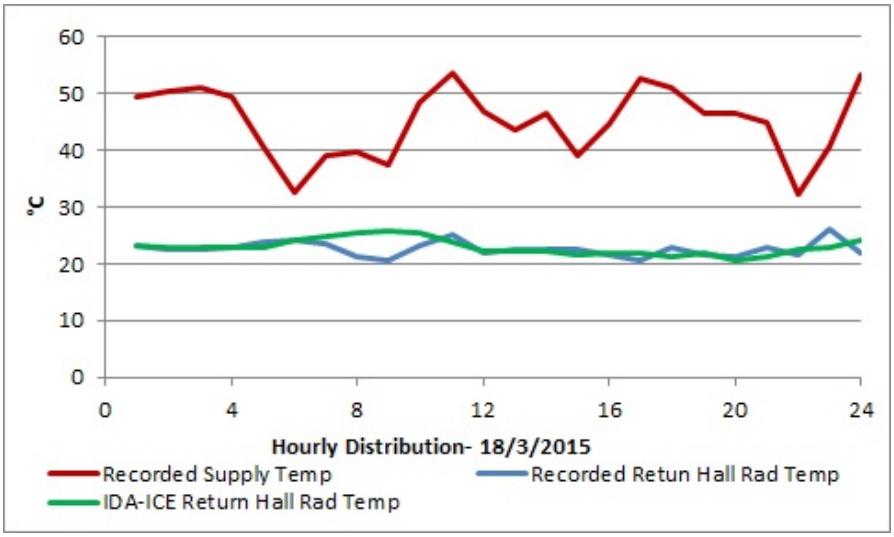

Figure 5.2: Hall radiators' temperature comparison

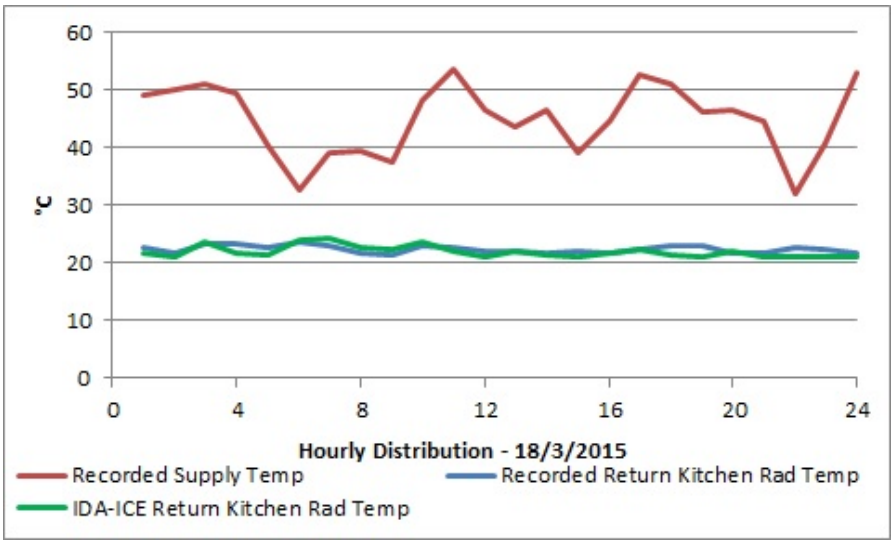

Figure 5.3: Kitchen radiators' temperature comparison

The results obtained show a good match between the simulations and the real measurements of the return temperatures for the period considered. The average return temperatures calculated by the software were 22.0 °C and 22.9 °C for the kitchen and hall respectively, whereas the average data collected were 22.4 °C and 22.5 °C. Therefore, the plate radiator unit available in IDA-ICE provides robust results and can be used to efficiently model the cooling of the return temperatures. It is also important to notice how the real data collected shows how existing hydronic radiators can be operated with low temperatures and potentially connected to LTDH, guaranteeing the expected indoor comfort.

5.3 Optimisation of operation of plate radiators based in the plan of connecting to LTDH

This section of the chapter illustrates the results obtained due to the application of the methodology presented in Chapter 4. Firstly, it is presented the hardware part and the relative selection of specific heating elements. Then the results of the optimisation are reported for the selected heating units.

5.3.1 Hardware analysis — selection of type of heating systems

The characterisation of the specific heating elements was evaluated and two different heating systems were chosen to investigate the application of the proposed method:

1. A heating system with low return temperatures — double string with plate

radiators

2. A heating system with high return temperatures — single string with plate radiators

The two selected heating systems were applied in turn to the single-family house considered in this study. Two main assumptions were made: the radiator were sized according to the steady-steady simulations, with no heat gains and winter design temperature according to building regulations; an efficiently controlled TRV was installed to each radiator. It was assumed for all the scenarios a direct connection without any heat exchanger. However, the performed analysis can also include the presence of heat exchangers by accounting for their efficiency.

5.3.2 Modelling part — calculation of heating demand of rooms and heating power of plate radiators in double string system

The developed method was intended to be applied to an area in the process of being connected to DH and it was supposed that the building chosen, for the case of double string with plate radiators, was representative of the urban area hypothesised. The application of the method was implemented on one selected room, the hall, and the results for the four steps described in the methodology are presented. The assumption infers that the selected room was the representative for the entire building. The scope of this part of the research was intended to illustrate and document the application of the proposed method to a Danish case study. The implementation of the strategy to all buildings and all rooms is presented in

Chapter 6 for the UK small scale DH case.

Step a: calculation of part load duration curve

According to the steady-state simulations based on the Danish standard [92], the design heat load calculated for the specific room was 884 W. Also, the dynamic simulation outputs obtained from IDA-ICE are presented in Figure 5.4 and depict the part load duration curve for the room in analysis on an hourly basis for the entire year.

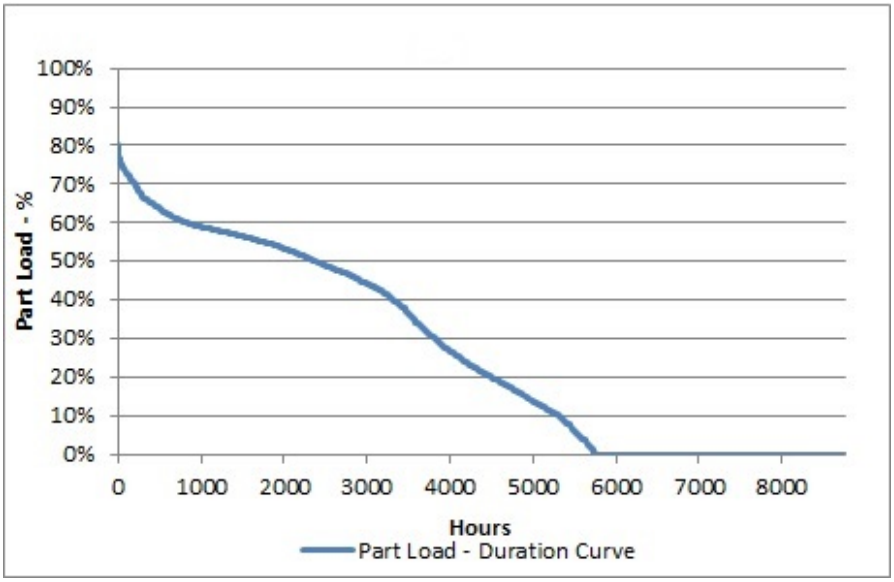

Figure 5.4: Step a: Part load duration curve

Step b: calculation of the relationship between part load and logarithmic mean temperature difference of the hydronic radiator elements

The results for step b presented in Figure 5.5 illustrate the relationship between each part load and the specific LMTD, expressing how the radiators need to be operated. It was assumed that the radiators in the double string configuration at design conditions were operated with supply and return temperatures of 80/40 °C.

In addition, to correctly perform the calculations of LMTD per each part load using Equation 4.2, n was assumed to be 1.3, Φ_0 was the design heat load of 884 W, whereas $LMTD_0$ was obtained from Equation 4.3 using the design temperatures of 80/40 °C and set indoor temperatures of 20 °C.

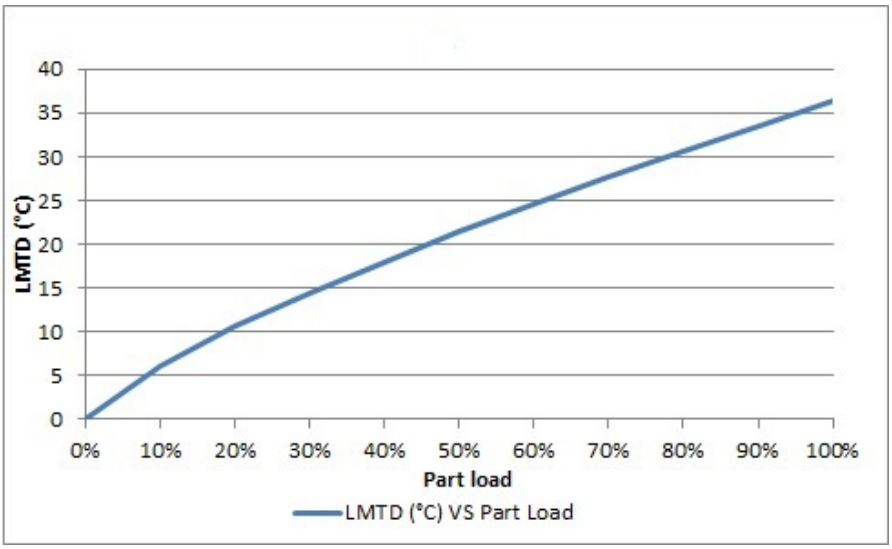

Figure 5.5: Step b: LMTD VS Part load

Step c: calculation of the duration curve of logarithmic mean temperature difference

The part load duration curve presented in Figure 5.4 and the general relation between the part load and LMTD in Figure 5.5 allowed calculation of the duration curve of LMTD on an hourly basis as described in Figure 5.6. The graphical combination of the curves of Figure 5.4, 5.5 and 5.6 provides a tool to clearly identify the number of hours per each range of part load or per each degree °C difference of LMTD, hence the exact amount of energy necessary to guarantee the expected indoor comfort through the radiators. These curves and in particular the curve of Figure 5.6 can be used to compare different buildings and different rooms, helping to define the conditions and the boundaries to be investigated for

implementing LTDH in an urban area.

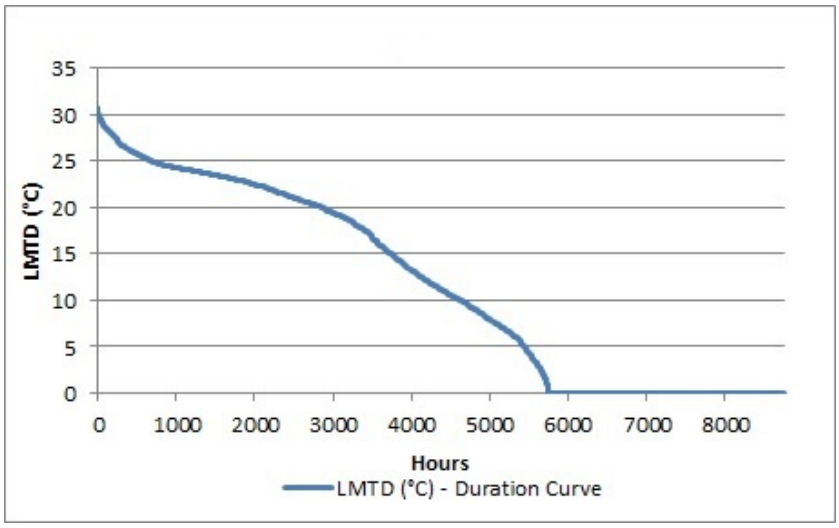

Figure 5.6: Step c: LMTD duration curve

Step d: calculation of the optimal supply and return temperature to provide the necessary logarithmic mean temperature difference

Two different scenarios, A and B, were investigated and consequently the formulation of the optimisation problem followed two different strategies. Both scenarios assess the impact that different DH markets have on the definition of the optimal combination of supply and return temperatures to operate the same hydraulic radiators. The results are presented in Figure 5.7 and illustrate on one hand the technical and economic factors affecting the selection of the optimal temperatures; on the other hand, to which extent these can be lowered without any intervention to the thermal envelop of the building or to the heating system.

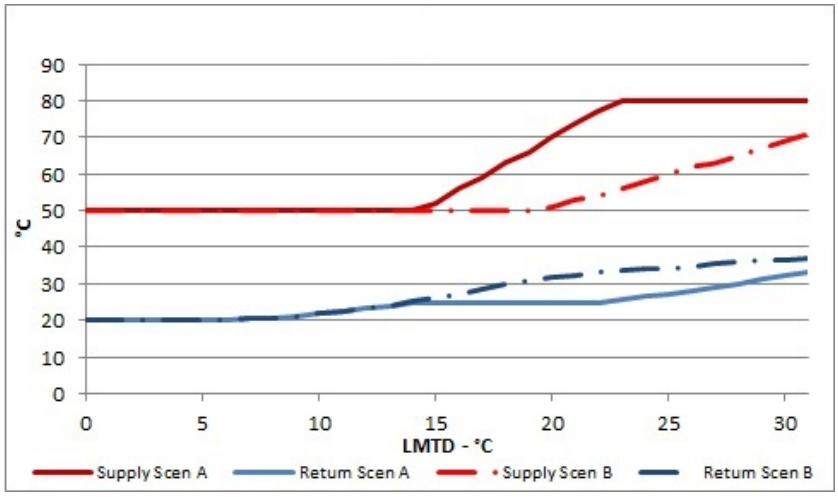

Figure 5.7: Step d: Optimised Supply and return temperatures

Scenario A: typical Danish DH network

In the Danish DH market more than 70% of heat is produced taking advantage of CHP technology and the price of heat unit only includes all the necessary costs related to supply heating, as DH companies are not allowed to make any profits [20]. Also, as achieving lower supply and return temperatures reduces the costs associated to heat generation and distribution losses, typically DH companies incentivize their customers through motivation tariffs to reduce temperatures in exchange of a discount in their energy bills. These are normally customized according to the specific characteristics of DH systems and relative end-users connected.

From this perspective, Scenario A was designed assuming the figures of a real motivation tariff related to an existing Danish DH company [107], where the heat generation is based on a biomass boiler with flue gas condenser. For the considered DH network, the company is able to guarantee to end users a discount of 1% in their energy bill (up to a maximum of 20%) for each °C lower in their return tem-

peratures compared to the reference DH yearly average return temperature. The assumed reference average yearly supply and return temperatures were 80/40 °C as typical for Danish DH networks. The discount offered is compensated by the savings made by the DH company due to the lower supply and return temperatures. In fact, at actual market conditions, according to their cost analysis [107], lower return temperatures have higher economic value due to the savings in buying energy at the generation point, compared to the reduction in the distribution heat losses due to lower supply and return temperatures.

Hence, the strategy of the optimisation was based on the minimisation of the supply and return temperatures of Equation 4.3 set equal to the specific LMTD for each value of the duration curve presented in Figure 5.6. The strategy followed three different paths clearly delimited by the breaking points related to LMTD of 14 °C and 23 °C corresponding to the change in the gradient of the optimised supply and return curves calculated — i.e. Figure 5.7. The objective functions and relative constraints are presented for all specific LMTD as follows:

i. For LMTD $< 14\,^{\circ}\mathrm{C}$:

$$minimise\ (T_R),\ for\ LMTD = \frac{T_S - T_R}{ln\left(\frac{T_S - T_i}{T_R - T_i}\right)} \tag{5.1}$$

Subject to:

$$T_S = 50\,^{\circ}\mathrm{C} \tag{5.2}$$

$$\dot{m} \leq \dot{m}_0 \tag{5.3}$$

ii. For $14\,^{\circ}\text{C} \leq LMTD \leq 23\,^{\circ}\text{C}$:

$$minimise\ (T_S), for\ LMTD = \frac{T_S - T_R}{ln\left(\frac{T_S - T_i}{T_R - T_i}\right)} \tag{5.4}$$

Subject to:

$$T_R = 25\,^{\circ}\text{C} \tag{5.5}$$

$$\dot{m} \leq \dot{m}_0 \tag{5.6}$$

iii. For LMTD $> 23\,^{\circ}\text{C}$:

$$minimise\ (T_R), for\ LMTD = \frac{T_S - T_R}{ln\left(\frac{T_S - T_i}{T_R - T_i}\right)} \tag{5.7}$$

Subject to:

$$T_S = 80\,^{\circ}\text{C} \tag{5.8}$$

$$\dot{m} \leq \dot{m}_0 \tag{5.9}$$

All the different components of the objective functions and constraints are: T_S is the supply temperature ($^{\circ}$C), T_R is the return temperature ($^{\circ}$C), T_i is the return temperature ($^{\circ}$C)(fixed at $20\,^{\circ}$C), $\dot{m}$ is the mass flow rate (kg/h) associated to the generic combination of T_S and T_R and $\dot{m}_0$ is the mass flow rate at design conditions (19 (kg/h)).

The max mass flow rate of 19 kg/h was obtained from Equation 5.10:

$$\Phi_0 = 3600 \cdot \dot{m}_0 \cdot c_p \cdot (T_{S_0} - T_{R_0}) \tag{5.10}$$

where Φ_0 is the nominal heating power at design conditions (W), $\dot{m}_0$ is the max mass flow rate (kg/h), T_{S_0} is the supply temperature at design conditions (°C) and T_{R_0} is the return temperature at design conditions (°C).

In the resolution of the optimisation problem all the combinations of temperatures fulfilled the constraints' criteria. The lower supply temperature limit of 50 °C is imposed by national standards to avoid the risk of Legionnaires' disease in DHW [45,49] and it was assumed that supply and return temperatures of 50/20 °C out of the heating season were enough to meet the DHW demand. The upper limit of 80 °C instead was assumed as the maximum inlet temperature according to the specific DH network.

In addition, according to normal operation practices of radiators, a target return temperature of 25 °C was set as a realistic value given the indoor room temperature of 20 °C. This was in fact one of the constraints in the minimisation of the supply temperatures for all LMTD included in the range between 14 °C and 23 °C. These two points, corresponding to the change in the gradient of the optimised curves proposed, illustrate that for LMTD lower than 14 °C, due to the combination of low heat demand and low mass flow rates, the return temperatures were always below the target temperature of 25 °C and supply temperatures could be set as low as 50 °C; contrarily, for a LMTD higher than 23 °C the combination

of high heat loads and high mass flow rates led to return temperatures always higher than 25 °C and supply temperatures were fixed to 80 °C to guarantee the expected indoor comfort and avoid unnecessary high return temperatures.

Compared to other studies where LTDH concept was applied to low-energy buildings [46, 63, 64] and to existing buildings at different levels of refurbishment [65, 66], the outcomes presented in Figure 5.7 show for this scenario that existing heating system based on double string radiators, if properly controlled, can be operated more efficiently and achieve low return temperatures for each LMTD without any intervention to the building, but simply adjusting temperatures to heat demand.

Thus, the calculated combination of supply and return temperatures can be used by the district heating company to efficiently operate the network, controlling the supply temperatures according to the optimal level. To this extent, Figure 5.8 presents the relationship between the optimised supply/return and outdoor temperatures. This outlines the strategy to be followed by the DH company to meet the heat demand for the hypothesized urban area, assuming that the building and the room chosen were representative.

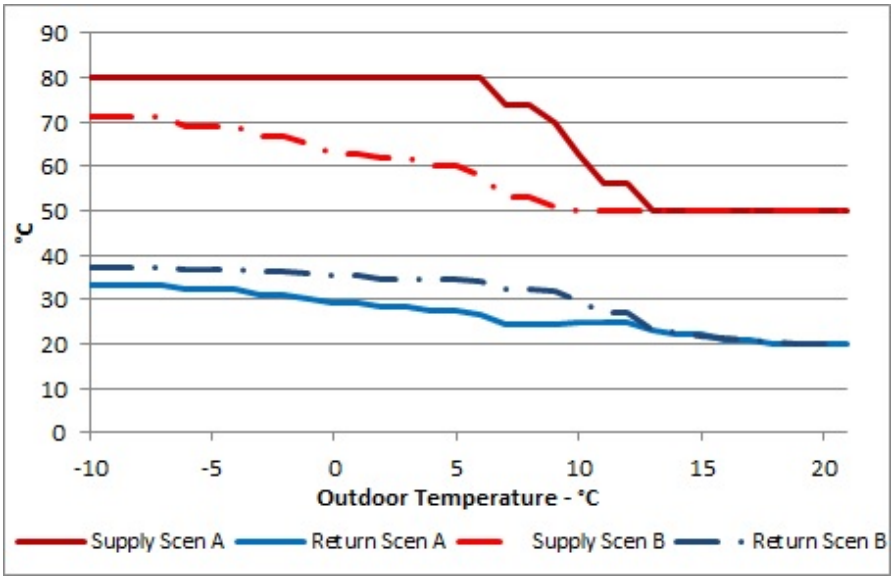

Figure 5.8: Scenario A and B: relation between optimised supply/return outside temperatures

The curves were calculated by finding the hourly peak load from the heat load profile of Figure 5.4 for each °C of the outdoor temperatures and associating for specific LMTD the optimal temperature combination from the results presented in Figure 5.7. The use of hourly peak loads for each °C of outdoor temperature is a conservative choice that guarantees the temperatures would deliver the heat demand in all conditions. Different approaches considering more realistic peak values, based on daily, 12 or 6 hour averages, are possible, but the evaluation has to be linked to the characteristic of the network in analysis and its capacity to adjust temperatures and pressures to the customers connected and to the use of weather forecasts.

Therefore, operating the DH network and the radiators as proposed would lead to implementing LTDH in the area and result in a possible discount of 14% in end users' energy bill according to the assumed motivation tariff, due to the lower return temperatures achievable compare to the reference yearly average of 40 °C

assumed.

Scenario B: future DH market

In the second scenario, the importance of integration of renewable and low carbon heat sources for future DH markets was evaluated. Lowering supply temperatures compared to the present market would increase the economic benefit for DH companies. Furthermore, lower supply temperatures allow heat sources such as heat pumps to operate more efficiently by increasing the COP, to recover waste heat, to connect solar plants with seasonal storage and to reduce the impact of distribution losses [45].

These future conditions were integrated in the analysis of this scenario, by assuming a motivation tariff where the DH company would guarantee a discount of 1% to end users in their energy bill (up to a maximum of 20%) for each °C lower in the average of supply and return temperatures compared to the reference DH average supply and return. These were assumed as 80/40 °C.

Therefore, the key element of the optimisation was expressed as the minimisation of the average of supply and return temperatures of Equation 4.3 set equal to the specific LMTD for each value of the duration curve defined in Figure 5.6. The objective function and constraints are presented as follows:

i. For all LMTD:

$$minimise\ (Average(T_S; T_R)),\ for\ LMTD = \frac{T_S - T_R}{ln\left(\frac{T_S - T_i}{T_R - T_i}\right)} \tag{5.11}$$

Subject to:

$$50\,^{\circ}\mathrm{C} \leq T_S \leq 80\,^{\circ}\mathrm{C} \tag{5.12}$$

$$\dot{m} \leq \dot{m}_0 \tag{5.13}$$

For this scenario the indoor temperature T_i was set at 20 °C and max mass flow rate $\dot{m}_0$ from Equation 5.10 was 19 kg/h. Each combination of supply and return temperatures fulfilled the constraints' criteria for hydraulic and supply temperature limits.

As presented in Figure 5.7, even in this case, well-controlled double string radiators can achieve low return temperatures. However, compared to scenario A, the outcomes illustrate that the optimal strategy to operate the radiators resulted in a reduction of the supply temperatures and an increased return temperature profile for each LMTD. This was related to the higher economic value associated to the supply temperatures in this scenario. A critical analysis of the curves presented in Figure 5.7 shows for LMTD up to 14 °C the optimal supply and return temperatures are identical for both cases; above that value the curves show the higher the supply temperatures the lower the return ones for each LMTD.

This clearly indicates the compromise to decide whether and to which extent lowering supply and return temperatures is strictly related to the economic benefit that those have for the specific DH system in analysis. To this extent, the strategy to operate the DH network in this scenario and deliver the heat demand

in the area by controlling the supply temperatures according to the optimal level is described in Figure 5.8. The curves show the relationship between the optimal supply and return temperatures linked to the hourly peak load associated to each 1 °C of outdoor temperature.

Hence, operating the DH network and the radiators as proposed would define the strategy to implement LTDH in the area. In fact, as presented in this study [46], LTDH is described as a system operating with supply temperature of 50–55 °C and return of 25–30 °C with the capability of increasing supply to 60–70 °C — with return of 40 °C — when necessary during very low outdoor temperatures. In addition, the new operation of the heating system would guarantee to end users a discount of 16% in their energy bills according to the assumed motivation tariff due to lower average supply and return temperatures obtained in comparison with the reference scenario.

5.3.3 Modelling part — calculation of heating demand of rooms and heating power of plate radiators in a single string system

Single string systems based on plate radiators are operated with higher mass flow rate and lower ΔT between supply and return temperatures. In the Danish experience, the typical operation of single string systems shows that in many cases it is difficult to obtain the expected cooling of return temperatures. In fact, as documented in this Danish report [108], although in same cases it could be necessary and recommended to replace these systems with double string ones,

it is appropriate as first step, technically and economically, to try to adjust the operation of these systems and improve the ΔT. In this direction, the objective of this part of the investigation was to illustrate the capability of the proposed methodology to improve the operation of single string systems. This was applied to the same single-family house assuming in this case the heating system based on single string with plate radiators for only one made up scenario. The hall room was the selected one to demonstrate the method and the outcomes are presented for the four steps as follow.

Step a: calculation of part load duration curve

The design heat load calculated for the specific room, as presented for the double string case, was 884 W according to the steady-state simulations based on the Danish standard [92]. In addition, the same dynamic simulation outputs are presented in Figure 5.9 and depict the room part load duration curve on an hourly basis.

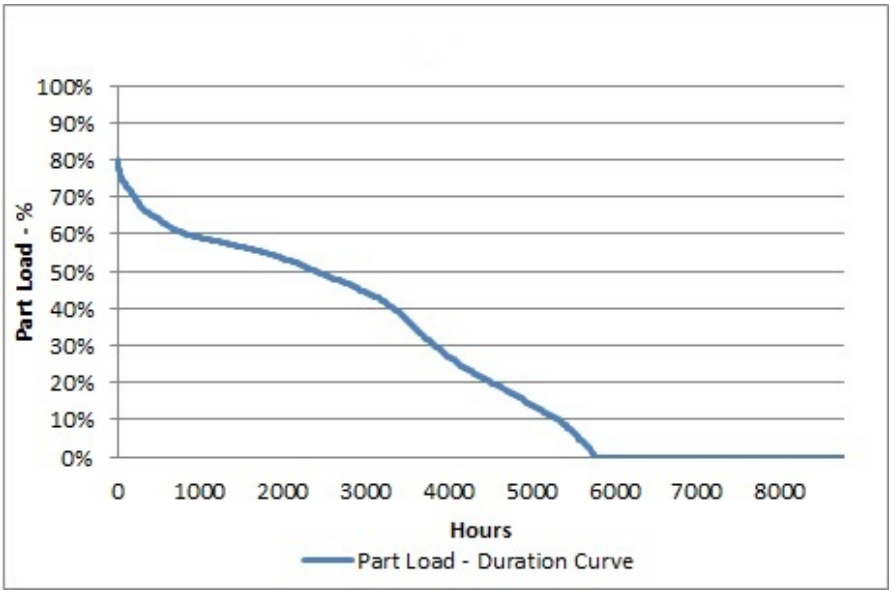

Figure 5.9: Step a: Part load duration curve

Step b: calculation of the relationship between part load and logarithmic mean temperature difference of the hydronic radiator elements

The relationship between each part load and the specific LMTD is presented in Figure 5.10 as a result of the calculations made in step b. The relationship defines how the radiators need to be operated to deliver the specific heat load outlined in step a. It was assumed in this case that the radiators in the single loop were operated at design conditions with supply and return temperatures of 80/75 °C. The calculations of LMTD for each part load were performed using Equation 1 and assuming: 1.3 for n, 884 W for Φ_0, while the $LMTD_0$ was calculated from Equation 2 using the design temperatures of 80/75 °C and set indoor temperatures of 20 °C.

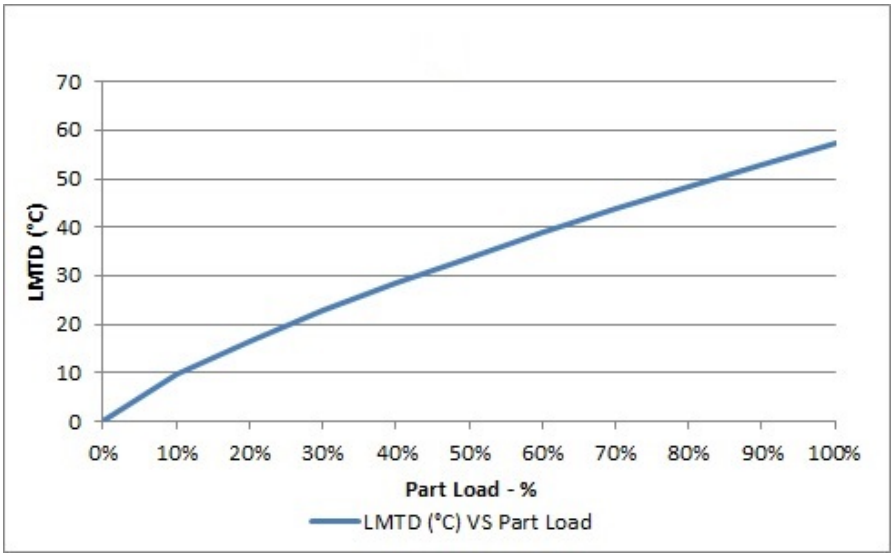

Figure 5.10: Step b: LMTD VS Part load

Step c: calculation of the duration curve of logarithmic mean temperature difference

The duration curve of LMTD based on hourly values is presented in Figure 5.11 and was obtained from the results of the part load duration curve obtained in step a and the relation of part load and LMTD defined in step b.

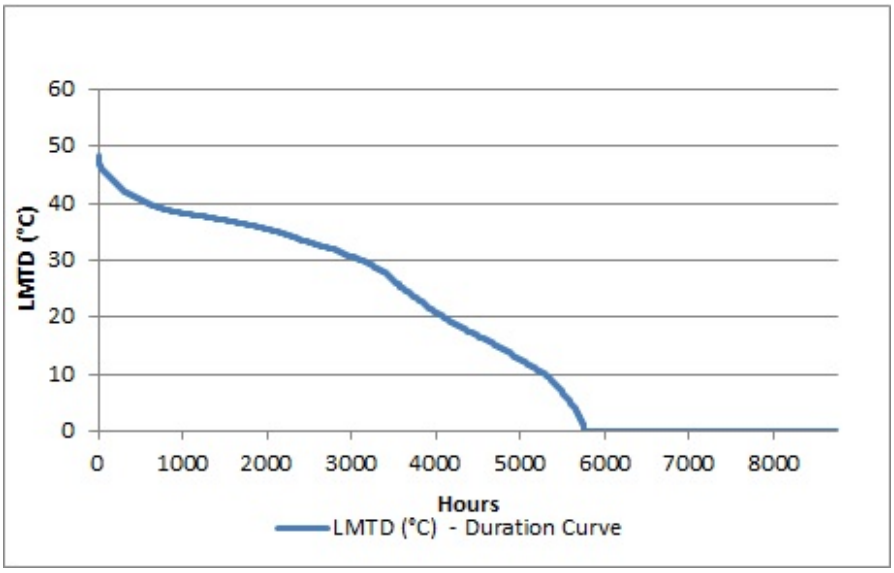

Figure 5.11: Step c: LMTD duration curve

Step d: calculation of the optimal supply and return temperature to provide the necessary logarithmic mean temperature difference

The single string systems based on plate radiators are operated with high mass flow rate to guarantee sufficient inlet temperature to all the radiators connected in series. Due to the typical small temperature difference, assuming a properly designed and controlled system, the strategy to obtain lower return temperatures is related to the possibility of keeping the supply temperatures as low as possible. It was hypothesized for this system a constant ΔT of 5 °C between the supply temperature in the first radiator — assumed as the radiator of the hall room —

and return temperature from the last one. A higher ΔT of 10 or 15 °C could have been considered, but the objective of the analysis was to test the method in the worst case possible. In addition, it was assumed for this scenario a motivation tariff defining a discount of 1% in the end users' energy bill (up to a max of 20%) for each 1 °C reduction in their average supply and return temperature compared to the reference case of the DH network where the building was ideally connected. The reference yearly average supply and return temperature assumed for the DH were 80/40 °C.

Hence, the main criterion of the optimisation was expressed as the minimisation of the average of supply and return temperatures of Equation 4.3 set equal to the specific LMTD for each value of the duration curve of Figure 5.11. The objective function and constraints for this scenario are presented as follows:

i. For all LMTD:

$$minimise\ (Average(T_S; T_R)),\ for\ LMTD = \frac{T_S - T_R}{ln\left(\frac{T_S - T_i}{T_R - T_i}\right)} \tag{5.14}$$

Subject to:

$$\Delta T = 5\,^{\circ}\mathrm{C} \tag{5.15}$$

$$50\,^{\circ}\mathrm{C} \leq T_S \leq 80\,^{\circ}\mathrm{C} \tag{5.16}$$

$$\dot{m} \leq \dot{m}_0 \tag{5.17}$$

The indoor temperature was fixed at 20 °C while the maximum mass flow rate

obtained from Equation 5.10 was 152 kg/h. All the optimal combinations of supply and return temperatures are presented in Figure 5.12 and fulfilled the constraints' criteria. In particular, as a constant ΔT of 5 °C was assumed, the optimized supply temperatures presented in Figure 5.12 is the optimized inlet temperature for the hall room radiator — assumed as the first in the single string system, whereas the return temperatures describe the temperatures out of the last radiator.

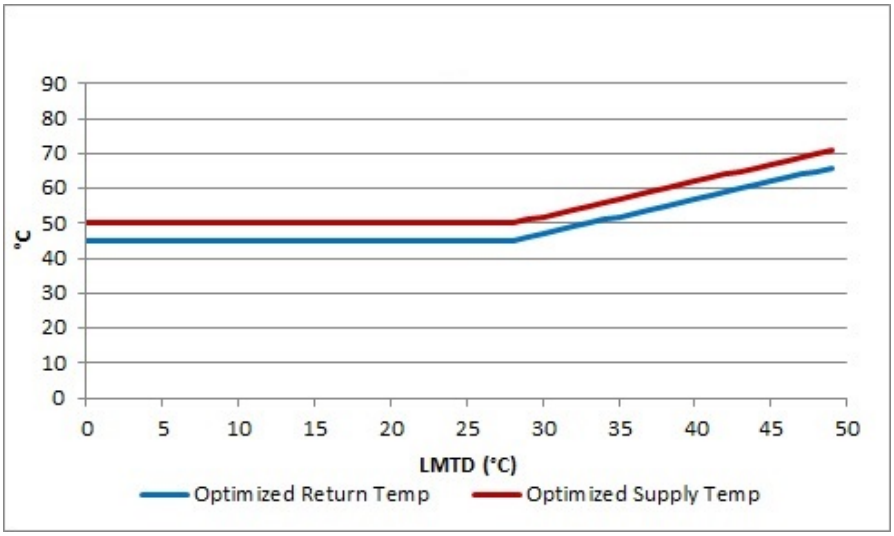

Figure 5.12: Step d: Optimised Supply and return temperatures

The ΔT of 5 °C, between supply and return temperatures, was always kept constant in order to ensure that even the last radiator of the loop would have been able to deliver the specific heat required. The supply temperatures instead are limited due to the same conditions presented for the double loop system and out of the heating season it was assumed that temperatures of 50/20 °C were enough to meet the DHW demand.

Although very low return temperatures — close to room temperature — were not achieved, the outcomes of the optimization show that these systems can be

operated more efficiently and in particular unnecessary high supply and return temperatures can be avoided. In fact, operating the single string system as proposed, if properly designed and controlled, a possible discount of 5% in the end users' energy bills could be obtained according to the hypothesized motivation tariff without any intervention to building or to the heating system.

5.4 Summary

The developed methodology was used to investigate and plan the application of LTDH to hydronic radiators in existing buildings. The results related to the double string scenarios showed the optimal operation of the existing plate radiators, properly controlled through TRVs and DH network, by adjusting the supply temperatures to the optimal level, achieved low return temperatures. This would allow existing buildings to be connected to LTDH without any intervention in the thermal envelope, through simply adjusting the temperatures according to demand, and obtain cost savings in the end users' energy bills. The strategy proposed for both scenarios A and B illustrated that a possible discount of 14% and 16% could be achieved in annual energy bills.

Also, the design curves suggest the strategy to be followed for lowering supply and return temperatures has to be related to the economic impact those have in the DH network in analysis. For the case of single string systems with plate radiators, the results illustrate that very low return temperatures were not possible due to the differences in the way these systems are operated. If the objective of the investigation in the area is the implementation of LTDH, if technically and economically feasible, these systems should be replaced or converted to double loop. However, it should be noted that the application of the method, even for this type of heating system, allowed the heating system to operate more efficiently and avoid unnecessary high supply and return temperatures. This was quantified for the assumed scenario by a possible discount of 5% in the end users' energy bills.

Only one building and one room were used in this study to demonstrate the reliability of the methodology. The full application of the developed method was investigated using a UK small scale DH network as case study as detailed in Chapter 6.

Chapter 6

Optimisation of operation of a UK small scale DH network

6.1 Introduction

This chapter presents the results of the analysis related to an existing small DH network located in the Nottinghamshire, UK. The research work, as highlighted in Section 1.4, took advantage of the collaboration with Sasie Ltd and DTU.

In this case study an accurate description of the existing DH network, building characteristics and heat loads were detailed. The Estate energy loads were both measured and modelled using the energy software IDA-ICE.

The network supply and return temperature optimisation was carried using the methodology illustrated in Chapter 4. The optimisation presented is focused on the buildings having double string hydronic radiators.

Once the new operating temperature profiles have been defined, a comparison is presented between the reference scenario and optimised one. The analysis is performed using TERMIS to simulate the heat network performances and the results illustrate the possible improvements in the distribution losses, operating temperatures and heat energy generation.

6.2 Site overview

This case study is based on an isolated small scale DH network supplying a mixture of buildings types on a farm north of Nottingham. Figure 6.1 shows the aerial view of the Estate.

Figure 6.1: Estate Google Earth view

The heat network was introduced in 2006 and its layout was modified before the heating season 2014/2015 to allow the connection of new buildings to the network. Eight different buildings are actually connected to the network. These

are a combination of offices (OF 1 and 2), domestic building (DB 1), live/work (LW 1 to 4) and a new live/work building (NB 1) built and connected at the end of 2015 as shown in Figure 6.1. The characteristic of the live/work buildings is that they combine in the same indoor environment both working and domestic spaces. A summary including area, activity and occupancy for each building is highlighted in Table 6.1, whereas detailed plans and drawings are included in Appendix I.

Table 6.1: Buildings' highlights

Building	**Occupants office**	**Occupants domestic**	**Total floor area (m^2)**
LW 1	4	2	256
LW 2	1	3	535
LW 3	5	-	535
LW 4	5	1	535
DB 1	-	2	209
OF 1	33	-	760
OF 2	40	-	564
NB 1	-	-	517

The heat network, fuelled by a condensing biomass boiler and connected to all the buildings of the Estate, covers only the SH demand, whereas the DHW is provided by individual electric heaters. The fuel for the biomass boiler, in the form of willow wood chips, is grown and coppiced on site.

6.2.1 Buildings description

An energy model was built for each building using the energy software IDA-ICE, considering the specific thermal properties in accordance to the UK building regulations. The Estate is composed by a mix of different buildings characterised by different energy consumption, activities and heating systems. OF 2, DB 1 and LW 1 are existing building renovated before 2006 and key data and construction elements are summarised in Table 6.2. LW 2, 3 and 4 instead are three identical new builings built according to UK Building Regulations 2006 part L1A and L2A [109,110] and key data and construction elements are presented in Table 6.3.

Table 6.2: Key data and construction elements for renovated buildings

Building construction elements	**U-value (W/m^2K)**
Brick cavity wall	0.7
Roof-tiles and insulation	0.7
Floors	0.7
Windows — double glazed	2.9
Design air permeability	**$m^3/h \cdot m^2$ at 50 Pa**
Renovated buildings	7.0

Table 6.3: Key data and construction elements for new buildings

Building construction elements	**U-value (W/m^2K)**
Brick cavity wall	0.35
Roof-tiles and insulation	0.35
Floors	0.35
Windows — double glazed	2.9
Design air permeability	**$m^3/h \cdot m^2$ at 50 Pa**
LW 2, 3 and 4	7.0

The largest building of the estate OF1, used as office space, is a listed "*Grade II*" building according to the UK application of part L of the building regulations to historic and traditionally constructed buildings [111]. The building is characterised by solid brick walls and single glazed windows with wooden frame. To preserve the architecture heritage, these buildings cannot be renovated and only the roof has been replaced as it was seriously damaged. The thermal properties of the building elements are given in Table 6.4. The Estate was granted a construction permit to build a new live/work home, NB 1, which was completed in 2015. The house was built according to the UK building regulations 2010 L1A and L2A [112, 113]and the thermal properties of the NB 1 elements are given in Table 6.5.

Table 6.4: Key data and construction elements for office 1 [114, 115]

Building construction elements	**U-value (W/m^2K)**
Solid bricks wall	2.09
Roof-tiles and insulation	0.35
Floors	0.7
Windows — single glazed wooden frame	4.9
Design air permeability	**$m^3/h \cdot m^2$ at 50 Pa**
OF 1	20.0

Table 6.5: Key data and construction elements for new building 1

Building construction elements	**U-value (W/m^2K)**
Wall	0.23
Roof	0.15
Floors	0.2
Windows	1.5
Design air permeability	**$m^3/h \cdot m^2$ at 50 Pa**
NB 1	5.0

In accordance to CIBSE standards [114], for office areas, typical values of heat gains of 12 and 15 W/m^2 were assumed respectively for lighting and equipment — including computers and office equipment; whereas 5 W/m^2 was considered for

internal heat gains for the case of domestic spaces. While the suggested value for lighting is kept constant regardless the occupancy of the offices, the values related to equipment vary according to density. The choice made is on the conservative end and reflects the fact that none of the offices have large and dense open-space working environments.

The indoor comfort for all buildings is controlled by implementing a night set-back strategy with target temperatures of 21/18 °C. This was supported by real measurements taken with the "EL-USB-1 Temperature Data Logger" — with accuracy of ±1 °C — during the months of January and February 2014 for one room of OF 1 and during January 2014 for one room of DB 1. An extract of the data are proposed in Figure 6.2 and 6.3 for one week in January and February 2014 for OF 1 and in Figure 6.4 for one week in January 2014 for DB 1.

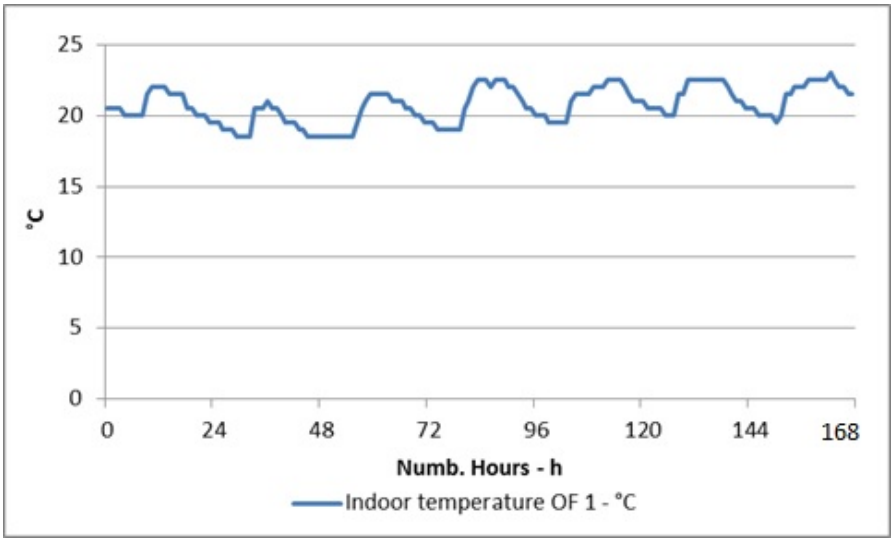

Figure 6.2: Indoor temperature OF 1 — 11/01/14 to 17/01/14

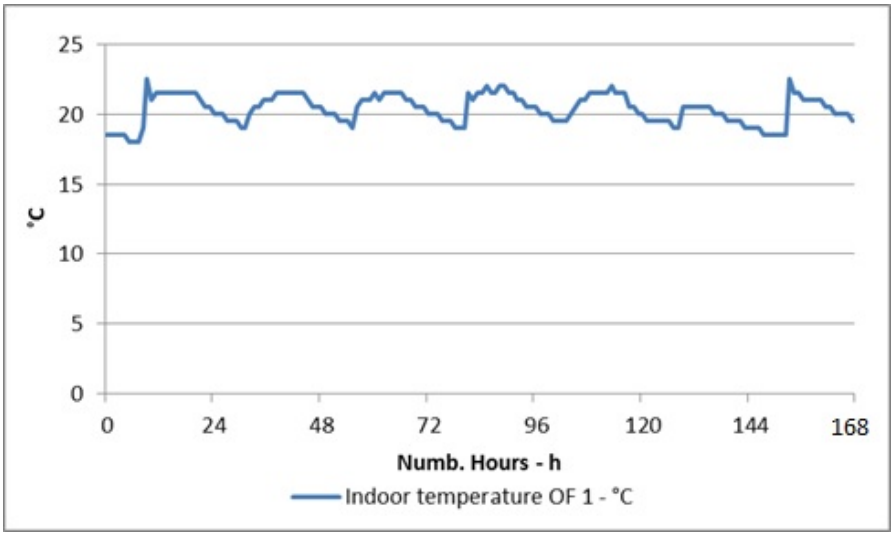

Figure 6.3: Indoor temperature OF 1 — 10/02/14 to 16/02/14

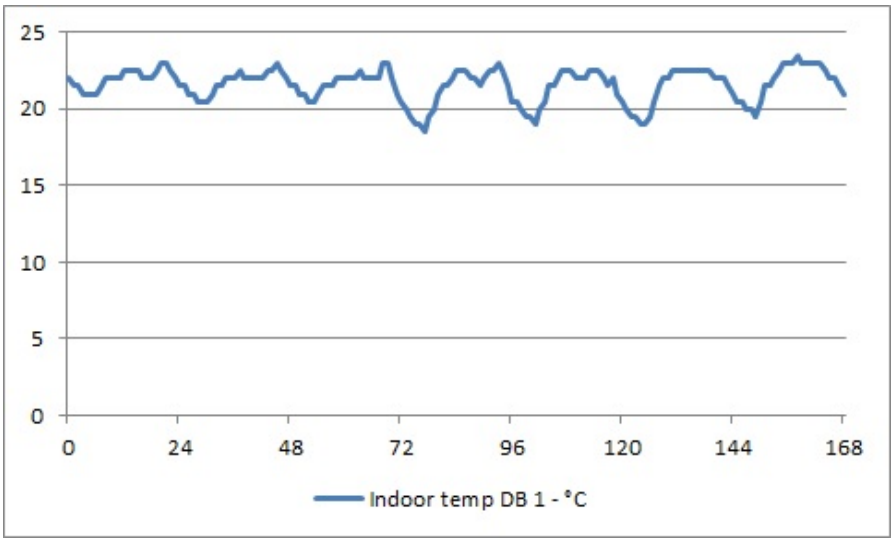

Figure 6.4: Indoor temperature DB 1 — 10/01/14 to 17/01/14

Furthermore, according to CIBSE standards [116] a dry-bulb temperature of $-3.9\,^{\circ}\mathrm{C}$ was assumed as winter design temperature for Nottingham and as described in Section 4.3.2, a CIBSE yearly weather data file was used as input in the IDA-ICE physical models. Finally, as part of the preliminary energy audit of the Estate, a thermal imaging survey was undertaken on the 5^{th} of March 2013 to assess the thermal performances of the buildings' envelopes. Even though the results

of the survey were not directly used in this investigation, these are summarised in Appendix H.

6.2.2 Heat Network

The heat network, fuelled by a biomass boiler, delivers heat to end-users to meet the SH demand, while DHW is provided by dedicated electric heaters installed in each building. A reconfiguration of the heat network was undertaken before the beginning of the heating season 2014/2015 to allow for the connection of NB 1 and other two buildings in the next 5 years.

A new condensing biomass boiler Schmid UTLS of 199 kW was installed on site and a detailed illustration of it is given in Figure 6.5. The boiler is able to burn both wood-chips and pellets with a maximum moisture content of 40%, modulate heat output capacity and work with maximum pressure of 3 bar.

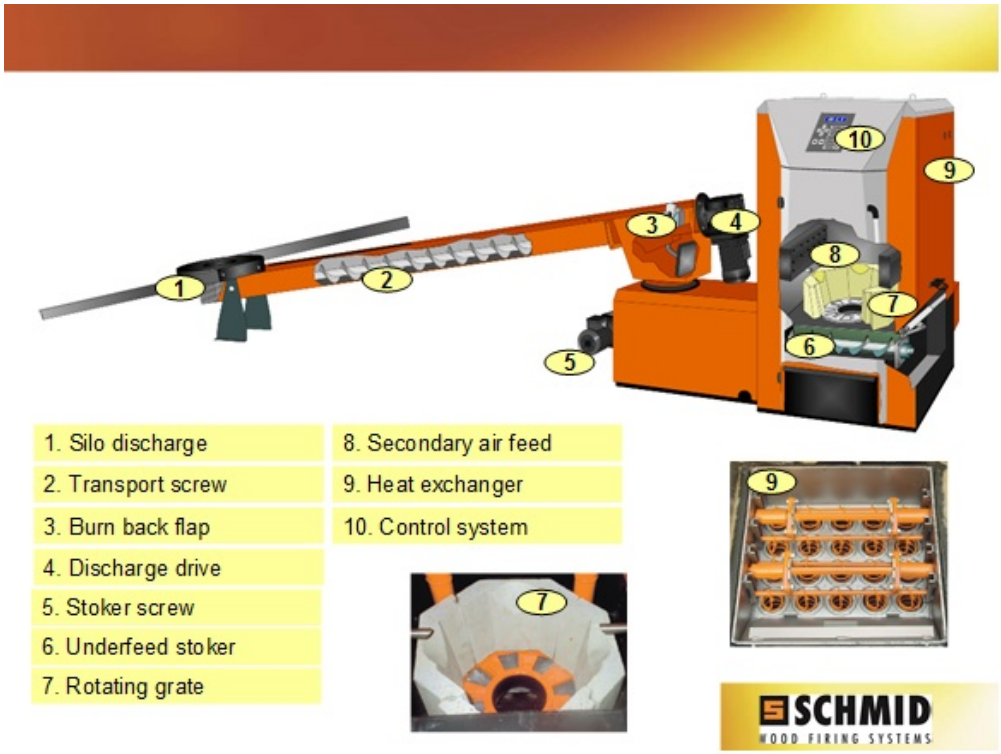

Figure 6.5: Schmid UTLS boiler [117]

The design choice of the new biomass boiler heating capacity of 199 kW was to displace part of the heat supplied by the current ageing boiler and maximise the renewable heat incentives (RHI) guaranteed by the UK government. The tariff for the specific case, connected before October 2014 is 8.63 p/kWh, while the historical database can be found through the Ofgem portal [118]. The old biomass condensing boiler of 300 kW — manufactured by Binder [119] — was also moved to the new plant room as back up solution. A dedicated smart meter was installed by Ofgem to monitor the heat generated on site by the biomass boilers. However, the data for which it was commercially sensitive were not made available.

The biomass boiler was coupled to a $5m^3$ Cordivari storage tank, as this is a typical requirement from manufacturers to let operate the boiler smoothly and

avoid on/off cycles which have a negative effect of the overall efficiency. In addition, a Groundfos twin-head pump — model Magna–3 65–150, see Figure 6.6 — with capability to adjust speed provides the mass flow rate in the network, with supply pressure of 1.5 bar. Technical specifications of equipment are enclosed in Appendix A, B and C .

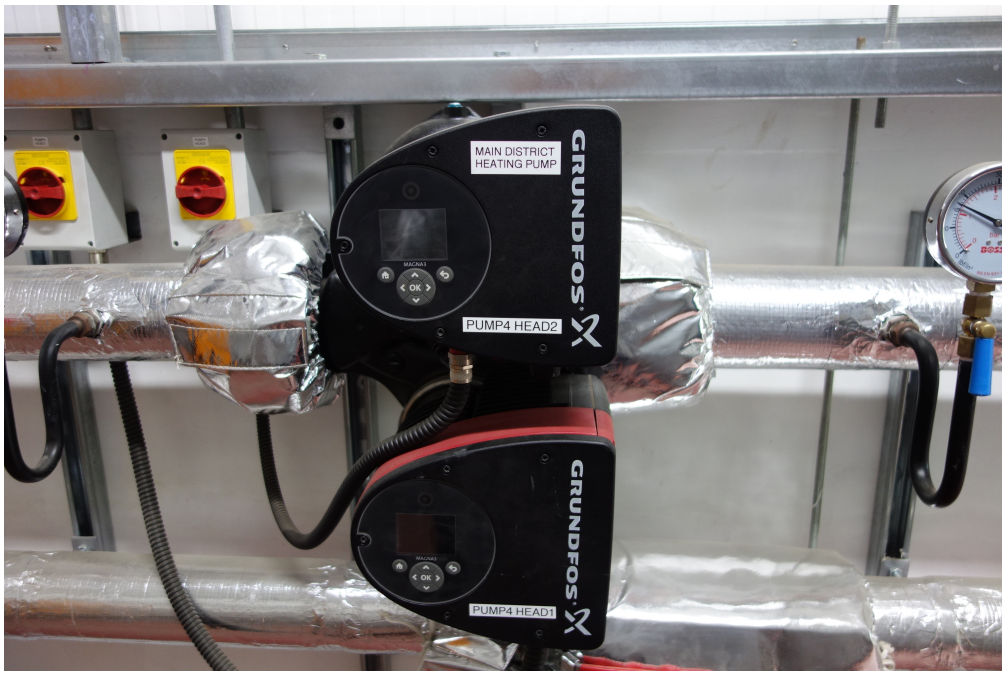

Figure 6.6: Groundfos twin-head pump

A schematic view of the small scale DH network is presented in Figure 6.7. The structure of the network has a typical tree configuration, with no loops. There is only one generation point and in the rearrangement of the network in 2014 new supply and return pipes were introduced, labelled in the schematic as A-D and B-C. The new lines allowed the integration of the old network to the new heat generation point through node D and to connect NB 1 through pipe B-C. The two new buildings planned to be built in the next five years will be placed in the area adjacent to NB 1 — see Figure 6.1.

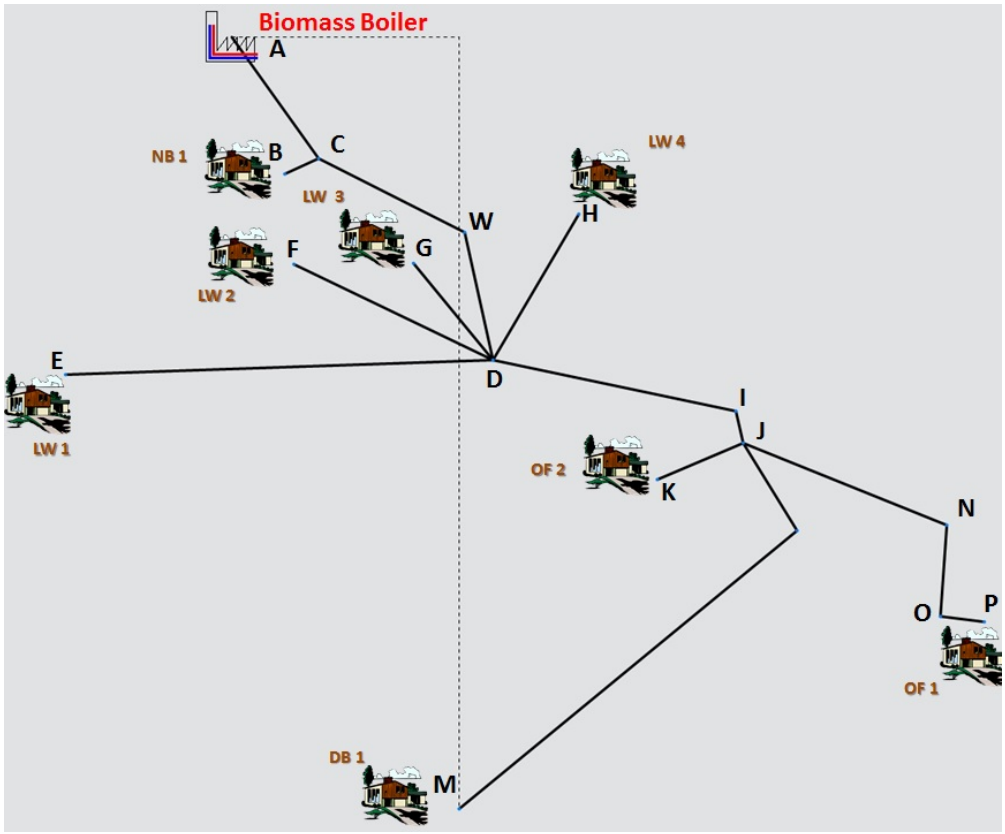

Figure 6.7: Heat network schematic

The network is composed of a mix of double and twin pre-insulated pipes using two different manufacturers: Rehau and Flexalen. Key data for each pipe are summarised in Table 6.6. Full technical specifications are attached in Appendix D and E.

Table 6.6: Rehau and Flexalen pipes key data

Pipe	**Manufacturer**	**DN (mm)**	**Thermal conductivity** (W/mK)	**Length (m)**
A-C	Re63Duo**	51.4	0.21	42
B-C	Re32Duo**	26.2	0.16	6
C-W	Re63Duo**	51.4	0.21	43
W-D	Re63Duo**	51.4	0.21	42
D-E	Flex40Duo**	32.6	0.23	116
D-F	Flex32Duo**	26.2	0.26	63
D-G	Flex32Duo**	26.2	0.26	29
D-H	Flex32Duo**	26.2	0.26	36
D-I	Flex63Uno*	51.4	0.28	60
I-J	Flex63Uno*	51.4	0.28	5
J-K	Flex32Duo**	26.2	0.26	20
J-L	Flex32Duo**	26.2	0.26	20
L-M	Flex32Duo**	26.2	0.26	54
J-N	Flex63Uno*	51.4	0.28	36
N-O	Flex63Uno*	51.4	0.2	20
O-P	Flex63Uno*	51.4	0.2	8

* UNO refers to double pipes

** DUO refers to twin pipes

The operation of the heat network was monitored for the heating season 2014/2015 and the average supply and return temperatures recorded were 72/55 °C. An extract of the data are presented in Figure 6.8 and 6.9, which shows the hourly temperature fluctuation for one week. The measurements were gathered by using a data logger — Datataker type 500 — and temperature sensors PT 100 — characterised by accuracy of ±0.1 °C — installed in the supply and return lines at the heat generation point.

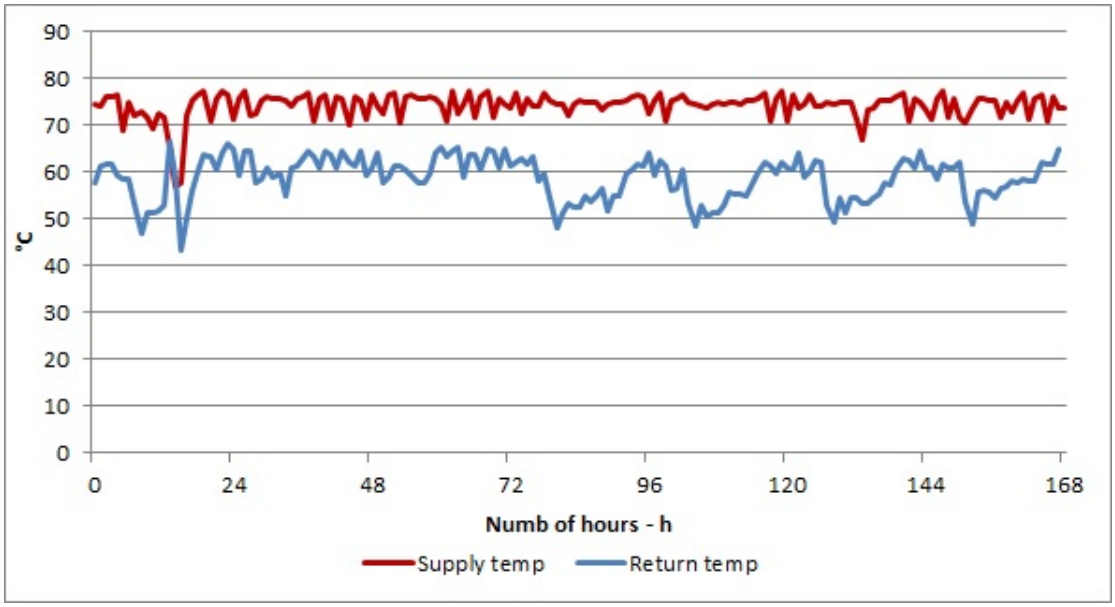

Figure 6.8: Supply and return temperature variation: 10/10/14 to 16/10/14

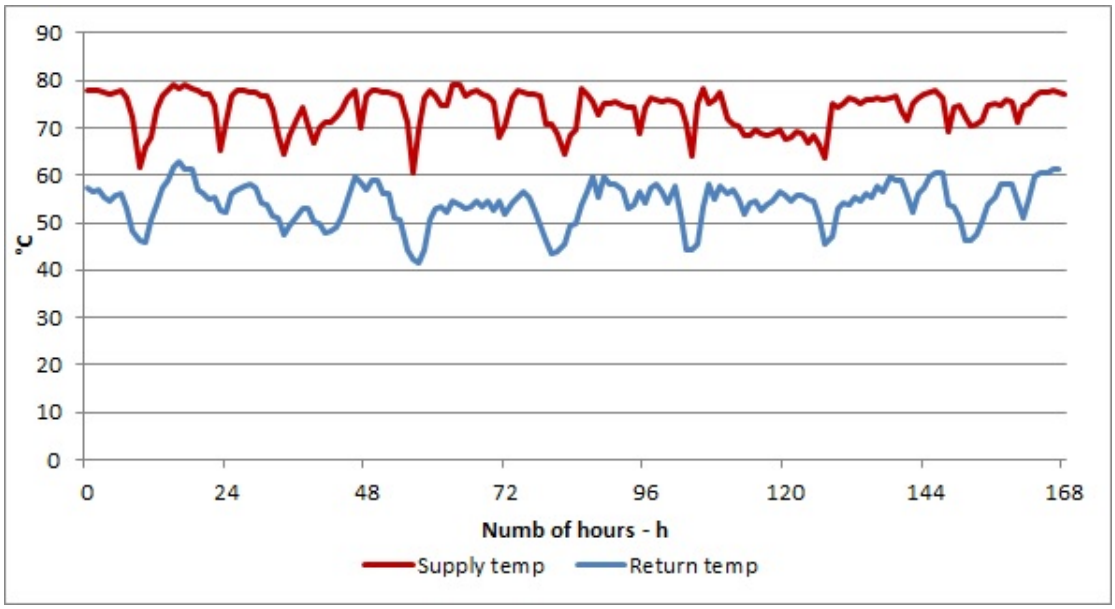

Figure 6.9: Supply and return temperature variation: 21/02/15 to 27/02/15

Each end-user is connected to the network through dedicated heat interface units (HIU). A typical installation of HIU in LW 2 is given in Figure 6.10. This was sized for a heat load of 50 kW, with design temperatures of 82/55 °C and 70/50 °C for the primary and secondary side respectively. The main components included in a typical HIU to interface end-users with DH networks are highlighted

in Figure 6.10 and listed as follow:

- Plate HE for SH demand
- Supply and return pipes from DH
- Supply and return pipes to UFH
- Pressure valve control
- Kamstrup smart meter
- Blending valve before UFH loops

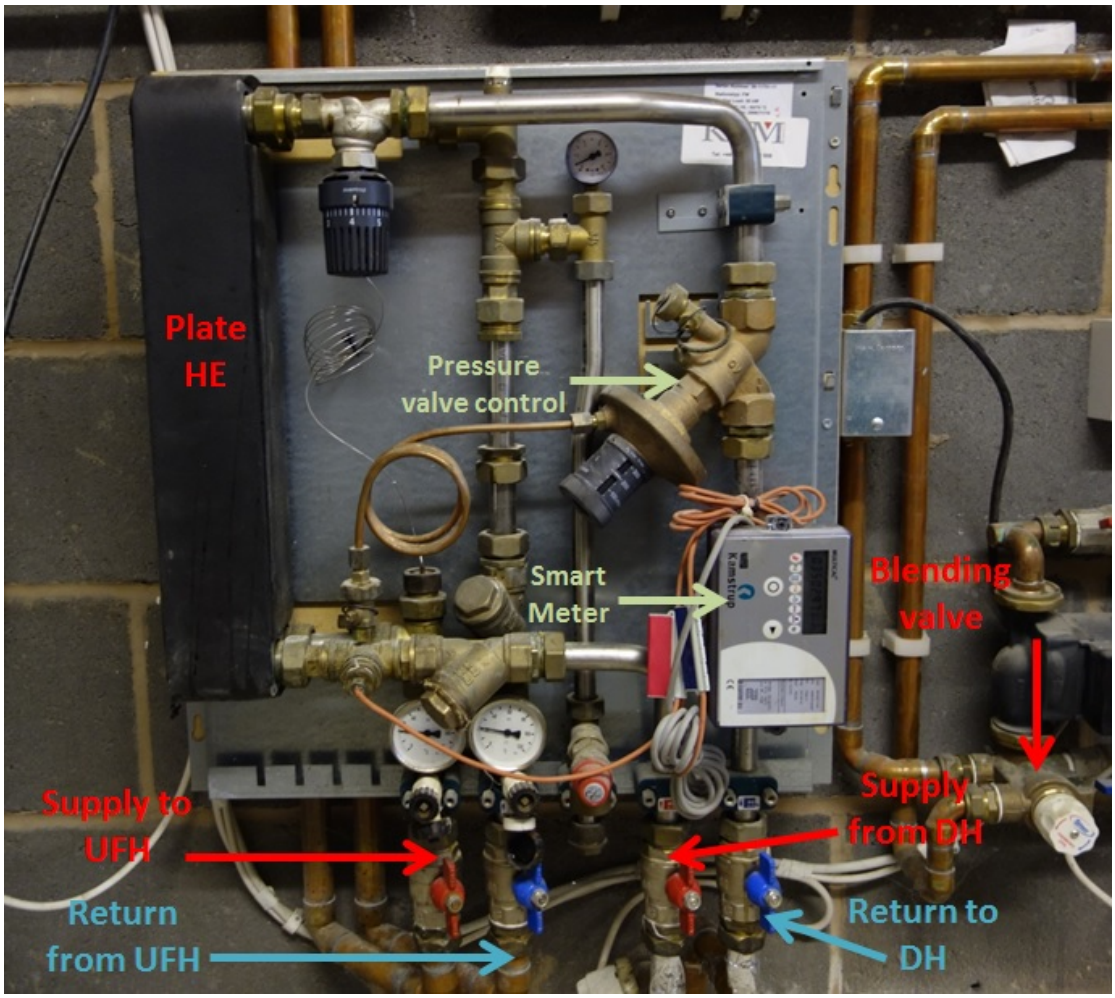

Figure 6.10: Heat interface unit at LW 2

The different heating systems associated to each building — UFH and double string plate radiators — are reported in Table 6.7. Typically, good operation of both DHW and SH systems allows to achieve good ΔT at the HIU and dictates the return temperature level in the DH network [10, 87]; as only SH demand is covered by the heat network of this case study, the efficient operation of the heating systems is crucial to achieve low return temperatures.

Table 6.7: Heat emitting systems installed in the buildings

Building	**UFH**	**Radiators**
LW 1	X	-
LW 2	X	-
LW 3	X	-
LW 4	X	-
DB 1	-	X
OF 1	-	X
OF 2	-	X

Access to monitor operating conditions of end-users was permitted only to LW 2. The gathered data from the HIU for the heating season 2014/2015 shows an average supply and return temperatures of 64/47 °C with a ΔT of 17 °C. An extract of the data are plotted on hourly basis in Figure 6.11 for one week during January 2015.

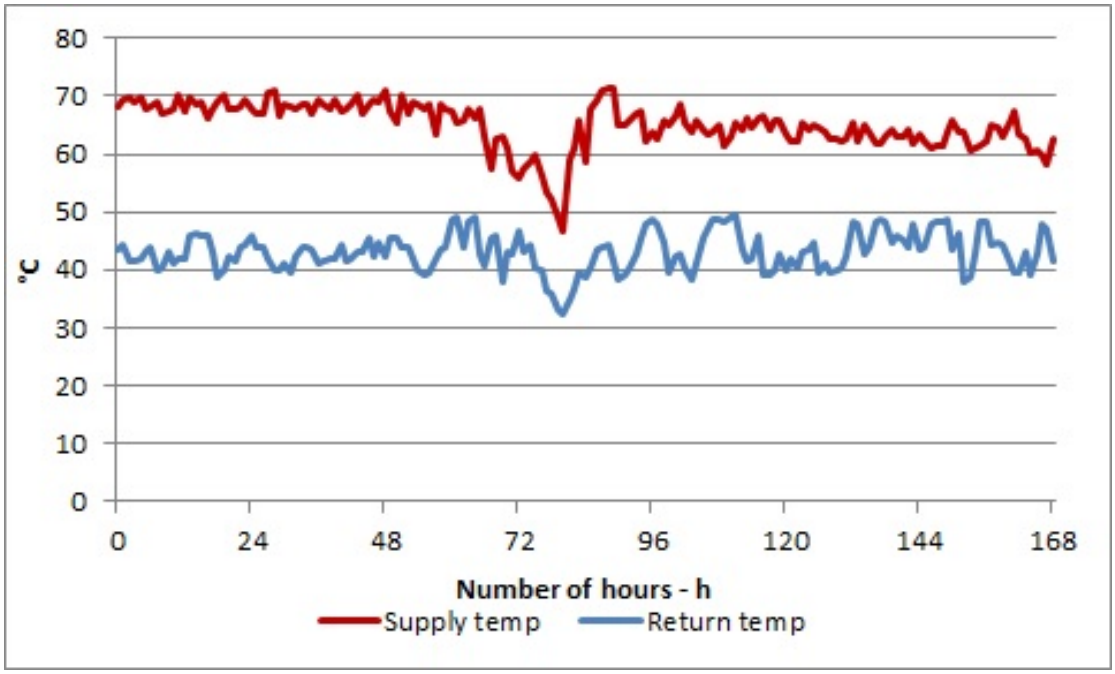

Figure 6.11: Supply and return temperature variations at HIU of LW 2: 20/01/15 to 26/01/15

Compared to typical operation of UFH systems, the measurements from the HIU of LW 2 clearly illustrate higher temperatures compared to what normally expected with UFH. In fact, these heating systems are usually designed to be operated with inlet temperatures within the range of 40–50 °C and ΔT of 5–10 °C [47, 93]. In low energy buildings, lower supply temperatures of 30 °C are possible, resulting in return temperature close to the occupied space temperature [57].

The reason for such high temperatures is related to the setting of the supply temperature at the blending valve installed before the inlet of the supply loop of the UFH — see Figure 6.10. This in fact is fixed at 60 °C as highlighted in Figure 6.12.

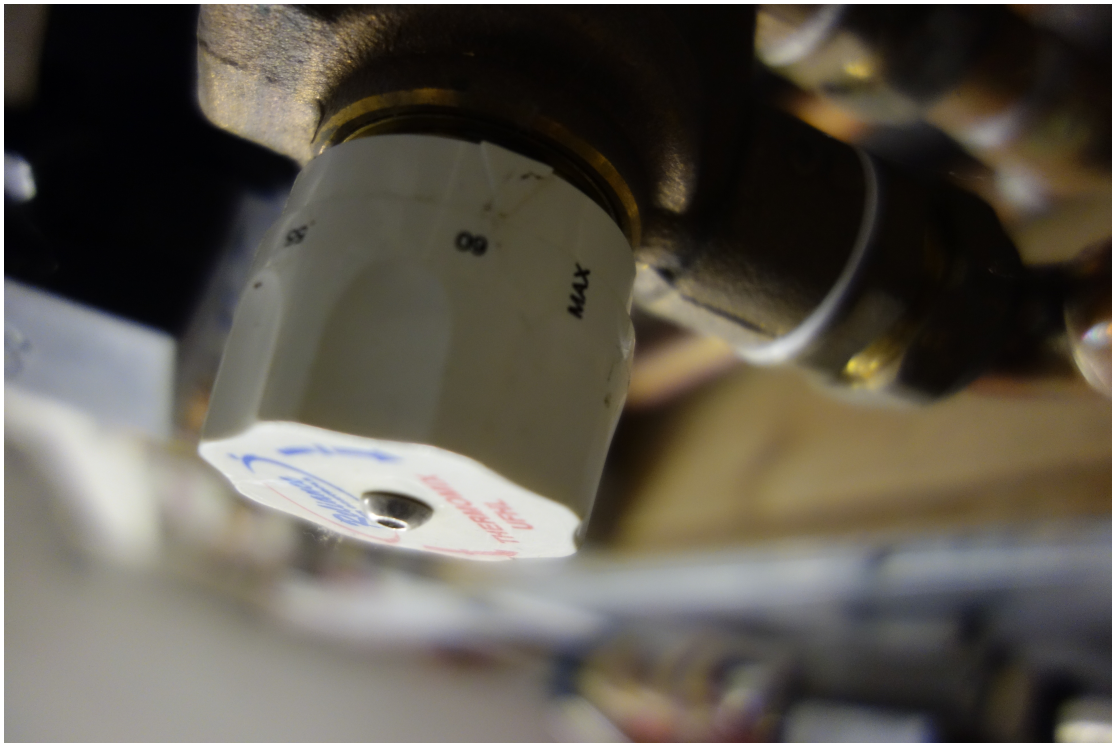

Figure 6.12: Blending valve setting of inlet circuit of the UFH of LW 2

Such high temperatures in UFH systems are typically the cause of indoor discomfort as well as the decay of the efficiency and durability of the installed components, as prescribed by manufactures. From this perspective, the recorded average supply and return temperatures for the small scale DH network of 72/55 °C clearly suggests that the inlet temperature of 60 °C, represents the chosen operational setting for the buildings with UFH. Therefore, this is one of the key areas assessed in the optimisation of the operation of the heat network analysed in this investigation.

6.3 Optimisation of operation of heating systems based on plate radiators

The first step in the optimisation of the operation of the small scale DH started with the analysis of the buildings with plate radiators — OF 1, LW 1 and DB 1. The results illustrate the full application of the method described in Chapter 4 and presented in Chapter 5 for one room and one building.

The approach considered two different scenarios:

- Scenario A: the indoor comfort is controlled with night set-back strategy, which represents the real conditions of the Estate
- Scenario B: a constant indoor temperature was set as an alternative strategy to control indoor comfort

6.3.1 Scenario A: indoor comfort controlled by night set-back strategy

A model was built in IDA-ICE for each building using the physical features presented in Section 6.2.1 and using 21/18 °C as night set-back control strategy. Figure 6.13 shows as an example the IDA-ICE model built for OF 1, whereas the other models are enclosed in Appendix F.

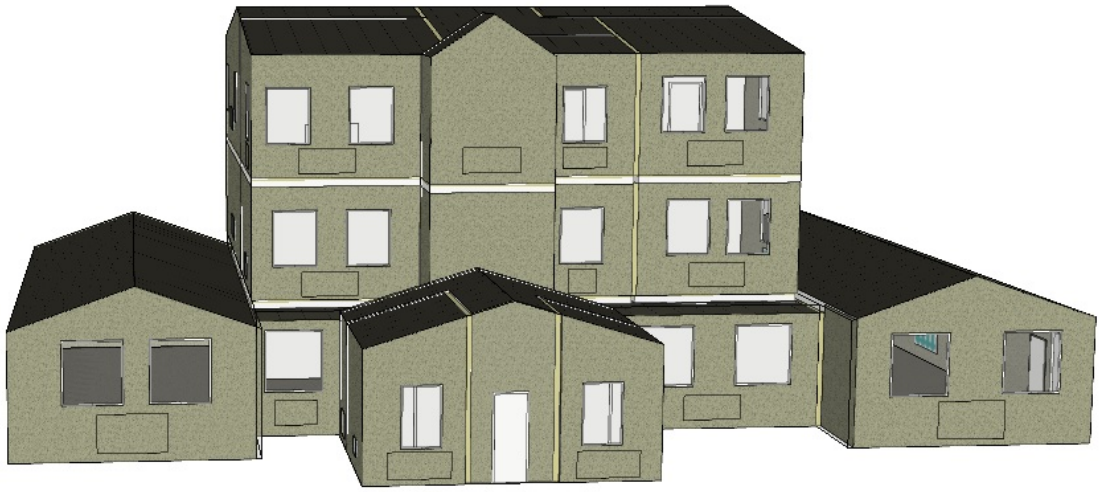

Figure 6.13: IDA-ICE model for OF 1

The results of the simulations for the annual energy consumption are compared with the real average annual energy consumptions for each building. These are obtained using recorded data from 2007 to 2012 and the comparison is presented in Table 6.8.

Table 6.8: Comparison between simulated and recorded annual energy consumption

Building	**Simulated results (MWh)**	**Recorded data (MWh)**
LW 1	26.7	26.3
LW 2	46.4	44.7
DB 1	26.7	27.7
OF 1	113.5	115.6
OF 2	71.8	70.4

The data is gathered from each building by dedicated smart heat meters — Kamstrup Multical 401 — which allow to monitor major operating parameters of the system as well as to quantify energy consumption for billing purpose. The results highlight good match between simulation and real energy consumption. It is important to notice that in the analysis and comparison presented in Table 6.8, LW 3, LW 4 and NB 1 are not included as no real measurements were available. LW 3 and 4 because no robust data was available, whereas NB 1 because was built and connected to the network in late 2015. However, this is not affecting the application of the proposed methodology, as the building in the Estate having double string plate radiators are OF 1, LW 1 and DB 1.

Step a: calculation of part load duration curve

The part load duration curves are the results of the dynamic simulations as presented in Figure 6.14 for the entire year on hourly base. Differently from what presented in Figure 5.4, the method was applied to all rooms and all buildings having hydronic radiators and connected to the network.

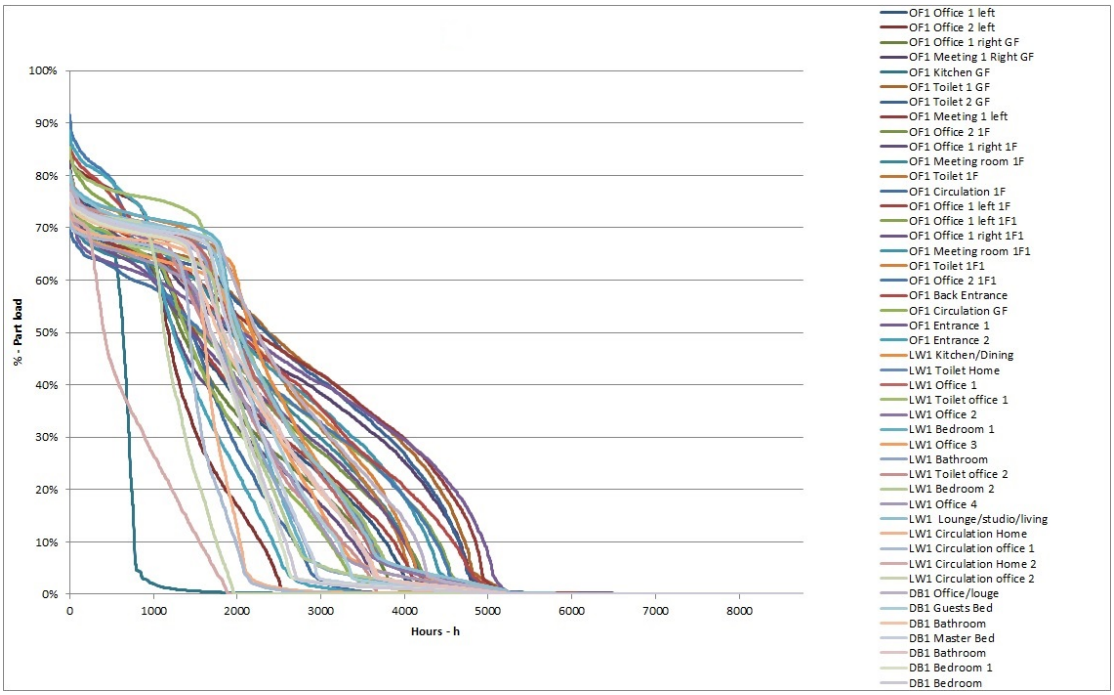

Figure 6.14: Step a — Part load duration curves for all rooms and all buildings

Step b: calculation of the relationship between part load and logarithmic mean temperature difference of the hydronic radiator elements

The results for step b presented in Figure 6.15 for one room of OF1 as an example — OF1 office 1 left — illustrate the relationship between each part load and the specific LMTD, expressing how the radiators need to be operated. According to UK design practise, it was assumed that the radiators in the double string configuration at design conditions were operated with supply and return temperatures of 82/70 °C and that the radiators in the rooms were sized accordingly. Hence, to correctly perform the calculations of LMTD per each part load using Equation 4.2, n was assumed to be 1.3, Φ_0 was the design heat load of 1940 W and $LMTD_0$ was obtained from Equation 4.3 using the design temperatures of 82/70 °C and set indoor temperatures of 20 °C.

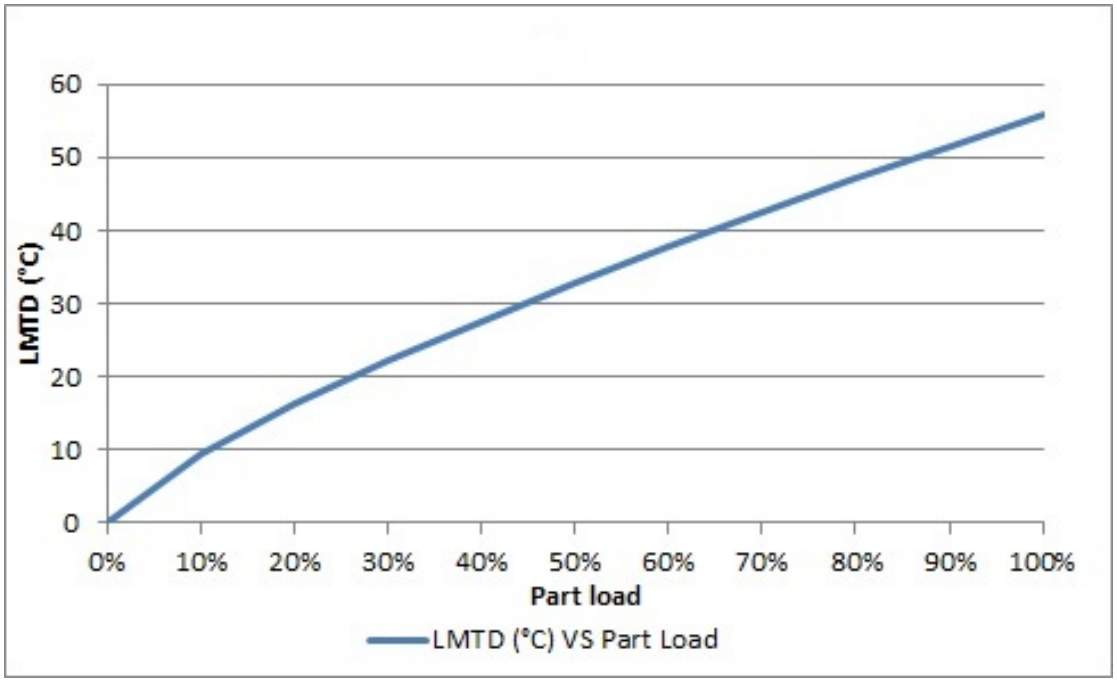

Figure 6.15: Step b — LMTD VS Part load

Step c: calculation of the duration curve of logarithmic mean temperature difference

The part load duration curve presented in Figure 6.14 and the general relation between the part load and LMTD in Figure 6.15 allowed the calculation of the duration curve of LMTD on an hourly basis for all rooms and all buildings as described in Figure 6.16.

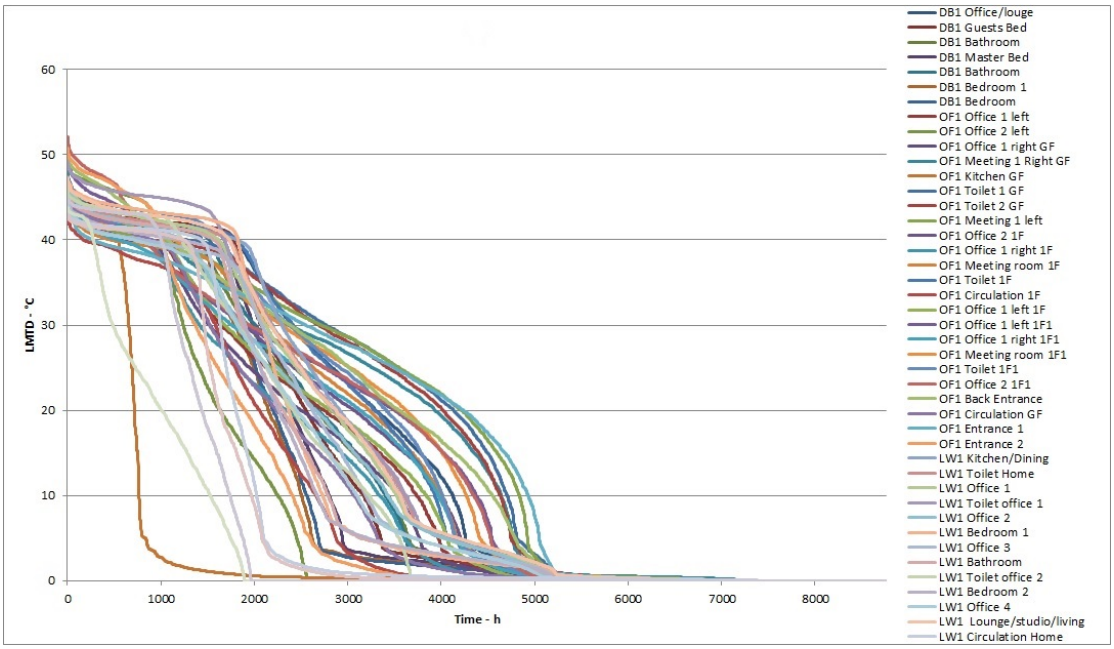

Figure 6.16: Step c — LMTD duration curves

The analysis of all curves allowed to compare and define for the specific case the conditions and the boundaries to be investigated for identifying to which extent operating temperatures can be lowered in the network. This is obtained by defining the curve representing the worst case as combination of the highest LMTD within all curves of all rooms for each time step as presented in Figure 6.17.

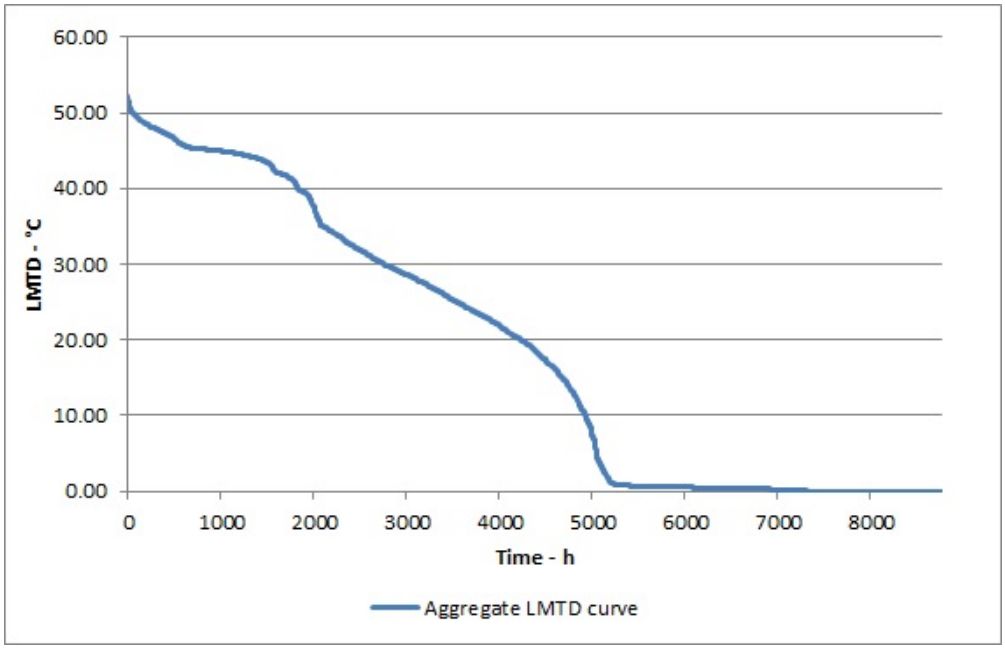

Figure 6.17: Step c — Aggregate LMTD duration curve based on highest LMTD

Step d: calculation of the optimal supply and return temperature to provide the necessary logarithmic mean temperature difference

As the network of this case study is fuelled by a biomass boiler with flue gas condenser, similarly to the Scenario A presented for double string radiators in Chapter 5, the formulation of the optimisation was mainly focused on the reduction of return temperature due to the higher economic value that this has with condensing boiler technologies compared to lower distribution losses.

It was hypothesised a motivation tariff to incentivise the customers connected to the network in analysis to achieve a better use of energy and obtain lower return temperatures in exchange of a discount in their energy bills. As the commercially sensisitive data for the site were not made available, the tariff was based on the example of the existing Danish DH company presented in Chapter 5 [107] and

customised to guarantee to the end users a discount of 1% in their energy bill (up to a maximum of 20%) for each °C lower in their return temperatures compared to the reference DH yearly average return temperature. The reference average supply and return temperature for the site are 72/55 °C as presented in the Section 6.2.2. The assumption made in the optimisation problem of weighting mostly the low return temperatures was also justified by the fact that the heat network in analysis has contained dimension in length, which implies that the distribution losses through the pre-insulated pipes have a minor impact in the overall efficiency and operational costs.

Hence, the optimisation focused on the minimisation of the supply and return temperatures of Equation 4.3 set equal to the specific LMTD for each value of the duration curve presented in Figure 6.17. The results are presented in Figure 6.18 for the set indoor temperatures of 21 and 18 °C respectively.

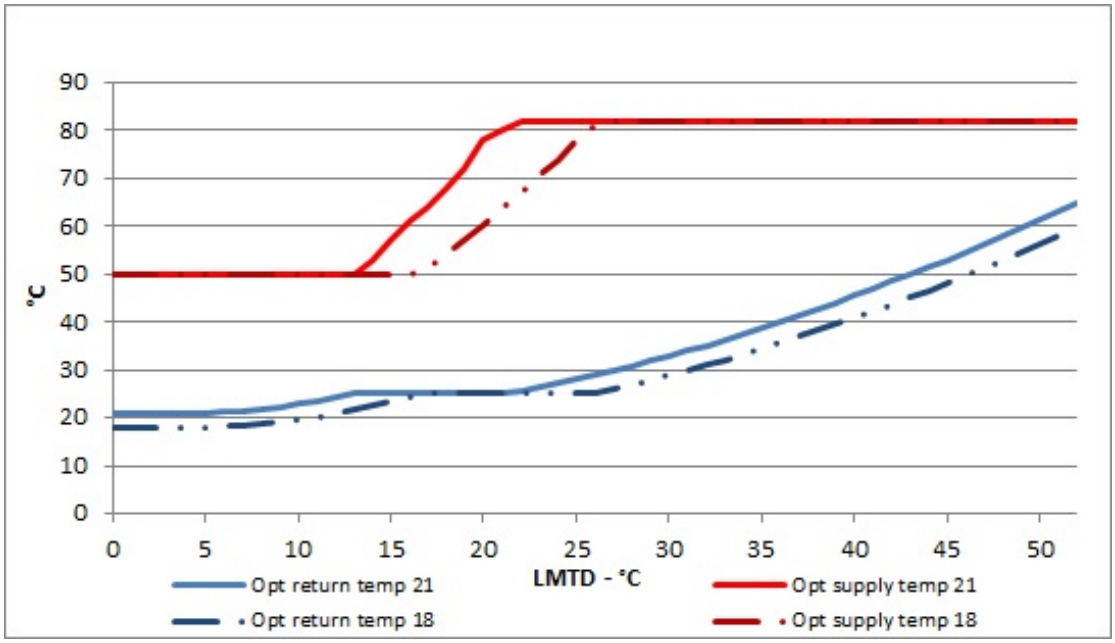

Figure 6.18: Step d — Optimised supply and return temperatures for set indoor temperatures of 21 and 18 °C

For the case of indoor temperature of 21 °C, the strategy followed three different paths clearly delimited by the breaking points related to LMTD of 13 °C and 22 °C. These correspond to the change in the gradient of the optimised supply and return curves calculated. The objective functions and relative constraints are presented for all specific LMTD as follows:

i. For LMTD $< 13\,^{\circ}\mathrm{C}$:

$$minimise\ (T_R),\ for\ LMTD = \frac{T_S - T_R}{ln\left(\frac{T_S - T_i}{T_R - T_i}\right)} \tag{6.1}$$

Subject to:

$$T_S = 50\,^{\circ}\mathrm{C} \tag{6.2}$$

$$\dot{m} \leq \dot{m}_0 \tag{6.3}$$

ii. For $13\,^{\circ}\mathrm{C} \leq LMTD \leq 22\,^{\circ}\mathrm{C}$:

$$minimise\ (T_S), for\ LMTD = \frac{T_S - T_R}{ln\left(\frac{T_S - T_i}{T_R - T_i}\right)} \tag{6.4}$$

Subject to:

$$T_R = 25\,^{\circ}\mathrm{C} \tag{6.5}$$

$$\dot{m} \leq \dot{m}_0 \tag{6.6}$$

iii. For LMTD $> 22\,^{\circ}$C:

$$minimise\ (T_R), for\ LMTD = \frac{T_S - T_R}{ln\left(\frac{T_S - T_i}{T_R - T_i}\right)} \tag{6.7}$$

Subject to:

$$T_S = 82\,^{\circ}\text{C} \tag{6.8}$$

$$\dot{m} \leq \dot{m}_0 \tag{6.9}$$

Similar profiles were obtained for the optimised supply and return temperature curves with indoor temperature of 18 °C. As illustrated by Figure 6.18, the change in the gradient of the optimised curves occurred in this case at LMTD of 16 and 27 °C highlighting the effect of the variation of the set indoor temperatures on the optimal operating temperatures of the radiators. The objective functions and relative constraints are presented for all specific LMTD as follows:

i. For LMTD $< 16\,^{\circ}$C:

$$minimise\ (T_R),\ for\ LMTD = \frac{T_S - T_R}{ln\left(\frac{T_S - T_i}{T_R - T_i}\right)} \tag{6.10}$$

Subject to:

$$T_S = 50\,^{\circ}\text{C} \tag{6.11}$$

$$\dot{m} \leq \dot{m}_0 \tag{6.12}$$

ii. For $17\,^{\circ}\text{C} \leq LMTD \leq 27\,^{\circ}\text{C}$:

$$minimise\ (T_S), for\ LMTD = \frac{T_S - T_R}{ln\left(\frac{T_S - T_i}{T_R - T_i}\right)} \tag{6.13}$$

Subject to:

$$T_R = 25\,^{\circ}\text{C} \tag{6.14}$$

$$\dot{m} \leq \dot{m}_0 \tag{6.15}$$

iii. For LMTD $> 27\,^{\circ}\text{C}$:

$$minimise\ (T_R), for\ LMTD = \frac{T_S - T_R}{ln\left(\frac{T_S - T_i}{T_R - T_i}\right)} \tag{6.16}$$

Subject to:

$$T_S = 82\,^{\circ}\text{C} \tag{6.17}$$

$$\dot{m} \leq \dot{m}_0 \tag{6.18}$$

In the resolution of the optimisation problem for both indoor temperatures all the combinations of temperatures fulfilled the constraints' criteria. In particular, the list of rooms defining the worst LMTD curve, including design heat load and max mass flow rates — calculated using Equation 5.10 with design temperatures of $82/70\,^{\circ}\text{C}$ — are presented in Table 6.9.

Table 6.9: Rooms design heat load and associated max mass flow rate

Building	**Design heat load (W)**	**Max Mass flow (kg/h)**
OF 1 Office 2 1F1	2374	170
OF 1 Entrance 2	1462	105
LW 1 Toilet office 1	593	43
LW 1 Bedroom 1	1399	100
LW 1 Kitchen/Dining	1503	108
OF 1 Toilet 1 GF	1331	95
OF 1 Meeting 1 left	8583	615
OF 1 Toilet 1 GF	1331	95
OF 1 Meeting 1 left	8583	615
OF 1 Entrance 1	1295	93

The constraints assumed for supply and return temperatures were the same of those illustrated for Scenario A of Chapter 5, a part for the upper limit of the supply temperature which in this case was set at 82 °C according to the different radiator design conditions. Also, the lower inlet temperature limit could have been potentially even lower than 50 °C, as the DHW demand is delivered by electric heaters. However, the future possibility of covering the DHW demand with the heat network through dedicated plate heat exchanger for instantaneous hot water preparation was the reason to fix it at 50 °C.

The outcomes presented in Figure 6.18 show even for this case that existing double string radiators, if properly controlled, can be operated more efficiently and achieve lower return temperatures without any intervention to the building, but simply adjusting temperatures to heat demand. Clearly, the UK old design practises of using high temperatures and small ΔT have an influence on the possibility of achieving lower return temperatures with existing radiators, as these affect their dimensions and as a consequence their capacity to be operated with lower temperatures. These old design practises have now been superseded as documented in the recent CIBSE and ADE publication [40], where 70/40 °C are recommended as the new design conditions for typical plate radiators.

The resolution of the optimisation problem led to achieve yearly average supply and return temperature of 81/41 °C. This would allow to obtain a possible discount of 14% in the end users' energy bill according to the assumed motivation tariff. In relation to the new operation of the heat network, rising supply temperature to 81 °C is not an issue with biomass condensing boiler, whereas the average return temperature returning to the plant room could be potentially even lower than 41 °C if the buildings with UFH would be correctly controlled and operated. This is illustrated in details in the last section of this Chapter.

6.3.2 Scenario B: indoor comfort controlled by constant set temperature

The night setback strategy is normally used to reduce the indoor temperature during night and according to the buildings' thermal mass can generate some en-

ergy savings. Nonetheless, this control strategy tends to a certain degree of heat load variability and for the operation of SH it can contribute to let the radiators work for more hours to higher part-load. This is emphasised especially during the mornings, when normally a higher peak heat demand is required due to the switching from night to day indoor temperature [10].

From this perspective, new simulations were performed for the buildings with plate radiators — OF 1, LW 1 and DB 1 — using the IDA-ICE models and setting a constant indoor temperature of 21 °C as new indoor control strategy. The new results expressing the annual energy consumption in comparison to those from Scenario A are presented in Table 6.10.

Table 6.10: Comparison between simulated annual energy consumption of Scenario A and B

Building	**Results Scenario A (MWh)**	**Results Scenario B (MWh)**	**Increase rate (%)**
LW 1	26.7	30.8	13
DB 1	26.7	30.5	13
OF 1	113.5	120.8	6

The results highlight that by setting constant indoor temperature of 21 °C the annual energy consumption was increased in each building. Hence, the objective of this scenario was to investigate the application of the method proposed in

Chapter 4 and verify if the increased energy consumption was justified by an effective improvement of the operating temperatures of the heating systems.

Step a: calculation of part load duration curve

The part load duration curves as results of the dynamic simulations are presented in Figure 6.19 on an hourly basis for the entire year. The new curves obtained with constant indoor temperature set at 21 °C show, as it was expected, smoother patterns with no flat shape within the part load range of 70–80% compared to those presented in Figure 6.19 for the scenario with night set-back.

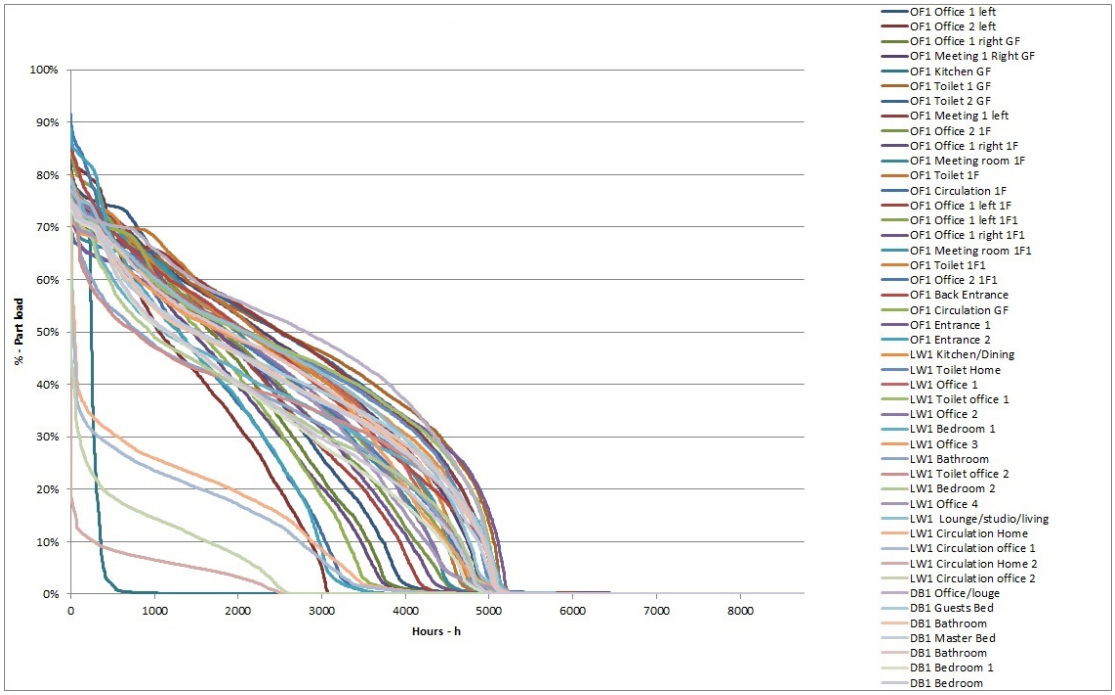

Figure 6.19: Step a — Part load duration curves for all rooms and all buildings

Step b: calculation of the relationship between part load and logarithmic mean temperature difference of the hydronic radiator elements

The results for step b presented in Figure 6.15 for one room of LW 1 as an example — LW 1 office 3 — illustrate the relationship between each part load and the

specific LMTD, expressing how the radiators need to be operated. It was assumed that the radiators in the double string configuration at design conditions were operated with supply and return temperatures of 82/70 °C and that the radiators in the rooms were sized accordingly. Hence, to correctly perform the calculations of LMTD for each part load using Equation 4.2, n was assumed to be 1.3, Φ_0 was the design heat load of 1351 W, whereas $LMTD_0$ was obtained from Equation 4.3 using the design temperatures of 82/70 °C and set indoor temperatures of 20 °C.

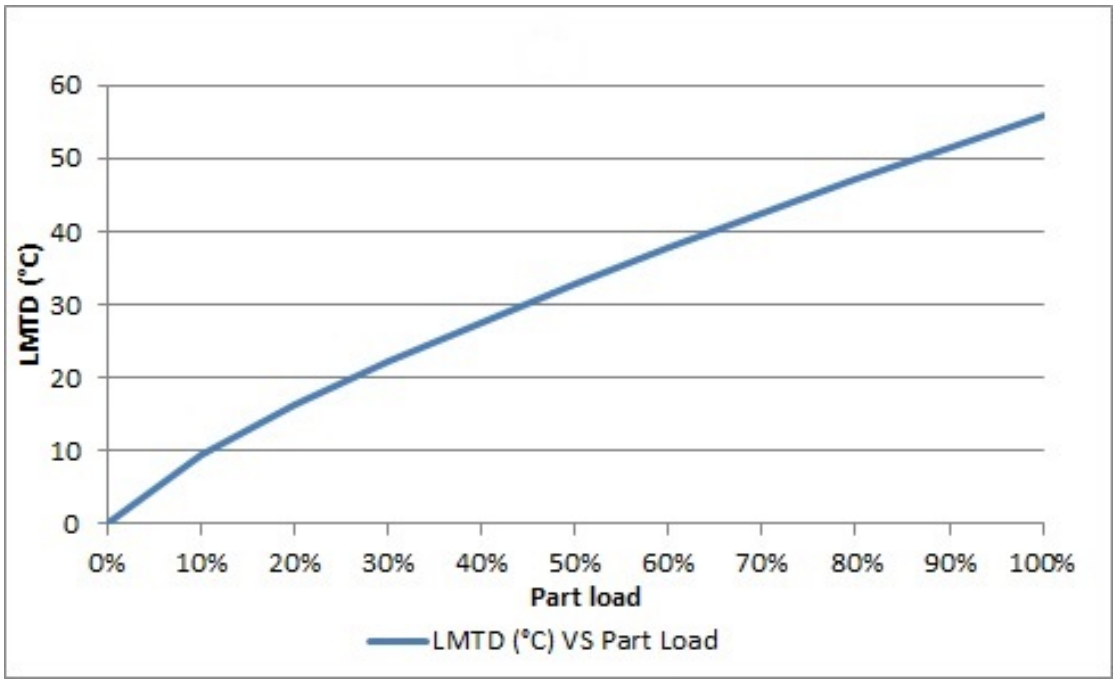

Figure 6.20: Step b — LMTD VS Part load

Step c: calculation of the duration curve of logarithmic mean temperature difference

The part load duration curve presented in Figure 6.19 and the general relation between the part load and LMTD in Figure 6.20 allowed the calculation of the duration curve of LMTD on an hourly basis for all rooms and all buildings as described in Figure 6.21.

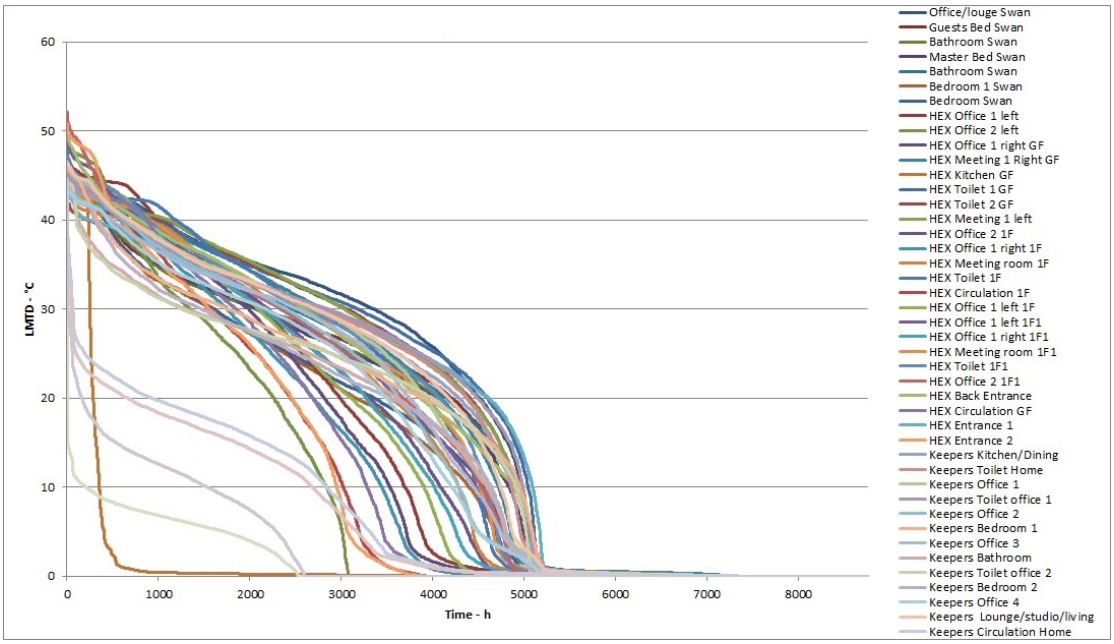

Figure 6.21: Step c — LMTD duration curve

The analysis of all curves allowed to easily compare and define the conditions and the boundaries to be investigated and identify to which extent operating temperatures can be lowered in the network. This is obtained, as presented in Figure 6.22, by defining for each time step the curve representing the worst case as combination of the highest LMTD within all curves of all rooms.

As highlighted in the profiles of the LMTD curves, the effect of the constant indoor temperature setting led to obtain a smoother swarm of curves with no flat shape due to the reduced effect of the load variability connected to the night set-back strategy.

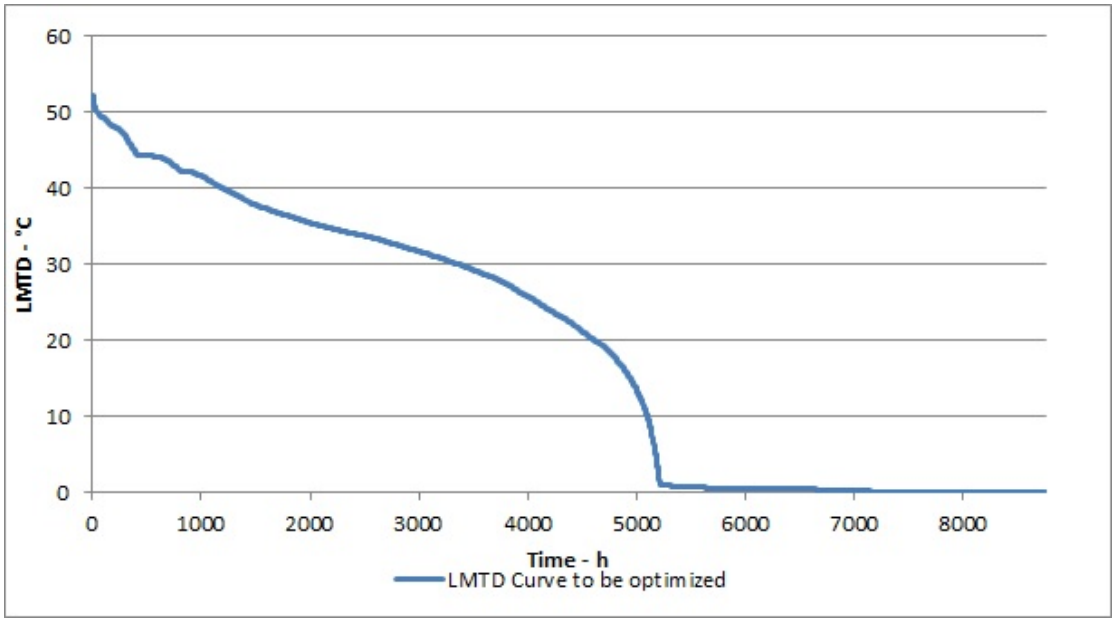

Figure 6.22: Step c — Aggregate LMTD duration curve based on highest LMTD

Step d: calculation of the optimal supply and return temperature to provide the necessary logarithmic mean temperature difference

Using the example of the existing Danish DH company presented in Chapter 5 [107], the same motivation tariff presented for the night set-back scenario was considered. This was customised to guarantee to the end users a discount of 1% in their energy bill (up to a maximum of 20%) for each °C lower in their return temperatures compared to the reference DH yearly average return temperature. The reference average supply and return temperature for the site are 72/55 °C as presented in the Section 6.2.2.

Hence, the optimisation focused on the minimisation of the supply and return temperatures of Equation 4.3 set equal to the specific LMTD for each value of the duration curve presented in Figure 6.22. The results are presented in Figure 6.23.

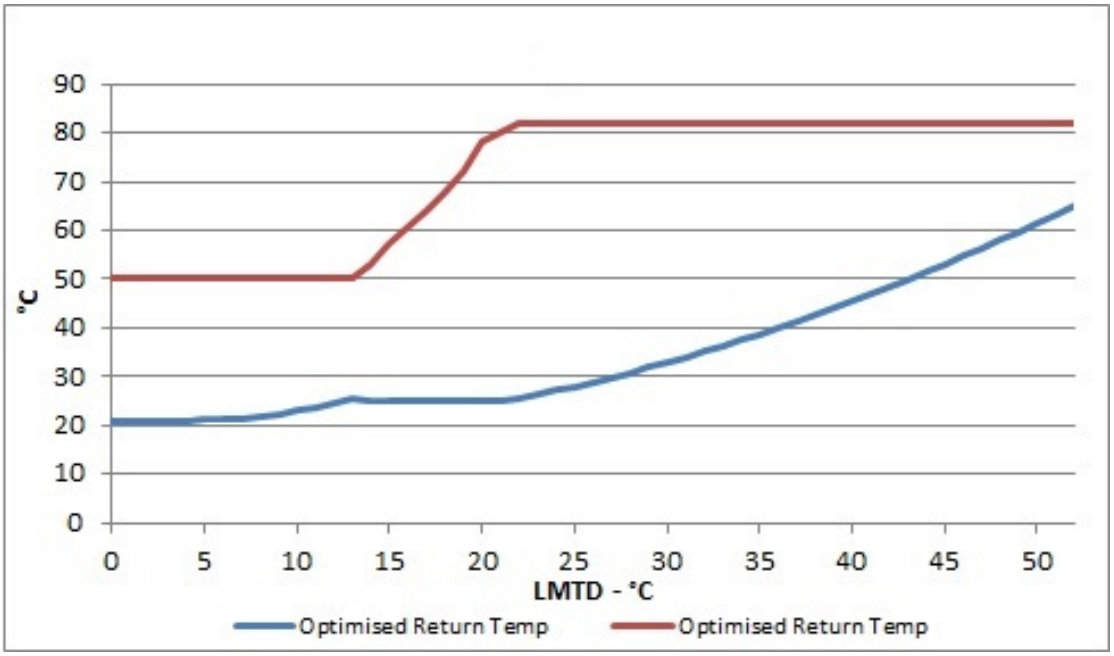

Figure 6.23: Step d — Optimised Supply and return temperatures with indoor temperature of 21 °C

The strategy followed three different paths clearly delimited by the breaking points related to LMTD of 13 °C and 22 °C corresponding to the change in the gradient of the optimised supply and return curves calculated — i.e. Figure 6.18. The objective functions and relative constraints are presented for all specific LMTD as follows:

i. For LMTD $< 13\,°C$:

$$minimise\ (T_R),\ for\ LMTD = \frac{T_S - T_R}{ln\left(\frac{T_S - T_i}{T_R - T_i}\right)} \tag{6.19}$$

Subject to:

$$T_S = 50\,°C \tag{6.20}$$

$$\dot{m} \leq \dot{m}_0 \tag{6.21}$$

ii. For 13 °C $\leq LMTD \leq$ 22 °C:

$$minimise\ (T_S), for\ LMTD = \frac{T_S - T_R}{ln\left(\frac{T_S - T_i}{T_R - T_i}\right)} \tag{6.22}$$

Subject to:

$$T_R = 25\,^{\circ}\mathrm{C} \tag{6.23}$$

$$\dot{m} \leq \dot{m}_0 \tag{6.24}$$

iii. For LMTD > 22 °C:

$$minimise\ (T_R), for\ LMTD = \frac{T_S - T_R}{ln\left(\frac{T_S - T_i}{T_R - T_i}\right)} \tag{6.25}$$

Subject to:

$$T_S = 82\,^{\circ}\mathrm{C} \tag{6.26}$$

$$\dot{m} \leq \dot{m}_0 \tag{6.27}$$

In the resolution of the optimisation problem all the combinations of temperatures fulfilled the constraints' criteria which were the same of those presented for the night set-back case. The specific list of rooms defining the worst LMTD curve are presented in Table 6.11, including the design heat loads and max mass flow rates — calculated using Equation 5.10 with design temperatures of 82/70 °C.

Table 6.11: Rooms design heat load and associated max mass flow rate

Building	**Design heat load (W)**	**Max Mass flow (kg/h)**
OF 1 Office 2 1F1	2374	170
OF 1 Entrance 2	1462	105
OF 1 Office 2 left	943	68
OF 1 Office 1 left	1940	139
OF 1 Toilet 1F	464	33
OF 1 Meeting 1 left	8583	615
DB 1 Office/lounge	1380	615
OF 1 Toilet 1 GF	1331	95
OF 1 Entrance 1	1295	93
OF 1 Toilet 1 GF	1331	95

The effect of setting constant indoor temperature of 21 °C, as discussed in step a and c, led to have smoother part load and LMTD curves due to the reduced impact of load variability and reheating during mornings. This was quantified in the resolution of the optimisation problem by obtaining new possible yearly average supply and return temperatures of 81/39 °C. This would guarantee a possible discount of 16% in the end users' energy bill according to the assumed motivation tariff. Although the new control strategy of the internal comfort would generate a higher discount for the end users and a lower average return temperature of 2 °C compared to the scenario with night set-back, these improvements will not be

enough to offset and justify the higher energy consumption presented in Table 6.10. Therefore, this scenario was not investigated further and the following analyses, based on TERMIS simulations, focus on the improvement of the operations of the heat network considering exclusively the case having night set-back indoor control strategy.

6.4 Improvement of the operation of the heat network

The results of the optimisation proposed in Section 6.3 were used to investigate the effects on the operation of the entire heat network. The small scale DH network was simulated with TERMIS. Two scenario were assessed:

- SCENARIO C: it represents the reference scenario. The heat network is simulated using the operating conditions extrapolated from recorded data
- SCENARIO D: it represents the optimised scenario. The heat network is simulated using the new operating strategy

6.4.1 Definition of the physical model and boundary conditions

The software TERMIS, as illustrated in Section 4.5, is one of the most advanced tools for both industry and academia to monitor and control on real time all the parameters of the heat networks as well as to dynamically simulate their operation in new area and/or in different scenarios. The first task was the definition of

the physical model for the heat network to be analysed. This was achieved by defining and drawing the basic object of the network, including nodes, pipes, heat generation plant and end-users, as presented in Figure 6.24.

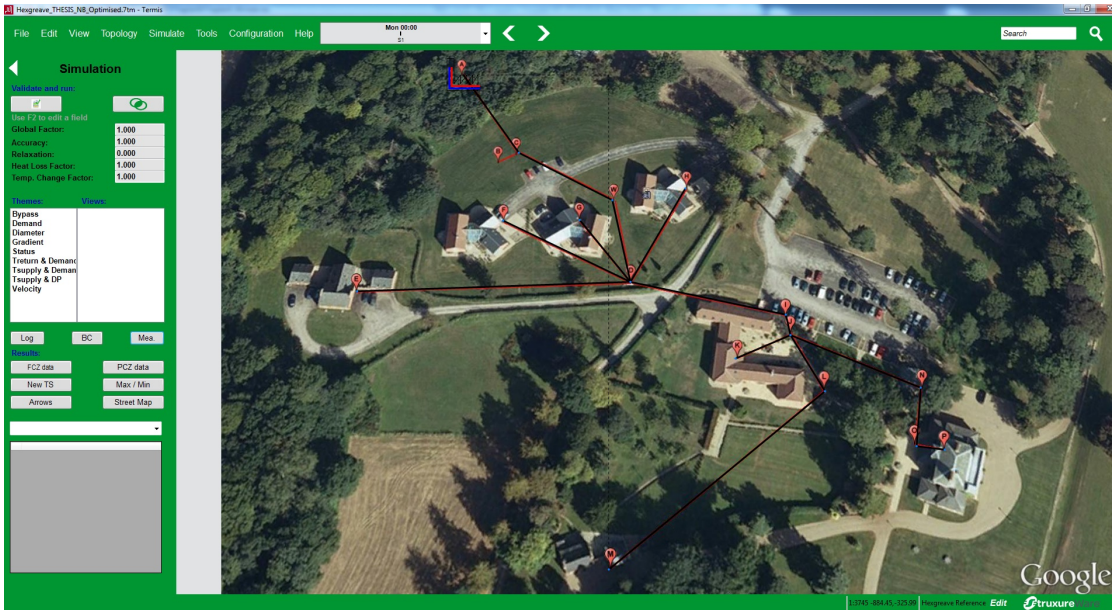

Figure 6.24: TERMIS heat network model

The pre-insulated pipes characteristics — including geometry, length and U-values — were introduced in the model as a catalogue based on the specifications summarised in Table 6.6. In order to correctly calculate the temperature propagation in the pipes and the heat losses for the heat network it was important to add the specific ground temperatures of the site. These were obtained from the CIBSE weather file used in this investigation and introduced in the model on monthly base as highlighted in Figure 6.25 [95].

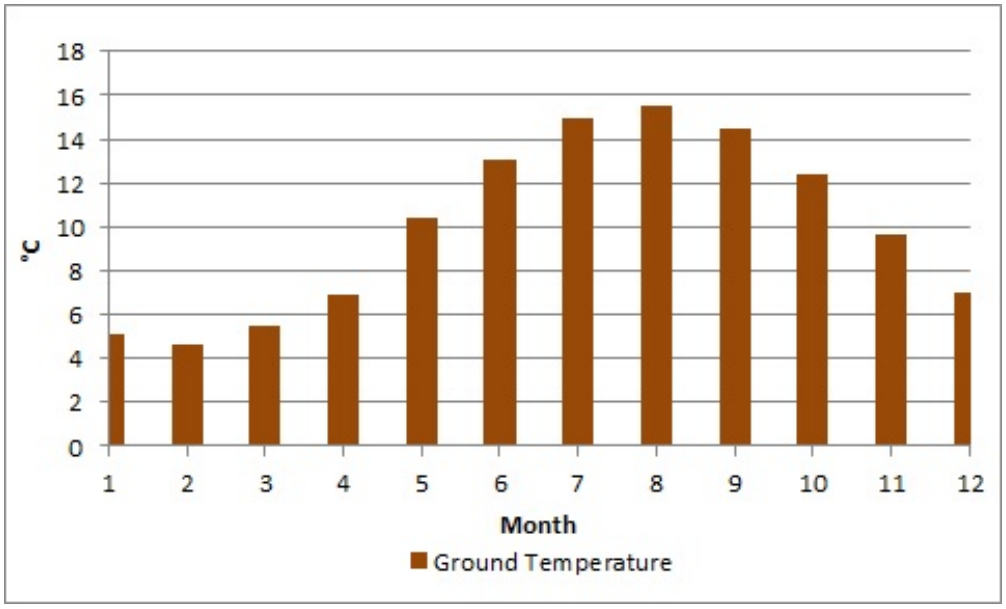

Figure 6.25: Monthly average ground temperature [95]

The equation used by the software to calculate the downstream temperature T_d in the pipe objects is defined as follows [120]:

$$T_d = \frac{M}{K} + \left(T_u - \frac{M}{K}\right) exp\left(\frac{-K \cdot L}{V}\right) \tag{6.28}$$

where T_u is the upstream fluid temperature (°C), L is the pipe length (m) and V is the velocity (m/s). Instead, the parameters K and M are defined as follows:

$$M = \frac{1}{\rho c_p} \cdot \left[(1 - c_p \cdot C_t) \cdot V \cdot \frac{\partial P}{\partial X} + \rho \frac{2f}{D} \mid V \mid V^2 + C_h \cdot \frac{T_a}{A}\right] \tag{6.29}$$

$$K = \frac{1}{\rho \cdot c_p} \cdot \left(\frac{C_h}{A}\right) \tag{6.30}$$

where T_a is the ambient temperature (°C), C_h is the overall heat transfer

coefficient governing the radial heat transport from the fluid to the environment (W/m °C), c_p is the water heat capacity at constant pressure (J/kg °C), C_t is the heat capacity at constant temperature of the water (J/kg °C), A is the cross sectional area of the pipe (m^2) and $\frac{\partial P}{\partial X}$ is the pressure gradient ($N/m^2/m$).

In addition, the software supports the calculation of temperature propagation and heat losses from twin pipes as presented in Figure 6.26. For instance for the supply leg, compared to conventional pipes, the heat transfer coefficient and the ambient temperature are defined by the software as follows [120]:

$$C_h{}^* = C_{h,s} + C_{h,twp} \tag{6.31}$$

$$T_a{}^* = \frac{C_{h,s} \cdot T_a + C_{h,twp} \cdot T_r}{C_{h,s} + C_{h,twp}} \tag{6.32}$$

where T_a is the ambient temperature (°C), $T_a{}^*$ is the ambient temperature (°C) corresponding to conditions for a conventional pipe, T_s is the fluid temperature in the supply line (°C), T_r is the fluid temperature in the return line (°C), $C_{h,s}$ is the heat transfer coefficient for the part of the supply pipe facing the ground (W/m °C), $C_{h,r}$ is the heat transfer coefficient for the part of the return pipe facing the ground (W/m °C), $C_{h,twp}$ is the heat transfer coefficient for the part of the supply and return pipes facing each other (W/m °C) and $C_h{}^*$ is the heat transfer coefficient corresponding to conditions for a conventional pipe (W/m °C).

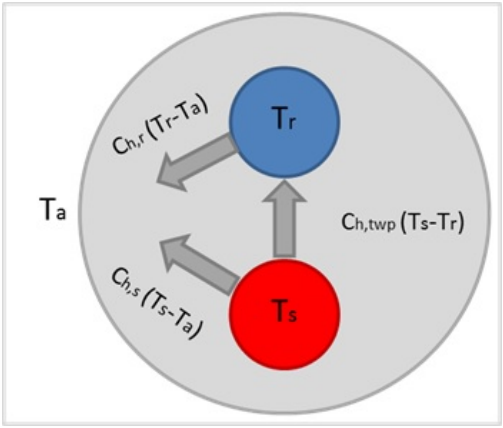

Figure 6.26: Schematic view of twin pipe [120]

Other important parameters to be configured were the heat loads associated to the nodes corresponding to the customers connected to the heat network. These were obtained from the IDA-ICE dynamic simulations with night set-back indoor temperature control and included in the model as monthly average for each of the buildings as presented in Figure 6.27. By introducing the demand at node level, the user defines the boundary condition and the software is able to calculate the pressure and the flows at each node. Few assumptions were made for what concerns the heat demand. Firstly, the NB 1 was not included in the model as this building, during the heating season 2014/2015, was not connected to the network yet. Moreover, as no data were available for the buildings LW 3 and 4, the same heat load of LW 2 was assumed as these three buildings, as described in Section 6.2.1, are identical. In addition, for each node acting as consumers, the software also requires to define the temperature difference or the return temperatures. These are illustrated in details in Section 6.4.2 and 6.4.3 for Scenario C and D.

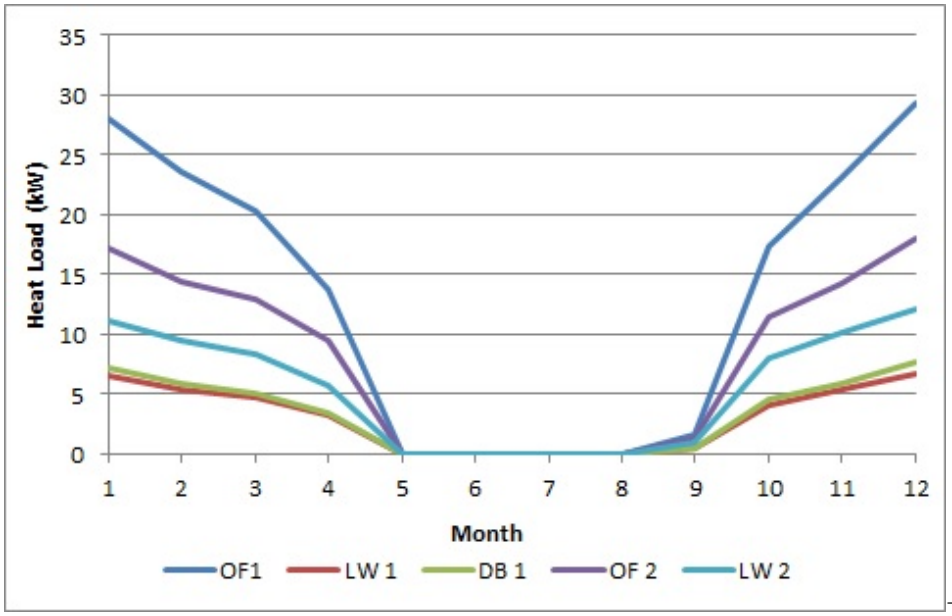

Figure 6.27: Monthly average heat load profiles

The last object configured in the model was the heat generation plant. It connects the supply and return lines and supplies energy to the network. The energy source can be any device and the details are not modelled by TERMIS. As software's requirements the inlet temperature and the static pressure — 1.5 bar in the supply line for the case in analysis — were defined in the plant object section. The supply temperatures vary according to the scenario considered and these are described in details in Section 6.4.2 and 6.4.3. The following equation controls the plant object [120]:

$$PWR = Q \cdot [T_s - T_r] \cdot c_v \tag{6.33}$$

where PWR is the lost power supplied by the plant, Q is the mass flow through the plant, T_s is the supply side temperature (must always be configured), T_r is the return side temperature and c_v is the heat capacity (at constant volume) of the fluid.

6.4.2 Scenario C: heat network operated at present conditions

This scenario evaluated the performances of the heat network in analysis considering the operating conditions extracted from the recorded data of the heating season 2014/2015 as presented in Section 6.2.2. Given the physical model built in TERMIS and described in Section 6.4.1, the monthly average supply temperatures from measurements were introduced in the heat generation plant object as well as the monthly average ΔT in the nodes corresponding to the consumers connected to the heat network. In particular, as access to monitor operating conditions at building level was possible only for LW 2, the monthly average ΔT recorded at the heat generation point were used as input to the nodes corresponding to the other buildings.

The results of the simulations corresponding to the operating temperatures and mass flow rate for the heat generation plant are presented in Figure 6.28 and 6.29. The estimated yearly average return temperature was 54.2 °C, showing a good match compared to the average return one of 55 °C from measurements. Instead, the yearly average mass flow rate obtained was 3790 kg/h — excluding the summer months and September as the system is switched on the 25^{th}. Although no gathered data for the mass flow rate circulating in the heat network are available to compare with the software outputs, the simulations show positive differential pressure, highlighting that the static pressure of 1.5 bar is enough to guarantee the necessary flow to each end users.

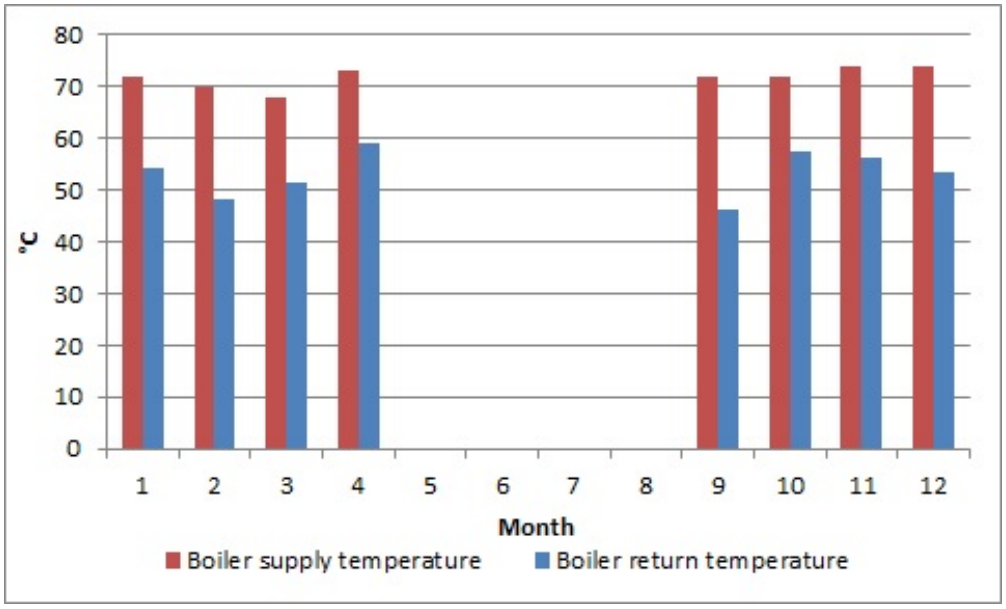

Figure 6.28: TERMIS simulations — Average supply and return temperatures in the boiler room

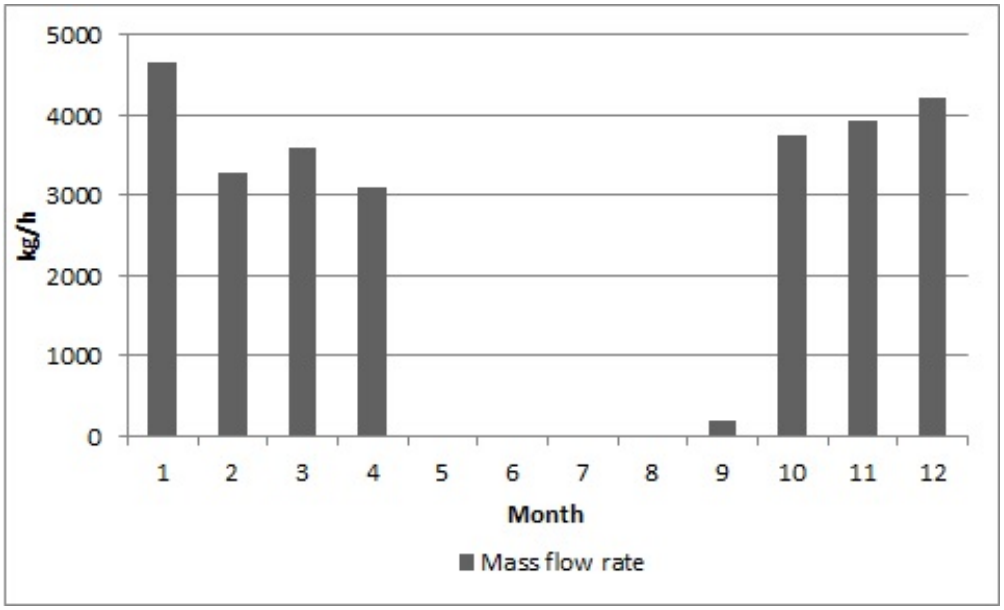

Figure 6.29: TERMIS simulations — Monthly pressure difference profiles

Furthermore, the energy generated and delivered as well as the distribution losses are summarised in Table 6.12 and presented as a bar chart on monthly base in Figure 6.30. The results depict a contained impact of the distribution losses quantified as only 4% of the total energy delivered. The reason of this low value, compared to the typical 20% found in more mature DH markets [44], is related to

the reduced dimension of this heat network and to the peculiarity of the system to cover only the SH demand of the Estate.

Table 6.12: TERMIS simulations — Energy profiles of the network

TERMIS results	**Scenario C**
Energy generated (MWh)	395.03
Energy delivered (MWh)	380.00
Distribution losses (MWh)	15.03

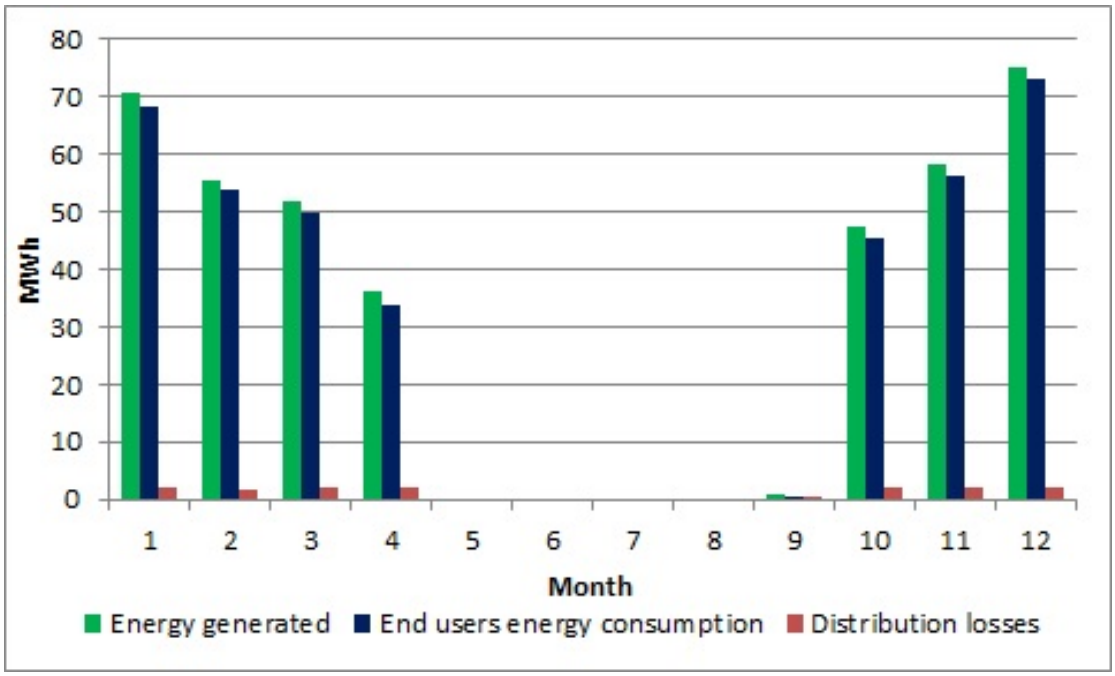

Figure 6.30: TERMIS simulations — Energy profiles of the network

The total energy delivered to the customers obtained from simulations is in line to the real figures measured on site. In fact, using the data of Table 6.8 and assuming the same energy demand for LW 2, 3 and 4, the average yearly energy consumption from measurements is 374 MWh, only 1.6% less than simulations.

These results represent the key parameters of the reference case and will be used to assess the effectiveness of the improvements proposed and illustrated in Scenario D.

Finally, the monthly average operating temperatures are presented in the Figure 6.31, 6.32 and 6.33 for OF 1, DB 1 and LW 2. These highlight the temperature variations at the end-users' level for an office space OF 1, a domestic building DB 1 and for mixed live/work space LW 2. According to the assumptions made in the definition of the TERMIS physical model, the simulations return for all the buildings an yearly average ΔT of 17 °C as observed from measurements.

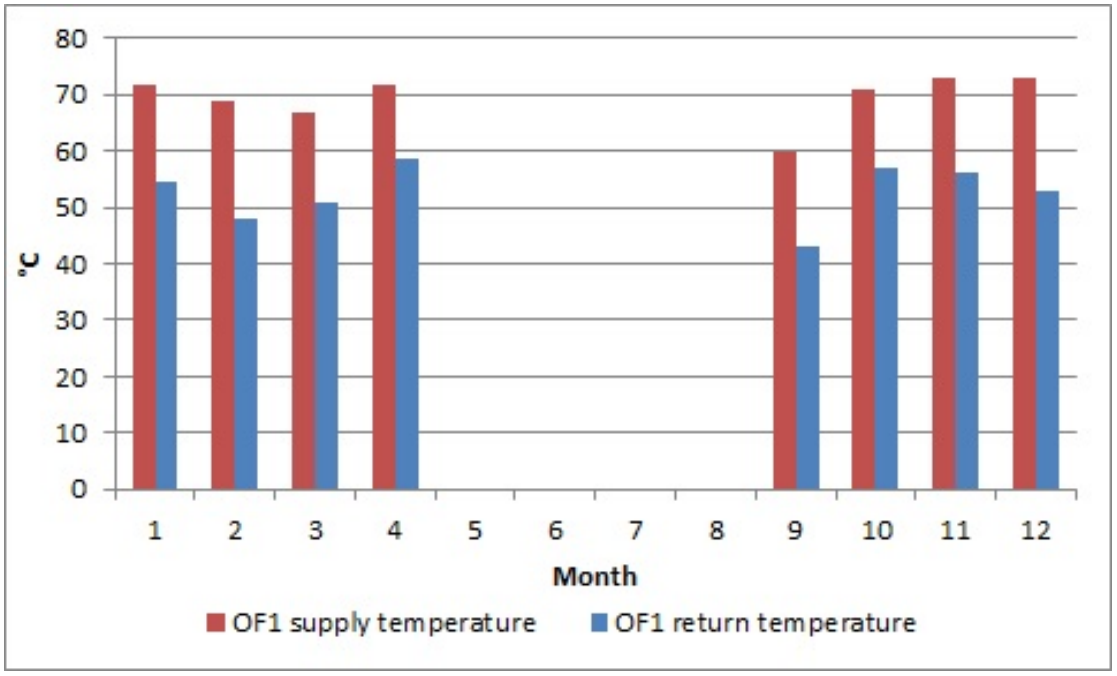

Figure 6.31: TERMIS simulations — OF 1 monthly operating temperature

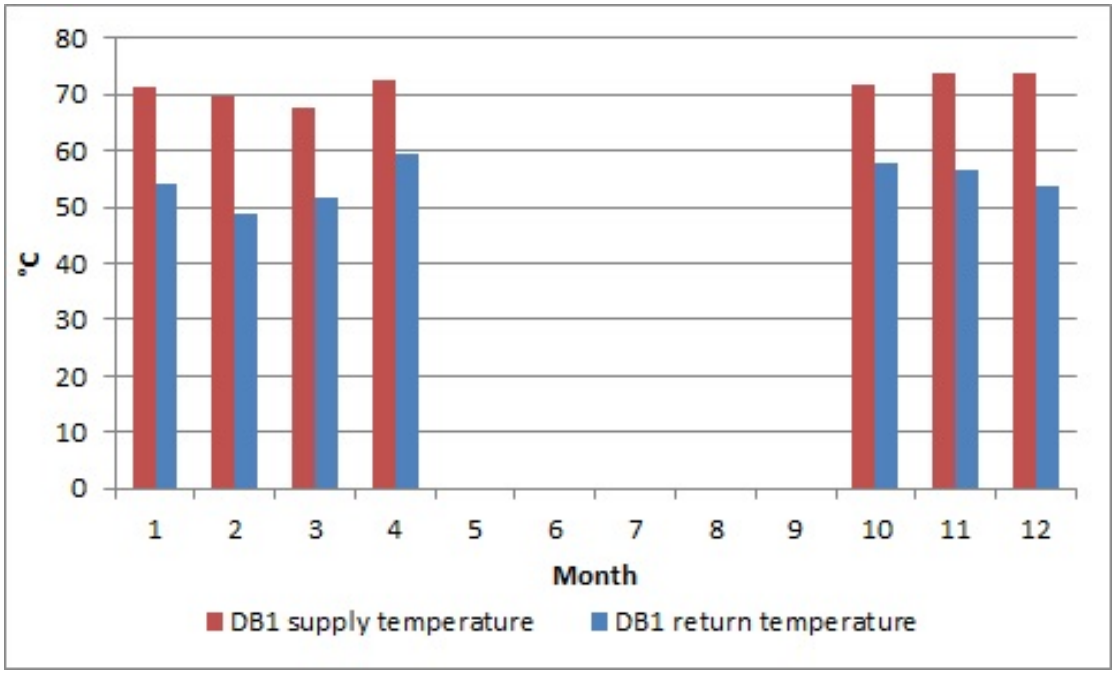

Figure 6.32: TERMIS simulations — DB 1 monthly operating temperature

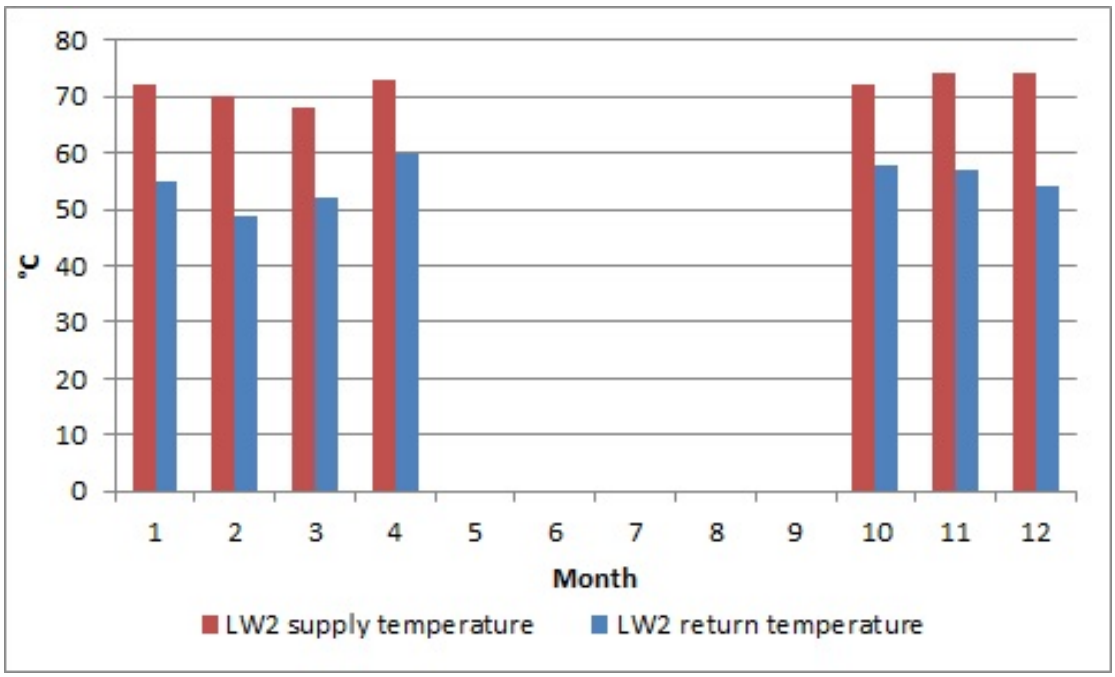

Figure 6.33: TERMIS simulations — LW 2 monthly operating temperature

6.4.3 Scenario D: optimised operation of the heat network

The core idea of this scenario was to propose a new strategy to operate the heat network for the UK case study and quantify in case the possible benefits achievable. Firstly, the buildings connected to the heat network cover their SH heating demand through either plate radiators or UFH systems. As the plate radiators are operated with higher temperatures, these determined the supply temperature profile in the heat network. Hence, the average supply temperature of 81 °C, obtained from the resolution of the optimisation problem presented in Section 6.3.1 for the buildings with radiators, was used as inlet temperature to configure the TERMIS heat generation plant object in this new scenario. In addition, in the node objects of the model, corresponding to the buildings with plate radiators, the optimal average return temperature of 41 °C was set as the new target temperature according to the calculations performed in Section 6.3.1.

Secondly, as documented in section 6.2.2, the buildings with UFH are operated with unnecessary high temperatures (blending valve set at 60 °C) which affect the system efficiency and the durability of equipment, leading as a consequence to higher return temperatures. To improve the operation of the UFH systems installed on site, 40/30 °C were assumed as the new operating temperatures for these systems, where 40 °C was supposed as the new setting for the blending valves placed before each UFH loop — see Figure 6.12 — and 30 °C was set in the model as target return temperature to each corresponding node object related to the buildings with UFH systems.

By keeping the same heat load profiles for the buildings connected to the heat network and the same static pressure of 1.5 bar in the plant object, the results of the simulations for the new operating temperatures and the mass flow rates are presented in Figure 6.34 and 6.35.

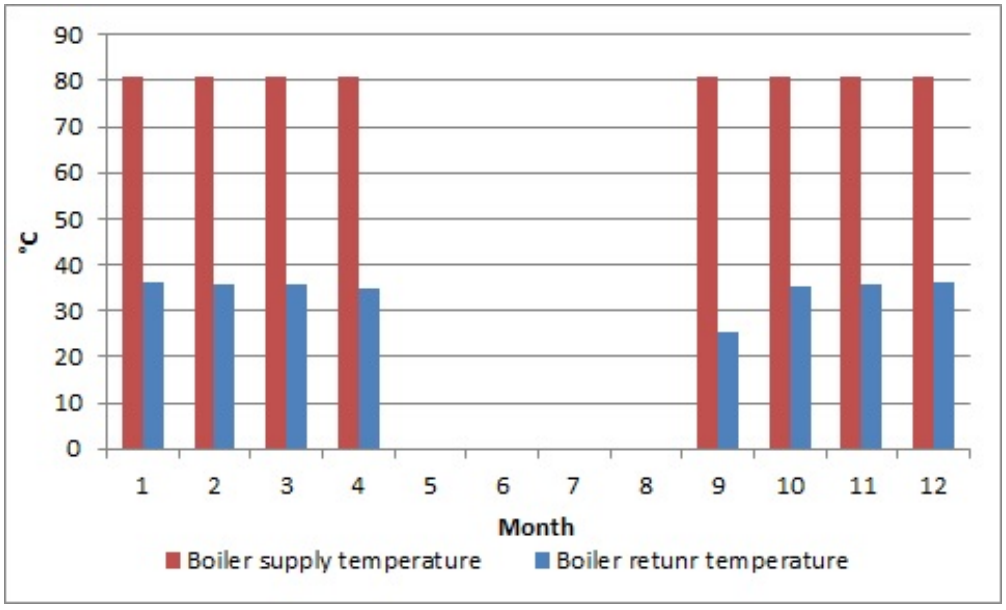

Figure 6.34: TERMIS simulations — Average supply and return temperatures in the boiler room

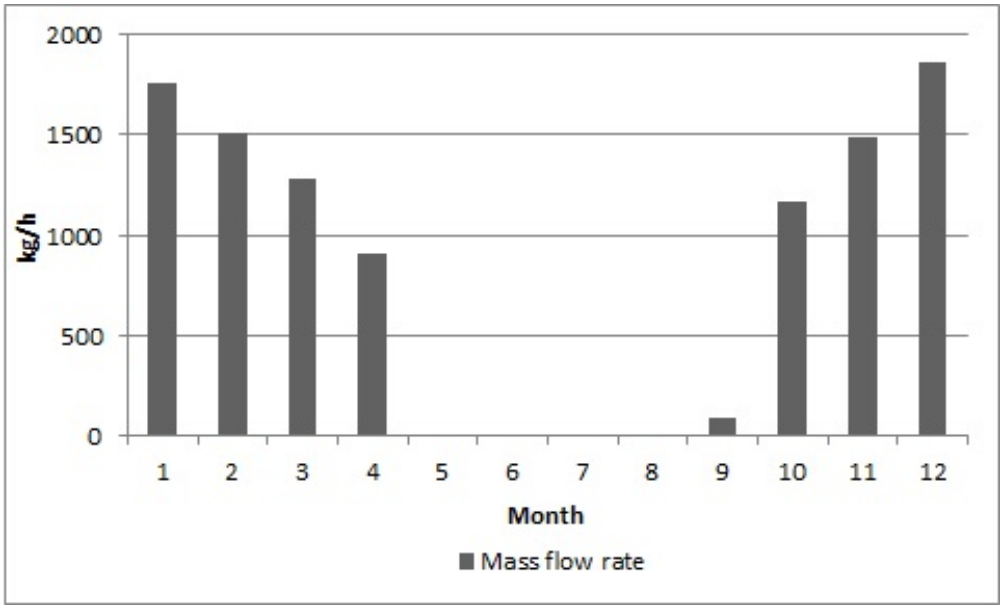

Figure 6.35: TERMIS simulations — Monthly pressure difference profiles

The results show that the new operation of the small scale DH network led

to obtain a yearly average return temperature of 35.6 °C, which correspond to a reduction of 18.6 °C compared to the reference case of Scenario C. In addition, a reduction in the mass flow rate circulating in the network was observed by comparing Figure 6.29 and 6.35, resulting for Scenario D in a yearly average of 1450 kg/h. This was possible due to the improved ΔT and as a consequence operating the heat network as proposed would also reduce the required pumping energy.

Furthermore, the results for energy generated, energy delivered and distribution losses are summarised and compared in Table 6.13 with the results of Scenario C and presented on monthly average in Figure 6.36.

Table 6.13: TERMIS simulations — Energy profiles of the network

TERMIS results	**Scenario C**	**Scenario D**
Energy generated (MWh)	395.03	393.75
Energy delivered (MWh)	380.00	380.00
Distribution losses (MWh)	15.03	13.75
Average return temperature (°C)	54.20	35.60

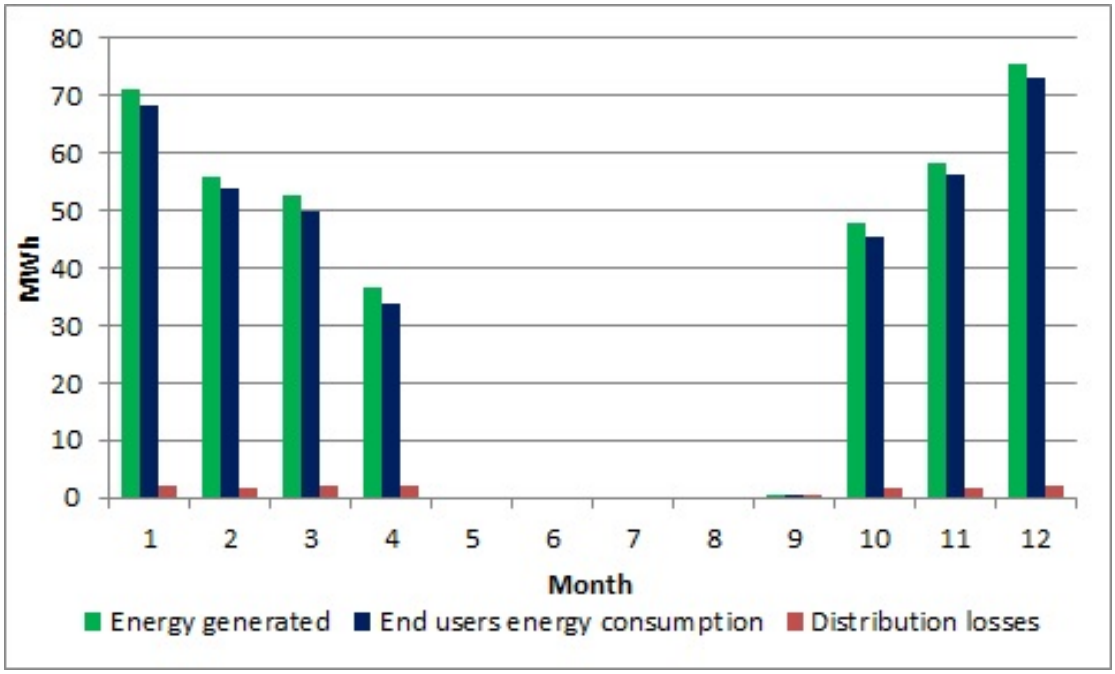

Figure 6.36: TERMIS simulations — Energy profiles of the network

The comparison of the two scenarios shows an improvement in the distribution losses due to the new operating strategy. These were quantified as 3.6% of the total energy delivered, corresponding to an improvement of 10% over the reference case of Scenario C.

Finally, as for Scenario C the monthly average operating temperatures for the office space OF 1, domestic building DB 1 and a live/work space are presented in Figure 6.37, 6.38 and 6.39, highlighting the temperature variations at the end-users' level and the improved average ΔT obtained by operating the heat network and the heating systems as proposed.

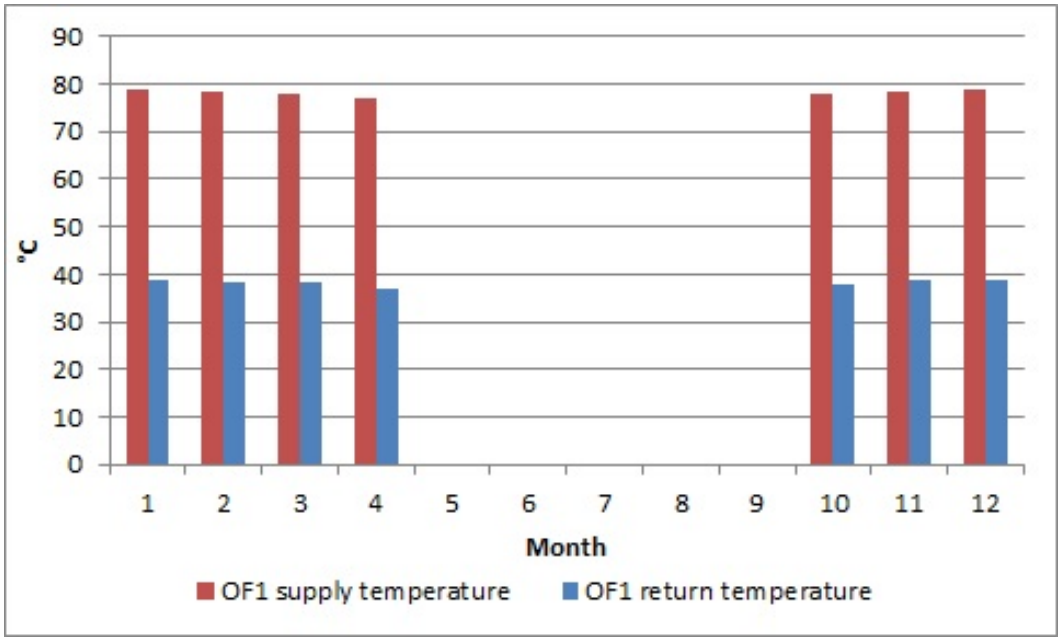

Figure 6.37: TERMIS simulations — OF 1 monthly operating temperature

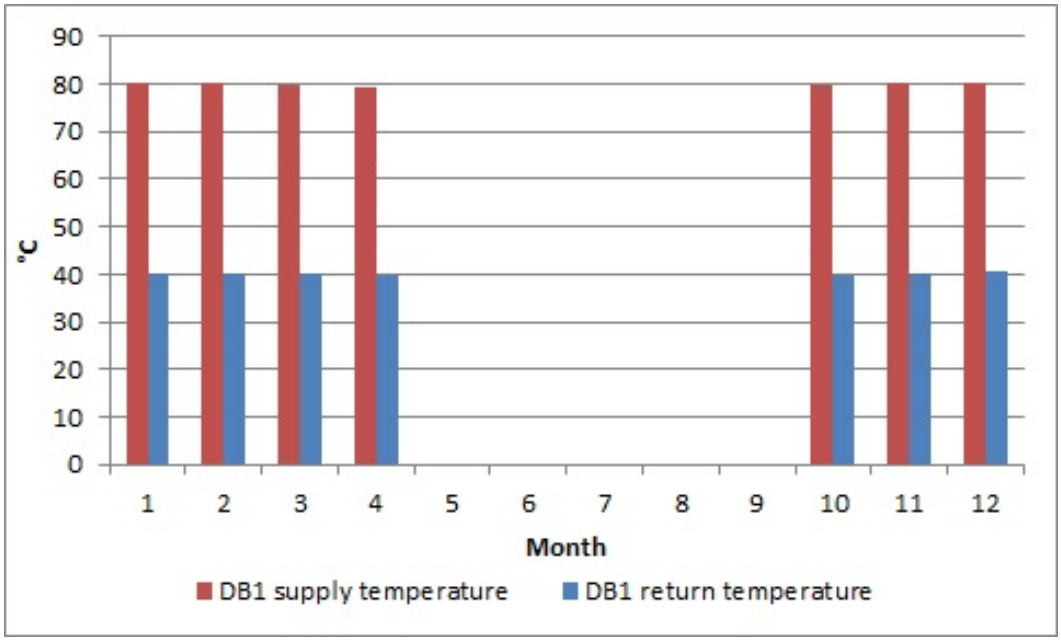

Figure 6.38: TERMIS simulations — DB 1 monthly operating temperature

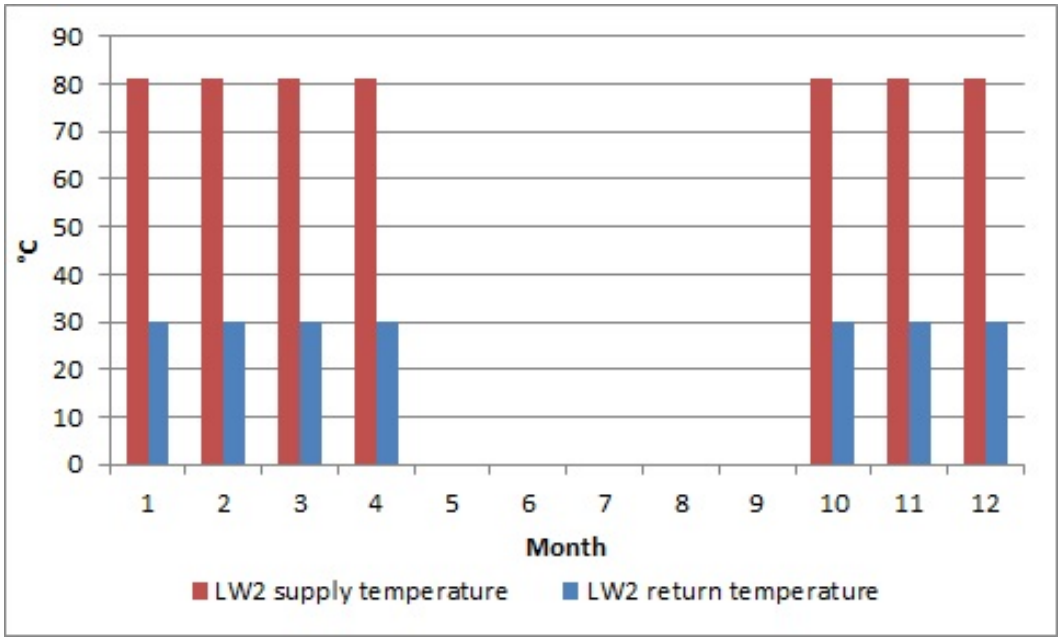

Figure 6.39: TERMIS simulations — LW 2 monthly operating temperature

6.4.4 Fuel consumption efficiency

The last part of the analysis is focused on evaluating the possible benefits achievable at the heat generation point. These would be possible due to the improved average return temperature obtained in Scenario D, which would guarantee a better condensation of the flue gases and improve the overall efficiency of the biomass boiler.

As presented in Section 6.1, a 199 kW Schmid UTLS biomass boiler is installed on site. The real efficiency curve as function of the return temperatures for the specific boiler has not been published by the manufacturer. Hence, it was assumed for the scope the efficiency curve related to condensing boilers available in the CIBSE Guide F [121] and presented in Figure 6.40.

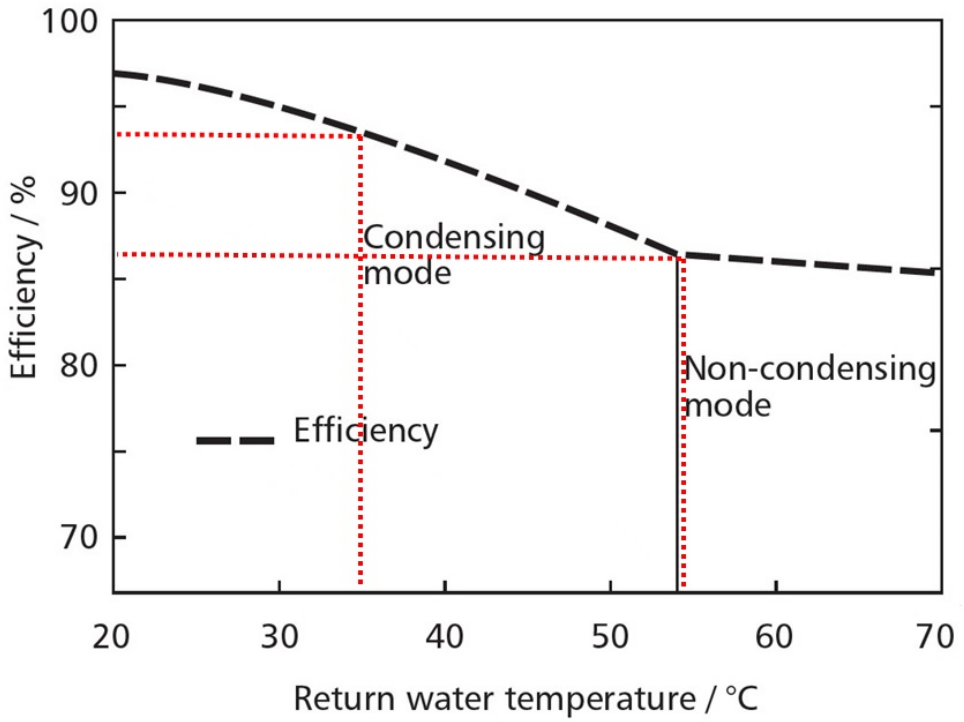

Figure 6.40: Operation of condensing boiler. Efficiency related to Scenario C and D

According to the specific return temperatures calculated for both Scenario C and D — 54.2 °C and 35.6 °C — the relative efficiency extrapolated from the curve are 86% and 94%. These values are used as inputs in Equation 6.34 to calculate the fuel consumption for the two cases.

$$m_f = \left(\frac{E_g}{CV \cdot \eta_b \cdot 1000} \right) \tag{6.34}$$

where m_f is the mass of fuel (tonne), E_g is the energy generated (kWh), CV is the net calorific value of the fuel — wood chips 30% moisture content — and η_b is relative efficiency of the boiler. All the inputs and results obtained are summarised in Table 6.14.

Table 6.14: Inputs and results of fuel analysis

	Scenario C	**Scenario D**
Average return temperature (°C)	54.20	35.60
Mass flow rate (kg/h)	3790	1450
Energy generated (MWh)	395.03	393.75
CV (kWh/kg) [122]	3.50	3.50
η_b — boiler efficiency	0.86	0.94
m_f (tonne)	133.00	121.00

By observing the results achieved, a reduction of 9% in the fuel consumption was estimated. This implies that it would be possible to deliver the same amount of energy to the end-users consuming less fuel by simply operating the small scale heat network as proposed in Scenario D. This further improvement, similarly to the other ones illustrated, was obtained by changing the operation of the heat network, without any intervention to either the heat network, buildings or heating systems. The method and the results obtained about the fuel consumption are reliable, however it is important to emphasise that the use of the real curve associated to the specific biomass boiler and/or changing in the moisture content of the fuel could slightly affect the results obtained.

6.5 Summary

The full implementation of the developed methodology was applied to the small scale DH network of the UK case study. The resolution of the optimisation problem, applied to the buildings with plate radiators, was performed to two different Scenarios A and B. The former replicates the actual control strategy for indoor comfort with night-set back. The latter instead assumed a constant indoor temperatures of 21 °C.

The calculation of the optimal operating conditions for the radiators would lead, in Scenario A, to achieve a possible discount of 14% in the end-users energy bill and an average return temperature of 41 °C. Although Scenario B would guarantee a discount in the end-users of 16%, corresponding to an average return temperature of 39 °C, this would not be enough to offset the increase in the energy consumption due to the constant indoor temperature setting of 21 °C.

Further analysis were performed to assess a new operation strategy for the entire heat network. Two Scenarios C and D were compared reflecting present and improved operating conditions. In the improved case, it was assumed that the UFH systems can be better operated by using more adequate supply and return temperatures of 40/30 °C. Also, as the buildings with plate radiators need high supply temperatures, 81 °C was assumed as average inlet one in the network. This was the result obtained from the resolution of the optimisation problem performed in Scenario A.

The results obtained by simulating the heat network with TERMIS for the two cases show that a reduction of 18.6 °C in the average return temperature and 10% in the distribution losses were achieved in the optimised scenario. This was obtained by simply adjusting temperatures according to heat demand, without any intervention to either the heating systems, buildings and/or network. Finally, the fuel analysis show that the strategy proposed would lead to deliver the same amount of energy to the end-users with a reduction of fuel consumption of 9%.

Chapter 7

Conclusions, discussions and future work

7.1 Introduction

DH technology has been successfully deployed in many countries to provide thermal comfort in buildings. DH is considered as one of the technologies that can play an important role in the transition towards a low carbon society. Applied at community level, DH offers economic, social and environmental benefits to many stakeholders including end users, utility energy providers (companies DNO, ESCO) and local/central governments. This chapter discusses the main research knowledge and contribution that was achieved in this work with the focus on the following:

- the development of an alternative methodology for connecting existing building to LTDH
- the application of the developed method to optimise heating systems oper-

ating conditions in two case studies

In addition, this chapter highlights future directions in terms of advancement of LTDH particularly in market like the UK.

7.2 Contribution

The research work conducted as part of this thesis contributed to the following:

1. A literature review of DH technology with a special focus to LTDH and UK heating market

2. An optimisation method to define the optimum supply and return temperatures for traditional plate radiators in existing DH connected buildings

3. The application of the method to two real case studies based on a Danish single-family house and to a UK small scale DH network

7.2.1 Review of DH technology and its role in the future heating market

The literature review on DH technology covered the main concepts, a detailed description of the evolution of traditional DH technology and projected future LTDH systems with the flexibility to making use of low-cost heat sources, heat recovery and renewable sources, leading the transition towards a low carbon economy.

This particularly focused on giving an insight into the actual heating and cooling sector in the EU context, the relative policy framework and future outlook. It

was assessed the DH penetration in the EU energy market; in particular the cases of Denmark and UK, leading and emerging country in the European DH industry, were deepened as part of the research performed in this investigation was related to a Danish and UK case study.

The concept of LTDH and its role in future energy market was also discussed, highlighting the immediate objective of achieving a load dependent temperatures with a target for supply and return 50/20 °C . Furthermore, the analysis illustrated the technical and economical challenges that the target temperatures will pose in future DH networks. This was explored in details for SH and DHW demand at building level, emphasising on one hand, the reason to limit supply temperatures to 50 °C due to the risk of Legionnaires' disease and on the other hand, to address the capability and differences of heating systems both in low-energy and existing buildings to guarantee the expected indoor comfort.

7.2.2 An optimisation method for operation temperatures of traditional plate radiators for buildings connected to DH

A method was designed to investigate and plan the connection of existing building to LTDH. This was applied in particular to existing buildings having traditional hydronic radiators, which is by far the most used heating elements in EU.

The heat demand is expressed as a function of the LMTD between the water

of radiator and the indoor temperature. The methodology of finding the optimal combination of supply and return temperatures needed to operate the radiators according to the specific LMTD was carried out and explained in a step-by-step procedure.

Different temperatures have different economical benefits to both end users and DH companies, thus the specific DH network would affect the way the plate radiators need to be operated. The method contributes to the engineering and scientific knowledge by presenting the results as an average reduction of the LMTD over the heating season compared to the design conditions and highlighting the different temperatures and possible energy savings in the end users' energy bills in relation to the specific DH market analysed.

7.2.3 Implementation of the methodology to a Danish single-family house and to a UK small scale DH network

To demonstrate the benefit of temperatures optimisation method, two case studies were considered to assess its reliability to provide an alternative strategy to operate DH networks and existing heating systems more efficiently and to which extent operating temperatures can be lowered.

A Danish single-family house from 1930 was used as case study. The investigation focused on defining the optimal operating temperatures for DH network and plate radiators comparing different scenarios:

- Double string plate radiators were hypothesized in the building, assuming to be connected to a traditional DH network based on a biomass CHP plant. The optimisation reflects the higher economical value of lower return temperatures to both end-users — trough a motivation tariffs — and DH company

- Double string plate radiators were hypothesized in the building, assuming to be connected to a future DH network where heat generation would be provided by a variety of heat sources as heat pumps, RE etc. The optimasation reflects in this case the higher economical value of lower supply and return temperatures for both the end-users and DH company

- Single string plate radiators were hypothesized in the building, assuming to be connected to a traditional DH network based on a biomass CHP plant. Due to the differences to operate single loop radiator systems, lower return temperatures can be obtained only by reducing supply temperatures too. Hence, the optimisation reflects the higher economical value of lower supply and return temperatures for both the end-users and DH company

Similarly, a UK small scale DH network, fuelled by a biomass condensing boiler, was investigated. The analysis began implementing the methodology and solving the optimisation problem for the buildings with double string plate radiators connected to the heat network. The optimisation took into account the higher economic value of lower return temperature for the both end-users and DH company. Next, the entire heat network was simulated comparing the reference scenario with the optimised one. The new operating temperatures for the buildings with radiators and UFH as well as for the heat network were changed, showing

the effectiveness of the proposed new strategy to operate the heating systems and the small scale DH network more efficiently.

7.3 Conclusion

The main key findings and contribution of this work are related to the optimisation of DH supply and return water temperatures associated mainly to the use of single and double string heat emitters.

7.3.1 Optimisation of hydronic radiators in a Danish single-family house

Double string plate radiators connected to a typical Danish DH network

The results related to this scenario, with the existing building in prevision to be connected to a typical Danish DH network, showed the optimal operation of the existing double string plate radiators. If properly controlled through TRVs and DH network, by adjusting the supply temperatures to the optimal level, low return temperatures can be achieved. The implementation of the proposed methodology in fact led to obtained a yearly average return temperature of 26 °C which corresponds to a discont of 14% in the end users' energy bill according to the assumed motivation tariff. This was obtained without any intervention in the thermal envelope of building nor to heating systems, through simply adjusting the temperatures according to demand.

Double string plate radiators connected to a future Danish DH network

In this scenario, the optimisation problem of the double string radiators was based on the minimisation of both supply and return temperatures due to the assumption of the higher economic value they will have, for both end users and DH companies, in the future DH market. The results illustrated that the plate radiators, if properly controlled through TRVs, can be operated with yearly average supply and return temperatures of 56/32 °C respectively. According to the assumed motivation tariff for this scenario, a possible discount of 16% could be achieved in the end users' energy bill. A critical analysis of the designed curves — Figures 5.7 and 5.8 — suggests that the strategy to be followed for lowering supply and return temperatures has to be related to the economic impact those have in the DH network in analysis. Hence, the optimal temperature level is strictly linked to the specific DH network where the building is or would be connected.

Single string plate radiators connected to a typical Danish DH network

For the case of single string systems with plate radiators, the results illustrate that low return temperatures were not possible due to the differences in the way these systems are operated. If the objective of the investigation in the area is the implementation of LTDH, if technically and economically feasible, these systems should be replaced or converted to double loop. However, it should be noted that the application of the method, even for this type of heating system, allowed the heating system to operate more efficiently and avoid unnecessary high supply and return temperatures. This was quantified for the assumed scenario by a possible discount of 5% in the end users' energy bills.

7.3.2 Optimisation of hydronic radiators and small scale DH network in a UK case study

Operating temperature optimisation for the buildings with double string plate radiators

The investigation of the UK small scale DH network started with the application of the proposed methodology to the building with double string plate radiators. As the heat network is fuelled by a biomass condensing boiler, the optimisation problem of the double string radiators was based on the minimisation of return temperatures due to the higher economic value these have for both end users and DH company. The methodology was applied to two scenario: one with night set-back, representing the current strategy to control the indoor comfort; the other one, with constant 21 °C as indoor temperature setting.

The results for the scenario with night set-back illustrated that the plate radiators, if properly controlled through TRVs, can be operated with yearly average supply and return temperatures of 81/41 °C. The reduction in the yearly average return temperature compared to the recorded one of 55 °C during the heating season 2014/2015 would result in a possible discount of 14% in the end users' energy bill according to the assumed motivation tariff.

The introduction of constant 21 °C as control strategy of the indoor comfort in the second scenario investigated provoked a smoother operation of the plate radiators due to the lower effect of load variability and reheating during mornings.

The results in fact showed that the radiators can be operated with yearly average supply and return temperatures of 81/39 °C. The improvements achieved in this scenario were quantified in a possible discount of 16% in the end users' energy bill due to the 2 °C difference in the yearly average return temperature compared to the scenario with night set-back control strategy. However, the possible benefits achievable in this scenario would not be able to offset the increase energy consumption quantified in 6% for OF1 and 13% for LW1 and DB1 respectively. Hence, the investigation on the optimisation of the operation of the small scale DH network was based on the scenario with night set-back control strategy.

Optimisation of the operation of the heat network

The optimisation of the operation of the UK small scale DH network was based on the comparison between the operation of the system at present conditions with the proposed new strategy. The simulations performed for the reference case resulted in a yearly average return temperature of 54.2 °C compared to recorded one of 55 °C with an average ΔT of 17 °C as observed in the measurements for the heating season 2014/2015. In addition, the estimated energy demand of the estate was 380 MWh from simulation, only 1.6% more of the average figure of 374 MWh obtained from recorded data. Next, the impact of the distribution losses was assessed and quantified as 4% of the total energy delivered. The value is justified by the small dimension of the heat network and its peculiarity of covering only the SH demand.

In the alternative scenario, few improvements in the operation of the network were proposed. Firstly, it was assumed to operate the buildings with plate radiat-

ors with yearly average supply and return temperatures of 81/41 °C as obtained from the optimisation performed for the case of night set-back control. Hence, 81 °C was set as the yearly average inlet temperature for the heat network, whereas for the buildings with UFH 40/30 °C were set as the new operating temperatures. The results of the new operation of the small scale DH network led to achieve a yearly average return temperature of 35.6 °C corresponding to a reduction of 18.6 °C compared to the reference case. This resulted in a overall reduction of the distribution losses of 10%, corresponding to the 3.6% of the total energy delivered.

Finally, the improved average return temperature would guarantee a better condensation of the flue gases improving the overall efficiency of the biomass boiler. This was quantified by calculating the fuel consumption for the two scenario, 133 and 121 tonne respectively for the reference and optimised one, which corresponded to a possible reduction of 9%.

7.4 Future work

The results of this work can form the basis for future development into low temperature heating and cooling in buildings in the following ways.

7.4.1 Application of the methodology to different DH networks

The methodology developed can be applied to other DH networks characterised by different energy generation, distribution and operation. This approach will

determine new optimal temperatures showing how the specific economic impact of lower supply and return temperatures affects the operation of both DH networks and heating systems with plate radiators.

7.4.2 MATLAB code to simulate heat networks

In the definition of the objectives of this research project as first goal it was agreed with the industrial partner to develop our own algorithm to simulate the performances of heat networks using the UK case study to test and validate it. The code, implemented in MATLAB environment, was designed to dynamically simulate the heat generation — including solar thermal — integrated with thermal storage, the temperature variation along the entire network as well as the quantification of the distribution losses and fuel consumption. However, changes in the commercial agreement between the industrial partner and the owner of the Estate of the UK case study had an effect on the development of this investigation and the algorithm was not validated through real measurements. As a result, the focus of the research was realigned to the development of the methodology to investigate and plan the connection of existing buildings to LTDH as described in Section 1.4. Therefore, further work would be carried out to validate the robust MATLAB code presented in Appendix G. There is currently great interest in the development of small scale community energy systems and this work will be of interest. The author is involved in the implementation of a novel heat network for the creative energy homes at the University of Nottingham, which will require the design and investigation of the heat network, as shown in Figure 7.1. Hence, the developed algorithm would be applied and tested in this new research project,

to be used in the future as a reliable tool for simulating the operation and the performances of heat networks.

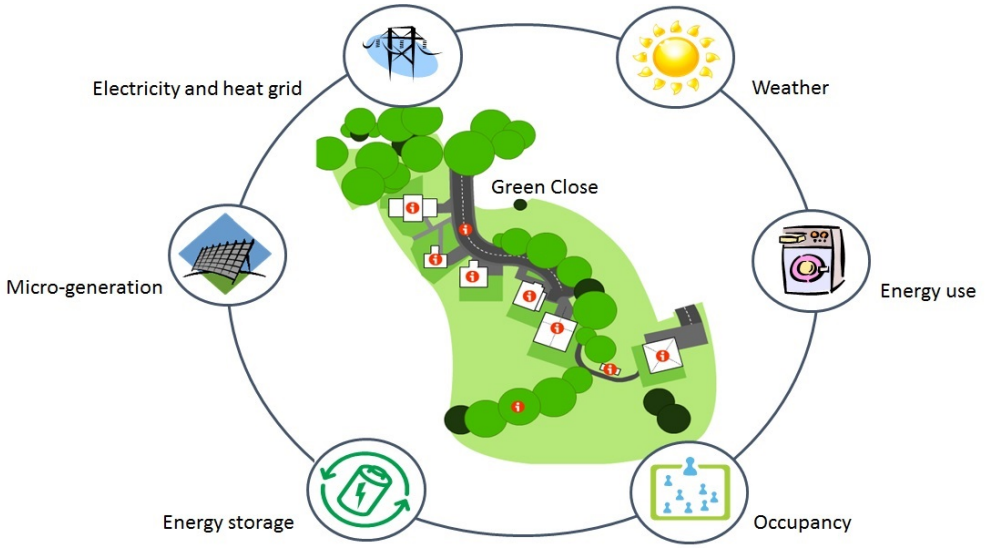

Figure 7.1: SCENIC (Smart Controlled Energy Networks Integrated in Communities) project at the University of Nottingham

7.4.3 Implementation of the developed methodology to the Scenic project

The creative energy homes LTDH network project will be also used as a case study to apply the proposed methodology. The first objective will be the definition of the optimal operating temperatures for the heating systems and the heat network according to the economical impact of supply and return temperatures. This will take into account the multiple heat generation technologies available on site which include biomass boiler, ASHPs, GSHP and solar thermal and the different heating systems. In addition, very detailed analysis will be performed in relation to the operation of the existing plate radiators with lower temperatures.

Appendix A

Schmid biomass boiler: technical specifications

Schmid UTSL Boiler

1

eco-fuels

The Schmid UTSL boiler is designed for the burning of Wood Chip and Wood Pellets up to 40% (W) moisture content whilst providing energy in the form of hot water and a maximum efficiency >93% thanks to low exhaust gas temperatures and clean combustion.

Combustion Chamber
The combustion chamber comprises of a underfeed screw feed stoker and a rotating grate. Controlled combustion air is introduced into the firebox chamber to ensure complete combustion and low emissions. The firebox chamber is lined with firebricks with low thermal storage to ensure rapid reaction time of the boiler. The combustion chamber is finished off with insulated panels.

Automatic De-Ashing
Both the rotating grate and heat exchanger are cleaned by a unique, specially developed mechanism. Removal of the ash can be either a drawer located at the front of the unit or an optional de-ash auger and collection bin.

Heat Exchange
The heat exchange is a 2 pass vertical tube system design ensuring good heat transfer and efficiency. The heat exchange is insulated with fibre insulation and finished with insulated panel.

Controls
The Schmid Controller controls and optimizes the combustion process via a lambda (oxygen) sensor.

- Clear display screen
- Mode of operation changeable at the press of a button
- Fault indicator
- Display cleaning program
- Factory tested

The result of these controls is an optimum utilization of fuel with high efficiency and low emissions to match. Remote monitoring, up to eight different heating circuits, water heater control, legionella control etc is available upon request.

Schmid UTSL Boiler

1

eco-fuels

UTSL & Spring Arm Mechanism

*This picture is for illustration purposes only and may not show the fuel handling equipment as specified within the quotation.

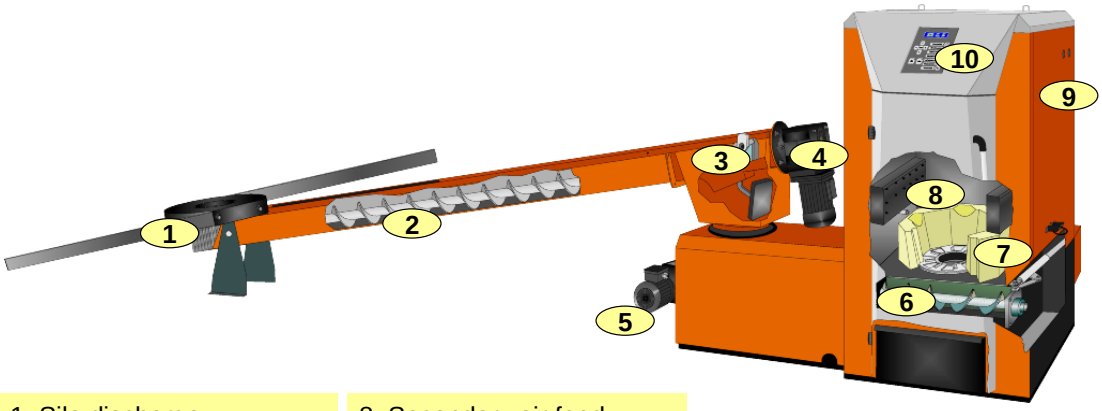

1. Silo discharge	8. Secondary air feed
2. Transport screw	9. Heat exchanger
3. Burn back flap	10. Control system
4. Discharge drive	
5. Stoker screw	
6. Underfeed stoker	
7. Rotating grate	

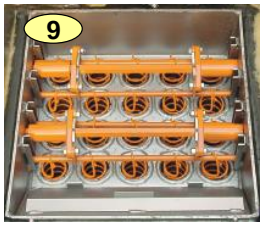

SCHMID
WOOD FIRING SYSTEMS

Technical Data

Combustion

Grate	Rotating
Capacity Regulation	100 – 30% Modulating

Output

Operating Medium	Hot water
Max. Working Pressure	3.0 Bar
Max. Working Temp	90°C

Fuel Input

Fuel Type	Woodchip & Wood Pellets
Fuel Size	40mm^3
Moisture Content of Fuel	w 10 – 35%

Schmid UTSL Boiler

1

eco-fuels

Boiler Type	Rated Power	Operating Range	Dims in mm			Weight	Chimney Size
	kW	kW	height	width	depth	In Kg's	180
UTSL 30 T	30	9 – 30	1330	630	1050	545	180
UTSL 40 T	40	12 – 40	1430	630	1050	575	180
UTSL 50 T	49	15 - 49	1430	770	1050	645	180
UTSL 65 T	65	20 – 65	1530	770	1050	690	200
UTSL 80 T	80	24 - 80	1520	870	1265	850	200
UTSL 99 / 110 T	110	30 – 100	1620	870	1265	950	200
UTSL 150 T	150	45 - 150	1810	1050	1465	1400	250
UTSL 199 T	199	70-199	1800	1175	2650	2100	250

Rotary Arm Bunker System

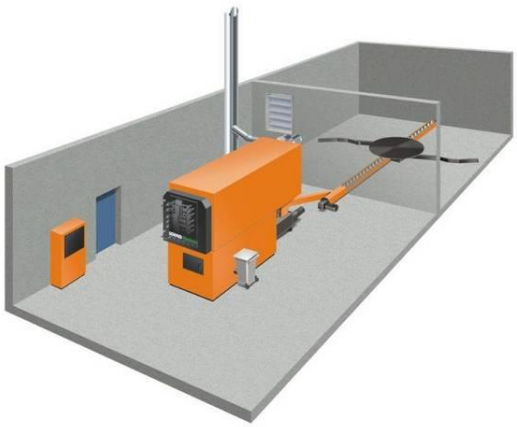

The rotary arm system comprises of a square storage bunker, centre fitted agitator arms and screw auger. Two flexible arms spin within the bunker to agitate the fuel whilst also moving material over the screw auger; the screw auger then transfers the fuel from the storage bunker to the boiler fuel feed connection point. The rate of fuel and operation is controlled via the Pyrotronic boiler controller. Fuel can either be blown in from the fuel delivery supplier or tipped in through an opening or hydraulic lid using machinery/tipper vehicles.
In cases where the storage bunker can't be positioned directly next to the boiler; additional intermediate screw augers are used to transfer the fuel between the bunker screw auger and boiler fuel feed connection.

Appendix B

Cordivari thermal storage: technical specifications

PUFFER VC VT - PUFFER VC SERP. VT

HEATING WATER BUFFER TANK WITH OR WITHOUT HEAT EXCHANGER

STORAGE		EXCHANGER	
Pmax	Tmax	Pmax	Tmax
3 bar	99°C	12 bar	110°C
		Coil version	

For temperature of exchanger > 110°C
see page 102

Capacity	PUFFER VC VT
[liters]	ART. NR.
200	3251162282501
300	3251162282502
500	3251162282503
800	3251162282504
1000	3251162282505
1500	3251162282506
2000	3251162282507
3000	3251162282508
5000	3251162282510

PUFFER VC VT (WITH COIL)		
Capacity	ART. NR.	Exchanger surface
[liters]		[m²]
300	3251162282201	1,0
500	3251162282202	2,1
800	3251162282203	2,5
1000	3251162282204	3,1
1500	3251162282205	3,8
2000	3251162282206	4,6
3000	3251162282207	6,2
5000	3251162282209	7,5

PROMPT DELIVERY

Grey highlighted products are dispatched in 1-5 working days. (Delivery time excluded)

Application
Production and Storage of heating hot water. Used to improve flexibility of pellets, stoves and burners.

Technical descriptions
Buffers are used in units with a typically discontinuous energy source .The buffer tank is connected with the heating system and do not need any coating inside. Made in carbon steel outside painted.
Version with heat exchanger allows use together with a solar installation.

Material
There is no need of any anti-corrosion treatment due to the fact that the buffer is in a closed circuit without any adding air.

Heat exchanger:
Carbon steel fixed coil

Insulation
100 mm soft polyester fibre with high Thermal insulation with Thermal conductivity: 0.035 W/mK. Fire resistance class B-s2d0 according to EN 13501.
Grey PVC external lining complete with top cover.

Warranty
-2 years See general sales conditions and warranty.

CONNECTIONS			
1 -3 6 -7	Heating return/To Generator 1" 1/2 Gas F	10	Connection for instrumentation 1/2" Gas F
2-5	Connection for instrumentation 1/2" Gas F	11-12 14-16	Heating delivery/From Generator 1" 1/2 Gas F
4	Heat exchanger outlet	13	Connection for instrumentation 1/2" Gas F
8	Heat exchanger inlet	15	
9	Connection for electrical integration 1" 1/2 Gas F	17	Heating delivery/From Generator 1" 1/2 Gas F
		18	Drain (for Capacity > 2000 lt)

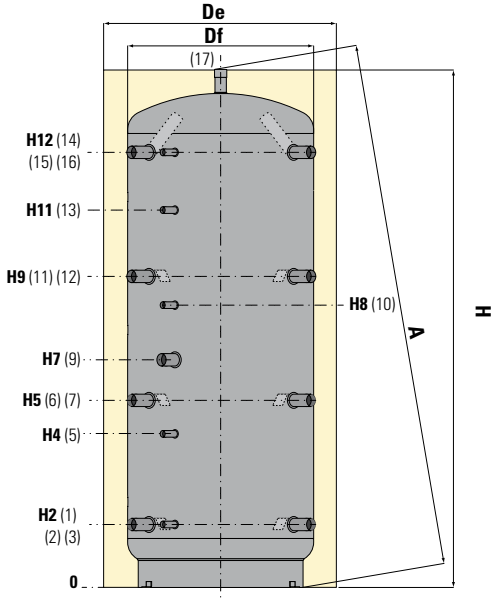

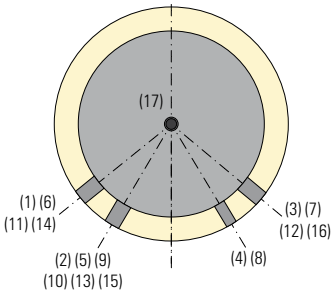

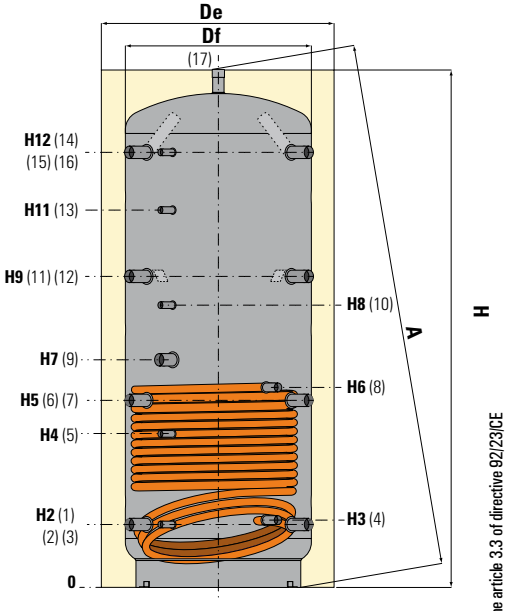

Puffer with coil

Capacity	Df	De	H	A	H2	H4	H5	H7	H8	H9	H11	H12	1-3-6-7-9-11-12-14-15-17	18	H3	H6	8 - 4
[liters]	[mm]														[mm]		CONNECTIONS Gas F
200	450	650	1349	1366	218	430	500	576	711	782	871	1064	1" 1/2	–	-	-	1"
300	550	750	1390	1413	232	444	514	590	725	796	885	1078	1" 1/2	–	217	514	1"
500	650	850	1720	1745	247	533	629	800	941	1011	1167	1393	1" 1/2	–	260	745	1"
800	790	990	1890	1925	265	584	690	823	988	1115	1332	1541	1" 1/2	–	278	762	1"
1000	790	990	2180	2210	265	656	787	1013	1188	1309	1588	1831	1" 1/2	–	284	953	1"
1500	950	1150	2300	2345	313	736	845	1061	1286	1377	1653	1909	1" 1/2	–	336	1006	1"
2000	1100	1300	2370	2430	347	770	879	1060	1300	1411	1687	1943	1" 1/2	–	370	1001	1"
3000	1250	1450	2854	2881	546	1007	1061	1683	1869	1776	2130	2392	2"	1"	569	1551	1"1/4
5000	1600	1800	3152	3186	669	1130	1184	1772	1972	1899	2242	2515	2"	2"	692	1323	1"1/4

P.E.D. product planned and produced in conformity to the article 3.3 of directive 92/23/CE

Appendix C

Groundfos pump: technical specifications

MAGNA3

Circulator pumps

50/60 Hz

Grundfos blueflux®

be
think
innovate

GRUNDFOS

1. Product description

The Grundfos MAGNA3 circulator pumps are designed for circulating liquids in the following systems:

- heating systems
- air-conditioning and cooling systems
- domestic hot-water systems.

The pump range can also be used in the following systems:

- ground source heat pump systems
- solar-heating systems.

Duty range

Data	MAGNA3 (N) Single-head pumps	MAGNA3 D Twin-head pumps
Maximum flow rate, Q	78.5 m^3/h	150 m^3/h
Maximum head, H	18 metres	
Maximum system pressure	1.6 MPa (16 bar)	
Liquid temperature	-10 to 110 °C	

TM05 8894 2813

Fig. 1 MAGNA3 pump ranges

Characteristic features

- $AUTO_{ADAPT}$.
- $FLOW_{ADAPT}$.
- Proportional-pressure control.
- Constant-pressure control.
- Constant-temperature control.
- Differential-temperature control.
- Constant-curve duty.
- Maximum or minimum curve duty.
- $FLOW_{LIMIT}$
- Automatic night setback.
- No external motor protection required.
- Insulating shells supplied with single-head pumps for heating systems.
- Large temperature range where the liquid temperature and the ambient temperature are independent of each other.

Benefits

- Low energy consumption. All MAGNA3 pumps comply with the EuP 2015 requirements.
- The $AUTO_{ADAPT}$ function ensures energy savings.
- $FLOW_{ADAPT}$ which is a combination of the well-known $AUTO_{ADAPT}$ control mode and a new $FLOW_{LIMIT}$ function.
- Built-in Grundfos differential-pressure and temperature sensor.
- Simple installation.
- No maintenance and long life.
- Extended user interface with TFT display.
- Control panel with self-explanatory push-buttons made of high-quality silicone.
- Work log history.
- Easy system optimisation.
- Heat energy meter.
- Multipump function.
- External control and monitoring enabled via add-on modules.
- The complete range is available for a maximum system pressure of 16 bar (PN 16).

Main applications

Heating systems

- Main pump
- mixing loops
- domestic hot water
- heating surfaces
- air-conditioning surfaces.

The MAGNA3 circulator pumps are designed for circulating liquids in heating systems with variable flows where you want to optimise the setting of the pump duty point, thus reducing energy costs.
The pumps are also suitable for domestic hot-water systems. Observe local legislation regarding pump house material.

To ensure correct operation, it is important that the sizing range of the system falls within the duty range of the pump.

The pump is especially suitable for installation in existing systems where the differential pressure across the pump is too high in periods with reduced flow demand. The pump is also suitable for new systems where automatic adjustment of pump head to actual flow demand is required, without using expensive bypass valves or similar components.

Furthermore, the pump is suitable for systems with hot-water priority as an external signal can immediately force the pump to operate according to the maximum curve, for example in solar-heating systems.

Type key

Code	Example	MAGNA3	(D)	80	-120	(F)	(N)	360
	Type range MAGNA3							
D	Single-head pump Twin-head pump							
	Nominal diameter (DN) of suction and discharge ports [mm]							
	Maximum head [dm]							
F	**Pipe connection** Flange							
N	**Pump housing material** Cast iron Stainless steel							
	Port-to-port length [mm]							

Model type

This data booklet covers model A and B and the model version is stated on the nameplate. See fig. 2.

Fig. 2 Model type on pump nameplate

The difference in model types can be seen in chapter *Functions*.

Performance range, MAGNA3 D single-head operation

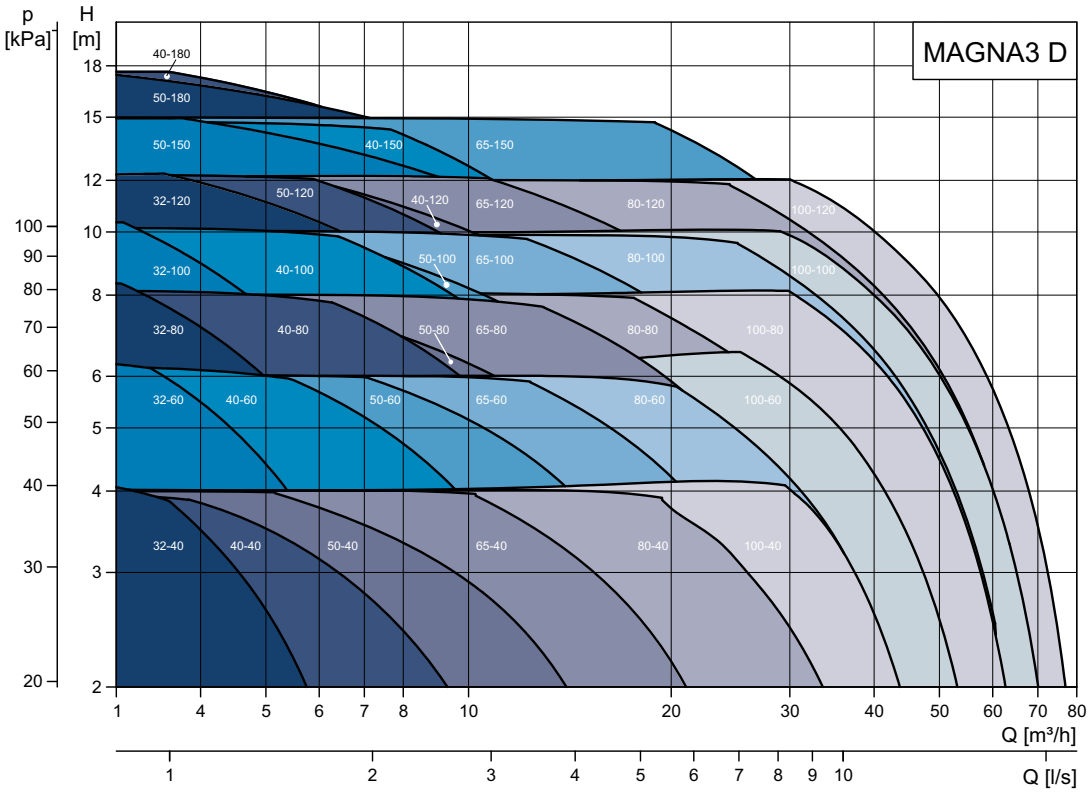

TM05 3937 2313

Fig. 4 Performance range, MAGNA3 D single-head operation

Performance range, MAGNA3 D twin-head operation

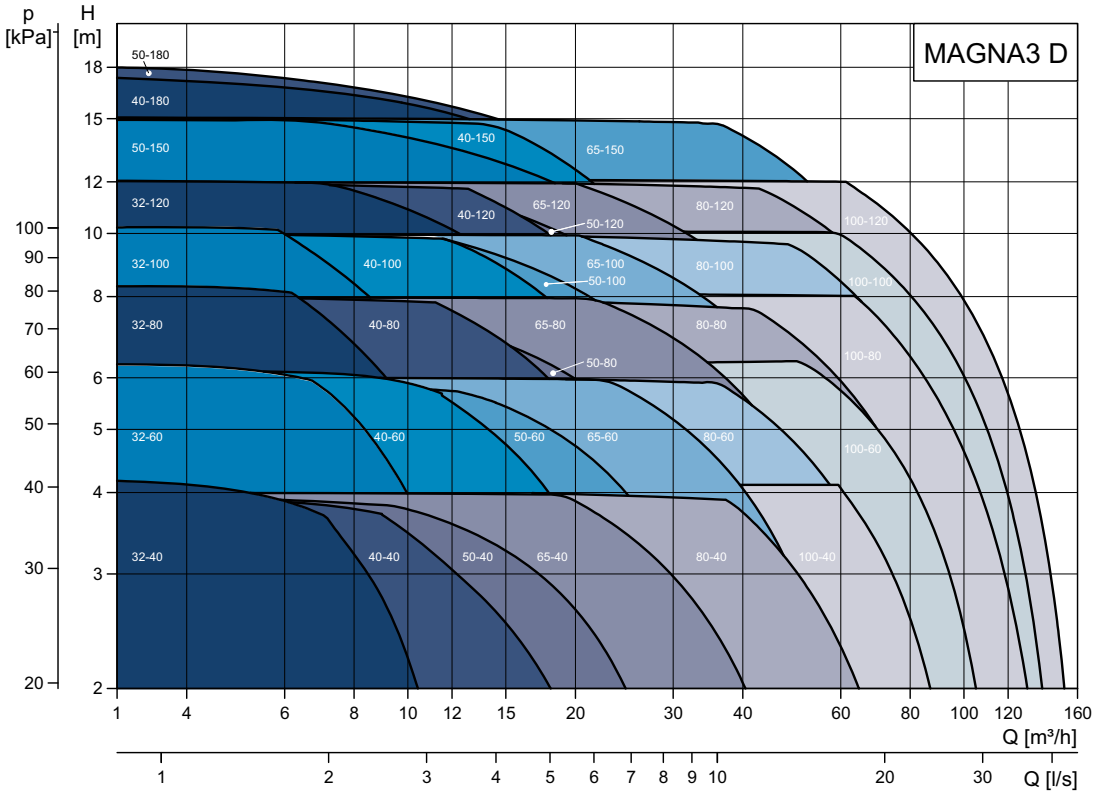

TM05 3938 2313

Fig. 5 Performance range, MAGNA3 D twin-head operation

Twin-head pumps

Pump type	Port-to-port length [mm]	Threaded pipe connection		Electrical connection	Data sheet Page
		Cast iron			
		PN 10	PN 16		
MAGNA3 D 32-40	180	•	•	Plug	51
MAGNA3 D 32-60	180	•	•	Plug	53
MAGNA3 D 32-80	180	•	•	Plug	55
MAGNA3 D 32-100	180	•	•	Plug	57

Pump type	Port-to-port length [mm]	Flange connection				Electrical connection	Data sheet Page
		Cast iron					
		PN 6	PN 10	PN 6/10	PN 16		
MAGNA3 D 32-40 F	220			•	•	Plug	60
MAGNA3 D 32-60 F	220			•	•	Plug	62
MAGNA3 D 32-80 F	220			•	•	Plug	64
MAGNA3 D 32-100 F	220			•	•	Plug	66
MAGNA3 D 32-120 F	220			•	•	Terminals	68
MAGNA3 D 40-40 F	220			•	•	Plug	70
MAGNA3 D 40-60 F	220			•	•	Plug	72
MAGNA3 D 40-80 F	220			•	•	Terminals	74
MAGNA3 D 40-100 F	220			•	•	Terminals	76
MAGNA3 D 40-120 F	250			•	•	Terminals	78
MAGNA3 D 40-150 F	250			•	•	Terminals	80
MAGNA3 D 40-180 F	250			•	•	Terminals	82
MAGNA3 D 50-40 F	240			•	•	Terminals	84
MAGNA3 D 50-60 F	240			•	•	Terminals	86
MAGNA3 D 50-80 F	240			•	•	Terminals	88
MAGNA3 D 50-100 F	280			•	•	Terminals	90
MAGNA3 D 50-120 F	280			•	•	Terminals	92
MAGNA3 D 50-150 F	280			•	•	Terminals	94
MAGNA3 D 50-180 F	280			•	•	Terminals	96
MAGNA3 D 65-40 F	340			•	•	Terminals	98
MAGNA3 D 65-60 F	340			•	•	Terminals	100
MAGNA3 D 65-80 F	340			•	•	Terminals	102
MAGNA3 D 65-100 F	340			•	•	Terminals	104
MAGNA3 D 65-120 F	340			•	•	Terminals	106
MAGNA3 D 65-150 F	340			•	•	Terminals	108
MAGNA3 D 80-40 F	360	•	•		•	Terminals	110
MAGNA3 D 80-60 F	360	•	•		•	Terminals	112
MAGNA3 D 80-80 F	360	•	•		•	Terminals	114
MAGNA3 D 80-100 F	360	•	•		•	Terminals	116
MAGNA3 D 80-120 F	360	•	•		•	Terminals	118
MAGNA3 D 100-40 F	450	•	•		•	Terminals	120
MAGNA3 D 100-60 F	450	•	•		•	Terminals	122
MAGNA3 D 100-80 F	450	•	•		•	Terminals	124
MAGNA3 D 100-100 F	450	•	•		•	Terminals	126
MAGNA3 D 100-120 F	450	•	•		•	Terminals	128

Note: The product numbers of the various pump variants can be found on page 131.

Appendix D

Flexalen pre-insulated pipes: technical specifications

Product Guide Flexalen™

FLEXENERGY®
INSULATED PIPE SOLUTIONS

www.flexenergy.co.uk

Material properties

Polybutene (carrier pipe)

Density	0,940 g/cm³
Melt index	0,4 g/10 min
Stretch tension	20 N/mm²
Tearing strength	35 N/mm²
Tearing expansion	300%
E-module	450 N/mm²
Shore-hardness	D60
Notch ductility	without breakage
Ductility	without breakage
Length expansion coefficient	0,13 mm/mK
λ-value	0,19 W/mK

Polyethylene (casing pipe)

Stretch tension	22 N/mm²
Tearing strength	32 N/mm²
Tearing expansion	800%
E-module	800 N/mm²
Notch ductility	without breakage
Ductility	without breakage
Length expansion coefficient	0,18 mm/mK
λ-value	0,043 W/mK

Polyolefine (insulation)

Volume weight	30 – 40 kg/m³
Temperature resistance	- 80 up to +95 ºC
λ-value	0,028 – 0,038 W/mK
closed cells	

Polyurethan (insulation)

Volume weight	50 – 80 kg/m³
Temperature resistance	- 40° C up to +110 ºC
λ-value	0,033 W/mK
closed cells	94%
Load resistance	>0,2 N/mm²

Flexibility of plastic pipes

Material	E-module (stiffness) [N/mm²]
PB	450
PE-X	600 (33% stiffer than Polybutene)
PP-R	800 (78% stiffer than Polybutene)

Operating pressure

at +95° C for pipes SDR 11 (z.B. 63 x 5,8)

Material	max. operating pressure [bar / PSI]	
PB	8 bar (116 PSI)	that is 33% higher
PE-X	6 bar (87 PSI)	
PP-R	–	

Did you know! …

that PB is extremely flexible? PB is 25% more flexible than PE-X and 44% more flexible than PP-R!

Flexalen 600™ – the professional pre-insulated pipe

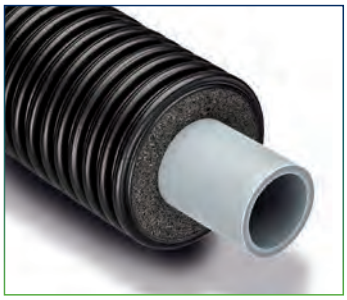

For heating, hot water and thermal pipes up to 95° C and 8 bar.

- Homogeneous connection between insulation and casing pipe
- Closed-cell, water tight Polyolefine insulation
- Polyolefine thermal insulation λ = 0,028 – 0,038 W/mK
- Homogeneous insulation also between double pipes
- Fully weldable system
- Strengthened jacket pipe
- High flexibility at low temperatures
- Continuous quality assurance by third party audits performed by acknowledged certification institute (KIWA)
- Temperature range -15° C up to +95° C
- It satisfies the requirements for sustainable construction

Temperature / Pressure rating

Dimension O.D. 16 – 110 mm

temperature	-15° C	0° C	20° C	40° C	60° C	70° C	80° C	90 °C	95° C
pressure (bar)	16 bar	16 bar	16 bar	15 bar	12 bar	10 bar	9 bar	8 bar	8 bar
pressure (PSI)	232	232	232	218	174	145	131	116	116

Dimension O.D. 125 – 225 mm

temperature	-15 °C	0 °C	20 °C	40 °C	60 °C	70 °C	80 °C	90 °C	95 °C
pressure (bar)	10 bar	10 bar	10 bar	10 bar	10 bar	8 bar	7 bar	6 bar	5 bar
pressure (PSI)	145	145	145	145	145	116	102	87	73

Flexible, pre-insulated pipe system with one carrier pipe for heating and hot water applications

- Homogenous connection between corrugated casing pipe and polyolefine insulation
- High flexibility
- Single pipes O.D.16 – O.D.125
- Pipe system for heating and hot water application
- Temperature range -15° C up to +95° C
- Fully weldable system
- It satisfies the requirements for sustainable construction
- Polyolefine insulation λ = 0,028 – 0,038 W/mK

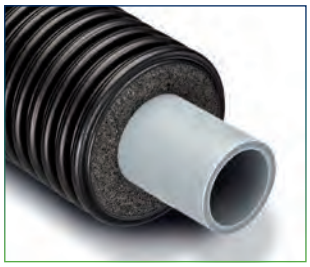

Product code	DN	Inch	Casing pipe O.D. [mm]	Carrier pipe**		Wall thickness [mm]	No. of carrier pipes	Minimum bending radius [m]	max. length* [m]	Weight [kg/m]
				O.D. [mm]	I.D. [mm]]					
VS-RS40A16	12	½	40	16	11,6	2,2	1	0,16	500	0,25
VS-RS40A20	15	½	40	20	14,4	2,8	1	0,20	500	0,28
VS-RS50A25	20	¾	50	25	20,4	2,3	1	0,30	500	0,37
VS-RS90A25	20	¾	90	25	20,4	2,3	1	0,40	500	0,75
VS-RS63A32	25	1	63	32	26,2	2,9	1	0,40	500	0,58
VS-RS125A32	25	1	125	32	26,2	2,9	1	0,40	300	1,85
VS-RS75A40	32	1 ¼	75	40	32,6	3,7	1	0,50	500	0,86
VS-RS125A40	32	1 ¼	125	40	32,6	3,7	1	0,50	300	1,98
VS-RS90A50	40	1½	90	50	40,8	4,6	1	0,60	500	1,21
VS-RS160A50	40	1 ½	160	50	40,8	4,6	1	0,70	150	2,40
VS-RS125A63	50	2	125	63	51,4	5,8	1	0,80	300	2,43
VS-RS160A63	50	2	160	63	51,4	5,8	1	0,80	150	2,75
VS-RS125A75	65	2 ½	125	75	61,4	6,8	1	0,80	300	2,89
VS-RS160A75	65	2 ½	160	75	61,4	6,8	1	0,80	150	2,97
VS-RS160A90	80	3	160	90	73,6	8,2	1	1,00	150	3,64
VS-R200A110	100	4	200	110	90,0	10,0	1	1,25	110	5,40
VS-R200A125	100	4	200	125	102,2	11,4	1	1,50	80	6,38

*) Any length within the maximum delivery length can be delivered, rounded up to the nearest whole metre.
**) The dimensions for the PB pipes refer to the pressure stage 8 bar at +95° C.

Temperature / Pressure rating

Dimension O.D. 16 – 110 mm

temperature	-15° C	0° C	20° C	40° C	60° C	70° C	80° C	90 °C	95° C
pressure (bar)	16 bar	16 bar	16 bar	15 bar	12 bar	10 bar	9 bar	8 bar	8 bar
pressure (PSI)	232	232	232	218	174	145	131	116	116

Dimension O.D. 125 – 225 mm

temperature	-15 °C	0 °C	20 °C	40 °C	60 °C	70 °C	80 °C	90 °C	95 °C
pressure (bar)	10 bar	10 bar	10 bar	10 bar	10 bar	8 bar	7 bar	6 bar	5 bar
pressure (PSI)	145	145	145	145	145	116	102	87	73

Flexible, pre-insulated pipe system with two carrier pipes for heating and hot water applications

- Homogenous connection between corrugated casing pipe and polyolefine insulation
- High flexibility
- Double pipes O.D.16 – O.D.63
- Pipe system for heating and hot water application
- Temperature range -15° C up to +95° C
- Fully weldable system
- It satisfies the requirements for sustainable construction
- Polyolefine insulation λ = 0,028 – 0,038 W/mK

Product code	DN	Inch	Casing pipe O.D. [mm]	Carrier pipe**		Wall thickness [mm]	No. of carrier pipes	Minimum bending radius [m]	max. length* [m]	Weight [kg/m]
				O.D. [mm]	I.D. [mm]					
VS-RS63A2/16	2 x 12	2 x ½	63	16	11,6	2,2	2	0,35	500	0,53
VS-RS75A2/20	2 x 15	2 x ½	75	20	14,4	2,8	2	0,40	500	0,69
VS-RS125A2/25	2 x 20	2 x ¾	125	25	20,4	2,3	2	0,60	300	1,80
VS-RS125A2/32	2 x 25	2 x 1	125	32	26,2	2,9	2	0,60	300	1,90
VS-RS160A2/40	2 x 32	2 x 1¼	160	40	32,6	3,7	2	0,80	150	2,46
VS-RS160A2/50	2 x 40	2 x 1½	160	50	40,8	4,6	2	0,80	150	3,00
VS-RS200A2/63	2 x 50	2 x 2	200	63	51,4	5,8	2	1,25	125	4,50

*) Any length within the maximum delivery length can be delivered, rounded up to the nearest whole metre.
**) The dimensions for the PB pipes refer to the pressure stage 8 bar at +95° C.

Temperature / Pressure rating

Dimension O.D. 16 – 110 mm

temperature	-15° C	0° C	20° C	40° C	60° C	70° C	80° C	90 °C	95° C
pressure (bar)	16 bar	16 bar	16 bar	15 bar	12 bar	10 bar	9 bar	8 bar	8 bar
pressure (PSI)	232	232	232	218	174	145	131	116	116

Dimension O.D. 125 – 225 mm

temperature	-15 °C	0 °C	20 °C	40 °C	60 °C	70 °C	80 °C	90 °C	95 °C
pressure (bar)	10 bar	10 bar	10 bar	10 bar	10 bar	8 bar	7 bar	6 bar	5 bar
pressure (PSI)	145	145	145	145	145	116	102	87	73

Flexalen 600™ heat losses according EN15632

Heat loss double pipe (flow & return)

Product code	Average service temperature [°C]						
	20	30	40	50	60	70	80
VS-RS63A2/16	3,527	5,878	8,230	10,581	12,932	15,284	17,635
VS-RS75A2/20	3,608	6,013	8,418	10,824	13,229	15,634	18,039
VS-RS125A2/25	2,992	4,987	6,981	8,976	10,971	12,965	14,960
VS-RS125A2/32	3,826	6,377	8,928	11,478	14,029	16,580	19,131
VS-RS160A2/40	3,356	5,680	8,004	10,328	12,652	14,976	17,300
VS-RS160A2/50	4,374	7,476	10,579	13,682	16,785	19,887	22,990
VS-RS200A2/63	4,374	7,800	11,226	14,652	18,078	21,504	24,930
	Heat loss [W/m]						

Thermal conductivity of soil	1,00 W/m.K
Thermal resistance factor of earth surface to ambient air	0,0685 m^2.K/W
Soil temperature	10° C
Soil covering	0,8 m

The mentioned heat loss values have been measured, calculated and proven by acknowledged testing institutes according EN 15632. During the expected lifetime this values will increase by 7 – 10%.

Flexalen 600™ heat losses according EN15632

Heat loss single pipe

Product code	Service temperature [°C]						
	20	30	40	50	60	70	80
VS-RS40A16	1,794	3,644	5,548	7,507	9,519	11,585	13,704
VS-RS40A20	2,354	4,776	7,264	9,819	12,439	15,123	17,870
VS-RS50A25	2,344	4,758	7,241	9,793	12,413	15,100	17,853
VS-RS90A25	1,390	2,824	4,302	5,822	7,385	8,990	10,638
VS-RS63A32	2,426	4,923	7,492	10,131	12,841	15,619	18,466
VS-RS125A32	1,411	2,863	4,357	5,892	7,469	9,086	10,743
VS-RS75A40	2,614	5,304	8,070	10,910	13,824	16,811	19,870
VS-RS125A40	1,678	3,405	5,181	7,005	8,877	10,796	12,763
VS-RS90A50	2,965	6,014	9,145	12,358	15,651	19,024	22,476
VS-RS160A50	1,730	3,506	5,327	7,193	9,105	11,060	13,060
VS-RS125A63	2,754	5,583	8,488	11,468	14,521	17,647	20,846
VS-RS160A63	2,109	4,273	6,491	8,764	11,090	13,470	15,904
VS-RS125A75	3,673	7,443	11,307	15,265	19,315	23,458	27,690
VS-RS160A75	2,521	5,106	7,756	10,470	13,248	16,089	18,992
VS-RS160A90	3,204	6,489	9,855	13,299	16,823	20,425	24,104
VS-R200A110	3,386	6,850	10,393	14,012	17,708	21,479	25,326
VS-R200A125	4,114	8,323	12,624	17,018	21,503	26,078	30,743
	Heat loss [W/m]						

Heat loss single pipe pair (flow & return)

Product code	Average service temperature [°C]						
	20	30	40	50	60	70	80
VS-RS40A16	3,376	6,781	10,279	13,868	17,732	21,313	25,168
VS-RS40A20	4,316	8,658	13,106	17,659	22,548	27,070	31,925
VS-RS50A25	4,308	8,644	13,091	17,647	22,553	27,078	31,950
VS-RS90A25	2,672	5,373	8,150	11,002	13,930	16,933	20,009
VS-RS63A32	4,449	8,926	13,516	18,218	23,281	27,949	32,976
VS-RS125A32	2,711	5,450	8,262	11,147	14,105	17,134	20,234
VS-RS75A40	4,762	9,550	14,457	19,479	24,884	29,865	35,225
VS-RS125A40	3,190	6,410	9,713	13,100	16,569	20,120	23,752
VS-RS90A50	5,327	10,677	16,152	21,751	27,770	33,309	39,265
VS-RS160A50	3,286	6,599	9,991	13,461	17,008	20,632	24,331
VS-RS125A63	5,008	10,042	15,195	20,463	26,113	31,340	36,945
VS-RS160A63	3,946	7,921	11,987	16,143	20,390	24,725	29,149
VS-RS125A75	6,426	12,866	19,442	26,151	33,346	39,959	47,052
VS-RS160A75	4,641	9,309	14,082	18,958	23,935	29,013	34,191
VS-RS160A90	5,741	11,505	17,390	23,395	29,811	35,759	42,113
VS-R200A110	6,040	12,102	18,280	24,574	31,267	37,503	44,134
VS-R200A125	7,135	14,281	21,558	28,964	36,851	44,156	51,937
	Heat loss [W/m]						

Thermal conductivity of soil	1,00 W/m.K
Thermal resistance factor of earth surface to ambient air	0,0685 m^2.K/W
Soil temperature	10° C
Soil covering	0,8 m

The mentioned heat loss values have been measured, calculated and proven by acknowledged testing institutes according EN 15632. During the expected lifetime this values will increase by 7 – 10%.

Appendix E

Rehau pre-insulated pipes: technical specifications

REHAU®

Unlimited Polymer Solutions

RAUVITHERM AND RAUTHERMEX PRE-INSULATED PIPE

TECHNICAL INFORMATION

www.rehau.co.uk/districtheating
Valid from August 2014
Subject to technical modifications

Building Solutions
Automotive
Industry

This Technical Information "REHAU RAUVITHERM and RAUTHERMEX systems for heat supply" is valid from April 2014.

With its publication the previous Technical Informations 817600EN (Date December 2013) and 463600EN (Date December 2013) become invalid.

Our current technical documents can be found at www.rehau.co.uk to download.

All dimensions and weights are reference values. Subject to errors and modifications.

2.4 Solutions for heat supply

2.4.1 RAUVITHERM - The highly flexible solution

Thanks to several soft insulating foam layers and the corrugated, resistant outer jacket RAUVITHERM is a pipe system that is highly flexible and very robust at the same time. This also enables extremely complex connections in heating networks as well as connections under cramped space conditions.

Fig. 2-1 Non-bonded pipe system RAUVITHERM

System properties

- Fully bonded outer jacket to the top layer of insulation
- Profiled outer jacket ensures flexibility with low bending forces and small bending radii
- Robust, solid jacket suitable for construction sites
- High thermal insulation due to the multi-layer composition and low thermal conductivity of the insulating layers
- High operating safety thanks to the corrosion resistance of the materials
- Coil lengths of up to 300 m reduces the use of connecting sleeves
- Complete pipe and fittings product range:
  - UNO pipes (up to 125 mm pipe diameter)
  - Efficient DUO pipes (up to 2 x 63 mm pipe diameter)

Fig. 2-2 RAUVITHERM pre-insulated pipe

2.4.2 RAUTHERMEX - The highly efficient solution

The excellent thermal insulation properties of the polyurethane foam insulation and the corrugated outer jacket make RAUTHERMEX a pipe system that keeps losses during heat transport particularly low, without lacking a high degree of flexibility.

Fig. 2-3 RAUTHERMEX bonded pipe system

System properties

- Highest thermal insulation in its class due to the special process technology, fine-pored PU foam and additional insulation thickness (Plus dimension)
- Coil lengths of up to 570 m enable very long sections without joints
- No expansion bellows or compensators required during installation
- Durable due to the corrosion-free materials, watertight secondary insulation and fully bonded pipe system
- Complete pipe and fittings product range:
- UNO pipes (up to 160 mm pipe diameter)
- DUO pipes (up to 2 x 63 mm pipe diameter)

Fig. 2-4 RAUTHERMEX pre-insulated pipe

3 MATERIAL PROPERTIES

3.1 Carrier pipes

The water-bearing carrier pipe in RAUTHERMEX and RAUVITHERM is made from high pressure crosslinked polyethylene (PE-Xa). The carrier pipes are crosslinked via the addition of peroxide under high pressure and at a high temperature during manufacturing. During this process the macromolecules combine to form a three-dimensional, stable network.

PE-Xa pipes are produced to DIN 16892 / DIN 16893 and DIN EN ISO 15875 in the pressure levels SDR 11 or SDR 7.4 (in accordance with the DVGW Worksheet W 544, W 270 and BGA KTW).

The term “SDR“ stands for “Standard Dimension Ratio“ and describes the ratio of the external diameter to the wall thickness of the pipe, see Fig. 3-1. The SDR number therefore serves indirectly to determine the pressure resistance. The smaller the SDR number, the thicker the walls of, and the more pressure-resistant the pipe.
SDR 11 demonstrates a high pressure resistance.

- Very high chemical resistance (DIN 8075 Supplementary sheet 1)
- Very low roughness (k = 0.007 mm)
- Permanently low pressure loss
- Long-term corrosion resistance
- High shape retention
- High temperature resistance, in the event of malfunctioning energy source control system
- High pressure resistance
- Robust and flexible at the same time
- Excellent resistance to point loads

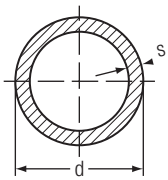

$$SDR = \frac{d}{s}$$

Fig. 3-1 SDR
d External diameter [mm]
s Wall thickness [mm]

Technical data carrier pipe

Description		Value	Standard
Density ρ		0.94 g/cm³	ISO 1183
Average thermal coefficient of linear expansion (0 °C - 70 °C)		$1.5 \cdot 10^{-4}$ /K	–
Thermal conductivity λ		0.35 W/m·K	Based on ASTM C 1113
Modulus of elasticity E at 20°C		600 N/mm²	ISO 527
Modulus of elasticity E at 80 °C		200 N/mm²	ISO 527
Surface resistance		10^{12} Ω	–
Building material class		B2 (normal flammability)	DIN 4102
Surface friction coefficient k		0.007 mm	–
Oxygen impermeability	at 40 °C	0.16 mg/(m³·d)	DIN 4726
	at 80 °C	1.8 mg/(m³·d)	

Tab. 3-1 Material properties PE-Xa carrier pipe

3.1.1 Carrier pipe SDR 11

The PE-Xa carrier pipes SDR 11 are predominantly used for the transport of recirculated water in the area of heating and cooling. For this reason, they have an additional oxygen diffusion barrier made of EVOH to DIN 4726. The colour of these pipes is orange.

Fig. 3-2 Carrier pipes SDR 11

Pressure and temperature resistance

The following temperature and pressure limits apply to DIN 16892 and DIN 16893 at continuous temperatures for carrier pipes SDR 11.
(Application: water; safety factor 1.25)

Temperature [C]	Max. pressure [bar]	Minimum service life [years]
40	11.9	50
50	10.6	50
60	9.5	50
70	8.5	50
80	7.6	25
90	6.9	15
95	6.6	10

Tab. 3-2 Pressure and temperature resistance SDR 11

In the case of varying pressures and temperatures the expected service life can be calculated according to the DIN 13760 “Miner‘s rule“ (see section 6.6. on Page 51).

Application temperatures

- Permanent operating temperature	maximum 85 °C
- Heating medium temperature	maximum 95 °C (sliding)
- Short-term excess temperature	up to 110 °C (failure)

3.1.2 Continuous quality inspection

REHAU is ISO 9001 certified and the quality of the carrier pipes is tested continuously by in-house accredited laboratories as well as external institutes.

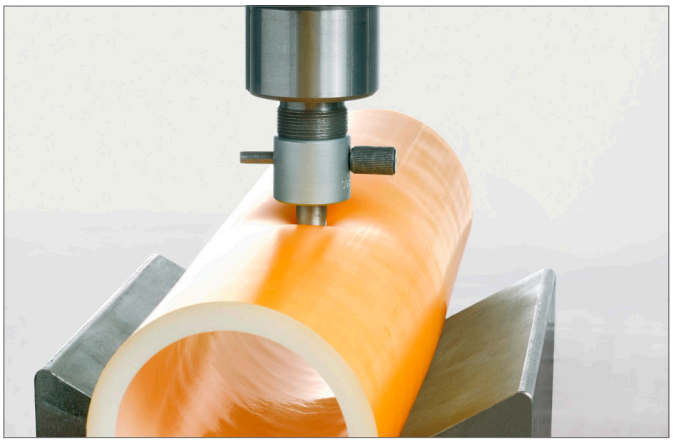

Fig. 3-3 Point load test

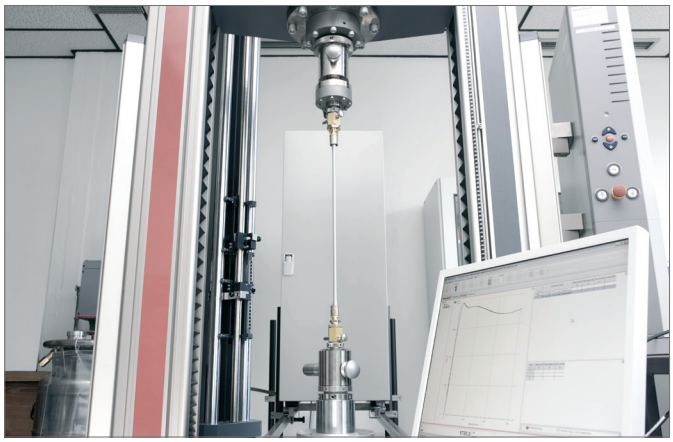

Fig. 3-4 Tensile test

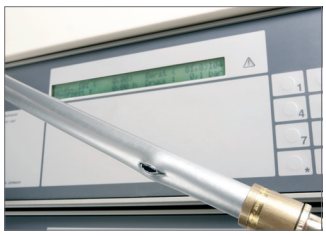

Fig. 3-5 Burst pressure test

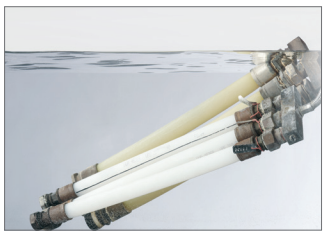

Fig. 3-6 Pressure test

3.2 RAUTHERMEX SDR 11

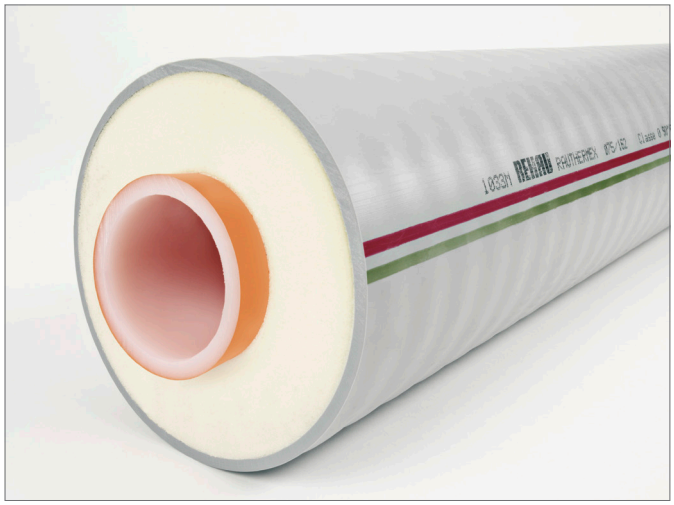

Fig 3-7 RAUTHERMEX composite pipe

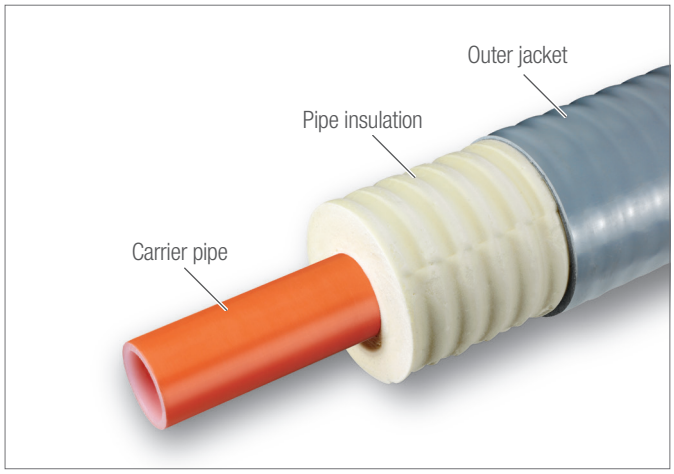

Fig 3-8 RAUTHERMEX pipe main components

3.2.1 Pipe insulation

The insulation of the RAUTHERMEX pipes in SDR 11 consists of pentane-blown PU foam. For coiled bundles the insulation is continuous, for cut lengths and custom components intermittent. The PU foam is therefore free from CFCs and HCFCs.

- Very fine-pored insulating foam structure
- Closed-cell factor ≥ 90 %
- High water vapour transfer coefficient

Technical data pipe insulation

Properties		Blowing agent pentane	Standard
Thermal conductivity $\lambda_{50, initial}$	W/m·K	≤ 0,0216 (0,0260 for rigid systems)	EN 15632
GWP (greenhouse potential)		0,5	
ODP (ozone depletion potential)		0	
Density ρ	kg/m³	> 50	EN 253
Compression strength	MPa	0,2	
Water absorption	%	≤ 10	EN 15632-1
Axial shear strength	kPa	≥ 90	EN 15632-2
Building material class		B2 (normal flammability)	DIN 4102

Tab. 3-3 Properties RAUTHERMEX pipe insulation

3.2.2 Outer jacket

RAUTHERMEX pipes have a corrugated outer jacket. The corrugation improves the structural properties, increases the flexibility and enables low bending radii. To increase the flexibility the outer jacket of the RAUTHERMEX pipes are made from the flexible material PE-LLD.

- Very good bond with the PU foam
- Extruded seamlessly around the PU foam

Technical data outer jacket

Description	Value	Standard
Thermal conductivity λ	0,33 W/m·K	DIN 52612
Crystallite melting range	122 °C	ISO 11357-3
Density ρ	0,92 g/cm³	ISO 1183
Modulus of elasticity E	325 N/mm²	–
Building material class	B2 (normal flammability)	DIN 4102

Tab. 3-4 Properties RAUTHERMEX outer jacket

3.2.3 Dimensions

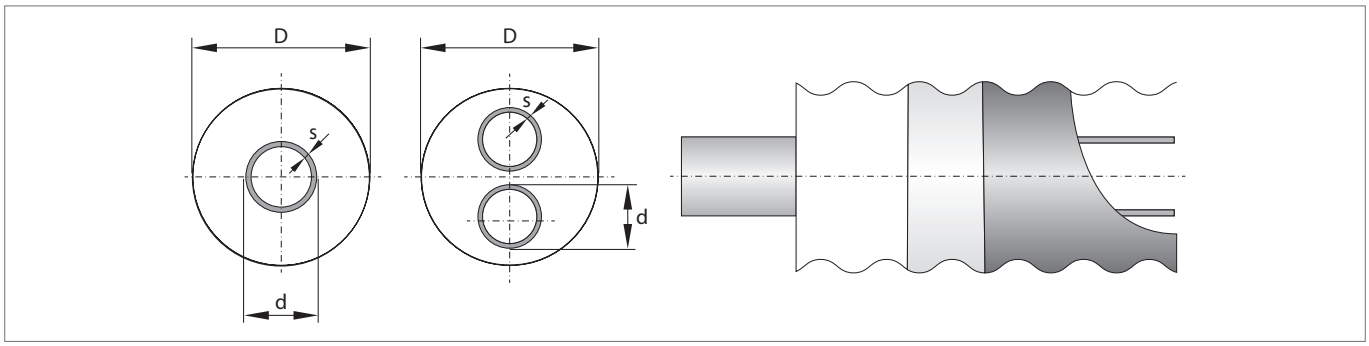

Fig. 3-9 RAUTHERMEX section

Size	d	s	D[2)]	Volume inner pipe	Weight empty	max. coil length 2.8 m x 0.8 m	max. coil length 2.8 m x 1.2 m	U-Value
	[mm]	[mm]	[mm]	[l/m]	[kg/m]	[m]	[m]	[W/m·K]
UNO 25/91	25	2.3	93	0.327	1.28	370	570	0.099
UNO 32/91	32	2.9	93	0.539	1.38	370	570	0.121
UNO 40/91	40	3.7	93	0.835	1.48	370	570	0.151
UNO 50/111	50	4.6	113	1.307	2.11	275	400	0.155
UNO 63/126	63	5.8	128	2.075	2.86	195	305	0.177
UNO 75/162	75	6.8	164	2.961	4.37	95	150	0.162
UNO 90/162	90	8.2	164	4.254	5.02	95	150	0.206
UNO 110/162	110	10	164	6.362	5.78	95	150	0.296
UNO 125/182	125	11.4	185	8.203	7.20	52	86	0.303
UNO 140/202	140	12.7	202	10.315	8.38	46	75	0.308
UNO 160/250	160	14.6	257	13.437	14.17	12 m lengths	–	0.303
DUO 25 + 25/111	25	2.3	113	2 x 0.327	1.85	275	400	0.139
DUO 32 + 32/111	32	2.9	113	2 x 0.539	2.11	275	400	0.183
DUO 40 + 40/126	40	3.7	128	2 x 0.835	2.75	195	305	0.211
DUO 50 + 50/162	50	4.6	164	2 x 1.307	4.25	95	150	0.195
DUO 63 + 63/182	63	5.8	185	2 x 2.075	5.45	52	86	0.238

Tab. 3-5 Dimensions RAUTHERMEX, SDR 11

[1)] maximum diameter at the peak

Size	d_1	s_1	D[1)]	Volume inner pipe	Weight empty	max. coil length 2.8 m x 0.8 m	max. coil length 2.8 m x 1.2 m	U–Value
	[mm]	[mm]	[mm]	[l/m]	[kg/m]	[m]	[m]	[W/m·K]
UNO 32/111	32	2.9	113	0.539	1.69	275	400	0.103
UNO 40/126	40	3.7	128	0.835	2.18	195	305	0.111
UNO 50/126	50	4.6	128	1.307	2.64	195	305	0.136
UNO 63/142	63	5.8	144	2.075	3.49	140	225	0.154
UNO 90/182	90	8.2	185	4.254	5.61	52	86	0.175
UNO 110/182	110	10	185	6.362	6.64	52	86	0.236
DUO 32 + 32/126	32	2.9	128	2 x 0.539	2.50	195	305	0.157
DUO 40 + 40/142	40	3.7	144	2 x 0.835	3.32	140	225	0.174
DUO 50 + 50/182	50	4.6	185	2 x 1.307	4.90	52	86	0.166
DUO 63 + 63/202	63	5.8	206	2 x 2.075	5.90	46	75	0.208

Tab. 3-6 Dimensions RAUTHERMEX Plus, SDR 11

[1)] maximum diameter at the peak

Appendix F

IDA-ICE buildings' models

As presented in Section 5.2 and 6.3.1 based on the characteristics of the buildings used in this investigation, detailed physical models were built in IDA-ICE for each of them. These are shown in the following Figures for both the Danish and UK case study.

Figure F.1: Floor plans, radiators (in red) and IDA-ICE model of the Danish single-family house [102]

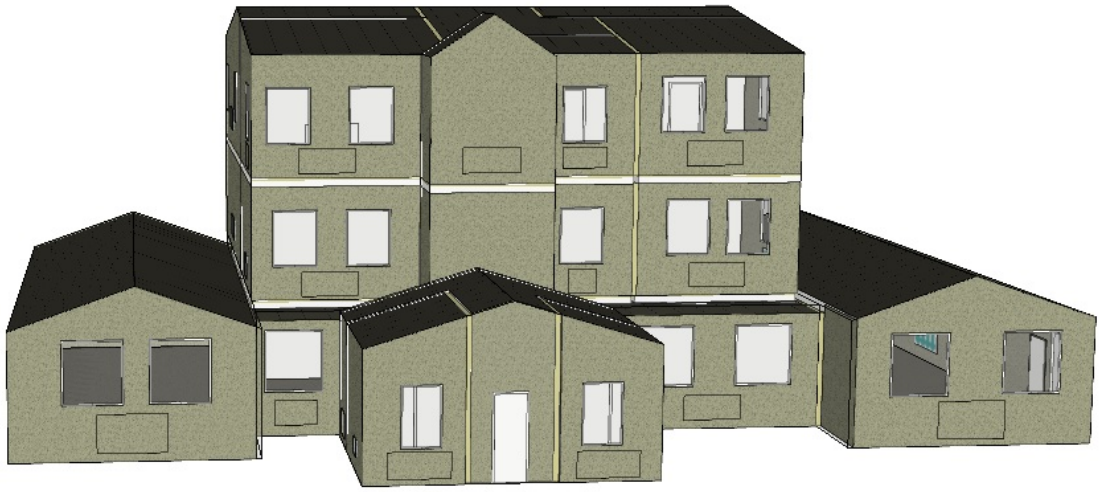

Figure F.2: IDA-ICE model for OF 1

Figure F.3: IDA-ICE model for OF 2

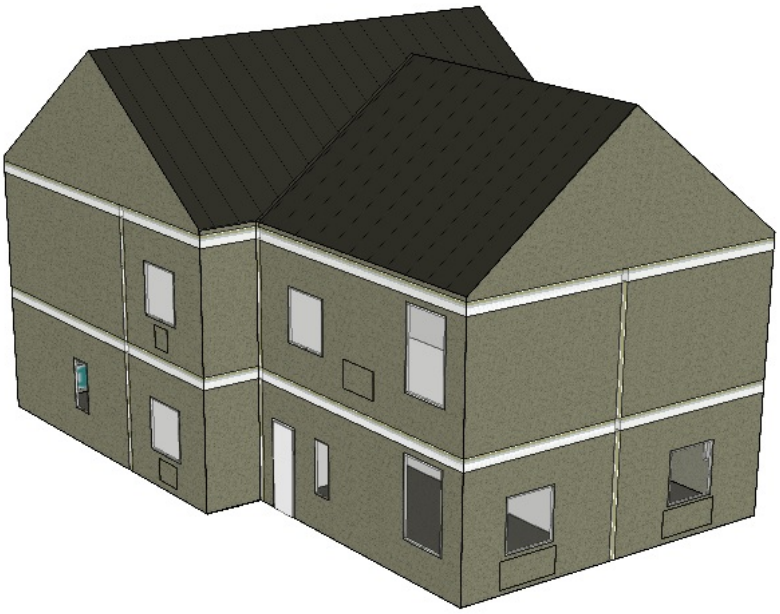

Figure F.4: IDA-ICE model for LW 1

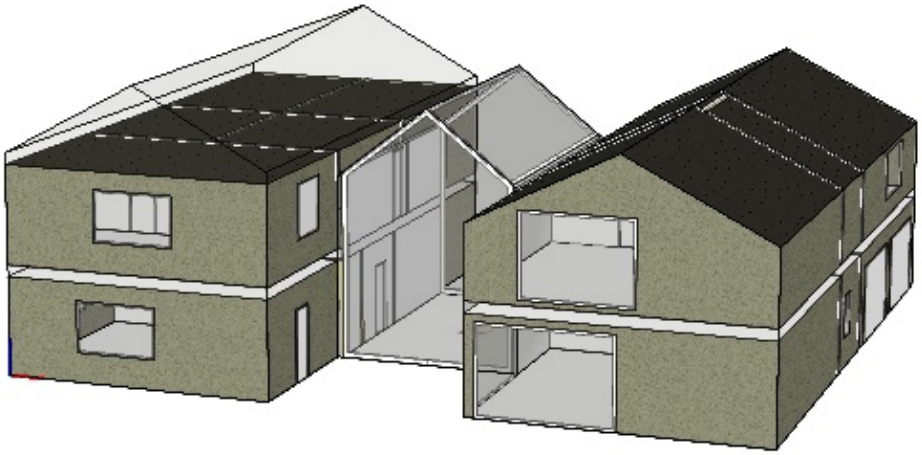

Figure F.5: IDA-ICE model for LW 2,3 and 4

Figure F.6: IDA-ICE model for DB 1

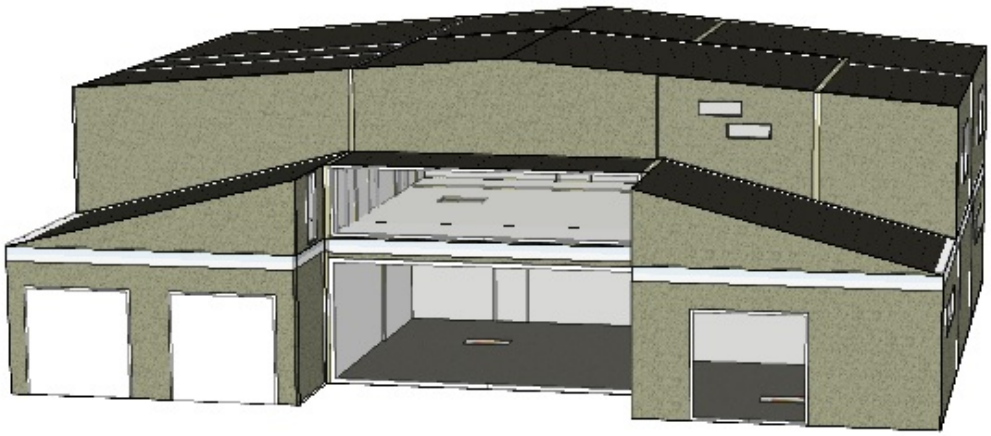

Figure F.7: IDA-ICE model for NB 1

Appendix G

MATLAB model: simulation of heat network operation

This Appendix outlines the programming work developed during the first part of this research project defining the theory and ideas behind the algorithm built in MATLAB. The first task was to delineate the general mathematical formulation, starting from the simplified case where only 2 branches and one user were considered; then the model was expanded and customised to perform a detailed analysis of UK small scale DH network.

G.1 Problem definition

The preliminary stage of the project was the definition of the physics of the problem looking at the simplest scenario. This is schematically presented in Figure G.1 and refers to one end-user and two branches (supply and return legs) network.

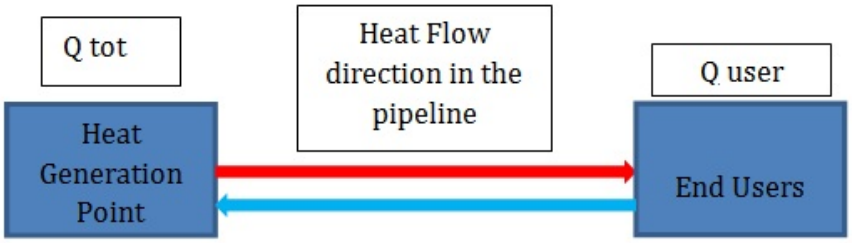

Figure G.1: Simplified scenario to define the physics of the problem

The idea was to clearly outline which ones are the main parts of the system, in order to define the strategy to correctly model the network. This can be summarised as follows:

- Definition of the heat load (Q tot) to be generated at the heat generation point
- Definition of the heat demand (Q user) for the end user
- Definition of heat Losses throughout the pipeline
- Definition of temperature propagation and mass flow rate circulating in the network

The concept, valid for one single end user, can be scaled up for large DH network by defining a combination of differential equations to dynamically simulate the operation of the heat network.

G.2 DH network

The mathematical model formulation of the DH network represents the major part of the computer programming. Using a combination of differential equations, it

defines the structure of the algorithm to dynamically simulate the heat network. The model consists in dividing each single pipe into homogeneous control volume element as shown in Figure G.2. The temperature distribution in each control volume of length dx is determined by applying the energy conservation laws as follows [123–125]:

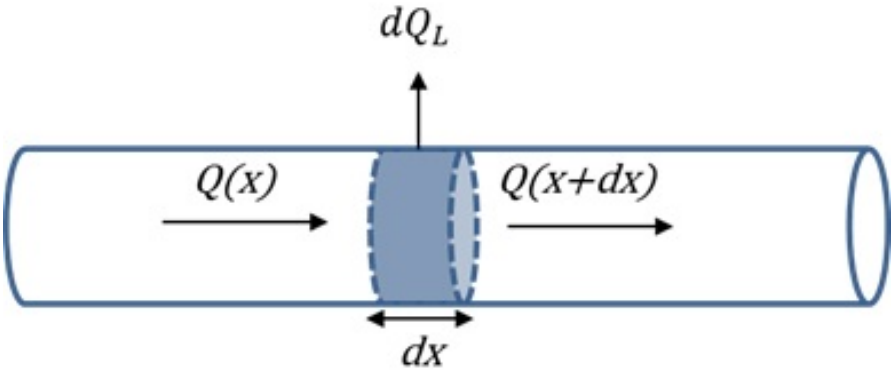

Figure G.2: Single pipe element to define mathematical formulation

$$m \cdot c_p \cdot \frac{\partial T}{\partial t} = -\dot{m}_x \cdot c_p \cdot \frac{\partial T}{\partial x} - dQ_L \tag{G.1}$$

where m is the mass of water of the control volume (kg), $\dot{m}_x$ is the mass flow rate (kg/s), T is the temperature of the control volume and dQ_L is the heat losses rate to the surrounding. The solution of the differential equation was obtained using the explicit finite element method as described in Equation G.2:

$$\begin{cases} \frac{\partial T}{\partial t}(x,t) = \frac{T(x,t)-T(x,t-\Delta t)}{\Delta t} \\ \\ \frac{\partial T}{\partial x}(x,t) = \frac{T(x,t)-T(x-\Delta x,t)}{\Delta x} \end{cases} \tag{G.2}$$

It was also necessary to define and formulate the heat losses (Q_L) of the insulated pipes buried in the ground. The mathematical description of the heat losses

from one single insulated pipe is given as follow [10, 124, 125]:

$$dQ_L = U \cdot \pi \cdot dx \cdot (T - T_g) \tag{G.3}$$

where $U = \frac{2\lambda_i L}{ln(D/d)}$ is the total heat transmission coefficient (W/m^2K, for circular pipe), λ_i is the heat conductivity for the insulation (W/mK), T is the water temperature (°C), T_g is the ground temperature (°C), d is the outer pipe diameter (m), D is the outer diameter including insulation (m) and L is the pipe length (m).

In normal practice, DH networks are often composed of two insulated buried pipes for supply and return, as presented in Figure G.3, and the thermal influence between the two pipes needs to be taken into account. Hence, the heat losses formulation is described as follows:

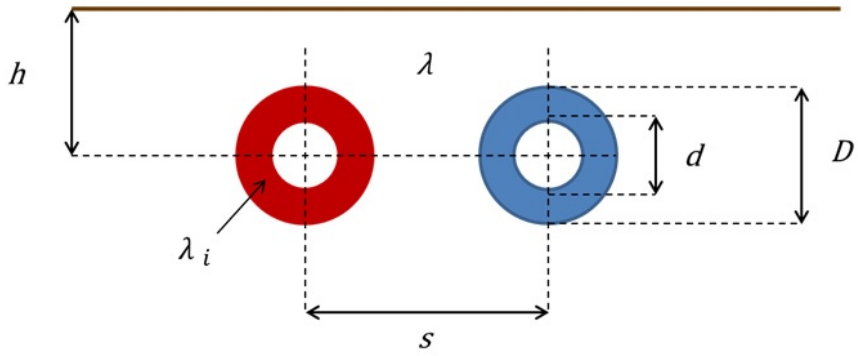

Figure G.3: Double pipe system

$$dQ_L = Q_{Ls} + Q_{Lr} = \frac{L\pi d(\theta_s + \theta_r)}{R_i + R_g + R_c} \tag{G.4}$$

where $R_i = (d/2\lambda_i) \cdot ln(D/d)$ is the insulation resistance (m^2 K/W), $R_g = (d/2\lambda) \cdot ln(4h/D)$ is the ground resistance (m^2 K/W), $R_c = (d/2\lambda) \cdot ln(((2h/s)^2 + 1)^0.5)$ is the coinciding temperature resistance (m^2 K/W), L is half pipe length,

D is the outer diameter including insulation (m), d d is the outer pipe diameter (m), s is the distance between pipes' centres (m), h is the distance between pipe centres and ground surface (m), $\theta_s = t_s - t_g$ (°C) and $\theta_r = t_r - t_g$ (°C). In the formulation of the mathematical model few assumptions were made:

- The fluid flow is developed in one direction
- Thermal and physical properties of water are assumed constant
- No leakages are considered

G.3 Heat exchanger

The heat transferred of a two stream heat exchanger, as described in the simplified representation of Figure G.4, considering a simple heat balance can be expressed in two equivalent ways as follows [125]:

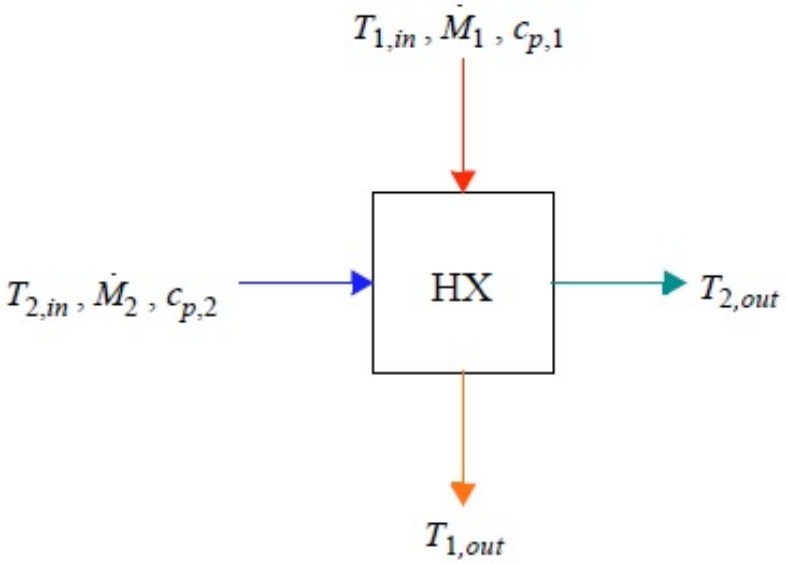

Figure G.4: Heat exchanger simplified representation

$$Q = (\dot{M}c_p)_1(T_{1,in} - T_{1,out}) = (\dot{M}c_p)_2(T_{2,out} - T_{2,in}) \tag{G.5}$$

$$Q = (\dot{M}c_p)_{smaller} \mid T_{in} - T_{out} \mid_{larger} = (\dot{M}c_p)_{larger} \mid T_{in} - T_{out} \mid_{smaller} \tag{G.6}$$

In addition, the thermal effectiveness of a heat exchanger is defined as the ratio of the heat transferred and thermodynamic maximum rate between the two streams as highlighted in Equation G.7.

$$\varepsilon = \frac{Q}{Q_{max}} \tag{G.7}$$

where

$$Q_{max} = (\dot{M}c_p)_{smaller}(T_{1,in} - T_{2,in}). \tag{G.8}$$

Hence, the effectiveness can be expressed as:

$$\varepsilon = \frac{\mid T_{in} - T_{out} \mid_{larger}}{T_{1,in} - T_{2,in}} \tag{G.9}$$

For the specific case study, characterised by end-users interfaced with the heat network through flat plates heat exchangers, the equations used for modelling and calculate the temperatures and mass flow rates at each time step and each end users are expressed as follows:

$$Q = \varepsilon \cdot \dot{m}_x \cdot c_p \cdot (T_s - T_u). \tag{G.10}$$

$$T_r = T_s - \varepsilon(T_s - T_u) \tag{G.11}$$

where ε is the effectiveness of the heat exchanger, $\dot{m}_x$ is the mass flow rate circulating in the DH network (kg/s), Q is the heat demand of the end user (kW), T_s is the DH supply temperature (°C), T_u is the heat exchanger inlet temperature at the end user side (°C), T_r is the DH return temperature (°C) and c_p is the heat capacity of water (kJ/kgK).

G.4 Solar thermal and thermal storage

The purpose of this section is to outline the basic theory involved for the implementation of solar thermal generation within the Matlab model. The strategy followed started with the definition of the solar radiation incident on a tilt surface. Given the latitude ϕ, slope β and the surface azimuth angle γ of a surface, it is possible to calculate the incidence radiation occurring on it [126]. Defining the solar declination δ and the hour angle ω, it is then possible to calculate the angle of incidence of a beam radiation on a tilted surface ϑ and on the horizontal surface ϑ_z as described in the following equations.

$$\delta = 23.45 \cdot sin\left(360 \cdot \frac{284+n}{365}\right) \tag{G.12}$$

$$\omega = 15 \cdot (12 - z) \tag{G.13}$$

$$\begin{aligned} cos\vartheta =& sin\delta \cdot sin\phi \cdot cos\beta - sin\delta \cdot cos\phi \cdot sin\beta \cdot cos\gamma \\ &+ cos\delta \cdot cos\phi \cdot cos\beta \cdot cos\omega + cos\delta \cdot sin\phi \cdot \\ &sin\beta \cdot cos\gamma \cdot cos\omega + cos\delta \cdot sin\beta \cdot sin\gamma \cdot sin\omega \end{aligned} \tag{G.14}$$

$$cos\vartheta_z = sin\delta \cdot sin\phi \cdot cos\delta \cdot cos\phi \cdot cos\beta \cdot cos\gamma \tag{G.15}$$

$$R_b = \frac{cos\vartheta}{cos\vartheta_z} \tag{G.16}$$

$$G_0 = G_{sc}\left(1 + 0.033cos\frac{360n}{365}\right)cos\vartheta_z \tag{G.17}$$

where n is the number of day of the year, z the specific hour of the day, R_b is the ratio between the incidence of beam radiation on the horizontal and tilted surfaces, G_0 is the radiation on a horizontal surface outside the earth's atmosphere (know as extra-terrestrial radiation) and $G_{sc} = 1362$ (W/m^2) is the solar constant.

The next step, having the clear index value k_t, is the calculation of the radiation on horizontal surface with Equation G.18.

$$k_t = \frac{H}{H_0} \tag{G.18}$$

Once calculated the horizontal radiation or if recorded data are available, the beam and diffuse components of hourly radiation can be evaluated by using the Erbs et al. correlation.

$$\frac{H_d}{H} = \begin{cases} 1.0 - 0.09k_t, & for k_t \leq 0.22 \\ 0.9511 - 0.160k_t + 4.388k_t^2 - 16.638k_t^3 + 12.336k_t^4 & for 0.22 \leq k_t \leq 0.8 \\ 0.165, & for k_t > 0.8 \end{cases}$$

Having the diffuse hourly radiation component, the beam component can be obtained as follows:

$$H_b = H - H_d \tag{G.19}$$

Given the beam radiation component and knowing the diffuse reflectance ρ_g of the surrounding, the radiation on tilted surfaces can be calculated by using the isotropic diffuse model:

$$H_t = H_b R_b + H_d \left(\frac{1 + cos\beta}{2} \right) + H\rho_g \left(\frac{1 - cos\beta}{2} \right) \tag{G.20}$$

Once the solar radiation available on the tilted surface is defined, the calculations for the useful energy out of the solar collectors can be calculated. Given a specific solar panel the equation to obtained the useful energy is expressed as follows:

$$Q_u = A_c F_r [H_t(\tau\alpha) - U_{L_{col}}(T_i - T_a)] \tag{G.21}$$

where Q_u is the useful energy out of the specific solar panel, A_c is the area of the collector, F_r is the heat removal factor, $\tau\alpha$ are the transmittance and

absorptance of the glass cover and the absorber plate respectively, $U_{L_{col}}$ is the heat loss coefficient. T_i is the inlet temperature and T_a is the ambient temperature. For what concerns the efficiency of the specific panel, two possible efficiency curves can be used:

$$\eta_{linear} = F_r(\tau\alpha) - \frac{F_r U_{L_{col}} \Delta T_m}{H_t} \tag{G.22}$$

$$\eta_{quadratic} = F_r(\tau\alpha) - \frac{F_r U_{L_{col1}} \Delta T_m}{H_t} - \frac{F_r U_{L_{col2}} \Delta T_m^2}{H_t} \tag{G.23}$$

Finally, it was considered in the model the equation to evaluate the temperature variation inside a specific thermal storage, assuming it would be part of the heat network. This is expressed as follows:

$$m \cdot c_p \cdot \frac{\partial T}{\partial t} = Q_u - Q_{load} - Q_{L_{tank}} \tag{G.24}$$

where m is the mass of water (kg), c_p is the specific heat capacity of water (kJ/kg K), Q_{load} is the heat extracted from the tank (kW), Q_u is the heat charging the thermal storage (kW) and $Q_{L_{tank}} = U_{L_{tank}} A_{L_{tank}} (T_{tank} - T_a)$ represents the heat losses through the tank (kW).

G.5 Algorithm to dynamically simulate the operation of an existing DH network

Content

- Main script to simulate the operation of the heat network
- Function to perform calculation supply line
- Function to perform calculation return line
- Function to perform calculation heat exchanger
- Solar thermal and thermal storage to be integrated in the main script
- Function for solar radiation calculation
- Function to model boiler operation
- Function for thermal storage mass balance
- Function for thermal storage energy balance

Main script to simulate operation of the heat network

```
% clear all;
% clc;
% % load('C:\Users\ezxmt\Dropbox\PhD\THIRD ...
   YEAR\WORKSPACE\WorkSpace Boiler December.mat');
% load('C:\Users\ezxmt\Dropbox\PhD\SECOND YEAR\Sim Model\Working ...
   Folder\FEM\Working Space\Workspace_Giusto.mat');
% the fie loaded in the work space defines the boundary ...
   conditions for the
% delivery points of the system. Specifically, Qload(from 1to 6) ...
   are the
% Heat Loads (kW) simulated with DB (providing hourly,monthly etc ...
   values;
```

```
% in this case 1h time step). Also, tg represent the temeprature ...
   of the
% ground for Nottingham and Tf represent the inlet temperature of ...
   the DH
% recorded last year.

%% %% Analysis of Hexgreave DH operating conditions
% the model intends to evaluate and integrate the temperatures, ...
   loads and mass flow
% rates caracterizing the specific DH case of study. In order to ...
   efficiently
% run the simulation and to optimize the computational capacity ...
   of the computers, all the output calculated,
% if needed, would be printed out of the workspace in a .cvs file ...
   in order
% to allow the user to correctly analyze and manipulate the data ...
   obtained

%% %% Network Data

n=3776; % number of time steps define the period of the year ...
   which the model would simulate
k=10; % number of nodes define the number of dx used to model ...
   each pipe
dt=3600; % Time step 15 min
ro=1000; % kg/m3
cp=4.186; % specific heat capacity of water kJ/kg*K
T_us=55; % User Temperature set for the HE
pump_max1= 2.777777778; % max pump limit for Hall and Coach House
pump_max2= 0.4166666667; % max pump limit for the rest of buildings
m_empty=0;
T_empty=0;


%% Pipe A
U_pA=0.00456; % Overall Heat Transfer COefficient teking into ...
   account the thermal properties of the specific pipe
L_A=27; % Pipe Lenght
dx_A=L_A/(k+1); % dx calculation for later implement the simulation
D_A=150; % pipe diameter
dV_A=((D_A/(2*1000))^2)*pi*dx_A; % infinitesimal volume element
dA_A=((D_A/1000)*dx_A*pi); % infinitesimal area element
area_A=((D_A/(2*1000))^2*L_A*pi); % total pipe area (area of ...
   cylinder)
node_1=1;
node_2=2;

%% Pipe B
U_pB=0.00096; % Overall Heat Transfer COefficient teking into ...
   account the thermal properties of the specific pipe
L_B=100; % Pipe Lenght
dx_B=L_B/(k+1); % dx calculation for later implement the simulation
D_B=126; % pipe diameter
dV_B=((D_B/(2*1000))^2)*pi*dx_B; % infinitesimal volume element
dA_B=((D_B/1000)*dx_B*pi); % infinitesimal area element
area_B=((D_B/(2*1000))^2*L_B*pi); % total pipe area (area of ...
   cylinder)
node_3=3;
```

```
%% Pipe C
U_pC=0.00106; % Overall Heat Transfer COefficient teking into ...
   account the thermal properties of the specific pipe
L_C=11; % Pipe Lenght
dx_C=L_C/(k+1); % dx calculation for later implement the simulation
D_C=111; % pipe diameter
dV_C=((D_C/(2*1000))^2)*pi*dx_C; % infinitesimal volume element
dA_C=((D_C/1000)*dx_C*pi); % infinitesimal area element
area_C=((D_B/(2*1000))^2*L_C*pi); % total pipe area (area of ...
   cylinder)
node_4=4;

%% Pipe D
U_pD=0.00162; % Overall Heat Transfer COefficient teking into ...
   account the thermal properties of the specific pipe
L_D=80; % Pipe Lenght
dx_D=L_D/(k+1); % dx calculation for later implement the simulation
D_D=76; % pipe diameter
dV_D=((D_D/(2*1000))^2)*pi*dx_D; % infinitesimal volume element
dA_D=((D_D/1000)*dx_D*pi); % infinitesimal area element
area_D=((D_D/(2*1000))^2*L_D*pi); % total pipe area (area of ...
   cylinder)
node_5=5;

%% Pipe E
U_pE=0.00153; % Overall Heat Transfer COefficient teking into ...
   account the thermal properties of the specific pipe
L_E=94; % Pipe Lenght
dx_E=L_E/(k+1); % dx calculation for later implement the simulation
D_E=76; % pipe diameter
dV_E=((D_E/(2*1000))^2)*pi*dx_E; % infinitesimal volume element
dA_E=((D_E/1000)*dx_E*pi); % infinitesimal area element
area_E=((D_E/(2*1000))^2*L_E*pi); % total pipe area (area of ...
   cylinder)
node_6=6;

%% Pipe F
U_pF=0.00153; % Overall Heat Transfer COefficient teking into ...
   account the thermal properties of the specific pipe
L_F=45; % Pipe Lenght
dx_F=L_F/(k+1); % dx calculation for later implement the simulation
D_F=76; % pipe diameter
dV_F=((D_F/(2*1000))^2)*pi*dx_F; % infinitesimal volume element
dA_F=((D_F/1000)*dx_F*pi); % infinitesimal area element
area_F=((D_F/(2*1000))^2*L_F*pi); % total pipe area (area of ...
   cylinder)
node_7=7;

%% Pipe G
U_pG=0.00153; % Overall Heat Transfer COefficient teking into ...
   account the thermal properties of the specific pipe
L_G=15; % Pipe Lenght
dx_G=L_G/(k+1); % dx calculation for later implement the simulation
D_G=76; % pipe diameter
dV_G=((D_G/(2*1000))^2)*pi*dx_G; % infinitesimal volume element
dA_G=((D_G/1000)*dx_G*pi); % infinitesimal area element
area_G=((D_G/(2*1000))^2*L_G*pi); % total pipe area (area of ...
```

```
   cylinder)
node_8=8;

%% Pipe H
U_pH=0.00153; % Overall Heat Transfer COefficient teking into ...
   account the thermal properties of the specific pipe
L_H=25; % Pipe Lenght
dx_H=L_H/(k+1); % dx calculation for later implement the simulation
D_H=76; % pipe diameter
dV_H=((D_H/(2*1000))^2)*pi*dx_H; % infinitesimal volume element
dA_H=((D_H/1000)*dx_H*pi); % infinitesimal area element
area_H=((D_H/(2*1000))^2*L_H*pi); % total pipe area (area of ...
   cylinder)
node_9=9;

%% Pipe I
U_pI=0.00153; % Overall Heat Transfer COefficient teking into ...
   account the thermal properties of the specific pipe
L_I=80; % Pipe Lenght
dx_I=L_I/(k+1); % dx calculation for later implement the simulation
D_I=76; % pipe diameter
dV_I=((D_I/(2*1000))^2)*pi*dx_I; % infinitesimal volume element
dA_I=((D_I/1000)*dx_I*pi); % infinitesimal area element
area_I=((D_I/(2*1000))^2*L_I*pi); % total pipe area (area of ...
   cylinder)
node_10=10;

%% Mass Flow rate Circulating

m_2=0.2; % mass flow rate for the specific building
m_4=0.2; % mass flow rate for the specific building
m_5=0.2; % mass flow rate for the specific building
m_7=0.2; % mass flow rate for the specific building
m_8=0.2; % mass flow rate for the specific building
m_9=0.2;  % mass flow rate for the specific building
m_10=0.2; % mass flow rate for the specific building

m_6=m_7+m_8+m_9+m_10; % Connection nodes of the network, ...
   important for return temepratures analysis
m_3=m_4+m_5+m_6;
m_4_5=m_4+m_5;
m_1=m_3+m_2;

%% Matrix Pipe A
T_A=zeros(k,2); % memory pre-allocation for calculating the ...
   Temperature propagation At the end of the for loop the model ...
   overwrites the first column and start calculating the new ...
   values at the new time step. the Entire matrix is saved in a ...
   csv file on Desktop.
T_A(:,1)=Tg(1,2); % Initial Condition : Temp of the water = temp ...
   of ground
T_rA=zeros(k,2);
T_rA(:,1)=Tg(1,2);

C_A=0;
B_A=0;
F_A=(U_pA*dA_A*dt/(dV_A*ro*cp));
Q_LsA=zeros(k,1);
```

```
Q_LrA=zeros(k,1);
% T_r1Conn=zeros(n,1);

%% Matrix Pipe B
T_B=zeros(k,2); % memory pre-allocation for calculating the ...
   Temperature propagation At the end of the for loop the model ...
   overwrites the first column and start calculating the new ...
   values at the new time step. the Entire matrix is saved in a ...
   csv file on Desktop.
T_B(:,1)=Tg(1,2); % Initial Condition : Temp of the water = temp ...
   of ground
T_rB=zeros(k,2);
T_rB(:,1)=Tg(1,2);

C_B=0;
B_B=0;
F_B=(U_pB*dA_B*dt/(dV_B*ro*cp));
Q_LsB=zeros(k,1);
Q_LrB=zeros(k,1);

% T_r1Conn=zeros(n,1);

%% Matrix Pipe C
T_C=zeros(k,2); % memory pre-allocation for calculating the ...
   Temperature propagation At the end of the for loop the model ...
   overwrites the first column and start calculating the new ...
   values at the new time step. the Entire matrix is saved in a ...
   csv file on Desktop.
T_C(:,1)=Tg(1,2); % Initial Condition : Temp of the water = temp ...
   of ground
T_rC=zeros(k,2);
T_rC(:,1)=Tg(1,2);

C_C=0;
B_C=0;
F_C=(U_pC*dA_C*dt/(dV_C*ro*cp));
Q_LsC=zeros(k,1);
Q_LrC=zeros(k,1);

% T_r3Conn=zeros(n,1);

%% Matrix Pipe D
T_D=zeros(k,2); % memory pre-allocation for calculating the ...
   Temperature propagation At the end of the for loop the model ...
   overwrites the first column and start calculating the new ...
   values at the new time step. the Entire matrix is saved in a ...
   csv file on Desktop.
T_D(:,1)=Tg(1,2); % Initial Condition : Temp of the water = temp ...
   of ground
T_rD=zeros(k,2);
T_rD(:,1)=Tg(1,2);

C_D=0;
B_D=0;
F_D=(U_pD*dA_D*dt/(dV_D*ro*cp));
Q_LsD=zeros(k,1);
Q_LrD=zeros(k,1);
```

```
% T_r4Conn=zeros(n,1);


%% Matrix Pipe E
T_E=zeros(k,2); % memory pre-allocation for calculating the ...
    Temperature propagation At the end of the for loop the model ...
    overwrites the first column and start calculating the new ...
    values at the new time step. the Entire matrix is saved in a ...
    csv file on Desktop.
T_E(:,1)=Tg(1,2); % Initial Condition : Temp of the water = temp ...
    of ground
T_rE=zeros(k,2);
T_rE(:,1)=Tg(1,2);

C_E=0;
B_E=0;
F_E=(U_pE*dA_E*dt/(dV_E*ro*cp));
Q_LsE=zeros(k,1);
Q_LrE=zeros(k,1);

% T_r6Conn=zeros(n,1);


%% Matrix Pipe F
T_F=zeros(k,2); % memory pre-allocation for calculating the ...
    Temperature propagation At the end of the for loop the model ...
    overwrites the first column and start calculating the new ...
    values at the new time step. the Entire matrix is saved in a ...
    csv file on Desktop.
T_F(:,1)=Tg(1,2); % Initial Condition : Temp of the water = temp ...
    of ground
T_rF=zeros(k,2);
T_rF(:,1)=Tg(1,2);

C_F=0;
B_F=0;
F_F=(U_pF*dA_F*dt/(dV_F*ro*cp));
Q_LsF=zeros(k,1);
Q_LrF=zeros(k,1);

%% Matrix Pipe G
T_G=zeros(k,2); % memory pre-allocation for calculating the ...
    Temperature propagation At the end of the for loop the model ...
    overwrites the first column and start calculating the new ...
    values at the new time step. the Entire matrix is saved in a ...
    csv file on Desktop.
T_G(:,1)=Tg(1,2); % Initial Condition : Temp of the water = temp ...
    of ground
T_rG=zeros(k,2);
T_rG(:,1)=Tg(1,2);

C_G=0;
B_G=0;
F_G=(U_pG*dA_G*dt/(dV_G*ro*cp));
Q_LsG=zeros(k,1);
Q_LrG=zeros(k,1);

%% Matrix Pipe H
```

```
T_H=zeros(k,2); % memory pre-allocation for calculating the ...
   Temperature propagation At the end of the for loop the model ...
   overwrites the first column and start calculating the new ...
   values at the new time step. the Entire matrix is saved in a ...
   csv file on Desktop.
T_H(:,1)=Tg(1,2); % Initial Condition : Temp of the water = temp ...
   of ground
T_rH=zeros(k,2);
T_rH(:,1)=Tg(1,2);

C_H=0;
B_H=0;
F_H=(U_pH*dA_H*dt/(dV_H*ro*cp));
Q_LsH=zeros(k,1);
Q_LrH=zeros(k,1);

%% Matrix Pipe I
T_I=zeros(k,2); % memory pre-allocation for calculating the ...
   Temperature propagation At the end of the for loop the model ...
   overwrites the first column and start calculating the new ...
   values at the new time step. the Entire matrix is saved in a ...
   csv file on Desktop.
T_I(:,1)=Tg(1,2); % Initial Condition : Temp of the water = temp ...
   of ground
T_rI=zeros(k,2);
T_rI(:,1)=Tg(1,2);

C_I=0;
B_I=0;
F_I=(U_pI*dA_I*dt/(dV_I*ro*cp));
Q_LsI=zeros(k,1);
Q_LrI=zeros(k,1);

%% Temperature and mass flow calculation, FEM main script for ...
   calculating the operating parameters of the system. few ...
   functions have been developed to correctly run the calculation
n=n+1;

for j=1:n-1,   %% Time Loop
        %% Coeff Calculation Pipe A
        B_A=(1+((m_2*dt/(dV_A*ro)))+(U_pA*dA_A*dt/(dV_A*ro*cp)));
        C_A=(m_2*dt/(dV_A*ro));

        %% Coeff Calculation Pipe B
        B_B=(1+((m_3*dt/(dV_B*ro)))+(U_pB*dA_B*dt/(dV_B*ro*cp)));
        C_B=(m_3*dt/(dV_B*ro));


        %% Coeff Calculation Pipe C
        B_C=(1+((m_4_5*dt/(dV_C*ro)))+(U_pC*dA_C*dt/(dV_C*ro*cp)));
        C_C=(m_4_5*dt/(dV_C*ro));

        %% Coeff Calculation Pipe D
        B_D=(1+((m_5*dt/(dV_D*ro)))+(U_pD*dA_D*dt/(dV_D*ro*cp)));
        C_D=(m_5*dt/(dV_D*ro));

        %% Coeff Calculation Pipe E
        B_E=(1+((m_6*dt/(dV_E*ro)))+(U_pE*dA_E*dt/(dV_E*ro*cp)));
```

```
        C_E=(m_6*dt/(dV_E*ro));

        %% Coeff Calculation Pipe F
        B_F=(1+((m_7*dt/(dV_F*ro)))+(U_pF*dA_F*dt/(dV_F*ro*cp)));
        C_F=(m_7*dt/(dV_F*ro));

        %% Coeff Calculation Pipe G
        B_G=(1+((m_8*dt/(dV_G*ro)))+(U_pG*dA_G*dt/(dV_G*ro*cp)));
        C_G=(m_8*dt/(dV_G*ro));

        %% Coeff Calculation Pipe H
        B_H=(1+((m_9*dt/(dV_H*ro)))+(U_pH*dA_H*dt/(dV_H*ro*cp)));
        C_H=(m_9*dt/(dV_H*ro));

        %% Coeff Calculation Pipe I
        B_I=(1+((m_10*dt/(dV_I*ro)))+(U_pI*dA_I*dt/(dV_I*ro*cp)));
        C_I=(m_10*dt/(dV_I*ro));

%%     Supply Network calculation

[T_A, Q_LsA]= Supply_Network_Calculation (Q_LsA, T_A, k, ...
   m_2,Tg(j,2),Tf(j,2), B_A, C_A, F_A, U_pA, dA_A);
[T_B, Q_LsB]= Supply_Network_Calculation (Q_LsB, T_B, k, ...
   m_3,Tg(j,2),Tf(j,2), B_B, C_B, F_B, U_pB, dA_B);
[T_C, Q_LsC]= Supply_Network_Calculation (Q_LsC, T_C, k, ...
   m_4_5,Tg(j,2),T_B(k,2), B_C, C_C, F_C, U_pC, dA_C);
[T_D, Q_LsD]= Supply_Network_Calculation (Q_LsD, T_D, k, ...
   m_5,Tg(j,2),T_D(k,2), B_D, C_D, F_D, U_pD, dA_A);
[T_E, Q_LsE]= Supply_Network_Calculation (Q_LsE, T_E, k, ...
   m_6,Tg(j,2),T_B(k,2), B_E, C_E, F_E, U_pE, dA_E);
[T_F, Q_LsF]= Supply_Network_Calculation (Q_LsF, T_F, k, ...
   m_7,Tg(j,2),T_E(k,2), B_F, C_F, F_F, U_pF, dA_F);
[T_G, Q_LsG]= Supply_Network_Calculation (Q_LsG, T_G, k, ...
   m_8,Tg(j,2),T_E(k,2), B_G, C_G, F_G, U_pG, dA_G);
[T_H, Q_LsH]= Supply_Network_Calculation (Q_LsH, T_H, k, ...
   m_9,Tg(j,2),T_E(k,2), B_H, C_H, F_H, U_pH, dA_H);
[T_I, Q_LsI]= Supply_Network_Calculation (Q_LsI, T_I, k, ...
   m_10,Tg(j,2),T_E(k,2), B_I, C_I, F_I, U_pI, dA_I);


%   After defining the function for the supply tempearure ...
   calculation the model calculates for each time step and dx
%   the temperature of the water circulating in every pipe of the ...
   network

     %% Heat exchange at building Level and return temperature ...
        calculation
%     ??Possible control of Qload for having T_s=T_r in case of ...
   not heat required

       [T_r2, m_2new]= HE_Calculation (T_A(k,2), QLoad(j,2), T_us, ...
          cp,pump_max1);
       [T_r4, m_4new]= HE_Calculation (T_C(k,2), QLoad1(j,2), ...
          T_us, cp,pump_max1);
       [T_r5, m_5new]= HE_Calculation (T_D(k,2), QLoad2(j,2), ...
          T_us, cp,pump_max2);
       [T_r7, m_7new]= HE_Calculation (T_F(k,2), QLoad3(j,2), ...
          T_us, cp,pump_max2);
```

```
      [T_r8, m_8new]= HE_Calculation (T_G(k,2), QLoad4(j,2), ...
         T_us, cp,pump_max2);
      [T_r9, m_9new]= HE_Calculation (T_H(k,2), QLoad5(j,2), ...
         T_us, cp,pump_max2);
      [T_r10, m_10new]= HE_Calculation (T_I(k,2), QLoad6(j,2), ...
         T_us, cp,pump_max2);

      m_6new=m_7new+m_8new+m_9new+m_10new;

      m_4_5new=m_4new+m_5new;

      m_3new=m_6new+m_4_5new;

      m_1new=m_2new+m_3new;


%     This part of the model is trying to evaluate the ...
   interaction between the primary network (DH) and the end users.
%     Therefore it provides at each time step, after defining an ...
   intial condition for the mass flow rate, the flow circulating
%     It also defines the return temperature after the heat echanger


        %%  Return Network Calculation
        %% Pipe A
        [T_rI,Q_LrI]= Return_Network_Calculation(node_10, k, ...
           m_10, m_empty,m_empty,m_empty,m_empty, B_I, C_I,F_I, ...
           U_pI, dA_I, Q_LrI, Tg(j,2), T_r10, T_rI, ...
           T_empty,T_empty,T_empty,T_empty);
        [T_rH,Q_LrH]= Return_Network_Calculation (node_9, k, m_9, ...
           m_empty,m_empty,m_empty,m_empty, B_H, C_H,F_H, U_pH, ...
           dA_H, Q_LrH, Tg(j,2), T_r9, T_rH, ...
           T_empty,T_empty,T_empty,T_empty);
        [T_rG,Q_LrG]= Return_Network_Calculation (node_8, k, m_8, ...
           m_empty,m_empty,m_empty,m_empty, B_G, C_G,F_G, U_pG, ...
           dA_G, Q_LrG, Tg(j,2), T_r8, T_rG, ...
           T_empty,T_empty,T_empty,T_empty);
        [T_rF,Q_LrF]= Return_Network_Calculation (node_7, k, m_7, ...
           m_empty,m_empty,m_empty,m_empty, B_F, C_F,F_F, U_pF, ...
           dA_F, Q_LrF, Tg(j,2), T_r7, T_rF, ...
           T_empty,T_empty,T_empty,T_empty);
        [T_rE,Q_LrE]= Return_Network_Calculation (node_6, k, m_7, ...
           m_8,m_9,m_10,m_6, B_E, C_E,F_E, U_pE, dA_E, Q_LrE, ...
           Tg(j,2), T_empty, T_rE, ...
           T_rF(k,2),T_rG(k,2),T_rH(k,2),T_rI(k,2));
        [T_rD,Q_LrD]= Return_Network_Calculation (node_5, k, m_5, ...
           m_empty,m_empty,m_empty,m_empty, B_D, C_D,F_D, U_pD, ...
           dA_D, Q_LrD, Tg(j,2), T_r5, T_rD, ...
           T_empty,T_empty,T_empty,T_empty);
        [T_rC,Q_LrC]= Return_Network_Calculation (node_4, k, ...
           m_4_5, m_4,m_5,m_empty,m_empty, B_C, C_C,F_C, U_pC, ...
           dA_C, Q_LrC, Tg(j,2), T_r4, T_rC, ...
           T_rD(k,2),T_empty,T_empty,T_empty);
        [T_rB,Q_LrB]= Return_Network_Calculation (node_3, k, m_3, ...
           m_4_5,m_6,m_empty,m_empty, B_B, C_B,F_B, U_pB, dA_B, ...
           Q_LrB, Tg(j,2), T_rC(k,2), T_rB, ...
           T_rE(k,2),T_empty,T_empty,T_empty);
        [T_rA,Q_LrA]= Return_Network_Calculation (node_1, k, m_1, ...
```

```
            m_2,m_3,m_empty,m_empty, B_A, C_A,F_A, U_pA, dA_A, ...
            Q_LrA, Tg(j,2), T_r2, T_rA, ...
            T_rB(k,2),T_empty,T_empty,T_empty);

        % Differently from the supply fuction, the return ...
            calculation have different cases, chosen by the model ...
            according to the node considered.
        % the main idea is that in presence of a connection node, ...
            say node1
        % the module define T_r1= ...
            m2*T_rA(k,2)+m3*T_rB(k,2)/m1(see network)


%% Switch and Outputs writing out of Matlab on csv

if j==1,
    % pipe A

    delete('C:\Users\ezxmt\Desktop\Output_Matlab\T_A.csv');
     dlmwrite('C:\Users\ezxmt\Desktop\Output_Matlab\T_A.csv', ...
        T_A(:,1)','-append');

    delete('C:\Users\ezxmt\Desktop\Output_Matlab\T_rA.csv');
     dlmwrite('C:\Users\ezxmt\Desktop\Output_Matlab\T_rA.csv', ...
        T_rA(:,1)','-append');

    delete('C:\Users\ezxmt\Desktop\Output_Matlab\m_2.csv');
     dlmwrite('C:\Users\ezxmt\Desktop\Output_Matlab\m_2.csv', ...
        m_2,'-append');

    delete('C:\Users\ezxmt\Desktop\Output_Matlab\m_1.csv');
     dlmwrite('C:\Users\ezxmt\Desktop\Output_Matlab\m_1.csv', ...
        m_1,'-append');

    delete('C:\Users\ezxmt\Desktop\Output_Matlab\B_A.csv');
     dlmwrite('C:\Users\ezxmt\Desktop\Output_Matlab\B_A.csv', ...
        B_A,'-append');

    delete('C:\Users\ezxmt\Desktop\Output_Matlab\Q_LsA.csv');
     dlmwrite('C:\Users\ezxmt\Desktop\Output_Matlab\Q_LsA.csv',
      Q_LsA(:,1)','-append');

     delete('C:\Users\ezxmt\Desktop\Output_Matlab\Q_LrA.csv');
     dlmwrite('C:\Users\ezxmt\Desktop\Output_Matlab\Q_LrA.csv',
      Q_LrA(:,1)','-append');


    % Pipe B
     delete('C:\Users\ezxmt\Desktop\Output_Matlab\T_B.csv');
     dlmwrite('C:\Users\ezxmt\Desktop\Output_Matlab\T_B.csv', ...
        T_B(:,1)','-append');

     delete('C:\Users\ezxmt\Desktop\Output_Matlab\T_rB.csv');
     dlmwrite('C:\Users\ezxmt\Desktop\Output_Matlab\T_rB.csv', ...
        T_rB(:,1)','-append');

     delete('C:\Users\ezxmt\Desktop\Output_Matlab\m_3.csv');
     dlmwrite('C:\Users\ezxmt\Desktop\Output_Matlab\m_3.csv', ...
```

```
    m_3,'-append');

 delete('C:\Users\ezxmt\Desktop\Output_Matlab\m_4.csv');
 dlmwrite('C:\Users\ezxmt\Desktop\Output_Matlab\m_4.csv', ...
    m_4,'-append');

delete('C:\Users\ezxmt\Desktop\Output_Matlab\B_B.csv');
 dlmwrite('C:\Users\ezxmt\Desktop\Output_Matlab\B_B.csv', ...
    B_B,'-append');

 delete('C:\Users\ezxmt\Desktop\Output_Matlab\Q_LsB.csv');
 dlmwrite('C:\Users\ezxmt\Desktop\Output_Matlab\Q_LsB.csv',
  Q_LsB(:,1)','-append');

  delete('C:\Users\ezxmt\Desktop\Output_Matlab\Q_LrB.csv');
 dlmwrite('C:\Users\ezxmt\Desktop\Output_Matlab\Q_LrB.csv',
  Q_LrB(:,1)','-append');

%% Pipe C

 delete('C:\Users\ezxmt\Desktop\Output_Matlab\T_C.csv');
 dlmwrite('C:\Users\ezxmt\Desktop\Output_Matlab\T_C.csv', ...
    T_C(:,1)','-append');

 delete('C:\Users\ezxmt\Desktop\Output_Matlab\T_rC.csv');
 dlmwrite('C:\Users\ezxmt\Desktop\Output_Matlab\T_rC.csv', ...
    T_rC(:,1)','-append');

 delete('C:\Users\ezxmt\Desktop\Output_Matlab\m_5.csv');
 dlmwrite('C:\Users\ezxmt\Desktop\Output_Matlab\m_5.csv', ...
    m_5,'-append');

 delete('C:\Users\ezxmt\Desktop\Output_Matlab\B_c.csv');
 dlmwrite('C:\Users\ezxmt\Desktop\Output_Matlab\B_c.csv', ...
    B_C,'-append');

 delete('C:\Users\ezxmt\Desktop\Output_Matlab\Q_LsC.csv');
 dlmwrite('C:\Users\ezxmt\Desktop\Output_Matlab\Q_LsC.csv',
  Q_LsB(:,1)','-append');

  delete('C:\Users\ezxmt\Desktop\Output_Matlab\Q_LrC.csv');
 dlmwrite('C:\Users\ezxmt\Desktop\Output_Matlab\Q_LrC.csv',
  Q_LrC(:,1)','-append');

%% Pipe D
 delete('C:\Users\ezxmt\Desktop\Output_Matlab\T_D.csv');
 dlmwrite('C:\Users\ezxmt\Desktop\Output_Matlab\T_D.csv', ...
    T_D(:,1)','-append');

 delete('C:\Users\ezxmt\Desktop\Output_Matlab\T_rD.csv');
 dlmwrite('C:\Users\ezxmt\Desktop\Output_Matlab\T_rD.csv', ...
    T_rD(:,1)','-append');

 delete('C:\Users\ezxmt\Desktop\Output_Matlab\m_4_5.csv');
 dlmwrite('C:\Users\ezxmt\Desktop\Output_Matlab\m_4_5.csv', ...
    m_4_5,'-append');

 delete('C:\Users\ezxmt\Desktop\Output_Matlab\B_D.csv');
```

```
dlmwrite('C:\Users\ezxmt\Desktop\Output_Matlab\B_D.csv', ...
    B_D,'-append');

delete('C:\Users\ezxmt\Desktop\Output_Matlab\Q_LsD.csv');
dlmwrite('C:\Users\ezxmt\Desktop\Output_Matlab\Q_LsD.csv',
 Q_LsD(:,1)','-append');

 delete('C:\Users\ezxmt\Desktop\Output_Matlab\Q_LrD.csv');
dlmwrite('C:\Users\ezxmt\Desktop\Output_Matlab\Q_LrD.csv',
 Q_LrD(:,1)','-append');

%% Pipe E
delete('C:\Users\ezxmt\Desktop\Output_Matlab\T_E.csv');
dlmwrite('C:\Users\ezxmt\Desktop\Output_Matlab\T_E.csv', ...
    T_E(:,1)','-append');

delete('C:\Users\ezxmt\Desktop\Output_Matlab\T_rE.csv');
dlmwrite('C:\Users\ezxmt\Desktop\Output_Matlab\T_rE.csv', ...
    T_rE(:,1)','-append');

delete('C:\Users\ezxmt\Desktop\Output_Matlab\m_6.csv');
dlmwrite('C:\Users\ezxmt\Desktop\Output_Matlab\m_6.csv', ...
    m_6,'-append');

delete('C:\Users\ezxmt\Desktop\Output_Matlab\B_E.csv');
dlmwrite('C:\Users\ezxmt\Desktop\Output_Matlab\B_E.csv', ...
    B_E,'-append');

delete('C:\Users\ezxmt\Desktop\Output_Matlab\Q_LsE.csv');
dlmwrite('C:\Users\ezxmt\Desktop\Output_Matlab\Q_LsE.csv',
 Q_LsE(:,1)','-append');

 delete('C:\Users\ezxmt\Desktop\Output_Matlab\Q_LrE.csv');
dlmwrite('C:\Users\ezxmt\Desktop\Output_Matlab\Q_LrE.csv',
 Q_LrE(:,1)','-append');

%% Pipe F
 delete('C:\Users\ezxmt\Desktop\Output_Matlab\T_F.csv');
dlmwrite('C:\Users\ezxmt\Desktop\Output_Matlab\T_F.csv', ...
    T_F(:,1)','-append');

delete('C:\Users\ezxmt\Desktop\Output_Matlab\T_rF.csv');
dlmwrite('C:\Users\ezxmt\Desktop\Output_Matlab\T_rF.csv', ...
    T_rF(:,1)','-append');

delete('C:\Users\ezxmt\Desktop\Output_Matlab\m_7.csv');
dlmwrite('C:\Users\ezxmt\Desktop\Output_Matlab\m_7.csv', ...
    m_7,'-append');

delete('C:\Users\ezxmt\Desktop\Output_Matlab\B_F.csv');
dlmwrite('C:\Users\ezxmt\Desktop\Output_Matlab\B_F.csv', ...
    B_F,'-append');

delete('C:\Users\ezxmt\Desktop\Output_Matlab\Q_LsF.csv');
dlmwrite('C:\Users\ezxmt\Desktop\Output_Matlab\Q_LsF.csv',
 Q_LsF(:,1)','-append');

 delete('C:\Users\ezxmt\Desktop\Output_Matlab\Q_LrF.csv');
```

```
dlmwrite('C:\Users\ezxmt\Desktop\Output_Matlab\Q_LrF.csv',
 Q_LrF(:,1)','-append');


 %% Pipe G
 delete('C:\Users\ezxmt\Desktop\Output_Matlab\T_G.csv');
dlmwrite('C:\Users\ezxmt\Desktop\Output_Matlab\T_G.csv', ...
    T_G(:,1)','-append');

delete('C:\Users\ezxmt\Desktop\Output_Matlab\T_rG.csv');
dlmwrite('C:\Users\ezxmt\Desktop\Output_Matlab\T_rG.csv', ...
    T_rG(:,1)','-append');

delete('C:\Users\ezxmt\Desktop\Output_Matlab\m_8.csv');
dlmwrite('C:\Users\ezxmt\Desktop\Output_Matlab\m_8.csv', ...
    m_8,'-append');

delete('C:\Users\ezxmt\Desktop\Output_Matlab\B_G.csv');
dlmwrite('C:\Users\ezxmt\Desktop\Output_Matlab\B_G.csv', ...
    B_G,'-append');

delete('C:\Users\ezxmt\Desktop\Output_Matlab\Q_LsG.csv');
dlmwrite('C:\Users\ezxmt\Desktop\Output_Matlab\Q_LsF.csv',
 Q_LsF(:,1)','-append');

 delete('C:\Users\ezxmt\Desktop\Output_Matlab\Q_LrG.csv');
dlmwrite('C:\Users\ezxmt\Desktop\Output_Matlab\Q_LrG.csv',
 Q_LrG(:,1)','-append');


% Pipe H
 delete('C:\Users\ezxmt\Desktop\Output_Matlab\T_H.csv');
 dlmwrite('C:\Users\ezxmt\Desktop\Output_Matlab\T_H.csv', ...
    T_H(:,1)','-append');

delete('C:\Users\ezxmt\Desktop\Output_Matlab\T_rH.csv');
 dlmwrite('C:\Users\ezxmt\Desktop\Output_Matlab\T_rH.csv', ...
    T_rH(:,1)','-append');

delete('C:\Users\ezxmt\Desktop\Output_Matlab\m_9.csv');
 dlmwrite('C:\Users\ezxmt\Desktop\Output_Matlab\m_9.csv', ...
    m_9,'-append');

delete('C:\Users\ezxmt\Desktop\Output_Matlab\B_H.csv');
 dlmwrite('C:\Users\ezxmt\Desktop\Output_Matlab\B_H.csv', ...
    B_H,'-append');

delete('C:\Users\ezxmt\Desktop\Output_Matlab\Q_LsH.csv');
 dlmwrite('C:\Users\ezxmt\Desktop\Output_Matlab\Q_LsH.csv',
  Q_LsH(:,1)','-append');

 delete('C:\Users\ezxmt\Desktop\Output_Matlab\Q_LrH.csv');
 dlmwrite('C:\Users\ezxmt\Desktop\Output_Matlab\Q_LrH.csv',
  Q_LrH(:,1)','-append');

% Pipe I
  delete('C:\Users\ezxmt\Desktop\Output_Matlab\T_I.csv');
 dlmwrite('C:\Users\ezxmt\Desktop\Output_Matlab\T_I.csv', ...
```

```
        T_I(:,1)','-append');

    delete('C:\Users\ezxmt\Desktop\Output_Matlab\T_rI.csv');
    dlmwrite('C:\Users\ezxmt\Desktop\Output_Matlab\T_rI.csv', ...
        T_rI(:,1)','-append')


    delete('C:\Users\ezxmt\Desktop\Output_Matlab\m_10.csv');
    dlmwrite('C:\Users\ezxmt\Desktop\Output_Matlab\m_10.csv', ...
        m_10,'-append');

    delete('C:\Users\ezxmt\Desktop\Output_Matlab\B_I.csv');
    dlmwrite('C:\Users\ezxmt\Desktop\Output_Matlab\B_I.csv', ...
        B_I,'-append');

    delete('C:\Users\ezxmt\Desktop\Output_Matlab\Q_LsI.csv');
    dlmwrite('C:\Users\ezxmt\Desktop\Output_Matlab\Q_LsI.csv',
     Q_LsI(:,1)','-append');

     delete('C:\Users\ezxmt\Desktop\Output_Matlab\Q_LrI.csv');
    dlmwrite('C:\Users\ezxmt\Desktop\Output_Matlab\Q_LrI.csv',
     Q_LrI(:,1)','-append');

end


% Pipe A
    dlmwrite('C:\Users\ezxmt\Desktop\Output_Matlab\T_A.csv', ...
        T_A(:,1)','-append');

    dlmwrite('C:\Users\ezxmt\Desktop\Output_Matlab\T_rA.csv', ...
        T_rA(:,1)','-append');

    dlmwrite('C:\Users\ezxmt\Desktop\Output_Matlab\m_2.csv', ...
        m_2,'-append');

    dlmwrite('C:\Users\ezxmt\Desktop\Output_Matlab\Q_LsA.csv', ...
        Q_LsA(:,1)','-append');

    dlmwrite('C:\Users\ezxmt\Desktop\Output_Matlab\m_1.csv', ...
        m_1,'-append');

    dlmwrite('C:\Users\ezxmt\Desktop\Output_Matlab\B_A.csv', ...
        B_A,'-append');

% Pipe B

    dlmwrite('C:\Users\ezxmt\Desktop\Output_Matlab\T_B.csv', ...
        T_B(:,1)','-append');

    dlmwrite('C:\Users\ezxmt\Desktop\Output_Matlab\T_rB.csv', ...
        T_rB(:,1)','-append');

    dlmwrite('C:\Users\ezxmt\Desktop\Output_Matlab\m_3.csv', ...
        m_3,'-append');

    dlmwrite('C:\Users\ezxmt\Desktop\Output_Matlab\m_4.csv', ...
        m_4,'-append');
```

```
    dlmwrite('C:\Users\ezxmt\Desktop\Output_Matlab\B_B.csv', ...
        B_B,'-append');

    dlmwrite('C:\Users\ezxmt\Desktop\Output_Matlab\Q_LsB.csv',
    Q_LsB(:,1)','-append');

    dlmwrite('C:\Users\ezxmt\Desktop\Output_Matlab\Q_LrB.csv',
    Q_LrB(:,1)','-append');

  %Pipe C

    dlmwrite('C:\Users\ezxmt\Desktop\Output_Matlab\T_C.csv', ...
        T_C(:,1)','-append');

    dlmwrite('C:\Users\ezxmt\Desktop\Output_Matlab\T_rC.csv', ...
        T_rC(:,1)','-append');

    dlmwrite('C:\Users\ezxmt\Desktop\Output_Matlab\m_5.csv', ...
        m_5,'-append');

    dlmwrite('C:\Users\ezxmt\Desktop\Output_Matlab\B_c.csv', ...
        B_C,'-append');

    dlmwrite('C:\Users\ezxmt\Desktop\Output_Matlab\Q_LsC.csv',
    Q_LsB(:,1)','-append');

    dlmwrite('C:\Users\ezxmt\Desktop\Output_Matlab\Q_LrC.csv',
    Q_LrC(:,1)','-append');

% Pipe E

    dlmwrite('C:\Users\ezxmt\Desktop\Output_Matlab\T_E.csv', ...
        T_E(:,1)','-append');

    dlmwrite('C:\Users\ezxmt\Desktop\Output_Matlab\T_rE.csv', ...
        T_rE(:,1)','-append');

    dlmwrite('C:\Users\ezxmt\Desktop\Output_Matlab\m_6.csv', ...
        m_6,'-append');

    dlmwrite('C:\Users\ezxmt\Desktop\Output_Matlab\B_E.csv', ...
        B_E,'-append');

    dlmwrite('C:\Users\ezxmt\Desktop\Output_Matlab\Q_LsE.csv',
    Q_LsE(:,1)','-append');

    dlmwrite('C:\Users\ezxmt\Desktop\Output_Matlab\Q_LrE.csv',
    Q_LrE(:,1)','-append');

   % Pipe F

    dlmwrite('C:\Users\ezxmt\Desktop\Output_Matlab\T_F.csv', ...
        T_F(:,1)','-append');

    dlmwrite('C:\Users\ezxmt\Desktop\Output_Matlab\T_rF.csv', ...
        T_rF(:,1)','-append');
```

```
 dlmwrite('C:\Users\ezxmt\Desktop\Output_Matlab\m_7.csv', ...
    m_7,'-append');

 dlmwrite('C:\Users\ezxmt\Desktop\Output_Matlab\B_F.csv', ...
    B_F,'-append');

 dlmwrite('C:\Users\ezxmt\Desktop\Output_Matlab\Q_LsF.csv',
 Q_LsF(:,1)','-append');

 dlmwrite('C:\Users\ezxmt\Desktop\Output_Matlab\Q_LrF.csv',
 Q_LrF(:,1)','-append');

% Pipe G

 dlmwrite('C:\Users\ezxmt\Desktop\Output_Matlab\T_G.csv', ...
    T_G(:,1)','-append');

 dlmwrite('C:\Users\ezxmt\Desktop\Output_Matlab\T_rG.csv', ...
    T_rG(:,1)','-append');

 dlmwrite('C:\Users\ezxmt\Desktop\Output_Matlab\m_8.csv', ...
    m_8,'-append');

 dlmwrite('C:\Users\ezxmt\Desktop\Output_Matlab\B_G.csv', ...
    B_G,'-append');

 dlmwrite('C:\Users\ezxmt\Desktop\Output_Matlab\Q_LsF.csv',
 Q_LsF(:,1)','-append');

 dlmwrite('C:\Users\ezxmt\Desktop\Output_Matlab\Q_LrG.csv',
 Q_LrG(:,1)','-append');


% Pipe H

dlmwrite('C:\Users\ezxmt\Desktop\Output_Matlab\T_H.csv', ...
    T_H(:,1)','-append');

dlmwrite('C:\Users\ezxmt\Desktop\Output_Matlab\T_rH.csv', ...
    T_rH(:,1)','-append');

dlmwrite('C:\Users\ezxmt\Desktop\Output_Matlab\m_9.csv', ...
    m_9,'-append');

dlmwrite('C:\Users\ezxmt\Desktop\Output_Matlab\B_H.csv', ...
    B_H,'-append');

dlmwrite('C:\Users\ezxmt\Desktop\Output_Matlab\Q_LsH.csv',
Q_LsH(:,1)','-append');

dlmwrite('C:\Users\ezxmt\Desktop\Output_Matlab\Q_LrH.csv',
Q_LrH(:,1)','-append');

%% Pipe I

 dlmwrite('C:\Users\ezxmt\Desktop\Output_Matlab\T_I.csv', ...
    T_I(:,1)','-append');
```

```
    dlmwrite('C:\Users\ezxmt\Desktop\Output_Matlab\T_rI.csv', ...
        T_rI(:,1)','-append')

    dlmwrite('C:\Users\ezxmt\Desktop\Output_Matlab\m_10.csv', ...
        m_10,'-append');

    dlmwrite('C:\Users\ezxmt\Desktop\Output_Matlab\B_I.csv', ...
        B_I,'-append');

    dlmwrite('C:\Users\ezxmt\Desktop\Output_Matlab\Q_LsI.csv',
    Q_LsI(:,1)','-append');

    dlmwrite('C:\Users\ezxmt\Desktop\Output_Matlab\Q_LrI.csv',
    Q_LrI(:,1)','-append');

% Switch

T_A(:,1)=T_A(:,2);
T_rA(:,1)=T_rA(:,2);

T_B(:,1)=T_B(:,2);
T_rB(:,1)=T_rB(:,2);

T_C(:,1)=T_C(:,2);
T_rC(:,1)=T_rC(:,2);

T_D(:,1)=T_D(:,2);
T_rD(:,1)=T_rD(:,2);

T_E(:,1)=T_E(:,2);
T_rE(:,1)=T_rE(:,2);

T_F(:,1)=T_F(:,2);
T_rF(:,1)=T_rF(:,2);

T_G(:,1)=T_G(:,2);
T_rG(:,1)=T_rG(:,2);

T_H(:,1)=T_H(:,2);
T_rH(:,1)=T_rH(:,2);

T_I(:,1)=T_I(:,2);
T_rI(:,1)=T_rI(:,2);



m_1=m_1new;

m_2=m_2new;

m_3=m_3new;

m_4=m_4new;

m_5=m_5new;

m_6=m_6new;
```

```
m_7=m_7new;

m_8=m_8new;

m_9=m_9new;

m_10=m_10new;

end
```

Function to perform calculations supply line

```
% Supply Network Calculation.
% Evaluate the temperature propagation inside a pipe
function [T,Q_Ls] = Supply_Network_Calculation (Q_Ls, T, k, m ...
   ,Tg,Tf, B_Pipe, C_Pipe, F_Pipe, U_p_Pipe, dA_Pipe)

            for  z=1:k-1, % accuracy of simulation relate to how ...
                many dx I decide to divide each pipe
                 if m==0,
                     T(1,2)=T(2,1); % initial condition if no flow ...
                         is circulating (cooling down process)
                 else T(1,2)= Tf; % initial condition: it could be ...
                     the temp coming from the boiler or other pipe; ...
                     it depends from the node/branch it would be ...
                     considered
                 end
                 T(z+1,2) = ...
                     (T(z+1,1)+(C_Pipe*(T(z,2)))+(F_Pipe*Tg))/B_Pipe; ...
                     % FEM calculation based on energy balance(B, ...
                     C, F parameters calculate at each time step, ...
                     according to the variation of mass flow etc, ...
                     see main script)
                 Q_Ls(z,1)=U_p_Pipe*dA_Pipe*(((T(z,1)+T(z+1,1))/2)-Tg); ...
                     % Losses in the supply network
            end
      % Almost same calculation applied to the return temperature

end
```

Function to perform calculations return line

```
 %%  Return Network Calculation.
% Evaluate the temperature propagation inside a pipe

function [T,Q_Lr, T_rCon] = Return_Network_Calculation ( node,k, ...
   m_1,m_2,m_3,m_4,m_5, B_Pipe, C_Pipe, F_Pipe, U_p_Pipe, ...
   dA_Pipe, Q_Lr, Tg, T_r, T,T_1,T_2,T_3,T_4)
```

```
        % DECLARE MATRIX U NEED node,k, B_Pipe, C_Pipe, F_Pipe, ...
           U_p_Pipe, dA_Pipe, Q_Lr, Tg, T_r, T

    switch node % according to the node the function switch to ...
       the proper case for correctly calculate the return ...
       temperatures

        case {5, 7, 8, 9, 10} % it is the simplest case ...
           applicable only to nodes 5, 7,8,9,10
%            disp('return');

              T(1,2)=T_r;
              for  z=1:k-1
                  T(z+1,2) = ...
                      (T(z+1,1)+(C_Pipe*(T(z,2)))+(F_Pipe*Tg))/B_Pipe;

                  Q_Lr(z,1)=U_p_Pipe*dA_Pipe*(((T(z,1)+T(z+1,1))/2)-Tg);
%                     T_rCon(z,1)=T(k,2);
              end

        case 1     %returnA
%        disp('returnA');

          T(1,2)=T_r;
             for  z=1:k-1,
                T(z+1,2) = ...
                    (T(z+1,1)+(C_Pipe*(T(z,2)))+(F_Pipe*Tg))/B_Pipe;
                     if m_1==0, % this is should be in the ...
                        input from main m_1
                       T_rCon=((T(k,2))+(T_1))/(2); % T_1 temp ...
                          coming from pipe B last dx, this ...
                          connection temperature is the mixing ...
                          one after coach (point 4) and Swan ...
                          (point 5)
                     else ...
                        T_rCon=((T(k,2)*m_2)+(T_1*m_3))/(m_1); ...
                        % m_2=m_2  m_3=m_3 from main script
                     end
                     Q_Lr(z,1)=U_p_Pipe*dA_Pipe*(((T(z,1)+T(z+1,1))/2)-Tg);
             end

          case {3 4}           %% Return ABC
%              disp('returnABC');

                if m_1==0, % it is m_4_5
                   T_rCon=((T_r)+(T_1))/(2); % T_1 Temp coming ...
                      from pipe D last dx
                else T_rCon=((T_r*m_2)+(T_1*m_3))/(m_1); % m_2 = ...
                   m_4 while m_3=m_5
                end
             T(1,2)=T_rCon;
             for  z=1:k-1,
                  T(z+1,2) = ...
                      (T(z+1,1)+(C_Pipe*(T(z,2)))+(F_Pipe*Tg))/B_Pipe; ...
                      % be careful when considering pipe B and C

                  Q_Lr(z,1)=U_p_Pipe*dA_Pipe*(((T(z,1)+T(z+1,1))/2)-Tg);
             end
```

```
        case 6            %% Return E
%               disp('returnE');

                  if m_5==0, % m_5=m_6
                     T_rCon=(T_1+T_2+T_3+T_4)/(4); % T_1 is the ...
                        final temp coming from pipe F, T_2 from ...
                        pipe G, T_3 from pipe H, T_4 from pipe I
                  else ...
                     T_rCon=((T_1*m_1)+(T_2*m_2)+(T_3*m_3)+(T_4*m_4))/(m_5); ...
                     % m_7=m_1, m_8=m_2, m_9=m_3, m_10=m_4
                  end
              T(1,2)=T_rCon;
              for  z=1:k-1
                 T(z+1,2) = ...
                    (T(z+1,1)+(C_Pipe*(T(z,2)))+(F_Pipe*Tg))/B_Pipe;

                 Q_Lr(z,1)=U_p_Pipe*dA_Pipe*(((T(z,1)+T(z+1,1))/2)-Tg);

              end

    end
end
```

Function to perform calculations for HEs

```
%% Heat exchange at building Level and return temperature calculation

function [T_r, m_next] = HE_Calculation (T_s, QLoad, T_us, ...
    cp,pump_max)
        % DECLARE MATRIX U NEED
%
     DeltaT_HE= T_s-T_us; % Delta Temp at the heat exchanger

     if DeltaT_HE <5, % Condition for the valve, if lower than 5 C ...
        no heat exchange
         cont_HE=0;
     else cont_HE=1;
     end
     if QLoad==0, % if no demand, no heat exchanged, therefore ...
        return temeprature equals supply temperature
         T_r=T_s;
     else T_r= T_s-(0.8*(T_s-T_us)*cont_HE); % Change the ...
        efficiency of the HE
     end

     % mass flow calculation
     Diff_in_out_HE= (T_s-T_r);

     if Diff_in_out_HE≤5,
         Diff_in_out_HE = 5;
     end

     m_next=QLoad/((0.8*Diff_in_out_HE*cp));
```

```
    if m_next > pump_max, %% max mass flow of the specific pump
        m_next=pump_max;
    end
end
```

Solar thermal and thermal storage to be integrated in the main script

```
% Solar Thermal and thermal Storage. this script needs to be ...
   integrated in the main one. It takes in to account the ...
   influence of the solar thermal and the boiler in the ...
   temperature  of the thermal storage. Further work is required ...
   to integrate this part with all the pipes of the heat network, ...
   as the temperature from the tank will define the inlet ...
   temperature in the network.

[T_c,Q_c,m_c]=Solar_Thermal_DH(Ta(j,1), ...
   T_Tank(NodesN,1),H_t_Hourly(j,1));


  Vector_ST_in={'Solar Thermal in',Q_c,T_c,m_c};
  Vector_ST_out={'Solar Thermal out',Q_c,T_Tank(NodesN,1),-m_c};


    if QLoad(j,1) ~= 0,


      if T_Tank(1,1) < T_tank_min,

          Test=1;


        % DISTRICT HEATING
        % Supply
        [T_A,Q_LsA]= Supply_Network_Calculation (Q_LsA,T_A, k, ...
           m_2,Tg(j,1),T_Boiler, B_A, C_A, F_A, U_pA, dA_A);
        %HE calculation
        [T_r2, m_2new]= HE_Calculation (T_A(k,2), QLoad(j,1), ...
           T_us, cp,pump_max1);
        %Return
        [T_rA,Q_LrA]= Return_Network_Calculation  (node_1, k, ...
           m_2,m_2new,m_2new,m_2new,m_2new, B_A, C_A,F_A, U_pA, ...
           dA_A, Q_LrA, Tg(j,1), T_r2, T_rA, ...
           T_A(k,2),T_A(k,2),T_A(k,2),T_A(k,2));


        Vector_DH_in = {'DH in',0,0,0};
        Vector_DH_out = {'DH out',0,0,0};

        if QLoad(j,1) < Q_Bmax,
          Boiler_nodeDistr = Model_Boiler_nodeDistr(Q_Bmax - ...
```

```
        QLoad(j,1), T_Boiler, T_Tank, T_Boiler_out_ref);
  elseif Q_Bmax≤QLoad(j,1),
    Boiler_nodeDistr = {'Boiler in',0,0,0,-1;'Boiler ...
       out',0,0,0,-1};
  end



elseif T_Tank(1,1) ≥ T_tank_min && T_Tank(1,1) < T_Limit,

    Test=2;

    Vector_DH_out = {'DH out',QLoad(j,1), T_Tank(1,1),-m_2};

  % DISTRICT HEATING
  % Supply
  [T_A,Q_LsA]= Supply_Network_Calculation (Q_LsA,T_A, k, ...
     m_2,Tg(j,1),T_Tank(1,1), B_A, C_A, F_A, U_pA, dA_A);
  %HE calculation
  [T_r2, m_2new]= HE_Calculation (T_A(k,2), QLoad(j,1), ...
     T_us, cp,pump_max1);
  %Return
  [T_rA,Q_LrA]= Return_Network_Calculation  (node_1, k, ...
     m_2,m_2new,m_2new,m_2new,m_2new, B_A, C_A,F_A, U_pA, ...
     dA_A, Q_LrA, Tg(j,1), T_r2, T_rA, ...
     T_A(k,2),T_A(k,2),T_A(k,2),T_A(k,2));

  Vector_DH_in={'DH in',QLoad(j,1), T_rA(k,2),m_2};

  Boiler_nodeDistr = Model_Boiler_nodeDistr(QLoad(j,1) - ...
     Q_c, T_Boiler, T_Tank, T_Boiler_out_ref);


elseif T_Tank(1,1) ≥ T_Limit,

    Test=3;

  % DISTRICT HEATING
  Vector_DH_out={'DH out',QLoad(j,1), T_Tank(1,1), -m_2};
  % Supply
  [T_A,Q_LsA]= Supply_Network_Calculation (Q_LsA,T_A, k, ...
     m_2,Tg(j,1),T_Tank(1,1), B_A, C_A, F_A, U_pA, dA_A);
  %HE calculation
  [T_r2, m_2new]= HE_Calculation (T_A(k,2), QLoad(j,1), ...
     T_us, cp,pump_max1);
  %Return
  [T_rA,Q_LrA]= Return_Network_Calculation  (node_1, k, ...
     m_2,m_2new,m_2new,m_2new,m_2new, B_A, C_A,F_A, U_pA, ...
     dA_A, Q_LrA, Tg(j,1), T_r2, T_rA, ...
     T_A(k,2),T_A(k,2),T_A(k,2),T_A(k,2));

  Vector_DH_in={'DH in',QLoad(j,1), T_rA(k,2),m_2};

  Boiler_nodeDistr = {'Boiler in',0,0,0,-1;'Boiler ...
     out',0,0,0,-1};

end
```

```
    elseif QLoad(j,1) == 0,

        Vector_DH_in = {'DH in',0,0,0};
        Vector_DH_out = {'DH out',0,0,0};
        Boiler_nodeDistr = {'Boiler in',0,0,0,-1;'Boiler ...
            out',0,0,0,-1};

        [T_A,Q_LsA]= Supply_Network_Calculation (Q_LsA,T_A, k, ...
            m_2,Tg(j,1),T_Tank(1,1), B_A, C_A, F_A, U_pA, dA_A);
        %HE calculation
        [T_r2, m_2new]= HE_Calculation (T_A(k,2), QLoad(j,1), ...
            T_us, cp,pump_max1);
        %Return
        [T_rA,Q_LrA]= Return_Network_Calculation  (node_1, k, ...
            m_2,m_2new,m_2new,m_2new,m_2new, B_A, C_A,F_A, U_pA, ...
            dA_A, Q_LrA, Tg(j,1), T_r2, T_rA, ...
            T_A(k,2),T_A(k,2),T_A(k,2),T_A(k,2));

    end

  Tank_IC = [Vector_DH_in; Vector_DH_out; Vector_ST_in; ...
     Vector_ST_out];

  [Tank_IC_NodeDistr,Check] = Calc_Node_Distr(Tank_IC,T_Tank);

%   Check_func=[Check_func;Check];

  Tank_IC_Node=[Tank_IC_NodeDistr; Boiler_nodeDistr];

  Tank_Input_Record=[Tank_IC_NodeDistr;Boiler_nodeDistr];

  Mass_Down = Tank_Mass_Balance(Tank_IC_Node);

  [T_Tank_Next,testres_f] = Tank_Energy_Balance(Tank_IC_Node, ...
     T_Tank, Mass_Down,j);

  testres = [testres; testres_f];
```

Function for solar radiation calculation

```
function [kt,H_t, H_t_daily,Yearly_Av_Radiation,H_t_Hourly]= ...
    solar_calculation_DH (d,n,lat,beta,azimut,Gsc,H,ro_g)
%% It calculates the total solar radiation on a tilted surface in ...
    a specific latitude
% (remember that irradiance is W/m2, while Irradiation J/m2)
% it starts with solar angle w(z) and the declination angle ...
    throughout the
% entire year. Then it assesses the incidence angle of the solar ...
    beam radiation teta
% it is also possible to obtain by calculations the ...
    extraterrestrial horizontal solar
% radiation on a surface. Once got H_o, having the measurement H ...
    data for the location,
```

```
% Nottingham in this case, we can calculate the clear index Kt ...
   and then the diffuse and beam
% radiation compoment, necessary for the Ht calculation using the
% isoentropic diffuse model (see Duffie & Beckman pag 90). On the ...
   calculation of the hourly
% radiation (see pag 75), close to sunset and sunrise, the ...
   calculation of
% teta is modified to get more accurate values and avoid errors ...
   in the calc
% (see pag. 88 duffie & Beckman)


declination=zeros(n,1);
sun_hour_angle=zeros(n,1);
w=zeros(24,1);
cos_teta=zeros(d,n);
cos_tetaz=zeros(d,n);
Rb=zeros(d,n);
H_0=zeros(d,n);
H_d=zeros(d,n);
H_b=zeros(d,n);
H_t=zeros(d,n);
H_t_daily=zeros(n,1);
H_t_Hourly=zeros(n*d,1);
kt=zeros(d,n);
time=1;
for z=1:24,
    w(z)=15*(12-z);

end
   for i=1:n,

        declination(i,1)=23.45*sind((360*(284+i)/365));
        sun_hour_angle(i,1)=(acosd(-(tand((lat))*tand((declination(i,1))))));

         for j=1:d,

            if sun_hour_angle(i,1)-15<= w(j,1) && ...
               w(j,1)<=sun_hour_angle(i,1)+15,

               cos_teta(j,i)= ...
                   (((sind(declination(i,1))*sind(lat)*cosd(beta))
               -(sind((declination(i,1))*cosd(lat)*sind(beta)*cosd(azimut))))
               *(pi*(w(j+1,1)-w(j,1))/180))+ ...
                   (((cosd(declination(i,1))*cosd(lat)*cosd(beta))
               +(cosd((declination(i,1))*sind(lat)*sind(beta)*cosd(azimut))))
               *(sind(w(j+1,1)-sind(w(j,1)))))-(((cosd(declination(i,1))
               *sind(beta)
               *sind(azimut)))*(cosd(w(j+1,1)-cosd(w(j,1)))));

               cos_tetaz(j,i)= ...
                   ((((cosd(declination(i,1)))*(cosd(lat)))
                             *(cosd(w(j+1,1))-cosd(w(j,1))))+(((sind(lat))
                             *(sind(declination(i,1))))
                             *(pi*(w(j+1,1)-w(j,1))/180)));


            elseif (-1)*sun_hour_angle(i,1)-15<= w(j,1) && ...
```

```
    w(j,1)≤(-1)*sun_hour_angle(i,1)+15,

    cos_teta(j,i)= ...
        (((sind(declination(i,1))*sind(lat)*cosd(beta))
    -(sind((declination(i,1))*cosd(lat)*sind(beta)*cosd(azimut))))
    *(pi*(w(j+1,1)-w(j,1))/180))+(((cosd(declination(i,1))
    *cosd(lat)*cosd(beta))+(cosd((declination(i,1))*sind(lat)
    *sind(beta)*cosd(azimut))))*(sind(w(j+1,1)-sind(w(j,1)))))
    -(((cosd(declination(i,1))*sind(beta)*sind(azimut)))
    *(cosd(w(j+1,1)-cosd(w(j,1)))));

    cos_tetaz(j,i)= ...
        ((((cosd(declination(i,1)))*(cosd(lat)))
    *(cosd(w(j+1,1))-cosd(w(j,1))))+(((sind(lat))
    *(sind(declination(i,1))))*(pi*(w(j+1,1)-w(j,1))/180)));

else cos_teta(j,i)= ...
    (sind((declination(i,1))))*(sind((lat)))
*(cosd((beta)))-((sind((declination(i,1))))*(cosd((lat)))*
(sind((beta)))*(cosd((azimut))))+((cosd((declination(i,1))))
*(cosd((lat)))*(cosd((beta)))*(cosd((w(j,1)))))+
((cosd((declination(i,1))))*(sind((lat)))*(sind((beta)))
*(cosd((azimut)))*(cosd((w(j,1)))))+((cosd((declination(i,1))))
*(sind((beta)))*(sind((azimut)))*(sind((w(j,1)))));

     cos_tetaz(j,i)=sind((declination(i,1)))*sind((lat))
     +(cosd((declination(i,1)))*cosd((lat))*cosd((w(j,1))));

end

if cos_tetaz(j,i)==0,
    Rb(j,i)=0;
else Rb(j,i)=cos_teta(j,i)/cos_tetaz(j,i);

end

H_0(j,i) = ...
    Gsc*(1+0.033*cosd((360*i/365)))*cos_tetaz(j,i)*time;

kt(j,i)=H(j,i)/H_0(j,i);

if kt(j,i)<0,

    kt(j,i)=0;
end
%
        if  kt(j,i)≤0.22,
            H_d(j,i)= H(j,i)*(1-0.09*kt(j,i));
            Bingo(j,i)=1;

        elseif 0.22<kt(j,i) && kt(j,i) ≤0.79,
            H_d(j,i)=H(j,i)*((0.9511-0.16004*kt(j,i))
            +(4.388*(kt(j,i))^2)-(16.638*(kt(j,i))^3)
            +(12.336*(kt(j,i))^4));

            Bingo(j,i)=2;

        elseif kt(j,i)>0.8,
```

```
                        H_d(j,i)=H(j,i)*0.165;
                        Bingo(j,i)=3;

                    end

                    H_b(j,i)=H(j,i)-H_d(j,i);

                    H_t(j,i)= ...
                        H_b(j,i)*Rb(j,i)+((H_d(j,i)*((1+cosd((beta)))/2)))
                            +(H(j,i)*ro_g(i,1)*((1-cosd((beta)))/2));

                                if H_t(j,i)<0,
                                H_t(j,i)=0;
                                end

        end
    H_t_daily(i,1)=sum(H_t(:,i))/1000;

    H_t_Hourly(1:d,1)=H_t(1:d,1);

    H_t_Hourly(i*d-23:i*d,1)=H_t(1:d,i);

    Yearly_Av_Radiation=mean (H_t_daily);

   end
end
```

Function to model boiler operation

```
function [Boiler_in_out]= Model_Boiler_nodeDistr(Q, T_Boiler, ...
    T_Tank, T_Boiler_out_ref)

global NodesN
global cp
Tollerance=10;

m_bi=Q/(cp*(T_Boiler - T_Boiler_out_ref));
Delta_T=zeros(NodesN,1);

    for z= 1:NodesN,
        Delta_T(z,1)=abs(T_Tank(z,1)-T_Boiler_out_ref);
    end

    %Define the exit node from the tank to the Boiler
    Delta_T(1,1) = 999999; % don't want the first one ....
    Delta_T(NodesN,1) = 999999;
    Node_out = max(find(Delta_T == min(Delta_T))); %in case of ...
        same Delta_T it will take the biggest
    T_Node_out = T_Tank(Node_out,1);

    if Q==0,
        Boiler_in_out = {'Boiler in',0,0,0,-1; };
        Boiler_in_out = [Boiler_in_out; {'Boiler out',0,0,0,-1; }];
```

```
    elseif T_Node_out < T_Boiler_out_ref - Tollerance,
        m_b = m_bi*((T_Boiler - T_Boiler_out_ref)/(T_Boiler - ...
            T_Node_out));

        Boiler_in_out = {'Boiler in', Q, T_Boiler, m_b, 1 };
        Boiler_in_out = [Boiler_in_out; {'Boiler out', ...
            Q,T_Node_out, - m_b,Node_out}];
    else
        Boiler_in_out={'Boiler in', Q, T_Boiler, m_bi, 1 };
        Boiler_in_out = [Boiler_in_out; {'Boiler out', ...
            Q,T_Node_out, - m_bi,Node_out}];
    end
```

Function for thermal storage mass balance

```
function [mass_down] = Tank_Mass_Balance(Tank_IC_Node)

global NodesN;

mass_down= zeros(NodesN,1);
cont_bal = 0;

% the first for loop is for calculating the mass balance between ...
    each node
% of the tank
    for z = 1:NodesN,
        %the second for loop account for the sum of in&out mass ...
            flow rate
        %to the tank
    mass_in_out=0;
        for x = 1: size(Tank_IC_Node,1),
            if isequal(Tank_IC_Node{x,5},z)
                mass_in_out = Tank_IC_Node{x,4} + mass_in_out;
            end
        end

%         if z ~= NodesN
% this is the mass balance per each one, where m_in + m_out + ...
    m_down + m_up
% = 0, also mass_down does not mean the direction, which instead ...
    is related
% to the sign it would come out after the calculation for ...
    mass_in_out above
        mass_down (z,1) = -(mass_in_out) - cont_bal;
        cont_bal =  -mass_down (z,1);

%         else  mass_down (z,1) = - mass_down (z-1,1);
%
%         end
    end

end
```

Function for thermal storage energy balance

```
function [T_Tank_Next,testres_1] = ...
    Tank_Energy_Balance(Tank_IC_Node, T_Tank, mass_down,j)

    global cp
    global NodesN
    global ro
    global dt

    Tank_Vol=10000; % Tank volume l
    Tank_Vol_Node = Tank_Vol/NodesN;
    U = 1.5/1000; %kW/m2K;
    h=2.5; % Tank height
    A_Base = (Tank_Vol/(ro*h)); %cross-sectional area
    r_Base = sqrt(A_Base/pi);
    A_Tank_Node = 2*r_Base*pi*(h/NodesN);
    Ta=15;
    T_Tank_Next = zeros(NodesN,1);

    testres = {};
    testres_1 = {};


    Wall_Thick = 0.005; % wall thickness
    k_wall= 50/1000; % Stainless Steel kW/mK
    k_water = 0.59/1000; % water conductivity kW/mK
    %A_wall = pi*((r_Base + Wall_Thick)^2); % cross-sectional ...
       area including wall
    A_wall=2*pi*((r_Base))*Wall_Thick;
    Delta_k = k_wall*( A_wall/A_Base); % the area of base it is ...
       not correct
    Coef_Cond =(k_water+Delta_k)*A_Base/(h/NodesN); % the area of ...
       base it is not correct



    for z = 1:NodesN,
        Energy_in_out = 0;
            for x = 1:size(Tank_IC_Node,1)
                if  isequal(Tank_IC_Node{x,5},z)
                    Energy_in_out = ...
                       (Tank_IC_Node{x,3}*Tank_IC_Node{x,4}*cp)+Energy_in_out;
%
                end
            end


     if z == 1,

            if mass_down (z,1) < 0,
                testres = [testres; [num2str(j)  ' ' num2str(z) ' ...
                   a']];
                testres_1 = [testres_1; [num2str(j)  ' ' ...
```

```
                num2str(Energy_in_out) ' ' num2str(mass_down ...
                (z,1)*T_Tank(z,1)*cp) ' 0' ' ' ...
                num2str(-U*A_Tank_Node*(T_Tank(z,1)-Ta)) ' ' ...
                num2str(Coef_Cond*(T_Tank(z+1,1)-T_Tank(z,1))) ...
                ' 0' ' a']];

            T_Tank_Next(z,1) = T_Tank(z,1) + dt*(((Energy_in_out)
                           +(mass_down (z,1)*T_Tank(z,1)*cp)
                           - (U*A_Tank_Node*(T_Tank(z,1)-Ta))
                           +(Coef_Cond*(T_Tank(z+1,1)-T_Tank(z,1))))
                           /(Tank_Vol_Node*cp));


            else T_Tank_Next(z,1) = T_Tank(z,1) + ...
                dt*(((Energy_in_out)+(
            mass_down (z,1)*T_Tank(z+1,1)*cp) - ...
                (U*A_Tank_Node*(T_Tank(z,1)-Ta))
            +(Coef_Cond*(T_Tank(z+1,1)-T_Tank(z,1))))/(Tank_Vol_Node*cp));

                testres = [testres; [num2str(j)  ' ' num2str(z) ' ' ...
                    b']];
                testres_1 = [testres_1; [num2str(j)  ' ' ...
                    num2str(Energy_in_out) ' ' num2str(mass_down ...
                    (z,1)*T_Tank(z+1,1)*cp) ' 0' ' ' ...
                    num2str(-U*A_Tank_Node*(T_Tank(z,1)-Ta)) ' ' ...
                    num2str(Coef_Cond*(T_Tank(z+1,1)-T_Tank(z,1))) ...
                    ' 0' ' b']];

            end

        elseif z == NodesN,

            if  mass_down (z,1) < 0,
                testres = [testres; [num2str(j)  ' ' num2str(z) ' ' ...
                    c']];
                testres_1 = [testres_1; [num2str(j)  ' ' ...
                    num2str(Energy_in_out) ' ' num2str(mass_down ...
                    (z,1)*T_Tank(z,1)*cp) ' 0' ' ' ...
                    num2str(-U*A_Tank_Node*(T_Tank(z,1)-Ta)) ' ' ...
                    num2str(Coef_Cond*(T_Tank(z-1,1)-T_Tank(z,1))) ...
                    ' 0' ' c']];
                T_Tank_Next(z,1) = T_Tank(z,1) + ...
                    dt*(((Energy_in_out)   + (mass_down ...
                    (z,1)*T_Tank(z,1)*cp) - ...
                    (U*A_Tank_Node*(T_Tank(z,1)-Ta))
                +(Coef_Cond*(T_Tank(z-1,1)-T_Tank(z,1))))/(Tank_Vol_Node*cp));

            else T_Tank_Next(z,1) = T_Tank(z,1) + ...
                dt*(((Energy_in_out) + (mass_down ...
                (z,1)*T_Tank(z-1,1)*cp)
            - (U*A_Tank_Node*(T_Tank(z,1)-Ta))
            +(Coef_Cond*(T_Tank(z-1,1)-T_Tank(z,1))))/(Tank_Vol_Node*cp));

                testres = [testres; [num2str(j) ' ' num2str(z) ' ' ...
                    d']];
                testres_1 = [testres_1; [num2str(j)  ' ' ...
                    num2str(Energy_in_out) ' ' num2str(mass_down ...
                    (z,1)*T_Tank(z-1,1)*cp) ' 0' ' ' ...
```

```
                num2str(-U*A_Tank_Node*(T_Tank(z,1)-Ta)) ' ' ...
                num2str(Coef_Cond*(T_Tank(z-1,1)-T_Tank(z,1))) ...
                ' 0' ' d']];


            end

        elseif z~=1 && z~=NodesN

            if mass_down (z,1) < 0,

                if - mass_down (z-1, 1) < 0,

            testres = [testres; [num2str(j) ' ' num2str(z) ' ...
                e']];
            testres_1 = [testres_1; [num2str(j)  ' ' ...
                num2str(Energy_in_out) ' ' num2str(mass_down ...
                (z,1)*T_Tank(z,1)*cp) ' ' num2str(-mass_down ...
                (z-1,1)*T_Tank(z,1)*cp) ' '  ...
                num2str(-U*A_Tank_Node*(T_Tank(z,1)-Ta)) ' ' ...
                num2str(Coef_Cond*(T_Tank(z-1,1)-T_Tank(z,1))) ...
                ' ' ...
                num2str(Coef_Cond*(T_Tank(z+1,1)-T_Tank(z,1))) ...
                ' e']];

                    T_Tank_Next(z,1) = T_Tank(z,1) + ...
                        dt*(((Energy_in_out) + (mass_down ...
                        (z,1)*T_Tank(z,
                    1)*cp) + (-mass_down (z-1,1)*T_Tank(z,1)*cp)
                     - (U*A_Tank_Node*(T_Tank(z,1)-Ta))
                     +(Coef_Cond*(T_Tank(z-1,1)-T_Tank(z,1)))
                     +(Coef_Cond*(T_Tank(z+1,1)-T_Tank(z,1))))
                     /(Tank_Vol_Node*cp));

                else T_Tank_Next(z,1) = T_Tank(z,1) + ...
                    dt*(((Energy_in_out)
                + (mass_down (z,1)*T_Tank(z,1)*cp) + ...
                    (-mass_down (z-1, 1)*T_Tank(z-1,1)*cp) -
                (U*A_Tank_Node*(T_Tank(z,1)-Ta))+(Coef_Cond*(T_Tank(z-1,1)
                -T_Tank(z,1)))+(Coef_Cond*(T_Tank(z+1,1)-T_Tank(z,1))))
                /(Tank_Vol_Node*cp));

            testres = [testres; [num2str(j) ' ' num2str(z) ' ...
                f']];
            testres_1 = [testres_1; [num2str(j)  ' ' ...
                num2str(Energy_in_out) ' ' num2str(mass_down ...
                (z,1)*T_Tank(z,1)*cp) ' ' num2str(-mass_down ...
                (z-1,1)*T_Tank(z-1,1)*cp) ' '  ...
                num2str(-U*A_Tank_Node*(T_Tank(z,1)-Ta)) ' ' ...
                num2str(Coef_Cond*(T_Tank(z-1,1)-T_Tank(z,1))) ...
                ' ' ...
                num2str(Coef_Cond*(T_Tank(z+1,1)-T_Tank(z,1))) ...
                ' f']];

                end

            elseif mass_down (z,1)≥ 0,
```

```
                    if - mass_down (z-1, 1) < 0,

                     T_Tank_Next(z,1) = T_Tank(z,1) + ...
                        dt*(((Energy_in_out)
                     +(mass_down ...
                        (z,1)*T_Tank(z+1,1)*cp)+(-mass_down (z-1,1)
                     *T_Tank(z,1)*cp)-(U*A_Tank_Node*(T_Tank(z,1)-Ta))
                     +(Coef_Cond*(T_Tank(z-1,1)-T_Tank(z,1)))
                     +(Coef_Cond*(T_Tank(z+1,1)-T_Tank(z,1))))
                     /(Tank_Vol_Node*cp));

                  testres = [testres; [num2str(j) ' ' num2str(z) ' ...
                     g']];
                  testres_1 = [testres_1; [num2str(j)  ' ' ...
                     num2str(Energy_in_out) ' ' num2str(mass_down ...
                     (z,1)*T_Tank(z+1,1)*cp) ' ' ...
                     num2str(-mass_down (z-1,1)*T_Tank(z,1)*cp) ' ...
                     '  num2str(-U*A_Tank_Node*(T_Tank(z,1)-Ta)) ' ...
                     ' ...
                     num2str(Coef_Cond*(T_Tank(z-1,1)-T_Tank(z,1))) ...
                     ' ' ...
                     num2str(Coef_Cond*(T_Tank(z+1,1)-T_Tank(z,1))) ...
                     ' g']];


                    else T_Tank_Next(z,1) = T_Tank(z,1) + ...
                        dt*(((Energy_in_out)
                     + (mass_down (z,1)*T_Tank(z+1,1)*cp)+
                     (-mass_down (z-1,1)*T_Tank(z-1,1)*cp)
                      -(U*A_Tank_Node*(T_Tank(z,1)-Ta))
                      +(Coef_Cond*(T_Tank(z-1,1)-T_Tank(z,1)))+
                      (Coef_Cond*(T_Tank(z+1,1)-T_Tank(z,1))))
                      /(Tank_Vol_Node*cp));

                  testres = [testres; [num2str(j) ' ' num2str(z) ' ...
                     h']];
                  testres_1 = [testres_1; [num2str(j)  ' ' ...
                     num2str(Energy_in_out) ' ' num2str(mass_down ...
                     (z,1)*T_Tank(z+1,1)*cp) ' ' ...
                     num2str(-mass_down (z-1,1)*T_Tank(z-1,1)*cp) ...
                     ' '  num2str(-U*A_Tank_Node*(T_Tank(z,1)-Ta)) ...
                     ' ' ...
                     num2str(Coef_Cond*(T_Tank(z-1,1)-T_Tank(z,1))) ...
                     ' ' ...
                     num2str(Coef_Cond*(T_Tank(z+1,1)-T_Tank(z,1))) ...
                     ' f']];
                    end
                            end

 end

end

for z = 1:NodesN-1,

     if T_Tank_Next (z,1)< T_Tank_Next (z+1,1),

         T_Tank_Next (z,1)= ((T_Tank_Next (z,1)+T_Tank_Next ...
```

```
                (z+1,1))/2)+2;
            T_Tank_Next (z+1,1) = ((T_Tank_Next ...
                (z,1)+T_Tank_Next (z+1,1))/2)-2;

        end
    end

end
```

Appendix H

Thermal imaging

In the preliminary energy audit of the UK case study a thermal imaging survey was carrier out. The inspection was performed on the 5^{th} March 2013, during a cold night (temperature recorded was -2) between 8 to 11 pm. The pictures around the Estate, for both buildings and heat network, were taken with a Flir thermal camera. Figure H.1, H.2, H.3 and H.4 illustrated the results obtained from the pictures taken for the buried pre-insulated pipes out of the old boiler room (before the replacement of the old biomass boiler) and connecting OF 1 and LW 2.

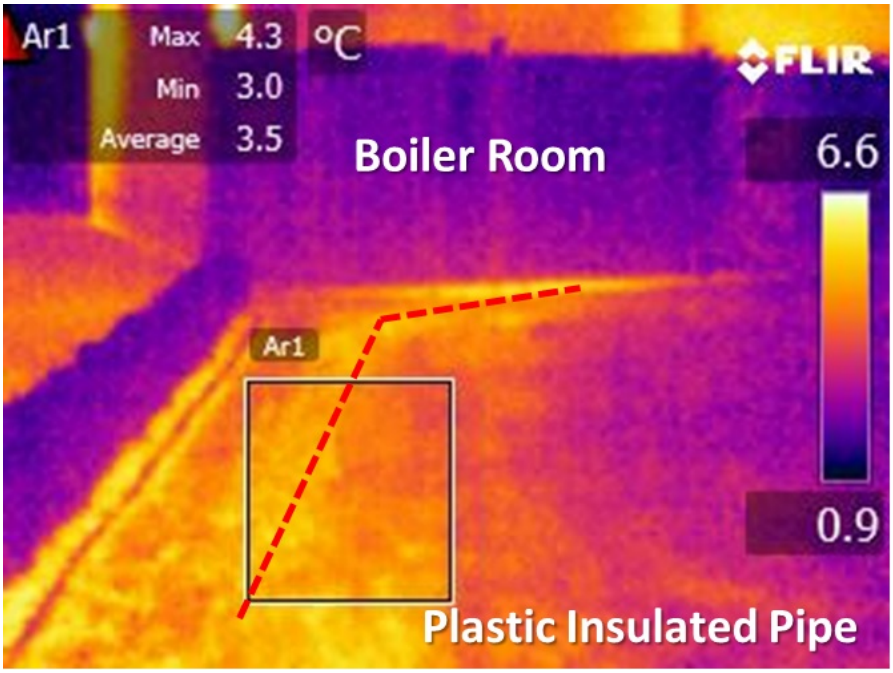

Figure H.1: Flir camera picture of pre-insulated pipes out of the boiler room

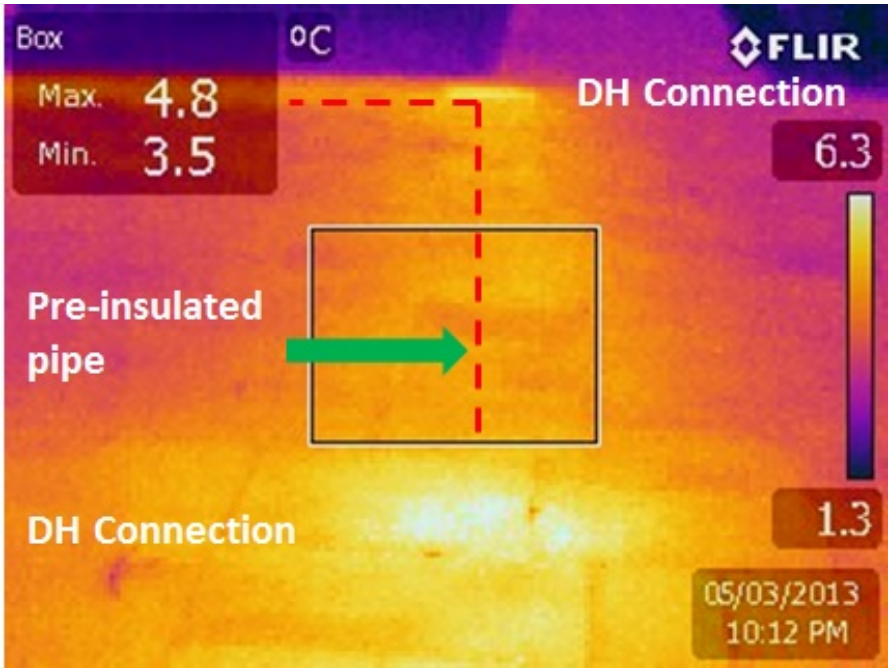

Figure H.2: Flir camera picture of pre-insulated pipes connecting OF 1

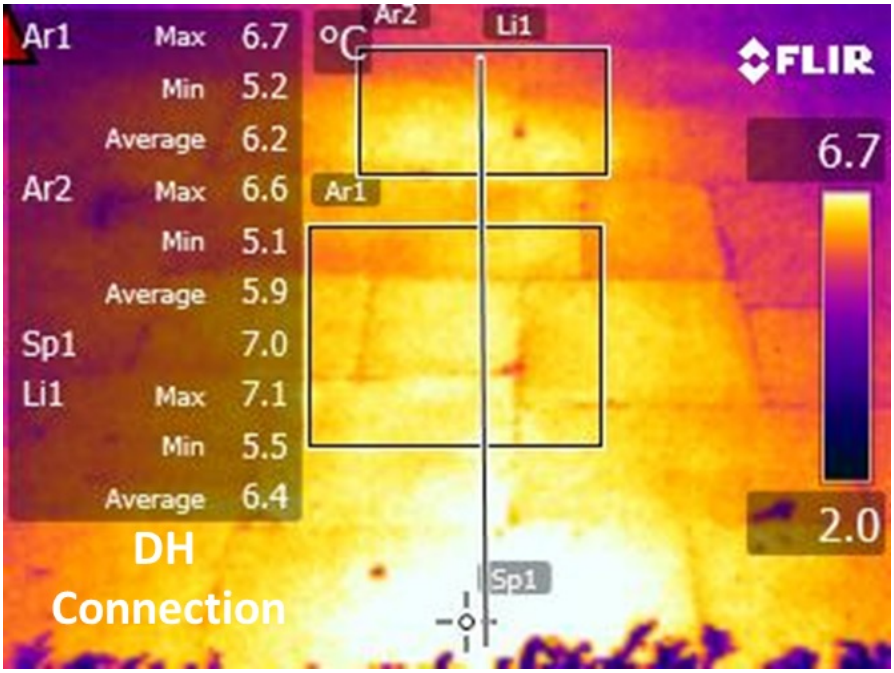

Figure H.3: Flir camera picture of pre-insulated pipes connecting OF 1

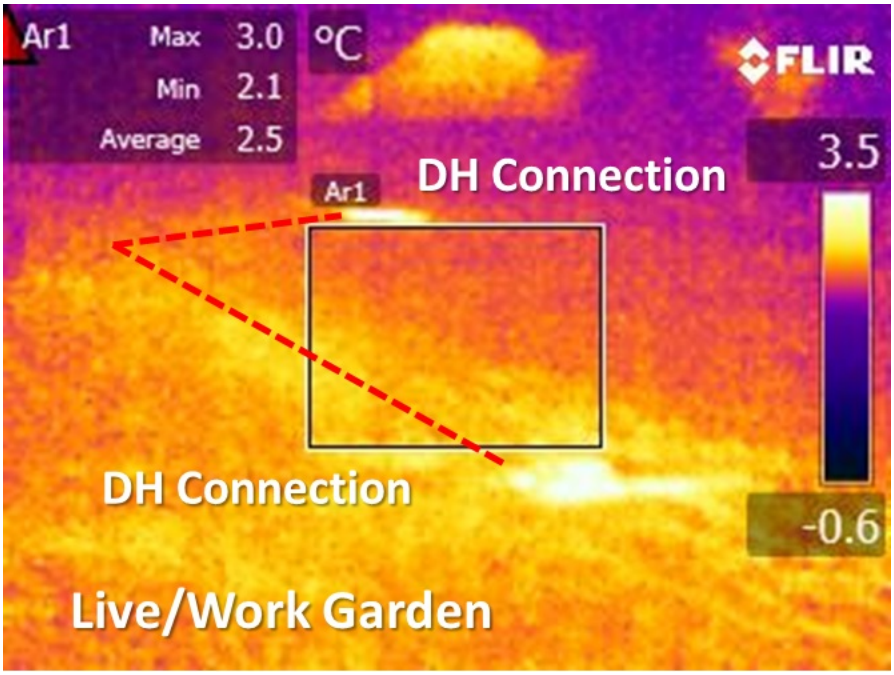

Figure H.4: Flir camera picture of pre-insulated pipes connecting LW 2

Although quantitative conclusions can not be drawn because the pictures does not take into account several aspects as typology of terrain, depth of pipelines and patterns of heat dispersion, nonetheless these can give a qualitative idea of the

distribution losses associated to the hot water circulating into the heat network.

Similarly, an evaluation of the thermal performances of the buildings' envelop was carried out. Figure H.5 and H.6 show the results for OF 2 and LW 2. The former picture shows a several discontinuities within the thermal envelop highlighting a disuniformity in the temperature distribution of the facade. Figure H.6 is still showing a thermal bridge in the discontinuity between first and second floor, but at the same time it presents a better temperature distribution on the facade as LW 2 built in 2006 is characterised by a better envelop compared to OF 2.

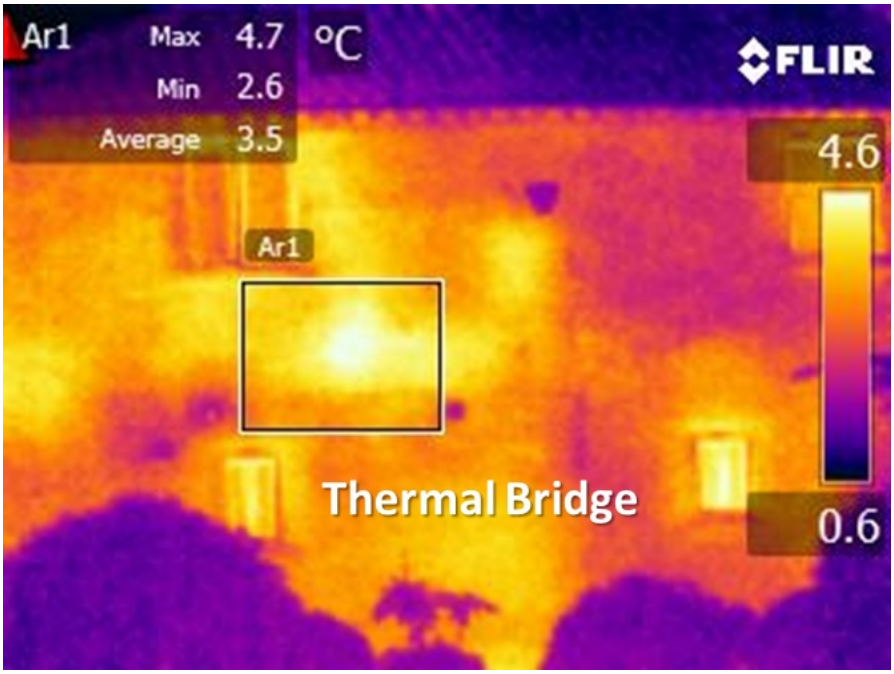

Figure H.5: Flir camera picture of thermal bridges OF 2

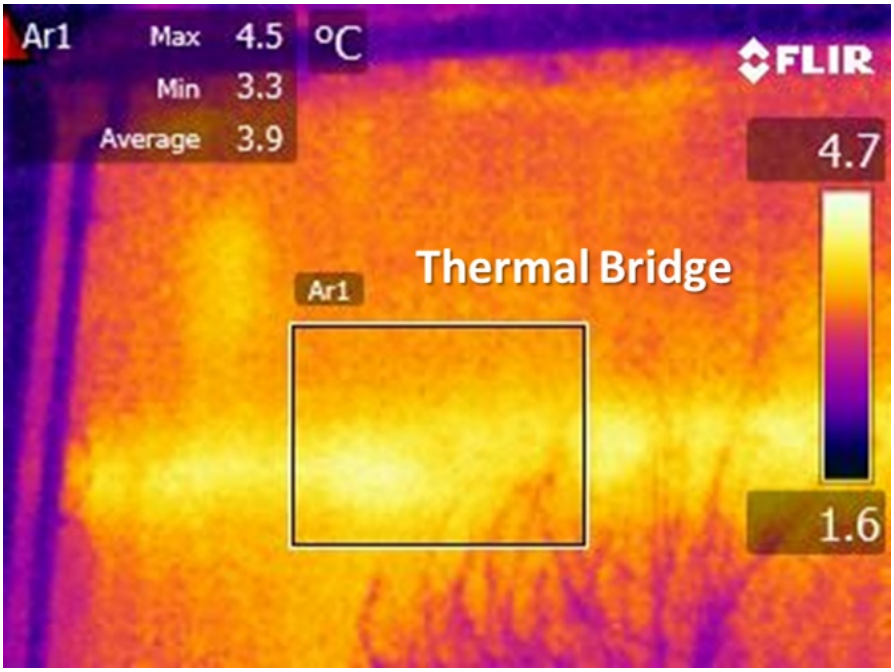

Figure H.6: Flir camera picture of thermal bridges LW 2

Appendix I

Site view and buildings' plans of the UK case study

All the key parameters and buildings' construction characteristics are summarised in Section 6.1 and 6.2.1. To correctly define the energy models of each building, with room height of 2.7 m, site maps and buildings' plans were also collected. These are presented as follow for each building of the UK Estate used as case study for this investigation.

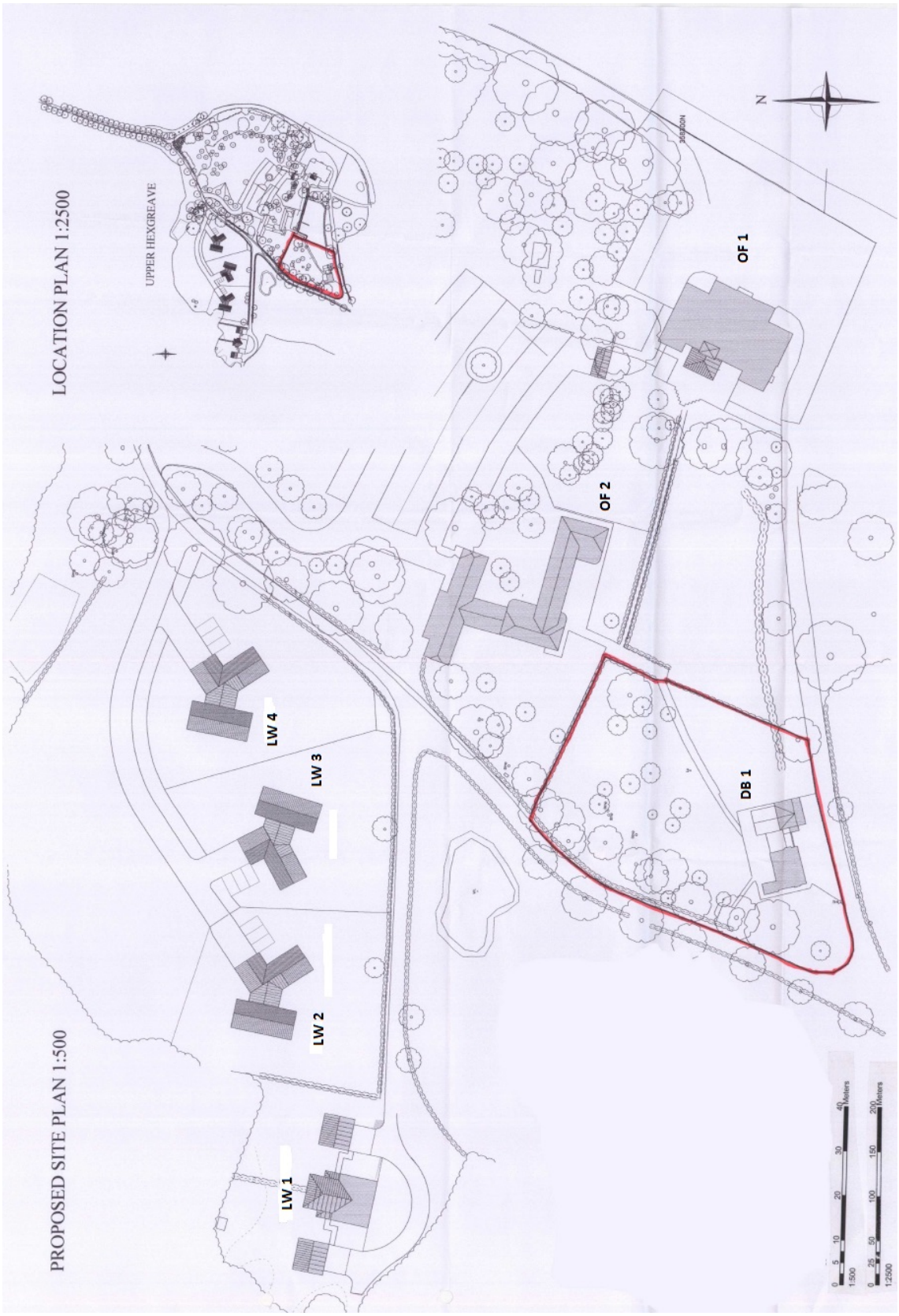

Figure I.1: UK case study: site plan

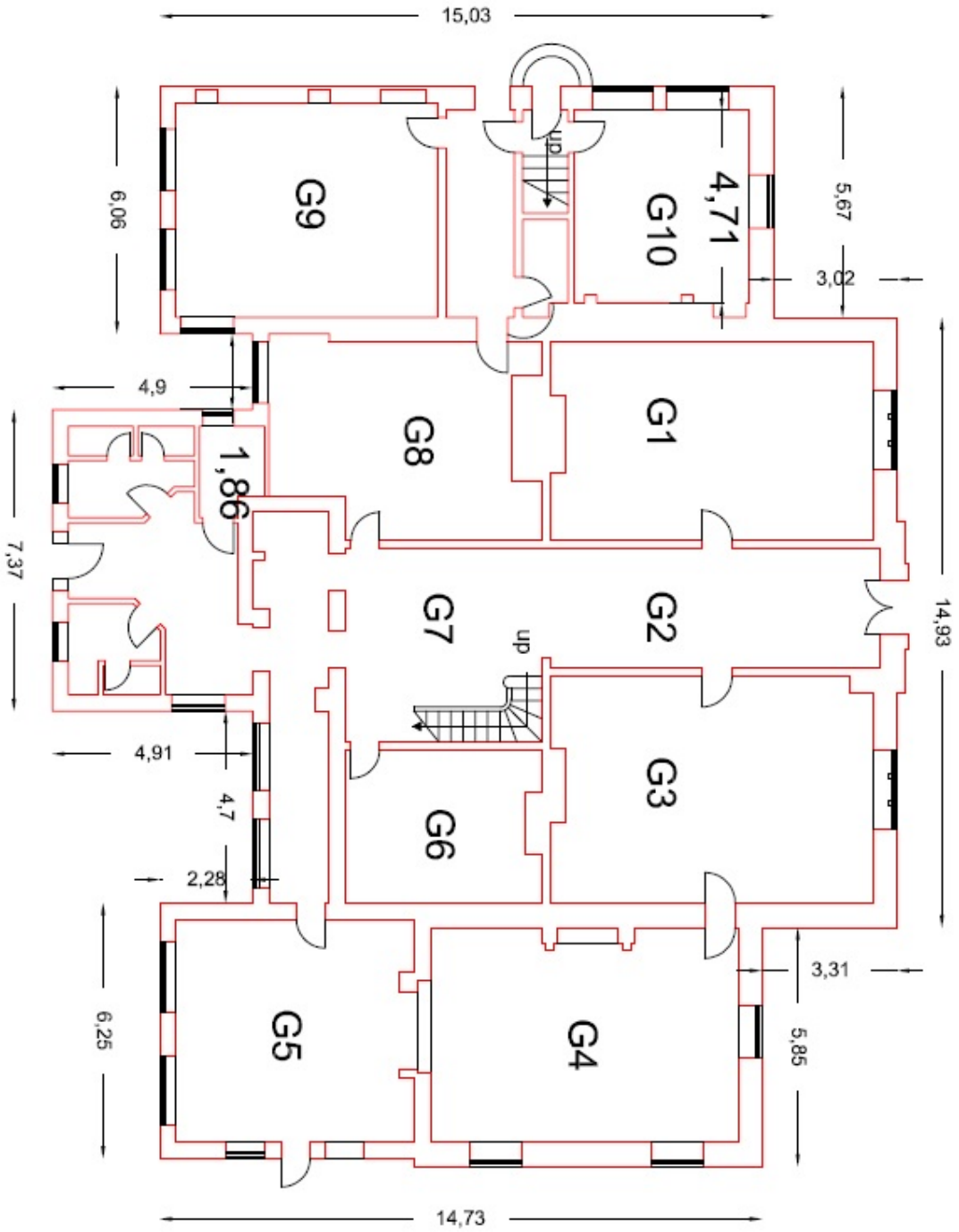

Figure I.2: OF 1: ground floor plan

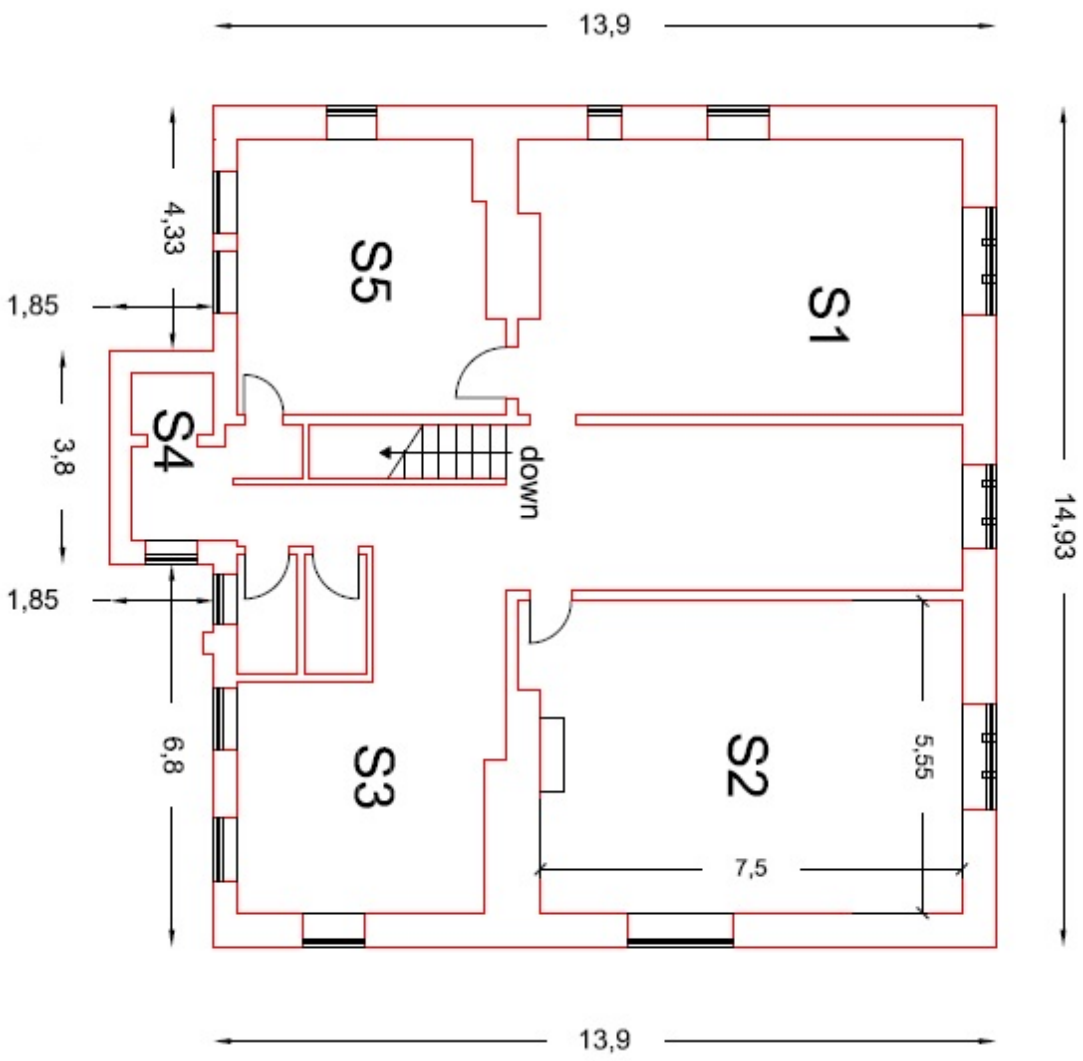

Figure I.3: OF 1: First and second floor plans

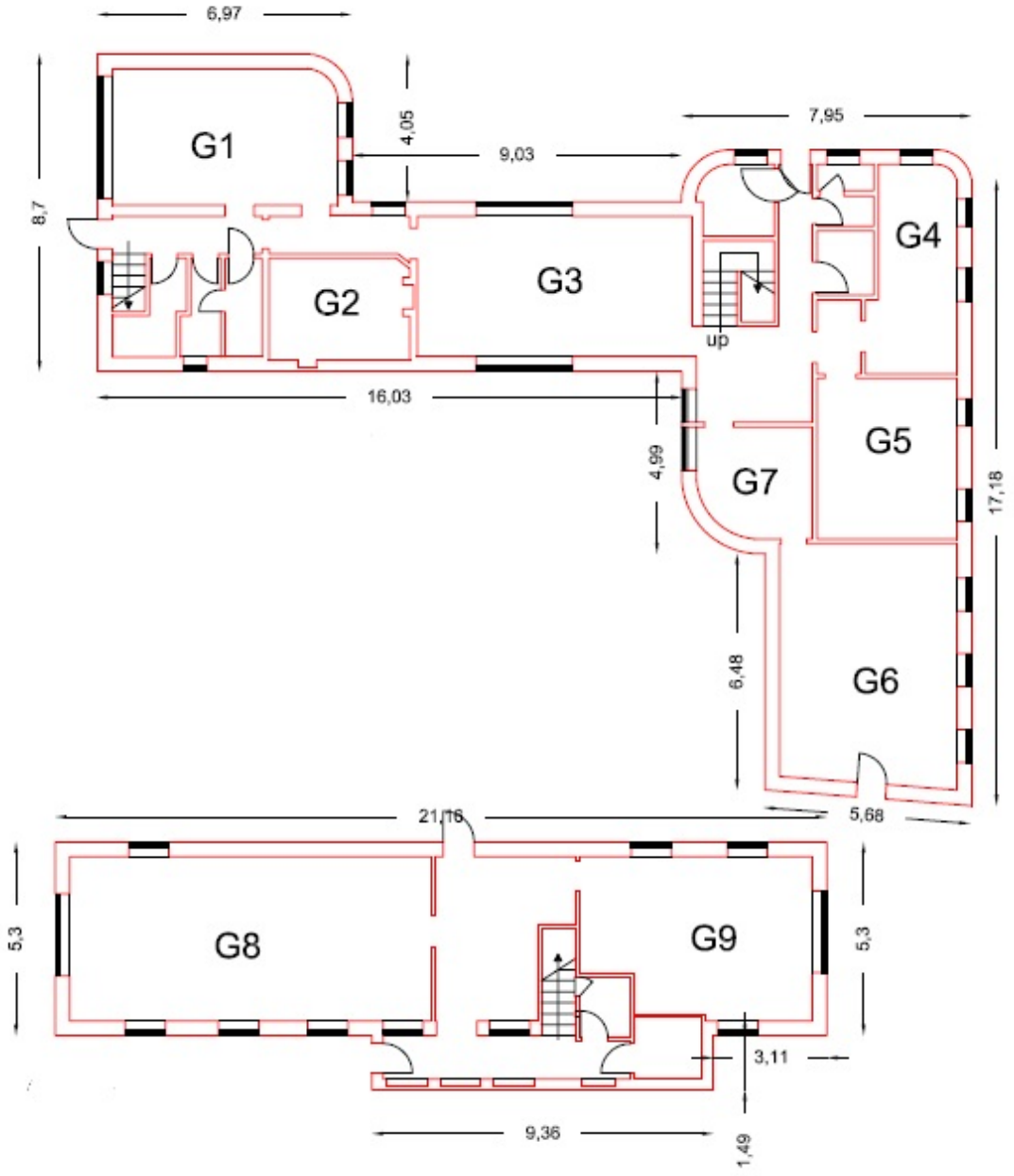

Figure I.4: OF 2: ground floor plan

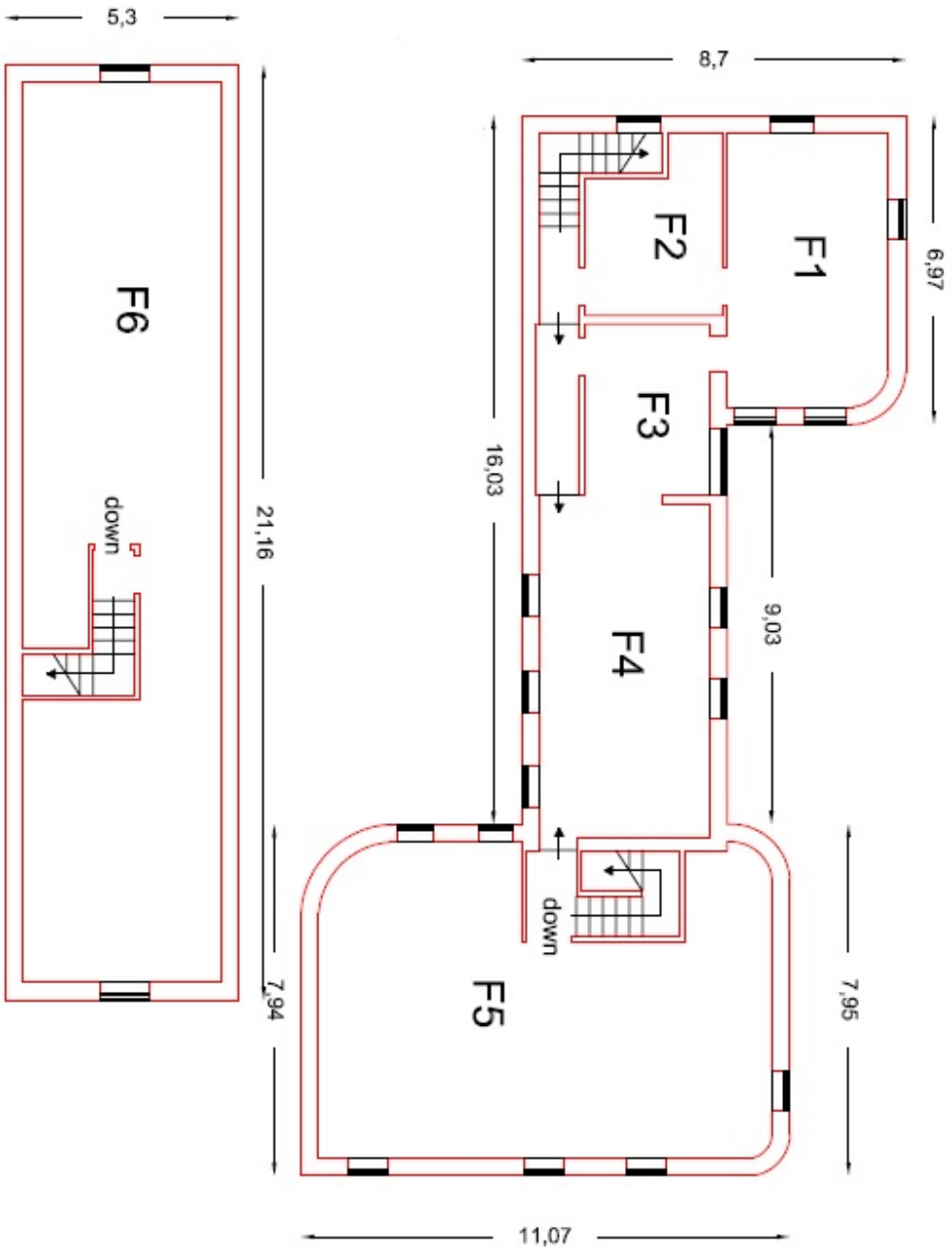

Figure I.5: OF 2: first floor plan

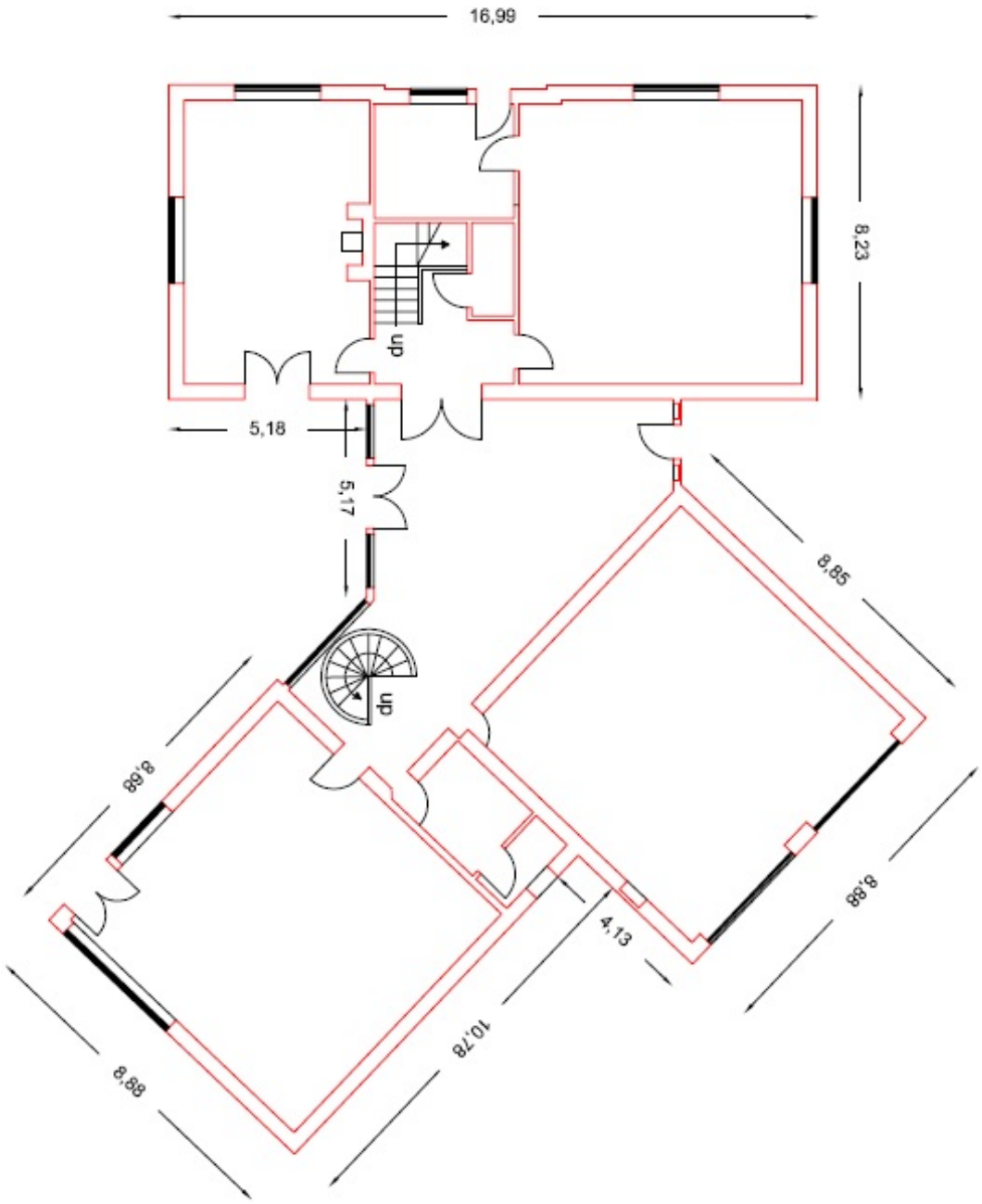

Figure I.6: LW 2, 3 and 4: ground floor plan

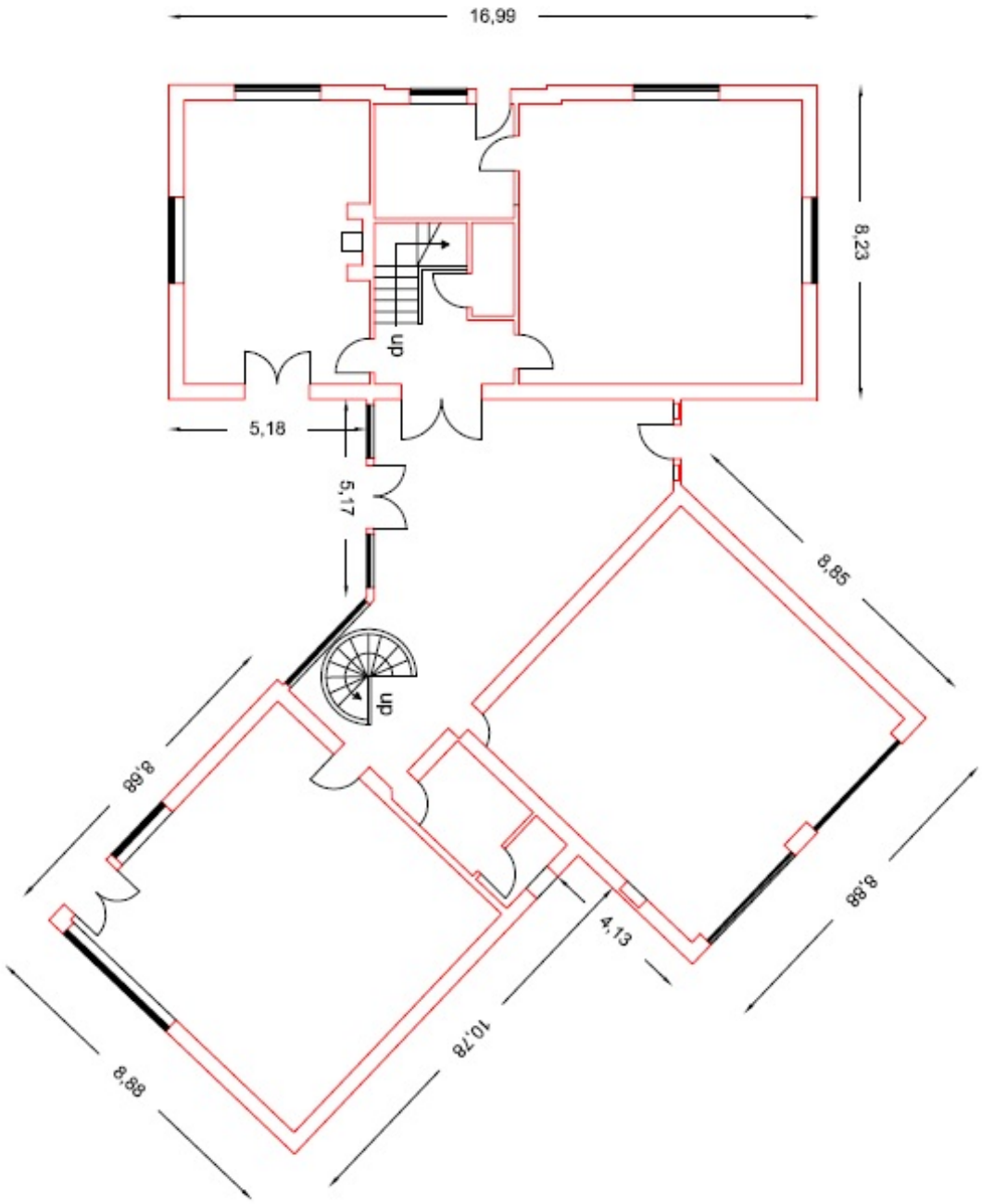

Figure I.7: LW 2, 3 and 4: first floor plan

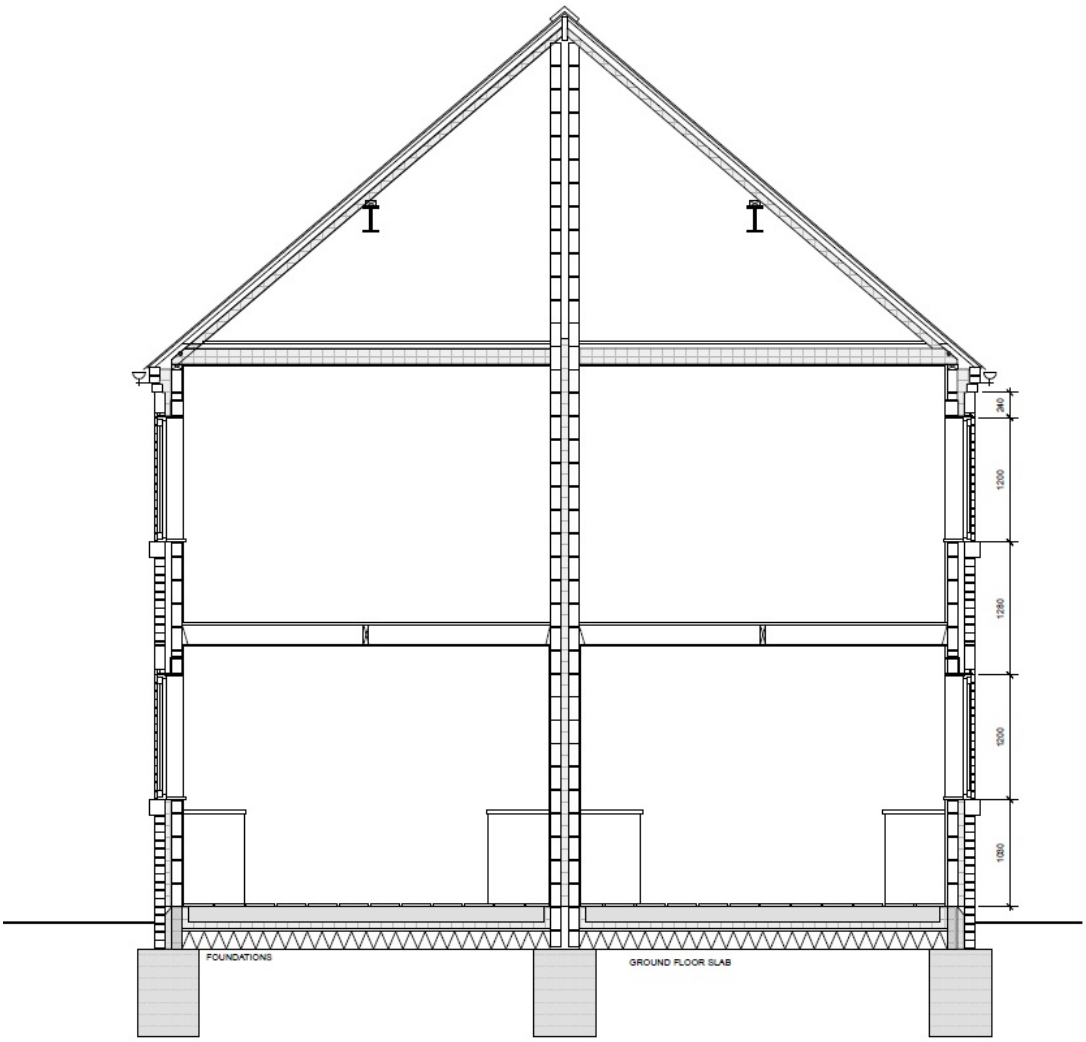

Figure I.8: LW 1: building section

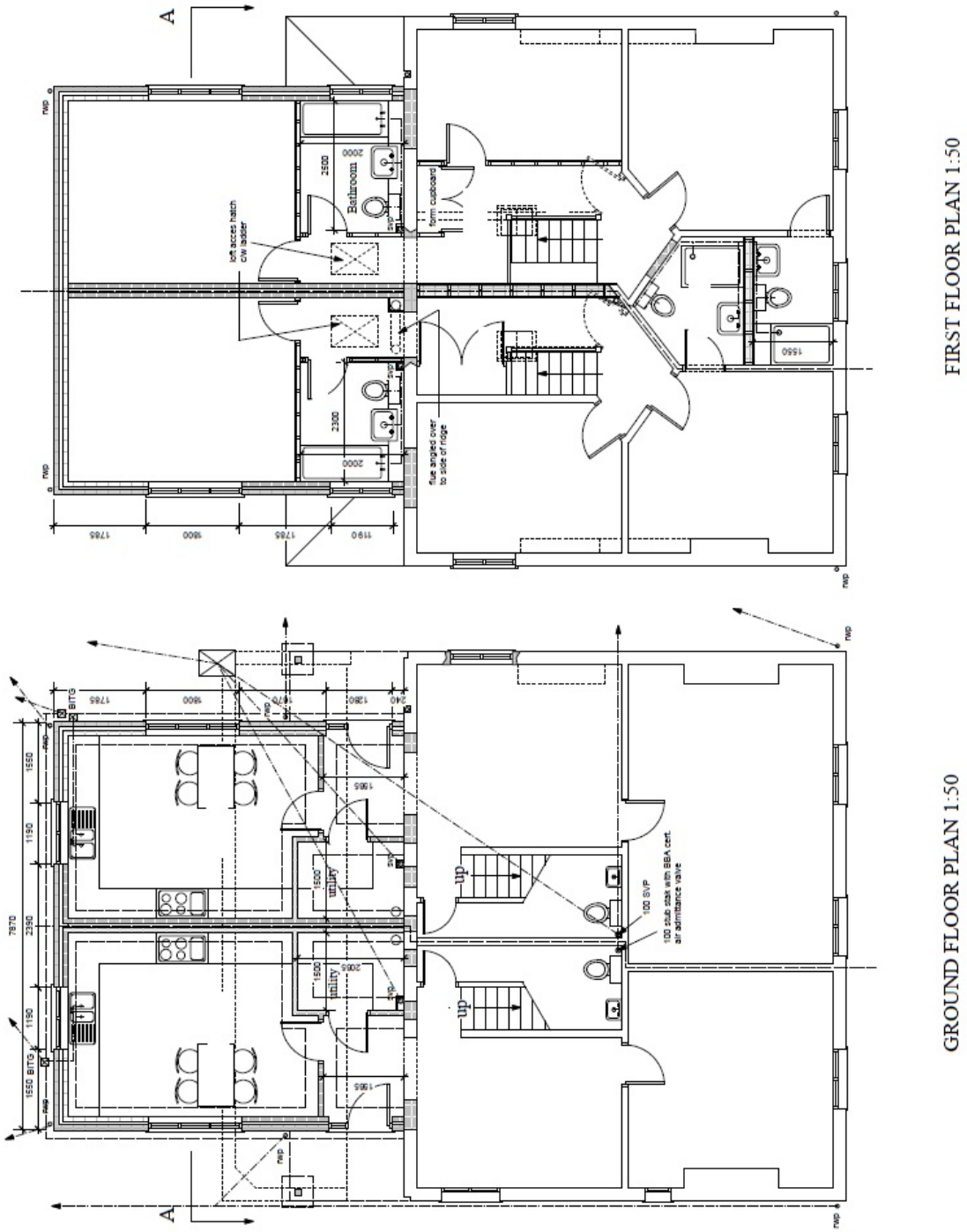

Figure I.9: LW 1: ground and first floor plans

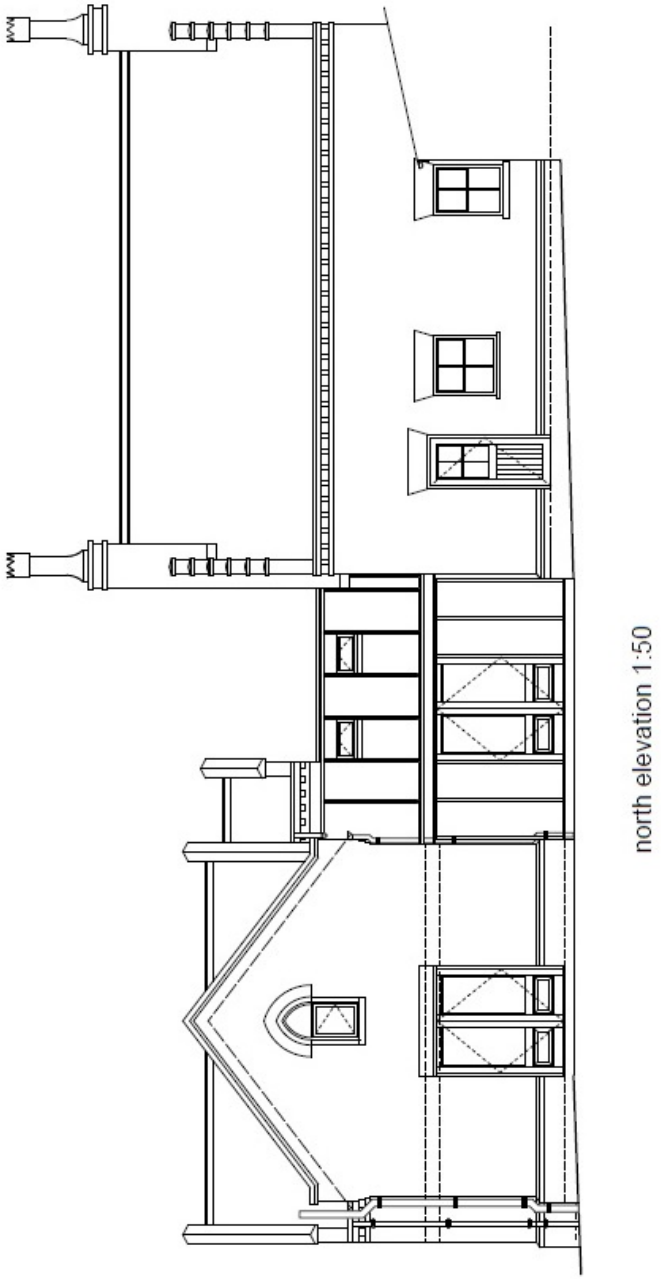

Figure I.10: DB 1: building section

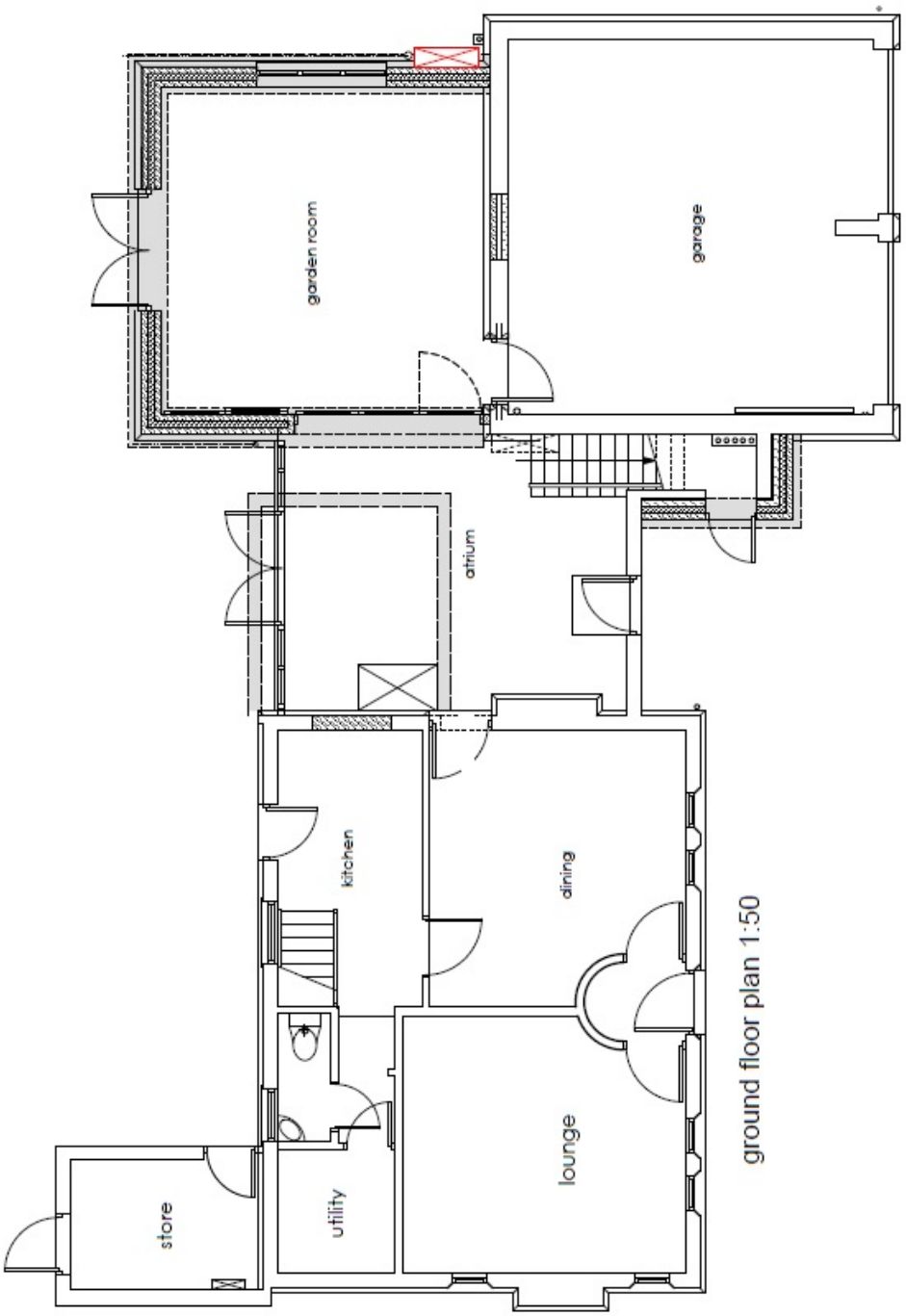

Figure I.11: DB 1: ground floor plan

References

[1] IEA. Key World Energy Statistics 2016. Technical report, International Energy Agengy, 2015.

[2] Enerdata. Global energy statistical yearbook 2016. https://yearbook.enerdata.net/#CO2-emissions-data-from-fuel-combustion.html.

[3] IPCC. Climate Change 2014 Synthesis Report Summary Chapter for Policymakers. Technical report, 2014.

[4] European Commission. Heating and cooling, 2016.

[5] European Commission. Communication from the Commission to the European Parliament, the Council, the European Economic and Social Committee and the Committee of the Regions - A Roadmap for moving to a competitive low carbon economy in 2050. Technical Report March, EU Commision, Brussels, 2011.

[6] EU. Analysis of options to move beyond 20% greenhouse gas emission reductions and assessing the risk of carbon leakage. 2010.

[7] European Commission. 2050 low-carbon economy. http://ec.europa.eu/clima/policies/strategies/2050/index{_}en.htm.

[8] L. D. Danny Harvey. *A handbook on low energy buildings and district energy fundamentals, Techniques and Examples*. EARTHSCAN, London, 2006.

[9] P. Woods and J. Overgaard. Historical development of district heating and characteristics of a modern district heating system . In *Advanced District Heating and Cooling (DHC) Systems*, chapter 1, pages 223–240. Elsevier Ltd., 2016.

[10] Svend Frederiksen and Sven Werner. *District Heating and Cooling*. Studentlitteratur, pag. 408, Sweden, 2013.

[11] Robin Wiltshire, Jonathan Williams, and Paul Woods. A technical guide to district heating. Technical report.

[12] Nicolas P Garcia, Kostantinos Vatopoulos, Alicia P Lopez, and Christian Thiel. Best available technologies for the heat and cooling market in the European Union. Technical report, 2012.

[13] Olof Jangsten, Antonio Aguiló-Rullán, Jonathan Williams, and Robin Wiltshire. A technical guide to district heating. Technical report, 2011.

[14] Bard Skagestad and Peter Mildenstein. *District Heating and Cooling Connection Handbook*. 2002.

[15] UNEP. District Energy In Cities: Unlocking the Potential of Energy Efficiency and Renewable Energy. Technical report, Copenhagen centre on energy efficiency, ICLEI, UNHABITAT, 2015.

[16] Urban Persson and Sven Werner. Heat distribution and the future competitiveness of district heating. *Applied Energy*, 88(3):568–576, 2011.

[17] European Commission. *EU energy in figures, Statistical Pocketbook 2015.* 2015.

[18] European Commission. An EU strategy on Heating and Cooling. Technical report, EU Commision, 2016.

[19] David Connolly, Brian Vad Mathiesen, and Poul Alberg Østergaard. Heat Roadmap Europe 2050 - First Prestudy. Technical report, 2012.

[20] Danish Energy Agengy. Regulation and planning of district heating in Denmark. Technical report, 2015.

[21] H Lund and B Mathiesen. Energy system analysis of 100% renewable energy systems - The case of Denmark in years 2030 and 2050. *Energy*, 34:524–531, 2008.

[22] Commitee on Climate Change. The Fourth Carbon Budget: Reducing Emissions Through the 1990s. Technical Report December, DECC, 2010.

[23] DECC. The Future of Heating : Meeting the challenge. Technical Report March, 2013.

[24] DECC. The Future of Heating:A strategic framework for low carbon heat in the UK. Technical report, 2012.

[25] Gareth Davies and Paul Woods. The potential and costs of district heating networks. Technical report, Poyry, 2009.

[26] Ecoheat4eu and Euroheat & Power. Recommendation report for the United Kingdom. Technical report, 2011.

[27] DECC. Assessment of the costs, performance, and characteristics of UK heat networks. Technical report, 2013.

[28] DECC. Summary evidence on district heating networks in the UK. Technical report, 2013.

[29] Enviroenergy. Nottingham district heating scheme. http://www.enviroenergy.co.uk.

[30] EU Commision. Remourban project. http://www.remourban.eu/.

[31] DECC. Birmingham district heating scheme. http://chp.decc.gov.uk/cms/district-heating-birmingham/.

[32] Aberdeen Heat & Power. Aberdeen district heating scheme. http://http://www.aberdeenheatandpower.co.ukl.

[33] Sheffield City Council. Sheffield district heating scheme. https://www.sheffield.gov.uk/environment/waste/reducingrecycling/districtheating.html.

[34] Cofely and Southampton City Council. Southampton district heating scheme. http://www.cofely-gdfsuez.co.uk/solutions/district-energy/district-energy-schemes/southampton-district-energy/.

[35] Coventry District Energy Company (CDEC). Coventry district heating scheme. http://business.engie.co.uk/embedded-generation/urban-energy/coventry/.

[36] Leicester District Energy . Leicester district heating scheme. http://www.leicester.gov.uk/news/news-story-details?nId=88794.

[37] Queen Elizabeth Olympic Park. Olympic park district heating scheme. `http://www.queenelizabetholympicpark.co.uk/the-park/attractions/around-the-park/energy-centre`.

[38] ADE. District heating map. `http://www.theade.co.uk/more-about-district-heating_3592.html`.

[39] David J K Hawkey. District heating in the UK: A technological Innovation System analysis. *Environmetal Innovation ans Societal Transition*, 5:19–32, 2012.

[40] CIBSE and ADE. *Heat networks : Code of Practice for the UK. Raising standards for heat supply.* CIBSE, 2015.

[41] DECC. Research into barriers to deployment of district heating networks. Technical report, 2013.

[42] Which?. Turning up the heat: getting a fair deal for district heating users. Technical report, 2015.

[43] D Hawkey. District heating in the UK : Prospects for a third national programme. *Science & Technology Studies*, 27:68–89, 2014.

[44] Brian Elmegaard, Torben Schmidt Ommen, Michael Markussen, and Johnny Iversen. Integration of space heating and hot water supply in low temperature district heating. *Energy and Buildings*, 2015.

[45] Henrik Lund, Sven Werner, Robin Wiltshire, Sven Svendsen, Jan Eric Thorsen, Frede Hvelplund, and Brian Vad Mathiesen. 4th Generation Dis-

trict Heating (4GDH) Integrating smart thermal grid into future sustainable energy system. *Energy*, 68:1–11, 2014.

[46] Peter Kaarup Olsen, Christian Holm Christiansen, Morten Hofmeister, Svend Svendsen, and Jan-Eric Thorsen. Guidelines for Low-Temperature District Heating. Technical Report April, Danish Energy Agency, 2014.

[47] Robin Wiltshire, Jonathan Williams, and Abhilash Rajan. The importance of energy quality in matching supply and demand. Technical report, 2012.

[48] Alessandro Dalla Rosa. *The development of a new district heating concept. Network design and optimization for integrating energy conservation and renewable energy use.* PhD thesis, technical University of Denmark, 2012.

[49] CEN. Recommendations for prevention of Legionella growth in installations inside buildings conveying water for human consumption. Technical report, CEN, 2012.

[50] Xiaochen Yang, Hongwei Li, and Svend Svendsen. Decentralized substations for low-temperature district heating with no Legionella risk, and low return temperatures. *Energy*, pages 1–10, 2015.

[51] CIBSE. *Minimising the risk of Legionnaires' disease.*, volume 296. 2013.

[52] British Standard Institution. *BS 8558 Guide to the design, installation, testing and maintenance of services supplying water for domestic use within buildings and their curtilages. Complementary guidance to BS EN 806.* BSI, second edition, 2015.

[53] HSE. *Legionnaires' disease. The control of legionella bacteria in water systems.* Health and Safety Executive, fourth edi edition, 2013.

[54] HSE. *Legionnaires' disease. Part 2: The control of legionella bacteria in hot and cold water systems.* Health and Safety Executive, 2014.

[55] A Della Rosa, H Li, and S Svendsen. Method for optimal design of pipes for low-energy district heating, with focus on heat losses. *Energy*, 36:2407–2418, 2011.

[56] A. Dalla Rosa, R. Boulter, K. Church, and S. Svendsen. District heating (DH) network design and operation toward a system-wide methodology for optimizing renewable energy solutions (SMORES) in Canada: A case study. *Energy*, 45(1):960–974, 2012.

[57] Peter Weitzmann. *Modelling building integated heating and cooling systems.* PhD thesis, 2004.

[58] A. Dalla Rosa and J. E. Christensen. Low-energy district heating in energy efficienty building areas. *Energy*, 36, 2011.

[59] Bruce Young, Alan Shiret, John Hayton, and Will Griffiths. Design of low-temperature domestic heating systems. Technical report, 2013.

[60] Patrick Lauenburg. *Improved supply of district heat to hydronic space heating systems.* PhD thesis, Lund University, 2009.

[61] R Langendries. Low return temperature (LRT) in district heating. *Energy and Buildings*, 12:191–200, 1988.

[62] P. Lauenburg and J. Wollerstrand. Adaptive control of radiator systems for a lowest possible district heating return temperature. *Energy and Buildings*, 72:132–140, 2014.

[63] Christian Holm Christiansen, Alessandro Dalla Rosa, Marek Brand, Peter Kaarup Olsen, and Jan Eric Thorsen. Technical paper results and experiences from a 2-year study with measurements on low-temperature DH system for low energy buidings. Technical report, Danfoss, 2012.

[64] Alessandro Dalla Rosa, Hongwei Li, Svend Svendsen, Sven Werner, Urban Persson, Karin Ruehling, Clemens Felsmann, Martin Crane, Robert Burzynski, and Ciro Bevilacqua. Toward 4 th Generation District Heating : Experience and Potential of Low-Temperature District Heating. Technical report, IEA, 2014.

[65] Marek Brand, Jan Eric Thorsen, and Svend Svendsen. Numerical modelling and experimental measurements for a low-temperature district heating substation for instantaneous preparation of DHW with respect to service pipes. *Energy*, 41:392–400, 2012.

[66] Ala Hasan, Jarek Kurnitski, and Kai Jokiranta. A combined low temperature water heating system consisting of radiators and floor heating. *Energy and Buildings*, 41(5):470–479, 2009.

[67] Donald R. Wulfinghoff. Radiators and convectors. In *Energy Efficiency Manual*, chapter 5. Energy Institute Press, 1999.

[68] ASHREA. Hydronic heat-distributing units and radiators. In *ASHRAE Handbook - Heating, Ventilating, and Air-Conditioning Systems and Equipment*, chapter 36, pages 1–12. ASHREA, 2012.

[69] CIBSE. Major components of heating systems. In *Non Domestic Hot Water Heating Systems*, pages 1–54. CIBSE, 2010.

[70] Doug Oughton and Ant Wilson. *Heating and air-conditioning of buildings*. Routledge, eleventh edition, 2015.

[71] S. Pettersson and B. Nyberg. Funktion hos 1–rörs radiatorsystem — avkylning, komfort och stabilitet [Function of the 1–pipe radiator systems — cooling, comfort and stability], 2003.

[72] Robert MacDowell. Hydronic systems. In *Fundamentals of HVAC Systems*, chapter 8, pages 103–116. 2006.

[73] Adnan Ploskić and Sture Holmberg. Performance evaluation of radiant baseboards (skirtings) for room heating. An analytical and experimental approach. *Applied Thermal Engineering*, 62(2):382–389, 2014.

[74] T. Kane, S.K. Firth, and K.J. Lomas. How are UK homes heated? A city-wide, socio-technical survey and implications for energy modelling. *Energy and Buildings*, 86:817–832, 2015.

[75] Robert Petitjean. *Balancing radiator systems*, volume 3. TA & Andersson AB, 2003.

[76] Baoping Xu, Ang Huang, Lin Fu, and Hongfa Di. Simulation and analysis on control effectiveness of TRVs in district heating systems. *Energy and Buildings*, 43(5):1169–1174, 2011.

[77] Z. Liao, M. Swainson, and a.L. Dexter. On the control of heating systems in the UK. *Building and Environment*, 40(3):343–351, 2005.

[78] Baoping Xu, Lin Fu, and Hongfa Di. Field investigation on consumer behavior and hydraulic performance of a district heating system in Tianjin, China. *Building and Environment*, 44(2):249–259, 2009.

[79] Valentina Monetti, Enrico Fabrizio, and Marco Filippi. Impact of low investment strategies for space heating control: Application of thermostatic radiators valves to an old residential building. *Energy and Buildings*, 95:202–210, 2015.

[80] Baoping Xu, Lin Fu, and Hongfa Di. Dynamic simulation of space heating systems with radiators controlled by TRVs in buildings. *Energy and Buildings*, 40(9):1755–1764, 2008.

[81] Micheal McNamara. Thermostatic Radiator Valve (TRV) Demonstration Project. 1995.

[82] EU Commission. EN 12828. Heating systems in buildings — Design for water-based heating systems, 2014.

[83] EU Commission. EN 12831. Heating systems and water based cooling systems in buildings — Method for calculation of the design heat load, 2014.

[84] EU Commission. European Standard — EN 442-1 — Radiators and convectors Part 1: Technical specifications and requirements, 2015.

[85] EU Commission. European Standard — EN 442-2 — Radiators and convectors. Part 2: tests methods and rating, 2015.

[86] P Ljunggren and J Wollerstrand. Optimum Performance of Radiator Space Heating Systems Connected to achieve lowest possible district heating return temperature. In *10th International Symposium on District Heating and Cooling*, number September, 2006.

[87] P. Lauenburg. Temperature optimization in district heating systems. In *Advanced District Heating and Cooling (DHC) Systems*, chapter Chapter 11, pages 223–240. Elsevier Ltd., 2016.

[88] EnergyPlus. EnergyPlus Documentation. `http://nrel.github.io/EnergyPlus/EngineeringReference/13b-EncyclopaedicRefs/#hot-water-baseboard-heater-with-radiation-and-convection`.

[89] Li Lianzhong and M. Zaheeruddin. Dynamic modelling and simulation of a room with hot water baseboard heater. *International Journal of Energy Research*, 30(6):427–445, 2006.

[90] L. Peeters, J. Van der Veken, H. Hens, L. Helsen, and W. D'haeseleer. Control of heating systems in residential buildings: Current practice. *Energy and Buildings*, 40(8):1446–1455, 2008.

[91] L. Hoon, K. Bong-Kyun, K. Youn-Hong, H. Lindkvist, A. Loewen, H. Seungkyu, H. Walletun, and M. Wigbels. Improvement of operational temperature differences in district heating systems, 2005.

[92] Danish Standard. DS 418:2011- Beregning af bygningers varmetab [Calculation of heat loss from buildings], 2011.

[93] CIBSE. CIBSE Guide B: Heating , ventilating , air conditioning and refrigeration. 2006.

[94] Peter Grunnet Wang, Mikael Scharling, Kristian Pagh Nielsen, Claus Kern-Hansen, and Kim Bjarne Wittchen. 2001–2010 Danish Design Reference Year: Reference Climate Dataset for Technical Dimensioning in Building, Construction and other Sectors. 2013.

[95] CIBSE. Nottingham weather data. `http://www.cibse.org/weatherdata`.

[96] Dorte Skaarup Østergaard and Svend Svendsen. Replacing critical radiators to increase the potential to use low-temperature district heating — A case study of 4 Danish single-family houses from the 1930s. *Energy*, 2016.

[97] Danish Standard, DS 469 — Heating and cooling systems in buildings, 2013.

[98] EQUA. Validation and certifications. `http://www.equa.se/en/ida-ice/validation-certifications`.

[99] Mikk Maivel and Jarek Kurnitski. Low temperature radiator heating distribution and emission efficiency in residential buildings. *Energy and Buildings*, 69:224–236, 2014.

[100] Mikk Maivel and Jarek Kurnitski. Radiator and floor heating operative temperature and temperature variation corrections for EN 15316-2 heat emission standard. *Energy and Buildings*, 99:204–213, 2015.

[101] Schneider. Termis software. `http://www.schneider-electric.com/en/product-range/61418-termis-software/`.

[102] EQUA. IDA Indoor Comfort Climate and Energy, 2015.

[103] Equa Simulation. Validation of IDA Indoor Climate and Energy 4 .0 with respect to CEN Standards EN 15255-2007 and EN 15265-2007. Technical report, 2010.

[104] S. Aggerholm and K. Grau. Bygningers energibehov - Pc - program og beregningsvejledning [Energy demand of buildings - Pc - program and calculation guide] - SBi -anvisning 213. Technical report, Danish Building research Institute, 2005.

[105] M. Brand, P. Lauenburg, J. Wollerstrand, and V. Zboril. Optimal Space Heating System for Low-Energy Single-Family House Supplied by Low-Temperature District Heating. In *Passivhusnorden*, 2012.

[106] E. Andersen, J. Dragsted, T. V. Kristensen, and L. Kokholm Andersen. Upgrade and Extension of the Climate station at DTU Byg. Technical report, 2014.

[107] Middelfart Fjernvarme [Info and data in Danish]. `http://www.middelfartfjernvarme.dk/wp-content/uploads/2015/09/Middelfart-`

Fjernvarme - Indf{%}C3{%}B8relse - af - motivationstarif - PIXI - udgave.pdf[InfoanddatainDanish].

[108] Jesper Toft. *Energy savings in multi-storey buildings.* Det økologiske råd, 2008.

[109] Office of the Deputy Prime Minister. The Building Regualtions 2000 L1A: Conservation of fuel and power in new dwellings. (April), 2006.

[110] Office of the Deputy Prime Minister. The Building Regualtions 2006 L2A: Conservation of fuel and power in new buildings other than dwellings. (April):1–39, 2006.

[111] English Heritage. Energy Efficiency and Historic Buildings. (April):1–61, 2012.

[112] Office of the Deputy Prime Minister. The Building Regualtions 2010 L1A: Conservation of fuel and power in new dwellings. 2010.

[113] Office of the Deputy Prime Minister. The Building Regualtions 2010 L2A: Conservation of fuel and power in new buildings other than dwellings. (l), 2010.

[114] CIBSE. *CIBSE Guide A - Environmental Design.* 2006.

[115] Brian Anderson. Conventions for U-value calculations. Technical report, BRE, 2006.

[116] CIBSE. *CIBSE Guide A - Environmental Design.* 2015.

[117] SCHMID energy solutions. Biomass boiler. http://www.schmid-energy.ch/en/schmid-group.

[118] Ofgem. Ofgem non-domestic rhi for great britain. https://www.ofgem.gov.uk/environmental-programmes/non-domestic-renewable-heat-incentive-rhi/tariffs-apply-non-domestic-rhi-great-britain.

[119] Binder. Binder biomass manufacturer, distributed by woodenergy. https://www.woodenergy.com/our-products/binder-biomass-boilers-200kw-10mw/.

[120] Schneider Electric. Termis District Heating Management — User Guide Version 6.1, 2014.

[121] CIBSE. Energy efficiency in buildings - CIBSE Guide F. Technical report, 2016.

[122] Biomass energy centre. Typical calorific values of fuels. https://http://www.biomassenergycentre.org.uk/portal/page?_pageid=75,20041&_dad=portal.

[123] Ursula Eiker Ilyes Ben Hassine. Impact of load structure variation and solar thermal energy integration on an existing district heating network. *Applied Thermal Engineering*, 50:1437–1446, 2013.

[124] DeWitt F. Incropera Bergmann, Lavine. Introduction to Heat Transfer . John Wiley & Sons, 2005.

[125] Yunus A Cengel. *Heat Transfer*. Mc Graw-Hill, 2003.

[126] John A Duffie & William A Beckman. *Solar Engineering of Thermal Processes*. John Wiley & Sons, Inc, Hoboken, New Jersey, 2006.